

**Best  
Available  
Copy**

AD701974

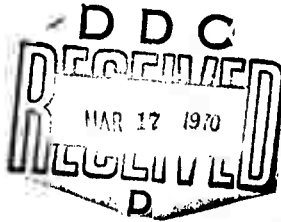
# FOREIGN TECHNOLOGY DIVISION



HYDRAULICS AND ITS APPLICATIONS ON AIRCRAFT

by

B. B. Nekrasov



Distribution of this document is unlimited. It may be released to the Clearinghouse, Department of Commerce, for sale to the general public.

Reproduced by the  
**CLEARINGHOUSE**  
for Federal Scientific & Technical  
Information Springfield Va 22151

Ho3

## EDITED TRANSLATION

HYDRAULICS AND ITS APPLICATIONS ON AIRCRAFT

By: B. B. Nekrasov

English pages: 393

Source: Gidravlika i Yeye Primeneniye na  
Letatel'nykh Apparatakh, Izd-vo  
"Mashinostroyeniye," Moscow, 1967,  
pp. 1-368.

Translated under: Contract No. F33657-68-D-0866P002

THIS TRANSLATION IS A RENDITION OF THE ORIGINAL FOREIGN TEXT WITHOUT ANY ANALYTICAL OR EDITORIAL COMMENT. STATEMENTS OR THEORIES ADVOCATED OR IMPLIED ARE THOSE OF THE SOURCE AND DO NOT NECESSARILY REFLECT THE POSITION OR OPINION OF THE FOREIGN TECHNOLOGY DIVISION.

PREPARED BY:

TRANSLATION DIVISION  
FOREIGN TECHNOLOGY DIVISION  
WP-APB, OHIO.

## NOTICE TO USERS

Portions of this document have been judged by the Clearinghouse to be of poor reproduction quality and not fully legible. However, in an effort to make as much information as possible available to the public, the Clearinghouse sells this document with the understanding that if the user is not satisfied, the document may be returned for refund.

If you return this document, please include this notice together with the IBM order card (label) to:

Clearinghouse  
Attn: 152.12  
Springfield, Va. 22151

## TABLE OF CONTENTS

Foreword . . . . .	v
Chapter I. Introduction. . . . .	1
§1. Hydraulics and Its Use on Aircraft. . . . .	1
§2. Forces Acting on a Fluid. Pressure in a Fluid. . . . .	5
§3. Basic Properties of Dropping Fluids. Fluids Used in Aviation and Rocket Engineering. . . . .	7
Chapter II. Fundamentals of Hydrostatics . . . . .	17
§4. Properties of Hydrostatic Pressure. . . . .	17
§5. Fundamental Equation of Hydrostatics. . . . .	19
§6. Differential Equilibrium Equations of a Fluid and Their Integration for the Simplest Case . . . . .	21
§7. Piezometric Height. Vacuum. Measurement of Pres- sure. . . . .	24
§8. Pressure Force of Fluid on Flat Wall. . . . .	28
§9. Pressure Force of Fluid on Cylindrical and Spherical Surfaces. Archimedean Law . . . . .	31
Chapter III. The Fluid at Relative Rest. . . . .	38
§10. Basic Concepts. . . . .	38
§11. Rectilinear Uniformly Accelerated Motion of a Container of Fluid. . . . .	39
§12. Uniform Rotation of Container of Fluid. . . . .	40
§13. Integration of Differential Equations of Equilib- rium of a Fluid for Particular Cases of Relative Rest. . . . .	43
Chapter IV. The Fundamental Equations of Hydraulics. . . . .	50
§14. Fundamental Concepts. . . . .	50
§15. Flow Rate. The Flow Rate Equation . . . . .	52
§16. Derivation of Bernoulli Equation for a Filament of Ideal Fluid. . . . .	54
§17. Derivation of the Differential Equations of Mo- tion of an Ideal Fluid and Their Integration. . . . .	59
§18. Bernoulli Equation for Viscous-Fluid Flow . . . . .	62
§19. Hydraulic Losses (in General) . . . . .	65
§20. Examples of Application of the Bernoulli Equation in Engineering. . . . .	68

Chapter V. Fluid Flow in Pipes. Hydrodynamic Similarity. . . . .	77
§21. Flows of Fluids in Pipes. . . . .	77
§22. Hydrodynamic Similarity . . . . .	80
§23. Cavitation Flow Regimes . . . . .	86
Chapter VI. Laminar Flow . . . . .	94
§24. Theory of Laminar Fluid Flows in a Round Pipe . . . . .	94
§25. The Initial Segment of Laminar Flow . . . . .	99
§26. Laminar Fluid Flow in Gaps. . . . .	101
§27. Special Cases of Laminar Flow . . . . .	106
Chapter VII. Turbulent Flow. . . . .	116
§28. Turbulent Flow of Fluid in Smooth Pipes . . . . .	116
§29. Fundamentals of Semiempirical Theory of Turbulent Pipe Flow . . . . .	120
§30. Turbulent Flow in Rough-Walled Pipes. . . . .	128
§31. Turbulent Flow in Noncircular Pipes . . . . .	133
Chapter VIII. Local Hydraulic Resistances. . . . .	138
§32. Local Resistances in General. Abrupt Expansion of the Channel . . . . .	138
§33. Diffusers . . . . .	141
§34. Constriction of Channel . . . . .	145
§35. Turns in the Channel. . . . .	147
§36. Local Resistances in Laminar Flow . . . . .	150
§37. Local Resistances in Aircraft Hydraulic Systems . . . . .	154
Chapter IX. Outflow of Fluid Through Holes and Mouthpieces . . . . .	159
§38. Hole in Thin Wall . . . . .	159
§39. Imperfect Contraction of Jet. Outflow Below Level . . . . .	164
§40. Outflow Through Mouthpieces . . . . .	167
§41. Outflow Under Variable Head (Drainage of Containers). . . . .	172
§42. Fundamentals of Hydraulic Automation. . . . .	176
§43. Spray Nozzles (Injectors) . . . . .	188
Chapter X. Relative and Nonsteady Motion of Fluid in Pipes . . . . .	199
§44. Bernoulli Equation for Relative Motion. Motion Under Conditions of Weightlessness. . . . .	199
§45. Nonsteady Fluid Flow in Pipes . . . . .	204
§46. Water Hammer in Pipes . . . . .	207
Chapter XI. Hydraulic Design of Pipelines. . . . .	219
§47. The Simple Constant-Section Pipeline. . . . .	219
§48. The Siphon. . . . .	224
§49. Series- and Parallel-Connected Pipes. . . . .	225
§50. Branched Pipelines. Calculations for the Complex Pipeline in the General Case. . . . .	227
§51. Pipeline with Pump Delivery of Fluid. . . . .	230

Chapter XII. Centrifugal Pumps . . . . .	243
§52. Pumps in General. . . . .	243
§53. Derivation of the Fundamental Equation of the Centrifugal Pump. . . . .	245
§54. Characteristic of the Ideal Pump. Pump Reaction Ratio . . . . .	248
§55. Transition to Finite Number of Vanes. . . . .	251
§56. Consideration of Hydraulic Losses in the Pump. Construction of Design Characteristic . . . . .	254
§57. Pump Efficiency . . . . .	256
§58. Similarity Formulas . . . . .	258
§59. The Speed Coefficient and Its Relation to Impeller Shape . . . . .	263
§60. Relation Between Speed Coefficient and Pump Efficiency. . . . .	265
§61. Calculations for Pump Scroll Chamber. . . . .	271
§62. Cavitation Calculations for Centrifugal Pumps (Method of S.S. Rudnev) . . . . .	273
§63. Determination of the Altitude Capability of Aircraft Fuel Systems with Centrifugal Booster Pumps . . . . .	278
§64. Selection of Pump Type. Features of Centrifugal Pumps Used in Aviation and Rocket Engineering . . . . .	282
§65. Basic Information on Turbulence Pumps . . . . .	287
Chapter XIII. Displacement Pumps . . . . .	292
§66. Basic Concepts. Piston Pumps. . . . .	292
§67. Rotor Pumps; Features and Varieties . . . . .	296
§68. Characteristics of Rotor Displacement Pumps . . . . .	310
§69. Fundamentals of the General Theory of Rotor Pumps and Hydraulic Motors. . . . .	314
Chapter XIV. Hydraulic Drives and Hydraulic Transmissions. . . . .	323
§70. Reciprocating Hydraulic Transmissions . . . . .	323
§71. Hydraulic Servo Drive (Hydraulic Booster) . . . . .	330
§72. Basic Subunits of Aircraft Hydraulic Systems. . . . .	339
§73. Rotary Displacement-Type Hydraulic Transmissions. . . . .	355
§74. Hydraulic-Mechanical Transmissions. . . . .	360
§75. Vane-Wheel Hydraulic Transmissions (Hydrodynamic Transmissions). . . . .	363
Chapter XV. Fundamentals of the Design of Gas Lines. . . . .	370
§76. Equation of Motion for an Inviscid Gas. . . . .	371
§77. Outflow of Gas Through Holes and Mouthpieces. . . . .	373
§78. Motion of Viscous Gas in Cylindrical Pipe . . . . .	376
§79. Possible Problems in the Synthesis of Gas Lines . . . . .	383
References . . . . .	391

ANNOTATION

This volume sets forth the laws of hydrostatics, the general equations of hydraulics, fluid-flow regimes in pipes, and the laws of outflow of fluids through holes and mouthpieces; it presents methods for hydraulic design of pipes.

Special sections are devoted to aviation-type centrifugal and displacement pumps, hydraulic drives and transmissions.

It is designed as a textbook for students in the aviation higher educational institutes and some of the mechanical-engineering schools.

There are 6 tables, 263 illustrations, and 36 source citations.

Reviewer: Prof. N.Ya. Fabrikant

Scientific Editor: Docent A.S. Shifrin, Candidate  
of Technical Sciences

## FOREWORD

The present textbook is based on the author's book Hydraulics (Voenizdat, 1960). The present edition has been extensively revised and expanded with new material.

The program of a hydraulics course may have a more or less specific slant, depending on the profile of the aviation-engineering school: design, production engineering, or operations; it may also vary in accordance with the specialization of the faculty.

It is the author's feeling that the present textbook can be used in all of the aviation schools.

\* In addition to the fundamentals of general hydraulics, with which the aviation engineer must be familiar, the text also incorporates the fundamentals of the theory of hydraulic machines (centrifugal and displacement pumps and hydraulic motors) and other hydraulic devices used on aircraft. These units include hydraulic-transmission (hydraulic-drive) systems and their elements (subassemblies of aircraft hydraulic systems).

The fundamentals of mathematical design for gas lines are considered in a special section.

The book casts light on a number of new problems not previously touched upon in student literature on hydraulics. They include laminar flow of a fluid with large pressure gradients, improvement of the laws of turbulent flow, outflow through nozzles, the elements of hydraulic automation (chokes, valves, flap nozzles, and pressure and flowrate regulators), motion of fluid under conditions of weightlessness, the classification, general

properties, and theoretical fundamentals of rotor displacement pumps and hydraulic motors, the hydraulic servodrives, hydro-mechanical transmissions, and, finally, a method for the mathematical design of gas lines that can be used for arbitrary dimensions and arbitrary subsonic velocities with adiabatic or isothermal flow.

Where the book sets forth theoretical fundamentals of hydraulics, the basic relationships for fluid equilibrium and for the case of motion of an ideal incompressible fluid (the Bernoulli equation) are derived by two methods - a simplified method that follows directly from the physics of the phenomenon and a more rigorous method in which the general Euler differential equations are integrated.

In setting forth the material, the author has made an effort to graduate it from the simple to the complicated, from the particular to the general, and from the ideal to the real.

Professors N.Ya. Fabrikant, K.F. Kosourov and S.S. Rudnev helped review the manuscript. Docent A.S. Shifrin, Candidate of Technical Sciences, performed yeoman service in the scientific editing of the manuscript. Further, the author was assisted with specific problems in preparation of the manuscript for the printer by Doctor of Technical Sciences V.N. Prokof'yev, Candidates of Technical Sciences V.V. Shul'gin and B.Ya. Shumyatskiy, and Engineer B.P. Borisov.

The author extends his heartfelt thanks to the above persons.

## CHAPTER I

### INTRODUCTION

#### §1. HYDRAULICS AND ITS USE ON AIRCRAFT

The division of mechanics that studies the equilibrium and motion of fluids and the dynamic interaction between fluids and bodies around which they flow or surfaces that restrict them is known as hydromechanics.

Hydraulics is one of the applied branches of hydromechanics. Usually, hydraulics is defined as the science of the laws of fluid equilibrium and motion and the application of these laws to the solution of practical problems. This definition requires a certain amount of refinement and qualification.

Hydraulics is concerned chiefly with fluid flows that are bounded and directed by solid walls, i.e., flows in open and closed channels. In our terminology, "channel" will include all walls that limit and direct the flow, and hence not only the channels of rivers, canals, and millraces, but also the various kinds of pipes, mouthpieces, and elements of hydraulic machines and other devices in which a fluid flows.

Thus, we might say that hydraulics is basically concerned with internal fluid flows and solves the so-called "internal" problem, as distinguished from the "external" problem, which involves flow of a continuous medium around bodies, such as occurs when a solid body moves in a liquid or gas (air). This "external" problem is examined in aerohydromechanics and has been

developed essentially in connection with the requirements of aeronautical and marine engineering.

We should note that the term "fluid" is often understood in a broader sense in hydrodynamics than we are used to in our everyday life. The "fluid" concept includes all bodies that have the property of fluidity, i.e., the ability to change shape without limit when acted upon by infinitesimally small forces. Thus, the notion includes both ordinary "dropping" liquids and gases.

The former are distinguished by the fact that they acquire spherical shape in small volumes and usually form a free surface in large ones. An important property of dropping fluids is that they undergo negligibly small changes in volume under a change in pressure, and are therefore usually regarded as incompressible. Gases, on the other hand, are capable of very large volume reduction under pressure and unlimited expansion in the absence of pressure, i.e., they are highly compressible.

In spite of this difference, the laws of motion of dropping fluids and gases can be considered identical under certain conditions. Fundamental among these conditions is a small value of the flow rate of the gas by comparison with the velocity of sound in it.

Hydraulics is concerned chiefly with the motions of dropping fluids and regards them as incompressible in the overwhelming majority of cases. As for internal flows of gas, they come into the jurisdiction of hydraulics only when their flow velocities are much smaller than the speed of sound and, consequently, the compressibility of the gas can be disregarded. Such cases of gas motion are encountered quite frequently in practice. An example is the flow of air in ventilation systems and certain other gas lines.

In the exposition that follows, the term "fluid" will mean a dropping liquid or a gas when the latter can be regarded as incompressible.

Investigation of the motion of liquids - not to mention gases - is a more difficult and complex problem than study of the motion of an absolutely rigid body. Galileo himself said that it was much easier to study the motion of celestial bodies infinitely distant from us than to study the motion of water in a rivulet at our feet. This becomes understandable when we remember that in the mechanics of the solid body we have a system of rigidly interconnected particles, while in fluid mechanics we are dealing with a medium that consists of a multitude of particles that have mobility with respect to one another.

Owing to these difficulties, the historical development of fluid mechanics took place in two different directions.

The first trend - exact mathematical analysis based on the laws of mechanics - was purely theoretical. It led to the

creation of theoretical hydromechanics, a science that long remained an independent discipline with no direct relation to experiment. This method is a highly seductive and at the same time highly effective scientific research instrument. However, it does not always answer the problems advanced by practice.

As a result, another science concerned with the motion of liquids arose out of the bread-and-butter problems of practical human engineering activity - hydraulics, in which the investigators took the second approach, that of extensive recourse to experiment and the accumulation of experimental data for use in engineering practice. In the early phase of its development, hydraulics was a purely empirical science. Now, however, the methods of theoretical hydrodynamics are coming into increasing use wherever possible and expedient for the solution of specific problems, and the theoretical branch is beginning to resort more and more often to experiment as a criterion for testing its conclusions. Thus, the distinction in the methods of these two sciences is gradually disappearing and the boundary between them is being effaced.

The method used in contemporary hydraulics to investigate fluid motions consists in the following. First, the phenomena to be studied are simplified and idealized and the laws of theoretical mechanics are applied to them. The results are then compared with experimental data, the extent of the discrepancies determined, and the theoretical conclusions and formulas improved and corrected to adapt them for practical use.

A whole series of phenomena that are so complex as to resist theoretical analysis quite stubbornly are investigated in hydraulics by purely experimental means, and the results of this research are presented in the form of empirical formulas. Hydraulics is therefore a semiempirical science.

It gives us methods for the mathematical design and construction engineering of a wide variety of hydraulic structures (dams, canals, sluices, pipelines to carry all types of liquids), hydraulic machines (pumps, hydraulic turbines, hydraulic transmissions), and other hydraulic devices that are used in many branches of engineering.

Hydraulics is especially important in mechanical engineering. Thus, at any modern machinery plant, we find the hydraulic drive in widespread use on metalcutting machine tools and forging-press equipment, along with applications of hydraulics in founding and plastics molding, etc.

One of the distinctive features of contemporary aeronautical engineering is the steadily increasing role of various types of equipment on the airplane, including hydraulic equipment - hydraulic transmissions (hydraulic systems), fuel systems, oil systems, air-and-oil shock absorbers, etc.

Aircraft hydraulic-drive systems have become considerably more complicated in recent years and have been made more powerful. While hydraulic transmissions were used on aircraft of the Second World War only to raise and lower landing gear, dozens of functions and more are performed by hydraulic transmissions on contemporary aircraft.

Hydraulic transmissions (hydraulic systems) on the airplane are usually used for flight control (deflection of tail control surfaces and ailerons), raising and lowering landing gear, steering the nose wheel, lowering and retracting flaps and airbrakes, operating wheel brakes, engine control (regulation of intake unit, exhaust nozzle, antisurge devices); control of doors and hatches; rotation of antennas, and so forth. There is a tendency to broaden the field of application of hydraulic transmissions even further on both airplanes and helicopters.

The largest and most crucial hydraulic transmission system - the airplane's hydraulic controls (hydraulic-amplifier or booster system) - is a finely tuned power servosystem on whose proper operation the possibility of flight depends.

The hydraulic drive is used successfully on aircraft as a synchronous-generator drive and thereby helps solve the problem of conversion of aircraft to alternating current with stable frequencies.

The fuel systems of modern jet aircraft have grown, owing to the very high fuel-consumption rates, into complex systems consisting of a number of tanks, a whole network of pipelines, a number of main and auxiliary pumps, and various other accessories.

The fuel-supply systems of liquid rocket engines, which consist basically of combustion chambers and these fuel systems, are particularly intricate and, at the same time, powerful. In turn, the fuel system is usually made up of two subsystems: one for supplying the fuel (for example, kerosene), and the other for oxidizer (for example, nitric acid or liquid oxygen). The two systems are coordinated by an automatic device that ensures supply of the propellants in the proper proportions with the engine operating under various conditions.

The lubricating systems of turbojet [TJE](TPA) and propjet [PJE](TBA) engines are crucially important hydraulic systems, each containing a number of pumps and special hydraulic accessories to cool and filter the oil, separate out water, etc.

Stationary and mobile fueling systems at airports are also hydraulic systems with high-delivery pumping units. And as for in-flight refueling of aircraft, successful solution of this problem is determined to a substantial degree by the use of adequately powerful and, at the same time, compact hydraulic equipment.

This by no means complete list shows how extensively various types of hydraulic devices are used in aeronautical engineering.

To understand the operation of these systems correctly and use them knowledgeably, to be able to diagnose trouble and find ways to correct it, and the more so to design and calculate these systems, it is necessary to have appropriate preparation in the field of hydraulics.

## §2. FORCES ACTING ON A FLUID. PRESSURE IN A FLUID

Hydraulics, and hydromechanics in general, dissociate themselves from the molecular structure of matter and treat fluids as continuous media that fill space without gaps and vacancies, i.e., as continua.



Fig. 1. Resolution of surface force into two components.

Because of the fluidity of the fluid (the mobility of its particles), concentrated forces cannot act in it, but only forces that are distributed continuously through its volume (mass) or over its surface. As a consequence, forces that act upon subject volumes of fluid and are external forces with respect to it are classified as mass (volume) and surface forces.

Mass forces are proportional to the mass of the fluid body, or, for homogeneous fluids, to the volume of the fluid. They include first the force of gravity and then the inertial forces of translational motion, which act on a fluid at relative rest in an accelerating container or one in relative motion in a channel that is subject to some form of acceleration.

The mass forces also include forces that are introduced by the D'Alembert principle in writing equations of fluid motion.

Surface forces are distributed continuously over the surface of a fluid and are proportional to the area of this surface (assuming uniform distribution). These forces are governed by direct action of neighboring volumes of fluid on a given volume or by the action of other bodies (solid or gaseous) that are in contact with the fluid body in question.

In the general case, the surface force  $\Delta R$  acting on an area  $\Delta S$  is directed at a certain angle to it, and  $\Delta R$  can be resolved into normal  $\Delta P$  and tangential  $\Delta T$  components (Fig. 1). The former is known as the pressure force if it is directed into the volume, while the latter is the force of friction.

In hydromechanics, both mass and surface forces are usually treated in the form of unit forces, i.e., forces referred to appropriate units. Mass forces are referred to a mass unit and surface forces to a unit area.

Since any mass force is equal to the product of a mass by an acceleration, it follows that the unit mass force is numerically equal to the corresponding acceleration.

The unit surface force, which is known as the stress of surface force, like the total force, is decomposed into normal and tangential stresses.

The normal stress, i.e., the stress of the pressure force, is known as the hydromechanical (or, for the case of rest, hydrostatic) pressure or simply the pressure, and is denoted by the letter  $p$ .

If the pressure force  $\Delta P$  is uniformly distributed over elementary area  $\Delta S$  or it is necessary to find the average value of a hydromechanical pressure, the latter is determined by the formula

$$p = \frac{\Delta P}{\Delta S}. \quad (1.1)$$

Generally, however, the hydromechanical pressure at a given point is equal to the limit to which the ratio of the pressure force to the area on which it acts tends as the area tends to zero, i.e., as the area contracts to a point.

$$p = \lim_{\Delta S \rightarrow 0} \frac{\Delta P}{\Delta S}. \quad (1.2)$$

If the pressure  $p$  is reckoned from zero, it is called absolute pressure, but if it is reckoned from atmospheric, it is known as the excess or gage pressure. Consequently, the absolute pressure is equal to the atmospheric pressure plus the excess pressure, i.e.,

$$p_{abs} = p_A + p_{ex}$$

The unit of pressure in the International System (SI) is the uniformly distributed pressure at which a force of 1 Newton acts on an area of 1 m<sup>2</sup>, i.e., 1 N/m<sup>2</sup>. The following derived units are also used: the decanewton per m<sup>2</sup> (daN/m<sup>2</sup>), the kilonewton per m<sup>2</sup> (kN/m<sup>2</sup>), and the meganewton per m<sup>2</sup> (MN/m<sup>2</sup>). Thus, we have

$$1 \text{ N/m}^2 = 10^{-1} \text{ daN/m}^2 = 10^{-3} \text{ kN/m}^2 = 10^{-6} \text{ MN/m}^2.$$

The MKGFS (meter, kilogram-force, second) system, in which the unit of pressure is 1 kgf/cm<sup>2</sup>, is still used in engineering. A nonsystem unit is also widely used - the technical atmosphere, which is equal to one kilogram-force per cm<sup>2</sup>, i.e.,

$$1 \text{ atm} = 1 \text{ kgf/cm}^2 = 10 \text{ 000 kgf/m}^2.$$

The relation between the pressure units in the SI and MKGFS systems is as follows:

$$1 \text{ N/m}^2 = 0.102 \text{ kgf/m}^2 \text{ or } 1 \text{ kgf/m}^2 = 9.81 \text{ N/m}^2.$$

The tangential stress in the fluid, i.e., the frictional stress, is denoted by  $\tau$  and expressed, like the pressure, as a limit:

$$\tau = \lim_{\Delta S \rightarrow 0} \frac{\Delta T}{\Delta S}, \quad (1.3)$$

while the units used for it are the same as those for pressure.

### §3. BASIC PROPERTIES OF DROPPING FLUIDS. FLUIDS USED IN AVIATION AND ROCKET ENGINEERING

Let us examine the basic physical properties of dropping fluids, with which hydromechanics is chiefly concerned.

The fundamental mechanical characteristic of a fluid is its density.

The density  $\rho$  is the mass of the fluid enclosed in a unit volume (for a homogeneous fluid), i.e.,

$$\rho = M/W \text{ [kg/m}^3 \text{] or [kgf}\cdot\text{s}^2/\text{m}^4 \text{]}, \quad (1.4)$$

where  $M$  is the mass of fluid in volume  $W$ .

We shall call the weight of a unit volume of fluid its specific or volume weight  $\gamma$ , i.e.,

$$\gamma = G/w \text{ [N/m}^3 \text{] or [kgf/m}^3 \text{]}, \quad (1.5)$$

where  $G$  is the weight of the fluid and  $W$  is its volume.

Thus, specific weight is a dimensional quantity, and its numerical value depends on the units in which it is expressed.

Thus, we have for water at  $4^\circ\text{C}$

$$\gamma = 1000 \text{ kgf/m}^3 = 0.001 \text{ kgf/cm}^3 = 9.81 \cdot 10^3 \text{ N/m}^3.$$

The relation between the specific weight  $\gamma$  and density  $\rho$  is easily found when we remember that  $G = gM$ ; we have

$$\rho = \frac{G}{gW} = \frac{\gamma}{g}. \quad (1.6)$$

If the fluid is inhomogeneous, Formulas (1.4) and (1.5) define only the average value of specific weight or density in a given volume. To determine the true  $\gamma$  or  $\rho$  at a given point, it is necessary to examine a vanishing volume and find the limit of the appropriate ratio.

The notion of the specific gravity  $\delta$  of a fluid is also in use; this is the ratio of the specific weight of the fluid to that of water at  $4^\circ\text{C}$ , i.e.,

$$\delta = \frac{\gamma_w}{\gamma_{\text{water}}} \quad (1.7)$$

Let us examine the following physical properties of dropping fluids: compressibility, thermal expansion, tensile strength, surface, tension, viscosity, and volatility.

1. Compressibility or the ability of a fluid to change its volume under pressure is characterized by the volumetric coefficient of compression  $\beta_p$ , which represents the relative volume change per unit of pressure, i.e.,

$$\beta_p = -\frac{1}{W_0} \frac{\Delta W}{\Delta p} \cdot [\text{m}^2/\text{N}] \text{ or } [\text{cm}^2/\text{kgf}]. \quad (1.8)$$

The minus sign in the formula is explained by the fact that a negative increment (i.e., a decrease) in the volume  $W$  corresponds to a positive increment of the pressure  $p$ .

Considering the pressure increment  $\Delta p = p - p_0$  and the volume change  $\Delta W = W - W_0$ , we obtain from Expression (1.8)

$$W = W_0(1 - \beta_p \Delta p)$$

or, applying (1.4),

$$\rho = \frac{\rho_0}{1 - \beta_p \Delta p} \quad (1.9)$$

where  $\rho$  and  $\rho_0$  are the density values at the pressures  $p$  and  $p_0$ .

The reciprocal of the coefficient  $\beta_p$  is the bulk elastic modulus  $K$ .

Expressing volume in terms of density and converting from finite differences to differentials, we obtain instead of (1.8)

$$K = -\frac{dp}{\rho^2 \left(\frac{1}{\rho}\right)} = \rho \frac{dp}{d\rho} \quad (1.10')$$

or

$$\frac{K}{\rho} = \frac{dp}{d\rho} = a^2, \quad (1.10)$$

where  $a$  is the velocity of propagation of longitudinal waves in an elastic medium, and is equal to the speed of sound (see physics textbooks).

For dropping fluids, the modulus  $K$  increases somewhat with increasing temperature and pressure. For water, it averages 20 000 kgf/cm<sup>2</sup>. Consequently, on a 1 kgf/cm<sup>2</sup> pressure increase, the volume of water decreases by 1/20 000, i.e., most insignificantly. The elastic moduli of other dropping fluids are also of the same order (see Table 1).

It follows from (1.9) that the density of AMG-1 fluid increases by only 3% when the pressure is raised to 400 kgf/cm<sup>2</sup>.

In most cases, therefore, dropping fluids may be regarded as practically incompressible, i.e., their densities  $\rho$  as independent of pressure. But at very high pressures and in elastic vibrations, the compressibility of fluids must be taken into account.

2. Thermal expansion is characterized by the coefficient of volume expansion  $\beta_t$ , which represents the relative change in volume on a 1°C change in the temperature  $t$ :

$$\beta_t = \frac{1}{W_0} \frac{\Delta W}{\Delta t} \quad (1.11)$$

Considering that  $\Delta W = W - W_0$ , we have from the above equation

$$W = W_0(1 + \beta_t \Delta t),$$

and, applying (1.4), we obtain

$$\rho = \frac{\rho_0}{1 + \beta_t \Delta t} \quad (1.12)$$

where  $\rho$  and  $\rho_0$  are the values of density at temperatures  $t$  and  $t_0$ .

For water, the coefficient  $\beta_t$  increases from  $14 \cdot 10^{-6}$  to  $700 \cdot 10^{-6}$  as the pressure is raised from 1 to 100 kgf/cm<sup>2</sup> or the temperature from 1 to 100°C. The coefficient  $\beta_t$  for AMG-10 aviation fluid may be assumed to average  $800 \cdot 10^{-6}$  in the pressure range from 1 to 150 kgf/cm<sup>2</sup>.

3. According to molecular theory, tensile strength may be quite considerable in dropping fluids - up to 10 000 kgf/cm<sup>2</sup>. Ephemeral tensile stresses of up to 230-280 kgf/cm<sup>2</sup> have been obtained experimentally in thoroughly purified and degassed water. However, technically pure liquids, which contain suspended solid particles and minute gas bubbles, do not withstand even insignificant tensile stresses. We shall therefore assume henceforth that tensile stresses are impossible in dropping fluids.

4. Surface tension forces act on the surface of a fluid, tending to impart a spherical shape to the volume of fluid and giving rise to a certain additional pressure in the fluid. However, this pressure makes its presence felt only in small

volumes. In small-diameter pipes, this additional pressure causes the level to rise above (or drop below) the normal level of the fluid in what is known as the capillary effect.

The height  $h$  to which fluid rises in a glass tube of diameter  $d$  is determined by the formula

$$h = \frac{k}{d} [\text{mm}],$$

where  $k$  has the following values in  $\text{mm}^2$ : +30 for water, -14 for mercury, and +12 for alcohol.

The capillary effect must be dealt with when glass tubes are used in instruments to measure pressure and in certain cases of fluid outflow. Surface tension becomes a major factor in a weightless fluid (see §44).

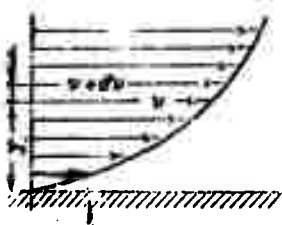


Fig. 2. Velocity profile in flow of viscous fluid along a wall.

5. Viscosity is the property of a fluid to resist shear or slip between its layers. It manifests in the appearance of tangential stresses in the fluid under certain conditions. Viscosity is the opposite of fluidity; more viscous fluids (glycerine, lubricating oils, etc.) are less fluid and vice versa.

When a viscous fluid flows along a solid wall, viscosity decelerates the flow (Fig. 2). The rate of motion  $v$  of the layers decreases with decreasing distance  $y$  from the wall, down to  $v = 0$  at  $y = 0$ , and slip, which is accompanied by the appearance of tangential (frictional) stresses, takes place between layers.

According to a hypothesis first advanced by I. Newton in 1686 and then confirmed experimentally by Prof. N.P. Petrov in 1882, the tangential stress in a fluid depends on the kind of fluid and the type of flow and varies in laminar flow in direct proportion to the so-called transverse velocity gradient, i.e., (for an infinite flat wall),

$$\tau = \mu \frac{dv}{dy}, \quad (1.14)$$

where  $\mu$  is the fluid's dynamic coefficient of viscosity and  $dv$  is the velocity increment corresponding to the coordinate increment  $dy$ .

The transverse velocity gradient  $dv/dy$  defines the change in viscosity per unit length in direction  $y$  and, consequently, characterizes the intensity of shear between layers of the fluid at a given point. If the wall is not infinite, i.e., if there is also a velocity gradient in the direction normal to the plane of the

figure (see Fig. 2), the total derivative in Formula (1.14) must be replaced by the partial derivative  $\partial v/\partial y$ .

In the case of constant tangential stress over the surface area  $S$ , the total tangential force (friction) acting on this surface is

$$T = \mu \frac{dv}{dy} S. \quad (1.15)$$

To determine the dimensions of the viscosity coefficient, let us solve Eq. (1.14) for  $\mu$ . We obtain

$$\mu = \tau(dy/dv) [\text{N}\cdot\text{s}/\text{m}^2] \text{ or } [\text{kgf}\cdot\text{s}/\text{m}^2].$$

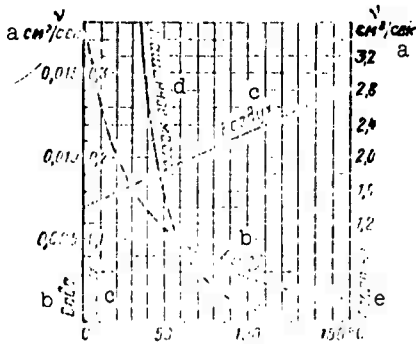


Fig. 3. Diagram of viscosity coefficient  $\nu$  as a function of temperature.  
KEY: (a)  $\text{cm}^2/\text{s}$ ; (b) water; (c) air; (d) machine oil; (e) oil.

In the CGS system, the viscosity unit is 1 poise = 1 dyne  $\times$   $\text{s}/\text{cm}^2$ .

Since 1 dyne =  $10^{-5}$  N =  $1.02 \cdot 10^{-6}$  kgf, and  $1 \text{ m}^2 = 10^4 \text{ cm}^2$ , we have 1 poise =  $0.1 \text{ N}\cdot\text{s}/\text{m}^2 = 1/98.1 \text{ kgf}\cdot\text{s}/\text{m}^2$ .

In addition to the viscosity coefficient  $\mu$ , the so-called kinematic coefficient of viscosity  $\nu$  is also used; it equals

$$\nu = \frac{\mu}{\rho} [\text{m}^2/\text{s}]. \quad (1.16)$$

The dimensions of this coefficient contain neither force nor mass, and this makes it easier to convert from one system of units to another.

The customary unit of measurement of the kinematic viscosity coefficient is 1 stoke =  $1 \text{ cm}^2/\text{s}$ . One one-hundredth of a stoke is a centistoke.

The viscosities of dropping fluids depend heavily on temperature, diminishing as the latter increases (Fig. 3). As for gases, however, their viscosities, to the contrary, rise with rising temperature. This is explained by the difference in the very nature of viscosity in liquids and gases.

In liquids, the molecules are much closer to one another than in gases, and viscosity is produced by forces of molecular cohesion. These forces diminish with rising temperature, so that viscosity drops.

In gases, viscosity is governed chiefly by disordered thermal motion of the molecules, whose intensity increases with

TABLE 1. Basic Physical Properties of Certain Fluids used in Aviation and Rocket Engineering

a Название жидкости	b	c Вязкость $\nu$ в сантистоксах при температуре $t$					d Упругости паров $P_t$ мм рт. ст.				e Объемный модуль упругости $K$ кг/см <sup>2</sup>	
		+70° C	+50° C	+20° C	0°	-20° C	-50° C	+60° C	+40° C	+20° C		
		t										
f Бензин авиационный Б95/130	0,750	—	0,54	0,73	0,93	1,26	2,60	—	195	50	13300	
g Керосин Т-1	0,899— 0,850	1,2	1,5	2,5	4,0	8,0	25	59	27	11,5	13000	
h Керосин Т-2	0,775	—	—	1,05	2,0	—	5,5	—	100	—	13000	
i Масло НК-20	0,895	65	185	1100	10160	J Значает					—	
k Масло МК-4	0,895	—	8,3	30	—	498	—	—	—	—	—	
l Вязкость пара при температуре кипения	0,850	7,5	10	15	42	130	1250	—	—	—	13300	
m Аэрозоль керосин-1	0,510	0,30	0,58	0,58	0,70	0,83	1,72	355	156	60	—	
n Этанолный спирт	0,790	—	—	1,32	—	—	6,5	352	135	44	—	
o Тетраэтил свинец	1,34	—	—	0,95	1,42	—	—	61,4	56,7	46,4	—	
p Жидкий кислород	1,15— 1,25	t										
		-175° C	-152° C	-132° C	-100° C	-200° C	-204° C	f	-140° C	-160° C	-180° C	-200° C
		q										
		0,125	0,170	0,193	0,257	0,237	0,237	0,237	0,237	0,237	0,237	0,237
		r										
		21	7	7	7	7	7	7	7	7	7	

KEY: (a) fluid; (b) specific gravity; (c) viscosity  $\nu$  in centistokes at temperature  $t$  of; (d) vapor pressure  $P_t$ , mmHg; (e) bulk modulus of elasticity  $K$ , kgf/cm<sup>2</sup>; (f) aviation gasoline B95/130; (g) kerosene T-1; (h) kerosene T-2; (i) oil MS-20; (j) solidifies; (k) oil MK-8; (l) AMG-10 hydraulic fluid; (m) nitric acid (98%); (n) ethyl alcohol; (o) hydrogen peroxide (80%); (p) liquid oxygen; (q)  $\nu$ , cSt; (r)  $P_t$ , atm.

temperature. As a result, gases become more viscous with increasing temperature.

The influence of temperature on the viscosity of fluids can be evaluated by the formula

$$\mu = \mu_0 e^{-\lambda(t-t_0)}, \quad (1.17)$$

where  $\mu$  and  $\mu_0$  are the viscosity values at temperatures  $t$  and  $t_0$ , and  $\lambda$  is a coefficient whose value varies from 0.023-0.033 for oils; for AMG-10 aviation fluid,  $\lambda = 0.028$  is assumed.

The viscosity of fluids also depends on pressure, but this relationship is manifested substantially only with relatively large pressure changes. With increasing pressure, the viscosities of most fluids rise, as we see from the formula

$$\mu = \mu_0 e^{\alpha(p-p_0)}, \quad (1.18)$$

where  $\mu$  and  $\mu_0$  are the values of viscosity at pressures  $p$  and  $p_0$ , and  $\alpha$  is a coefficient whose value varies in the range 0.0023-0.003 for oils.

It follows from the law of friction (1.14) that a frictional stress is possible only in a moving fluid, i.e., the viscosity of a fluid is evident only when it flows. We shall assume the tangential stresses in a quiescent fluid to be zero.<sup>1</sup>

All this leads us to the conclusion that friction in fluids, which is governed by viscosity, is subject to a law that differs fundamentally from the law of friction for solids.

6. Volatility is inherent to all dropping fluids, but the rates of evaporation differ for different fluids and depend on the conditions prevailing for it.

One of the indicators that characterize the volatility of a fluid is its boiling point at standard atmospheric pressure. The higher the boiling point, the lower the volatility of the fluid. In aircraft hydraulic systems, standard atmospheric pressure is only a particular case; usually, it is necessary to deal with vaporization and sometimes even boiling of fluids in closed volumes at various temperatures and pressures. Hence the saturation vapor pressure  $p_1$ , given as a function of temperature, must be regarded as a more complete characteristic of volatility. The higher the saturation vapor pressure at a given temperature, the higher the volatility of the fluid. The pressure  $p_1$  increases with temperature, but to different degrees in different fluids.

While the  $p_1 = f(t)$  relationship is quite definite for a given simple fluid, the pressure  $p_t$  depends in complex fluids, i.e., multicomponent mixtures such as gasoline, etc., not only on

<sup>1</sup>See page 15 for footnote.

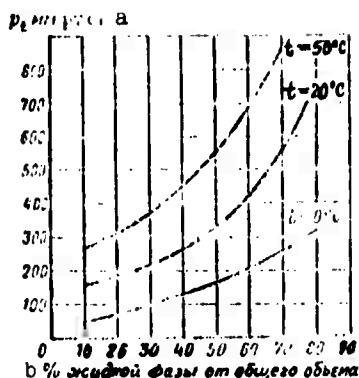


Fig. 4. Vapor pressure of gasoline as a function of phase ratio and temperature.

KEY: (a) mmHg; (b) % of total volume occupied by liquid phase.

their physicochemical properties and the temperature, but also on the proportions by volume of the liquid and vapor phases. The saturation vapor pressure increases with the part of the volume occupied by the liquid phase. By way of example, Fig. 4 shows the saturation vapor pressure of gasoline as a function of the proportions of liquid and vapor phases for three temperatures.

The basic physical properties of certain fluids used in aviation and rocket engineering are given in Table 1.

**Footnote**

Manu-  
script  
page

13

<sup>1</sup>There are certain so-called anomalous or nonnewtonian fluids (suspensions, colloids), in which tangential stresses are possible even at rest and the viscosity coefficient is found to depend on flow velocity.

### Symbol List

Manu- script page	Symbol	English equivalent	
6	абс	abs	absolute
6	изб	izb	excess
8	ж	zh	fluid
8	вод	vod	water

## C H A P T E R    I I

### FUNDAMENTALS OF HYDROSTATICS

#### §4. PROPERTIES OF HYDROSTATIC PRESSURE

As we noted above, only one type of stress is possible in a fluid at rest: compressive stress, i.e., hydrostatic pressure.

The following two properties of hydrostatic pressure in a fluid must be remembered:

1. On the outer surface of the fluid, hydrostatic pressure is always directed along normals into the volume of fluid under consideration.

This property follows directly from the definition of pressure as the stress of a normal compressive force (see §2).

The external surfaces of a fluid should be understood as including not only the interface between it and the environment, but also the surfaces of elementary volumes that we abstract from the total volume of fluid.

2. At any point inside a fluid, the hydrostatic pressure is the same in all directions, i.e., it does not depend on the inclination angle of the elementary area on which it acts at a particular point.

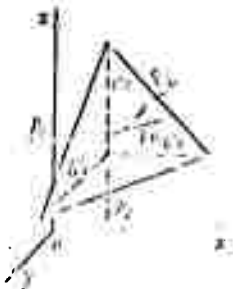


Fig. 5. Illustrating discussion of properties of hydrostatic pressure.

To demonstrate this property, let us isolate an elementary volume in an immobile fluid in the form of a right tetrahedron with sides parallel to the coordinate axes and equalling  $dx$ ,  $dy$ , and  $dz$ , respectively (Fig. 5).

Let a unit mass force whose components equal  $X$ ,  $Y$ , and  $Z$  act on the fluid in the neighborhood of our chosen volume.

Let us denote by  $p_x$  the hydrostatic pressure acting on the face normal to the  $ox$ -axis, by  $p_y$  the pressure on the face normal to the  $oy$ -axis, and so forth. The hydrostatic pressure acting on the inclined face will be denoted by  $p_n$  and the area of this face by  $dS$ . All of these pressures are directed along normals to the corresponding surfaces.

Let us first write the equilibrium equation of our selected fluid volume in the direction of the  $ox$ -axis.

The projection of the pressure forces onto the  $ox$ -axis is

$$p_x \frac{1}{2} dy dz - p_n dS \cos(\hat{n}, x).$$

The mass of the tetrahedron is equal to the product of its volume by its density, i.e.,  $\frac{1}{6} dx dy dz \rho$ ; consequently, the mass force acting on the tetrahedron along the  $ox$ -axis equals

$$\frac{1}{6} dx dy dz \rho X.$$

The equilibrium equation of the tetrahedron is written in the form

$$\frac{1}{2} dy dz p_x - p_n dS \cos(\hat{n}, x) + \frac{1}{6} dx dy dz \rho X = 0.$$

We divide this equation term by term by the area  $\frac{1}{2} dy dz$ , which is the projection of the inclined face  $dS$  onto the  $yOz$  plane and is therefore equal to

$$\frac{1}{2} dy dz - dS \cos(\hat{n}, x).$$

We have

$$p_x - p_n + \frac{1}{3} dx X = 0.$$

As the dimensions of the tetrahedron tend to zero, the last term of the equation, which contains the multiplier  $dx$ , will also tend to zero, but the pressures  $p_x$  and  $p_n$  will remain nonzero quantities.

We therefore obtain at the limit

$$p_x - p_n = 0,$$

or

$$p_x = p_n.$$

Writing the equations of equilibrium along the Oy and Ox axes in the same way, we obtain by similar reasoning

$$p_y = p_n, p_z = p_n$$

or

$$p_x = p_y = p_z = p_n. \quad (2.1)$$

Since the dimensions  $d_x$ ,  $d_y$ , and  $d_z$  of the tetrahedron were taken arbitrarily, the slope of area  $dS$  is also arbitrary and, consequently, the pressure at the point to which the tetrahedron shrinks at the limit will be the same in all directions.

This proposition can also be proven easily on the basis of strength-of-materials formulas for the stresses in compression along two and three mutually perpendicular directions.<sup>1</sup> For this it is sufficient to set the tangential stress equal to zero in the above formulas to obtain

$$\sigma_x = \sigma_y = \sigma_z = -p.$$

This property of hydrostatic pressure in an immobile fluid also applies for an inviscid fluid in motion. In motion of a viscous fluid, however, tangential stresses arise, with the result that hydromechanical pressure does not, strictly speaking, exhibit this property in a viscous fluid.

## §5. FUNDAMENTAL EQUATION OF HYDROSTATICS

We shall examine the fundamental case of fluid equilibrium in which gravity is the only mass force acting on the fluid, and derive for this case an equation with which we can find the hydrostatic pressure at any point in a subject volume of fluid. As we know, the free surface of the fluid in this case is a horizontal plane.

Suppose that the fluid occupies a container (Fig. 6) and that a pressure  $p_0$  acts on its exposed surface. Let us find the hydrostatic pressure  $p$  at an arbitrarily chosen point M, which is situated at depth  $h$ .

With point M as its center, let us take an elementary horizontal unit area  $dS$  and construct a vertical cylindrical volume of height  $h$  on it. We shall examine the equilibrium condition of

<sup>1</sup>See page 36 for footnote.

this fluid volume in isolation from the total mass of fluid. The pressure of the fluid on the lower base of the cylinder will now be an external pressure and will be directed along normals into the volume, i.e., upward.

Let us write the sum of all forces acting on this volume in the vertical direction. We shall have

$$p dS - p_0 dS - \gamma h dS = 0,$$

where the last term is the weight of the fluid in our volume. The pressure forces on the sides of the cylinder do not appear in the equation, since they are normal to this surface.

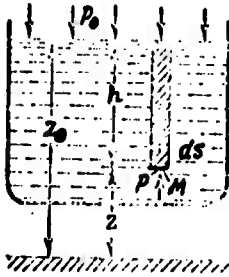


Fig. 6. Illustrating derivation of fundamental equation of hydrostatics.

Cancelling  $dS$  and regrouping terms,

$$p = p_0 + \gamma h. \quad (2.2)$$

This equation is known as the fundamental equation of hydrostatics; it enables us to compute the pressure at any point on a quiescent fluid. As we see from the equation, this pressure has two components: the pressure on the outer surface of the fluid,  $p_0$ , and the pressure governed by the weight of the superjacent layers of fluid.

The quantity  $p_0$  is the same for all points in the fluid volume; we can therefore say, considering the second property of hydrostatic pressure, that the pressure applied to the outer surface of the fluid is transmitted to all points of this fluid and equally in all directions (Pascal's law).

As we see from (2.2), the fluid pressure rises linearly with increasing depth and is constant at a given depth.

A surface at all of whose points the pressures are the same is called a level surface. In this case, the level surfaces are horizontal planes, and the exposed surface is one of the level surfaces.

Let us select, at an arbitrary height, a horizontal comparison plane from which we shall reckon the  $z$ -coordinate vertically upward. Denoting the coordinate of point  $M$  by  $z$  and the coordinate of the exposed fluid surface by  $z_0$  and substituting  $z_0 - z$  for  $h$  in (2.2),

$$z + \frac{p}{\gamma} = z_0 + \frac{p_0}{\gamma}.$$

But since we took  $M$  arbitrarily, we can state that for the entire volume of immobile fluid under consideration

$$z - \frac{p}{\gamma} = \text{const.} \quad (2.3)$$

The  $z$ -coordinate is known as the level height. The quantity  $p/\gamma$  also has the dimensions of length and is known as the piezometric height. The sum  $z + (p/\gamma)$  is called the hydrostatic head.

Thus, the hydrostatic head is a constant for the entire volume of an immobile fluid.

The same results can be derived more rigorously by integrating the differential equations of equilibrium of the fluid.

### §6. DIFFERENTIAL EQUILIBRIUM EQUATIONS OF A FLUID AND THEIR INTEGRATION FOR THE SIMPLEST CASE

We shall derive the differential equations of equilibrium of a fluid for the general case, in which the fluid is acted upon not only by gravity, but also by other mass forces, such as inertial forces of translational motion in a state of so-called relative rest (see Chapter III).

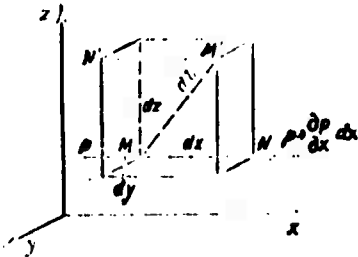


Fig. 7. Illustrating derivation of differential equations of equilibrium of a fluid.

Let us take an arbitrary point  $M$  with the coordinates,  $x$ ,  $y$ , and  $z$ <sup>2</sup> and pressure  $p$  in an immobile fluid. In the fluid, we isolate an elementary volume in the form of a rectangular parallelepiped with its sides parallel to the coordinate axes and equalling respectively  $dx$ ,  $dy$ , and  $dz$ . Let point  $M$  be one of the vertices of the parallelepiped (Fig. 7). Let us examine the equilibrium conditions for our isolated fluid volume. Let the fluid in this volume be acted

upon by a resultant mass force whose components, referred to the mass unit (see §2), are  $X$ ,  $Y$ , and  $Z$ . Then the mass forces acting on the isolated volume in the directions of the coordinate axes will be equal to these components multiplied by the mass of the isolated volume.

The pressure  $p$  is a function of the coordinates,  $x$ ,  $y$ , and  $z$ , but it is the same near point  $M$  on all three faces of the parallelepiped, as follows from the property of hydrostatic pressure proven above (see §4). On passage from point  $M$  to, for example, point  $N$ , only the single coordinate  $x$  changes by an infinitesimal amount  $dx$ , with the result that the function  $p$  acquires an increment equal to the partial differential

$$\frac{\partial p}{\partial x} dx.$$

<sup>2</sup>See page 36 for footnote.

The pressure at point N will therefore be

$$p + \frac{\partial p}{\partial x} dx,$$

where  $\partial p/\partial x$  is the pressure gradient in the direction of the  $x$ -axis near point N.

Examining the pressures at other corresponding points on the face normal to the  $x$ -axis, for example, at points N' and M', we see that these pressures differ by the same (accurate to higher-order infinitesimals) amount, which is equal to

$$p - \left( p + \frac{\partial p}{\partial x} dx \right) = - \frac{\partial p}{\partial x} dx.$$

As a result, the difference in the pressure forces acting on the parallelepiped in the direction of the  $x$ -axis will be equal to the above value multiplied by the area of the face, i.e.,

$$- \frac{\partial p}{\partial x} dx dy dz.$$

The differences of the pressure forces acting on the parallelepiped in the directions of the other two axes are expressed similarly, but in terms of pressure gradients  $\partial p/\partial y$  and  $\partial p/\partial z$ .

Only the indicated mass forces and the pressure-force differences will act upon the isolated parallelepiped. Thus the equilibrium equations of the parallelepiped in the directions of the three coordinate axes will be written

$$\left. \begin{aligned} X \rho dx dy dz - \frac{\partial p}{\partial x} dx dy dz &= 0; \\ Y \rho dx dy dz - \frac{\partial p}{\partial y} dx dy dz &= 0; \\ Z \rho dx dy dz - \frac{\partial p}{\partial z} dx dy dz &= 0. \end{aligned} \right\} \quad (2.4)$$

We divide these equations by the mass  $\rho dx dy dz$  of the parallelepiped and let  $dx$ ,  $dy$ , and  $dz$  tend to zero as a limit, i.e., let the parallelepiped shrink to the original point M. We then obtain the equations of equilibrium of the fluid referred to point M at the limit:

$$\left. \begin{aligned} X - \frac{1}{\rho} \frac{\partial p}{\partial x} &= 0; \\ Y - \frac{1}{\rho} \frac{\partial p}{\partial y} &= 0; \\ Z - \frac{1}{\rho} \frac{\partial p}{\partial z} &= 0. \end{aligned} \right\} \quad (2.5)$$

The system of differential equations of hydrostatics (2.5) is referred to as the Euler equations.<sup>3</sup>

For practical use, it is helpful to replace equation system (2.5) by a single equivalent equation that does not contain partial derivatives. For this we multiply the first equation of (2.5) by  $dx$ , the second by  $dy$ , and the third by  $dz$  and add all three equations to obtain

$$Xdx + Ydy + Zdz - \frac{1}{\rho} \left( \frac{\partial p}{\partial x} dx + \frac{\partial p}{\partial y} dy + \frac{\partial p}{\partial z} dz \right) = 0. \quad (2.6')$$

The trinomial in the parentheses is the total differential of pressure, i.e., of the function  $p(x, y, z)$ . Equation (2.6') can therefore be rewritten

$$Xdx + Ydy + Zdz - \frac{dp}{\rho} = 0$$

or

$$\rho p = \rho(Xdx + Ydy + Zdz). \quad (2.6)$$

The resulting equation expresses the pressure increment  $dp$  due to changes in the coordinates by  $dx$ ,  $dy$ , and  $dz$  in the most general case of fluid equilibrium.

If we assume that gravity is the only mass force acting on the fluid and direct the  $z$ -axis vertically upward, then  $X = Y = 0$ ,  $Z = -g$ , and instead of Eq. (2.6) we obtain for this fundamental particular case of fluid equilibrium

$$dp = -\rho g dz = -\gamma dz. \quad (2.7)$$

Integration yields

$$p = -\gamma z + C.$$

The constant of integration  $C$  is found from the condition  $z = z_0$  on the exposed surface, at which  $p = p_0$  (see Fig. 6), so that

$$C = p_0 + \gamma z_0.$$

Hence

$$p = p_0 + (z_0 - z)\gamma \quad (2.8')$$

or

$$z + \frac{p}{\gamma} = z_0 + \frac{p_0}{\gamma} = \text{const.} \quad (2.8)$$

Substituting  $h$ , the depth of point  $M$ , for the difference  $z_0 - z$  in Eq. (2.8'), we obtain another form of Relation (2.8):

<sup>3</sup>See page 36 for footnote.

$$p = p_0 + h\gamma.$$

We have arrived at the same fundamental equation of hydrostatics (2.2) and (2.3) that we derived by another method in the preceding section.

Subsequently, we shall examine integration of (2.6) for other cases of fluid equilibrium (see §13).

### §7. PIEZOMETRIC HEIGHT. VACUUM. MEASUREMENT OF PRESSURE

The piezometric height  $p/\gamma$  is the height of a column of a given fluid that corresponds to a given pressure  $p$  (absolute or excess). The piezometric height corresponding to the excess pressure can be read from a so-called piezometer, a rudimentary device for pressure measurement. A piezometer is a vertical glass tube whose upper end is open to the atmosphere, while its lower end is attached to the volume of fluid in which the pressure is to be measured (Fig. 8).

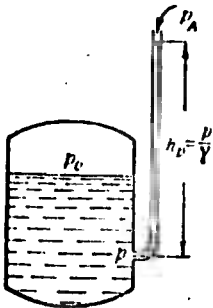


Fig. 8. Piezometer connected to tank.

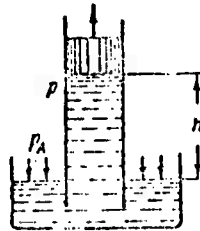


Fig. 9. Suction of fluid by piston.

Applying Formula (2.2) to the fluid in a piezometer, we obtain

$$p_{abs} = p_A + h_p\gamma,$$

where  $p_{abs}$  is the absolute pressure in the fluid at the level of the piezometer connection and  $p_A$  is atmospheric pressure.

Hence the fluid in the piezometer rises to a height

$$h_p = \frac{p_{abs} - p_A}{\gamma} = \frac{p_{ex}}{\gamma}, \quad (2.9)$$

where  $p_{ex}$  is the excess pressure at the same level.

Obviously, if atmospheric pressure acts on the exposed surface of the quiescent fluid, the piezometric height for any point

in the subject volume of fluid is equal to the depth of that point.

Pressures in liquids or gases are often expressed numerically in the form of the corresponding piezometric-height pressure according to (2.9).

For example, one technical atmosphere corresponds to

$$h_1 = \frac{p}{\gamma_{H_2O}} = \frac{10000}{1000} = 10 \text{ mH}_2\text{O};$$

$$h_2 = \frac{p}{\gamma_{Hg}} = \frac{10000}{136000} = 0,735 \text{ mmHg}.$$

If the absolute pressure in a liquid or gas is below atmospheric, we have an underpressure or vacuum. An underpressure or vacuum is expressed as a pressure difference, i.e.,

$$p_v = p_A - p_t$$

or

$$h_v = \frac{p_A - p_t}{\gamma}$$

NOT REPRODUCIBLE

Let us take, for example, a tube with a piston fitted tightly to it, lower the bottom end of the tube into a container of fluid, and gradually raise the piston (Fig. 9). The fluid will follow the piston and rise with it to a certain height  $h$  above the exposed surface, which is under atmospheric pressure. Since the depth of points under the piston is negative with respect to the exposed surface, the absolute pressure of the fluid under the piston will, according to Eq. (2.2), equal

$$p = p_A - \gamma h \tag{2.10}$$

and the vacuum will be

$$p_v = p_A - p = \gamma h$$

or

$$h_v = \frac{p_A - p}{\gamma} = h$$

As the piston rises, the absolute pressure of the fluid under it will decrease. The lower limit for the absolute pressure in the fluid is zero, and the maximum value of the vacuum is numerically equal to atmospheric pressure; consequently, the maximum height to which the fluid can rise in this example, i.e., the maximum "suction" height of the fluid, will be determined from (2.10) if we set  $p = 0$  (or, more precisely,  $p = p_t$ ) in it.

Thus, without consideration of the vapor pressure  $p_t$ , we have

$$h_{\max} = \frac{P \cdot A}{\gamma}$$

Under normal atmospheric pressure (1.033 kgf/cm<sup>2</sup>), the height  $h_{\max}$  is 10.33 m for water, 13.8 m for gasoline ( $\gamma = 750$  kgf/m<sup>3</sup>), 0.760 m for mercury, and so forth.

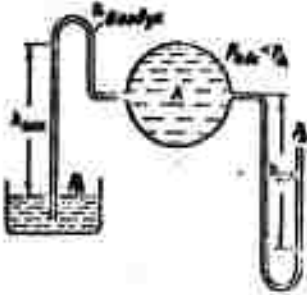


Fig. 10. Elementary vacuum gages.  
KEY: (a) air.

The glass tube, two versions of which are shown in Fig. 10, can serve as an elementary vacuum-measuring device. The vacuum in fluid volume A can be measured either with the U-tube (at the right in the drawing) or with the inverted U-tube, one end of which is immersed in the container with the fluid (on the left in the figure).

In addition to piezometers, various types of manometers, which are classified as liquid and mechanical types, are used to measure fluid and gas pressures under laboratory conditions.

Figure 11 shows diagrams of liquid manometers. The so-called U-tube manometer (Fig. 11a) is a mercury-filled bent glass tube.

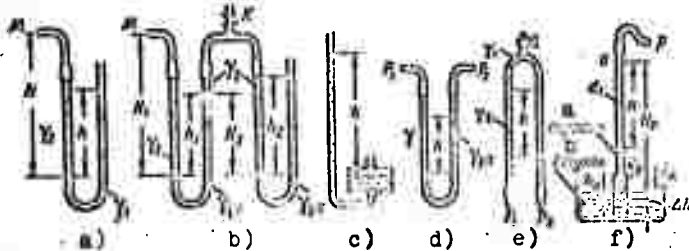


Fig. 11. Diagrams of liquid manometers.  
KEY: (a) kerosene; (b) mercury.

For measurement of low gas pressures, the mercury is replaced by alcohol, water, or sometimes tetrabromoethane ( $\delta = 2.95$ ). If the fluid pressure is being measured at point M and the connecting tube is filled with the same fluid, it is necessary to take the height of the manometer above point M into consideration. Thus, we have for the excess pressure at point M

$$P_M = P_1 N_1 - h_2 N_2$$

If the pressure  $p_M$  to be measured is quite large and the height  $h$  corresponding to it does not diminish within a single U-tube, several U-tubes are connected in series, containing, for example, mercury ( $\gamma_{rt}$ ) and a fluid with a smaller specific weight

$\gamma_2$ . For the two tubes shown in Fig. 11b (K is a cock or clamp for releasing air), we have

$$P_2 = \gamma_1(h_1 + H) + \gamma_2(H_2 + H)$$

or, in the general case for several tubes,

$$P_2 = \sum \gamma_i h_i + \gamma_2 H$$

The dish manometer (Fig. 11c) is more convenient than the foregoing, in that it is necessary to record the position of only one fluid level. When the dish diameter is large enough by comparison with the tube diameter, the fluid level in the dish can be regarded as constant. A dish-type micromanometer with an inclined tube is used for high precision in measurement of low gas pressures. The length of the fluid column to be measured is then increased in inverse proportion to the sine of the tube inclination angle, and the accuracy of the measurement increases accordingly.

Differential manometers, simplest among which is the U-tube manometer (Fig. 11d), are used to measure pressure differences between two points. If a mercury-filled manometer of this type is used to measure the difference between pressures  $p_1$  and  $p_2$  in a fluid of specific weight  $\gamma$  that completely fills the connecting tubes, it is evident that

$$P_1 - P_2 = h(\gamma_1 - \gamma)$$

A two-liquid micromanometer is used to measure small water-pressure gradients; this device is an inverted U-tube with oil or kerosene at the top (Fig. 11e). We have for this case

$$P_1 - P_2 = h(\gamma - \gamma_1)$$

The two-liquid dish manometer (Fig. 11f) is designed to measure air pressures or vacuums in the approximate range from 0.1 to 0.5 atm, i.e., when the alcohol or water manometer has too high a liquid column and is therefore clumsy to use, while the mercury manometer does not yield the required accuracy because the mercury column is too short. Manometers of this type are used, for example, in experiments in high-speed wind tunnels.

Mercury is poured into the dish and alcohol, kerosene, or some other fluid into the tube. Kerosene is highly recommended by its low volatility.

By appropriate selection of the diameters of the upper and lower segments of the tube ( $d_1$  and  $d_2$ ), we can produce any effective specific weight ( $\gamma_{ef}$ ) in the formula

$$\gamma_{ef} = H\gamma_2,$$

where  $p$  is the pressure (or vacuum) to be measured and  $H$  is the manometer reading.

We find the expression for  $\gamma_{ef}$  from the following equations (see Fig. 10f): the equilibrium equation of the mercury and kerosene columns at  $p = p_A$

$$H_0 \gamma_k = h_0 \gamma_m;$$

the equilibrium equation for  $p > p_A$

$$p \cdot \left( H_0 + H + \Delta h \right) \gamma_k = \left( h_0 + \Delta h \right) \gamma_m;$$

and the equation of volumes (the volume of kerosene that has transferred from the upper tube  $d_1$  to the lower  $d_2$  is equal to the volume of displaced mercury)

$$H d_1^2 = \Delta h d_2^2.$$

Substituting and rearranging,

NOT REPRODUCIBLE

$$\gamma_m = \frac{d_1^2}{d_2^2} \gamma_k \cdot \left( 1 - \frac{d_1^2}{d_2^2} \right) \gamma_k.$$

For example, we have for  $d_2 = 2d_1$ :  $\gamma_{ef} = 0.25 \cdot 13\,600 + 0.75 \cdot 800 = 4000 \text{ kgf/m}^3$ .

Spring or membrane-box mechanical manometers are used to measure pressures above 2-3 atm. Their operating principle is based on the deformation of a hollow spring or a membrane under the pressure to be measured. A mechanism transmits this deformation to a needle, which indicates the measured pressure on a dial.

Manometers are used on aircraft to monitor the pressure of fuel being supplied to gas-turbine engine nozzles or piston-engine carburetors, oil line pressures, etc.

The most common type of aviation manometer at the present time is the electrical manometer, and mechanical types are used less often. The sensitive element (sender) of an electric manometer is a membrane. Under the action of the pressure to be measured, the membrane deforms and, working through a transmission linkage, moves the wiper of a potentiometer, which is connected into the electrical circuit together with an indicator.

## §8. PRESSURE FORCE OF FLUID ON FLAT WALL

Let us use the fundamental equation of hydrostatics (2.2) to find the total pressure force of a fluid on a flat wall that is inclined at an arbitrary angle  $\alpha$  to the horizontal (Fig. 12). We calculate the pressure  $P$  exerted by the fluid on a certain area of this wall that is enclosed by an arbitrary contour and has an area of  $S$ .

We direct the  $ox$ -axis along the line of intersection of the wall plane with the open fluid surface and the  $oy$ -axis perpendicular to this line in the plane of the wall.

First, we write an expression for the elementary pressure force applied to an infinitesimally small area  $dS$ :

$$dP = p dS = (p_0 + h\gamma) dS = p_0 dS + h\gamma dS,$$

where  $p_0$  is the pressure on the exposed surface and  $h$  is the depth at which elementary area  $dS$  is located.

To determine the total force  $P$ , we integrate over the entire area  $S$ :

$$P = p_0 \int dS + \gamma \int h dS = p_0 S + \gamma \sin \alpha \int y dS,$$

where  $y$  is the coordinate of the center of area  $dS$ .

As we know from mechanics, the last integral represents the static moment of area  $S$  about the  $ox$ -axis and is equal to the product of this area by the coordinate of its center of gravity (point  $C$ ), i.e.,

$$\int y dS = y_C S.$$

Consequently,

$$P = p_0 S + \gamma \sin \alpha y_C S = p_0 S + \gamma h_C S,$$

(here  $h_C$  is the depth coordinate of the center of gravity of area  $S$ ), or

$$P = (p_0 + \gamma h_C) S = p_C S, \quad (2.11)$$

i.e., the total pressure force of the fluid on the flat wall equals the product of the wall area by the hydrostatic pressure at the center of gravity of this area.

If the pressure  $p_0$  is atmospheric, the force of the fluid excess pressure on the flat wall is

$$P_{\text{excess}} = h_C \gamma S = p_{C, \text{excess}} S. \quad (2.11')$$

Let us now find the position of the center of pressure, i.e., the coordinate of the intersection of the fluid pressure force on the wall with the plane of the wall.

Since the external pressure  $p_0$  is transmitted identically to all points on area  $S$ , the resultant of this pressure will be applied at the center of gravity of area  $S$ . To find the point of application of the fluid excess-pressure force (point  $D$ ), we use an equation of mechanics whose import is that the moment of the resultant pressure force about the  $ox$ -axis equals the sum of the moments of the component forces, i.e.,

$$P_{\text{excess}} y_D = \int y dP_{\text{excess}}$$

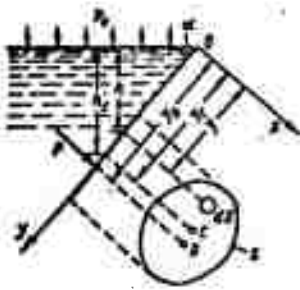


Fig. 12. Illustrating determination of fluid force on flat wall (wall indicated in two projections).

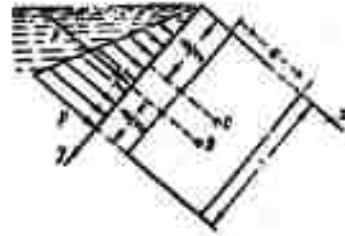


Fig. 13. Diagram of pressure on rectangular wall.

where  $y_D$  is the coordinate of the application point of force  $P_{1zb}$ .

Expressing  $P_{1zb}$  and  $dP_{1zb}$  in terms of  $y_C$  and  $y$  and determining  $y_D$ , we have

$$y_D = \frac{\gamma \sin \alpha \int y^2 dS}{\gamma \sin \alpha y_C S} = \frac{J_x}{y_C S},$$

where  $J_x = \int y^2 dS$  is the moment of inertia of area  $S$  about the  $ox$ -axis.

Remembering that

$$J_x = J_{x_0} + y_C^2 S$$

( $J_{x_0}$  is the moment of inertia of area  $S$  about the central axis, which is parallel to  $ox$ ), we obtain finally

$$y_D = y_C + \frac{J_{x_0}}{y_C S}. \quad (2.12)$$

Thus, the point of application of force  $P_{1zb}$  is below the center of gravity of the wall area; the distance between these points is

$$\Delta y = \frac{J_{x_0}}{y_C S}.$$

If the pressure  $p_0$  is atmospheric and acts on both sides of the wall, point  $D$  will also be the center of pressure. When  $p_0$  is above atmospheric, the pressure center will be found according to the rules of mechanics as the point of application of the resultant of two forces:  $h_C \gamma S$  and  $p_0 S$ . Here, the greater the second

force is by comparison with the first, the nearer, obviously, will the center of pressure be to the center of gravity of area  $S$ .

We have defined only the one center-of-pressure coordinate  $y_D$ . To determine the other coordinate  $x_D$ , we must write the equation of moments with respect to the  $Oy$ -axis.

In the particular case in which the wall is rectangular, and one of the sides of the rectangle coincides with the exposed surface of the fluid, the center-of-pressure position is very easy to find. Since the diagram of the fluid's pressure on the wall is a right triangle (Fig. 13) whose center of gravity lies at  $1/3$  of the height  $h$  of the triangle, the fluid's center of pressure will be at  $1/3$  of  $h$ , measuring downward.

It is frequently necessary to deal in aviation engineering with the action of a fluid-pressure force on flat walls, e.g., on the walls of pistons in various hydrostatic machines and devices (see, for example, Chapter XIV); here the pressure  $p_0$  is usually so high that the center of pressure can be regarded as coinciding with the center of gravity of the wall area.

#### §9. PRESSURE FORCE OF FLUID ON CYLINDRICAL AND SPHERICAL SURFACES. ARCHIMEDEAN LAW

In the general case, solution of the problem of the pressure force exerted by a fluid on an arbitrarily shaped surface reduces to determination of three components of the resultant force and three moments. It is usually necessary to deal with cylindrical or spherical surfaces having a vertical plane of symmetry. In these cases, the pressure of the fluid is reduced to an equivalent force lying in the plane of symmetry.

Let us take a cylindrical surface  $AB$  whose generatrix is perpendicular to the plane of the drawing (Fig. 14) and attempt to determine the pressure force of the fluid on this surface in two cases: fluid above (a) and below (b) the surface.

In case "a," we isolate a volume of fluid that is bounded by the subject surface  $AB$ , by vertical planes passing through the boundaries of this area, and the exposed surface of the fluid, i.e., volume  $ABCD$ , and examine its equilibrium conditions for the vertical and horizontal directions. If the fluid acts on surface  $AB$  with a force  $P$ , surface  $AB$  will also exert the same pressure  $P$  on the fluid, but in the opposite direction. Figure 14 shows this reaction force decomposed into two components: horizontal  $P_g$  and vertical  $P_v$ .

The equilibrium condition for volume  $ABCD$  in the vertical direction takes the form

$$P_v = p_0 S_g + G, \quad (2.13)$$

where  $p_0$  is the pressure on the exposed fluid surface,  $S_g$  is the

area of the horizontal projection of surface AB, and G is the weight of the isolated fluid volume.

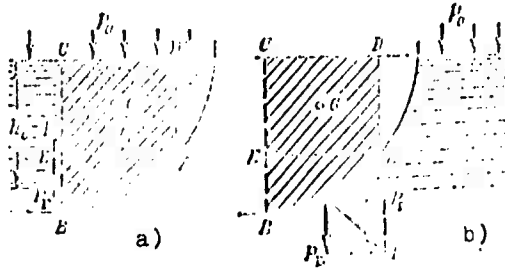


Fig. 14. Pressure of fluid on cylindrical surface.

The equilibrium condition for the same volume in the horizontal direction is written with consideration of the fact that the pressure forces of the fluid on surfaces EC and AD cancel one another, leaving only the pressure force on area BE, i.e., on the vertical projection  $S_v$  of surface AB:

$$P_v = S_v h c + p_0 S. \quad (2.14)$$

Using Formulas (2.13) and (2.14) to determine the vertical and horizontal components of the total pressure force P, we find this force:

$$P = \sqrt{P_v^2 + P_h^2}. \quad (2.15)$$

When the fluid is below the surface (case "b," see Fig. 14), the hydrostatic pressures at all points of surface AB will have the same values as in case "a," but the opposite directions, and the resultant forces  $P_v$  and  $P_g$  will be given by the same formulas (2.8) and (2.9), but their signs will be the opposite. Here, G should be understood, as in case "a," as the weight of the fluid in volume ABCD, even though this volume is not filled with fluid.

The position of the center of pressure on a cylindrical wall is easily found if the forces  $P_v$  and  $P_g$  are known and if the center of pressure on the vertical projection of the wall or the center of gravity of the isolated volume ABCD is determined. The problem is substantially simpler when the cylindrical surface under consideration is circular, since the resultant force then intersects the axis of the surface. This follows from the fact that any elementary pressure force dP is normal to the surface, i.e., radially directed.

The above method of determining the pressure force on cylindrical surfaces is also applicable to spherical surfaces. In this case, the resultant force also passes through the center of



Fig. 15. Illustrating proof of Archimedean law.

the surface and lies in the vertical plane of symmetry.

Let us apply the above method of finding the vertical fluid-pressure-force component on a curvilinear wall to prove the well-known law of Archimedes.

Suppose that a body of arbitrary shape and of volume  $W$  is immersed in a liquid (Fig. 15). Let us project this body onto the exposed liquid surface and draw a projecting cylindrical surface tangent to the surface of the body along a closed contour. This curve separates the upper surface  $ACB$  of the body from its lower surface  $ADB$ . The vertical component of the fluid excess pressure force on the top part of the surface,  $P_{v_1}$ , is directed downward and equals the weight of fluid in volume  $AA'B'BCA$ . The vertical component of the fluid pressure force on the lower part of the body's surface,  $P_{v_2}$ , is directed upward and equals the weight of the fluid in volume  $AA'B'BDA$ .

This implies that the vertical resultant fluid pressure force on the body will be directed upward and will be equal to the weight of the fluid in a volume equal to the difference between the above two volumes, i.e., in the volume of the body:

$$P_a = P_{v_2} - P_{v_1} = G_{\text{fluid}} V_{\text{body}}$$

This is the Archimedean law, which is usually formulated thus: a body immersed in a liquid loses a weight equal to the weight of the liquid that it displaces. The law of Archimedes is, of course, also valid for bodies that are partially immersed in a liquid.



Fig. 16. Diagram of hydraulic press (jack).

The force  $P_a$  as known as the Archimedean force or buoyant force, and the point of its application, i.e., the center of



Fig. 17. Diagram of hydraulic multiplier.

gravity of volume  $W$ , as the center of displacement.

Three cases are possible, depending on the relation between the body's weight  $G$  and the Archimedean force  $P_A$ : 1)  $G > P_A$ , body sinks; 2)  $G < P_A$ , body emerges from liquid; 3)  $G = P_A$ , body floats.

In addition to the force equality  $G = P_A$ , equilibrium of a floating body also requires zero resultant moment. This last condition is met when the body's center of gravity is on the same vertical as the center of displacement. The problem of equilibrium stability of floating bodies will not be discussed here.

**Example 1.** Figure 16 is a schematic diagram of a hydraulic press and can also be used to represent a hydraulic jack. For the jack case, body 1 is the load to be raised, while for the case of the press it is a stationary support attached to a foundation by columns 8 (indicated by dashed lines); body 2 then becomes the material to be pressed.

Hand pump 3, which is fitted with intake 5 and delivery 4 valves, sets up in cylinder 6 a pressure that acts on system 7 and produces a force  $P$  along the piston.

Determine this force for the following data:  $R = 20$  kgf;  $a/p = 1/9$ ;  $D/d = 10$ .

**Solution.**

$$P = R \left( \frac{D}{d} \right)^2 = 20 \cdot 10 \cdot 100 = 20000 \text{ kgf.}$$

**Example 2.** A hydraulic multiplier (Fig. 17) is used to raise the pressure  $p_1$  obtained from a pump or accumulator. Pressure  $p_1$  is applied to cylinder 1, which contains a sliding hollow cylinder 2 of weight  $G$  and diameter  $D$ . The latter slides along stationary plunger 3, whose diameter is  $d$  and whose bore ducts fluid under an increased pressure  $p_2$ .

Determine pressure  $p_2$  for the following data:  $G = 300$  kgf;  $D = 125$  mm;  $p_1 = 100$  kgf/cm<sup>2</sup>;  $d = 50$  mm.

Disregard friction in the packings.

**Solution.** We have from the equilibrium condition for cylinder 2

$$p_1 \cdot \frac{\pi D^2}{4} = \frac{\pi d^2}{4} p_2 + G.$$

from which

$$P_2 = P_1 \left( \frac{D}{d} \right)^2 = \frac{4G}{\pi d^2} \cdot 100 \left( \frac{125}{50} \right)^2 = \frac{4 \cdot 300}{\pi \cdot 5^2} = 610 \text{ kgf/cm}^2.$$

### Footnotes

Manu-  
script  
page

19 <sup>1</sup>These formulas are as follows:

$$\sigma_n = \sigma_x \cos^2 \varphi + \sigma_y \sin^2 \varphi; \tau = -\frac{1}{2} (\sigma_x - \sigma_y) \sin 2\varphi.$$

21 <sup>2</sup>We attach the coordinate system rigidly to the vessel containing the fluid.

23 <sup>3</sup>Leonard Euler (1707-1783) was a famous mathematician, mechanician, and physicist. He was born and educated at Basel (Switzerland). He lived for more than 30 years at St. Petersburg, working at the Russian Academy of Sciences.

### Symbol List

Manu- script page	Symbol		English equivalent
24	абс	abs	absolute
24	изб	izb	excess
25	вод	vod	water
25	рт	rt	mercury
25	вак	vak	vacuum
27	эф	ef	effective
28	к	k	kerosene
31	г	g	horizontal
31	в	v	vertical

## C H A P T E R    I I I

### THE FLUID AT RELATIVE REST

#### §10. BASIC CONCEPTS

In the preceding chapter, we were basically concerned with the equilibrium of a fluid when acted upon by a single mass force - its own weight. This is the case only when the fluid is at rest in a container that is not in motion relative to the earth, or in a container in uniform rectilinear motion.

If, on the other hand, the container with the fluid is in nonuniform or nonrectilinear motion, then all particles of the fluid are acted upon, in addition to their own weight, by the inertial forces of the translational motion. Under these forces, assuming that they are constant in time, the fluid assumes a new equilibrium position, i.e., it becomes stationary relative to the walls of the container. This case of equilibrium is, as we noted in §6, known as relative rest.

In this state, the exposed surface of the fluid and other level surfaces (see §5) may differ substantially from the level surfaces when the fluid is at rest in a stationary container, i.e., from a family of horizontal planes. Determination of the shape and position of the exposed surface of a fluid at relative rest is guided by the basic property of all level surfaces according to which the resultant mass force always acts normal to a level surface.

Indeed, if the resultant mass force were not in fact normal, but acted at some other angle to the level surface, the tangential

component of this force would cause motion of fluid particles along the level surface. At relative rest, however, there are no fluid-particle displacements either relative to the container walls or with respect to one another. Consequently, the only possible direction for the resultant mass force is the normal to the free surface and to other level surfaces.

It must also be remembered that level surfaces cannot intersect, since otherwise we should have along the line of intersection of two such surfaces a row of points at which the pressure had two different values at the same time, which is impossible.

Let us examine two characteristic cases of relative rest of a fluid:

- a) in a container in rectilinear and uniformly accelerated motion;
- b) in a container rotating uniformly about a vertical axis.

#### §11. RECTILINEAR UNIFORMLY ACCELERATED MOTION OF A CONTAINER OF FLUID

Suppose that a container of fluid, such as an aircraft fuel tank, is in straight-line motion with a constant acceleration  $\underline{a}$ . In this case, the resultant mass force acting on the fluid is found as the vector sum of the inertial force, which is directed oppositely to the acceleration  $\underline{a}$ , and the force of gravity (Fig. 18).

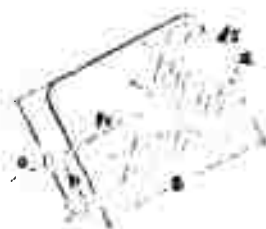


Fig. 18. Relative rest of fluid in container in rectilinear uniformly accelerated motion.

Using  $\underline{j}$  to denote the resultant mass force referred to unit mass, we have

$$\underline{j} = -\underline{a} + \underline{g}$$

The resultant mass forces are parallel to one another for all particles in the volume of fluid under consideration, and the level surfaces are perpendicular to these forces, so that all level surfaces, including the free surface, are parallel planes. The angle of inclination of these planes to the horizon is determined from their perpendicularity to the force  $\underline{j}$ .

To resolve fully the question as to the position of the fluid's free surface in a container in straight-line uniformly accelerated motion, it is necessary to complement the above condition with the equation of volumes, i.e., it is necessary to know the volume of the fluid in the container and express it in terms of the container dimensions  $B$  and  $H$  and the original fluid level  $h$ .

An equation that can be used to find the pressure at any point in the fluid volume can be derived in much the same way as was done in §5.

For example, we take at point M an elementary area  $dS$  parallel to the free surface and construct on this area a cylindrical volume whose generatrix is normal to the free surface. The equilibrium condition for this fluid volume in the direction of the normal to the free surface will take the form

$$p dS = p_0 dS + j \rho l dS,$$

where the last term represents the total mass force acting on the isolated fluid volume and  $l$  is the distance from point M to the free surface.

On cancelling the  $dS$ , we obtain

$$p = p_0 + j \rho l. \quad (3.1)$$

In the particular case with  $a = 0$ ,  $j = g$  and Formula (3.1) becomes the fundamental equation of hydrostatics (2.2).

In analysis of cases in which an inertial force acts, it is customary in aviation practice to use the notion of the load factor, which is equal (in straight-line level flight) to

$$n_x = \frac{a}{g}.$$

When the airplane maneuvers in flight, the load factor may be tangential ( $n_x$ ) or normal ( $n_y$ ). The latter case occurs in curvilinear flight (entering and pulling out of a dive, turning), but relative rest of the fluid, as in the airplane's fuel tanks, is then possible only in a steady turn in the horizontal plane. In this case, the unit mass force of translational-motion inertia, which is numerically equal to the acceleration, is given by

$$a = \frac{V^2}{R},$$

where  $V$  is the airplane's speed and  $R$  is the radius of the turn.

We should note that the normal load factors are usually substantially larger than the tangential factors for airplanes (by factors of 8-10).

If large load factors are acquired when the fuel in the tanks is low, the fuel-system pickup may be starved and the fuel supply cut off. Special devices are provided around the pickup hole to prevent this.

## §12. UNIFORM ROTATION OF CONTAINER OF FLUID

First, let us take an open cylindrical vessel that contains a fluid and set it in rotation about its vertical axis at a constant

angular velocity  $\omega$ . The fluid gradually acquires the same angular velocity as the container, and its free surface changes shape: the fluid level drops at the center and rises at the walls, and the entire free surface of the fluid becomes a surface of revolution (Fig. 19).

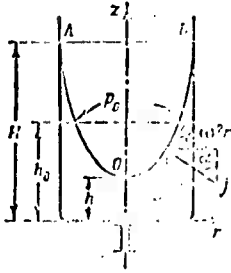


Fig. 19. Rotation of open container of fluid about its vertical axis.

In this case, the fluid will be acted upon by two mass forces: gravity and centrifugal force; referred to the unit mass, these will be  $\underline{g}$  and  $\omega^2 r$ , respectively.

The resultant mass force  $\underline{j}$  increases with increasing radius by virtue of its second component, while its inclination angle to the horizon becomes smaller. This force is normal to the free surface of the fluid, with the result that the inclination of this surface increases with increasing radius.

Let us find the equation of curve AOB in  $z, r$ -coordinates with the origin at the center of the bottom of the container. Remembering that the force  $\underline{j}$  is normal to curve AOB, we find from the drawing that

$$\tan \alpha = \frac{dz}{dr} = \frac{\omega^2 r}{g}$$

From this,

$$dz = \frac{\omega^2 r}{g} dr,$$

or, after integration,

$$z = \frac{\omega^2 r^2}{2g} + C.$$

It follows from the condition for the intersection point of curve AOB with the rotation axis that  $C = h$ , so that we finally obtain

$$z = h + \frac{\omega^2 r^2}{2g}, \quad (3.2)$$

i.e., curve AOB is a parabola, and the free surface of the fluid is that of a paraboloid of revolution.

Applying (3.2), we can determine the position of the free surface in the container, e.g., the maximum height  $H$  to which the fluid rises and the height  $h$  of the vertex of the paraboloid at a given speed  $\omega$ . However, this also requires use of an equation of volumes: the volume of the stationary fluid is equal to its volume during rotation.

In practice, the case most frequently encountered is that of rotation of a container of fluid with the axis horizontal (or in an arbitrary position) and the angular velocity  $\omega$  so high that gravity can be disregarded by comparison with the centrifugal forces.

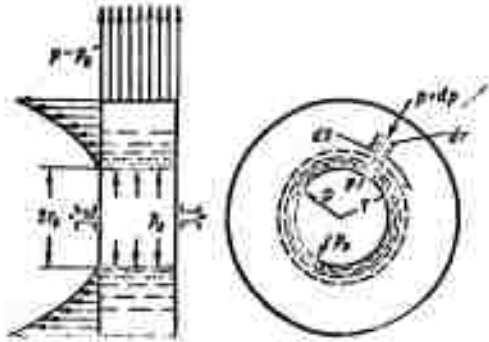


Fig. 20. Rotation of container of fluid around a horizontal axis.

The law of pressure variation in the fluid is easily obtained for this case by considering the equilibrium equation of an elementary volume with base area  $dS$  and height  $dr$ , taken along the radius (Fig. 20). This fluid element is acted upon by pressure and centrifugal forces. Denoting the pressure at the center of area  $dS$  on radius  $r$  by  $p$  and that at the center of the other base of the volume (at radius  $r+dr$ ) by  $p+dp$ , we obtain the following equilibrium equation for the isolated volume in the radial direction:

$$pdS - (p+dp)dS + \rho\omega^2 r dr dS = 0$$

or

$$dp = \rho\omega^2 r dr.$$

Integration yields

$$p = \rho\omega^2 \frac{r^2}{2} + C.$$

We find the constant  $C$  from the condition that  $p = p_0$  at  $r = r_0$ , so that

$$C = p_0 - \rho\omega^2 \frac{r_0^2}{2}.$$

Finally, we obtain the relation between  $p$  and  $r$  in the form

$$p = p_0 + \rho \frac{\omega^2}{2} (r^2 - r_0^2). \quad (3.3)$$

Obviously, the level surfaces in this case will be circular cylindrical surfaces with a common axis - the fluid's axis of rotation. If the container is only partly filled with fluid, its free surface, as a level surface, will also be cylindrical, and it will be convenient to denote its radius by  $r_0$  and the pressure on it by  $p_0$ .

It is often necessary to compute the pressure force exerted by the fluid rotating with a container on a wall normal to the axis of rotation (or on an annular segment of this wall).

This requires first writing an expression for the pressure force acting on an elementary annular area of radius  $r$  and width  $dr$ . Using (3.3), we obtain

$$dP = p dS = \left[ p_0 + \rho \frac{\omega^2}{2} (r^2 - r_0^2) \right] 2\pi r dr,$$

and then integrate between the appropriate limits.

A quite considerable resultant pressure force can be obtained on the walls of a container by setting the fluid in it rotating at high speed. This effect is used in certain friction clutches in aviation engines where large normal-pressure forces are required to engage two shafts. The method indicated above is used to compute the axial-pressure force of the fluid on the impellers of centrifugal pumps.

The same formulas can be derived for these cases of relative rest by solving the fluid's differential equations of equilibrium.

### §13. INTEGRATION OF DIFFERENTIAL EQUATIONS OF EQUILIBRIUM OF A FLUID FOR PARTICULAR CASES OF RELATIVE REST

Here we shall use the general differential equation of fluid equilibrium (2.6), as derived in §6, to analyze fluids at relative rest.

Writing this equation,

$$dp = \rho(Xdx + Ydy + Zdz)$$

and examining it, we see that the trinomial in the parentheses, like the left member of the equation, must be a total differential of a certain function  $U(x, y, z)$ .

This function must have the following property: its partial derivatives with respect to the coordinates  $x$ ,  $y$ , and  $z$  must equal  $X$ ,  $Y$ , and  $Z$ , respectively, i.e.,

$$\frac{\partial U}{\partial x} = X; \quad \frac{\partial U}{\partial y} = Y; \quad \frac{\partial U}{\partial z} = Z.$$

The function  $U$  is known as the force function. As we know from

theoretical mechanics, this function is equal to the potential of the forces taken with the opposite sign.

We may therefore conclude that equilibrium of the fluid is possible only under the action of mass forces that have a potential.

Introducing the function  $U$  into the fundamental equation (2.6),

or

$$\rho \operatorname{grad} U = -\operatorname{grad} p \quad (3.4')$$

NOT REPRODUCIBLE

$$\rho = -\rho' U \quad (3.4)$$

After integration, we obtain in the general form

$$p = U + G \quad (3.5')$$

We find the constant of integration from boundary conditions: let  $p = p_0$  at  $U = U_0$ ; then

$$p = \rho(U - U_0) + p_0 \quad (3.5)$$

The surface that satisfies the condition

$$\rho = \text{const} \quad \text{or} \quad p = \text{const}$$

will also satisfy the condition

$$\rho = 0 \quad \text{or} \quad p(x, y, z) = \text{const}$$

Consequently, such a surface is a level surface or an equipotential surface. This means that a surface of constant pressure is at the same time a surface of constant mass-force potential, and that the pressure in the fluid can be changed only by changing the force potential and vice versa.

We may also conclude from the above that the density of an inhomogeneous dropping fluid must be a function of  $U$ :

$$\rho = \rho(U)$$

For this case, Formula (3.4) is written

$$\rho(U) \operatorname{grad} U = -\operatorname{grad} p \quad (3.6)$$

or, after integration,

$$p = \int \rho(U) dU + G \quad (3.7)$$

For an inhomogeneous dropping fluid, therefore, the level surfaces will also be surfaces of equal density. This means that an inhomogeneous dropping fluid at equilibrium has layers of equal

density corresponding to its level surfaces, and that higher pressures correspond to higher density values and vice versa. This property is used to separate inhomogeneous liquid mixtures in devices known as centrifuges.

Let us introduce into consideration the resultant unit mass force  $\underline{j}$ , whose projections onto the coordinate axes equal X, Y, and Z, i.e., let us take the total acceleration caused by the action of all mass forces at a given point. We note then that dx, dy, and dz are the projections of an infinitesimally short segment dl, which represents the distance between two closely spaced points M and M' (see Fig. 7), onto the coordinate axes.

On this basis, we can write the equations

$$X = j \cos(j, x); \quad Y = j \cos(j, y); \quad Z = j \cos(j, z)$$

and

$$dx = dl \cos(dl, x); \quad dy = dl \cos(dl, y); \quad dz = dl \cos(dl, z).$$

We now apply a formula used in analytical geometry to determine the cosine of the angle between two straight lines and, noting the foregoing expressions, write

$$\cos(j, dl) = X dx + Y dy + Z dz / j dl = \cos(j, x) \cos(dl, x) + \cos(j, y) \cos(dl, y) + \cos(j, z) \cos(dl, z) = j dl \cos(j, dl).$$

NOT REPRODUCIBLE

Substituting the expression obtained for dU into (3.4), we have

$$dU = \rho dl \cos(j, dl). \quad (3.8)$$

We see from (3.8) that the largest pressure increment is obtained in the direction of the resultant mass force  $\underline{j}$ , since  $\cos(j, dl)$  is then equal to unity.

For any segment dl on a level surface, the increment dp = 0. But in the general case  $\underline{j}$  and dl are nonzero, so that

$\cos(j, dl) = 0$ , i.e., the resultant mass force is normal to the level surface. This important property of the level surface has already been derived (§10) on the basis of simple reasoning.

Let us carry out the integration of the differential equations of fluid equilibrium for the two cases of relative rest examined above.

1. Let the fluid be in a container that is in straight-line uniformly accelerated motion, i.e., let it be at relative rest, as considered in §11. In this case, it is convenient to use

(3.8), placing the direction  $l$  along the resultant mass force  $\underline{j}$  (see Fig. 18).

We then have

$$\cos(\hat{j}, \hat{l}) = 0$$

and, consequently,

$$dp = \rho j dl$$

On integration,

$$p = \rho j l + C$$

Since  $p = p_0$  for  $l = 0$ , we have  $C = p_0$  and finally arrive at the familiar equation

$$p = p_0 + \rho j l$$

2. Let the fluid be in a container that is in uniform rotation at angular velocity  $\omega$  about its vertical axis, i.e., let it be in the state of relative rest examined in §12. Placing the origin at the center of the bottom of the container and pointing the  $z$ -axis vertically upward, we obtain the following expressions for the components of the unit mass force:

$$X = \omega^2 r \cos(\hat{r}, \hat{x}) = \omega^2 x;$$

$$Y = \omega^2 r \cos(\hat{r}, \hat{y}) = \omega^2 y;$$

$$Z = -g.$$

Substituting these expressions into the general equilibrium equation (2.6),

$$dp = \rho(\omega^2 x dx + \omega^2 y dy - g dz)$$

or

$$dp = \frac{\rho}{g} \omega^2 (x dx + y dy) - \rho dz.$$

If we remember that

$$x dx + y dy = d\left(\frac{r^2}{2}\right),$$

we obtain after integration

$$p = \frac{\rho}{2g} \omega^2 r^2 - \rho z + C.$$

At  $r = 0$  and  $z = h$ ,  $p = p_0$ , so that

$$C = p_0 + \rho h.$$

Finally, therefore,

$$p = p_0 + \gamma(h - z) + \frac{\gamma}{2g} \omega^2 r^2. \quad (3.9)$$

Formula (3.9) enables us to determine the pressure at any point in a volume of fluid rotating about a vertical axis (see Fig. 19).

The equation of the fluid's free surface can be obtained by setting  $p = p_0$  in (3.9). After cancelling and rearranging, we have

$$z = h + \frac{\omega^2 r^2}{2g},$$

which agrees with the earlier Formula (3.2).

If we disregard gravity ( $z = 0$ ) in the above derivation and determine the constant of integration from the condition  $p = p_0$  at  $r = r_0$ , we obtain Formula (3.3):

$$p = p_0 + \gamma \frac{\omega^2}{2g} (r^2 - r_0^2).$$

Thus, the relationships already known to us for relative rest of a fluid are obtained more rigorously by integrating the differential equations of fluid equilibrium.

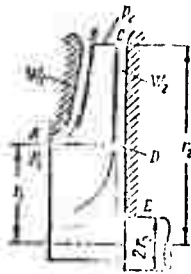


Fig. 21. Illustrating determination of axial force in centrifugal pump.

(in spaces  $W_1$  and  $W_2$ ) is rotating at an angular velocity equal to half the pump speed and that negligible fluid passes through clearance A (Fig. 21).

**Example.** Determine the axial-pressure force of a fluid on the impeller of a liquid-rocket-engine centrifugal pump on the assumption that the fluid between the impeller disks and the casing of the pump

The excess pressure at the impeller exit is  $p_2 = 38$  atm, and  $p_1 = 0$  at the inlet. The pump speed  $n = 16\,500$  rev/min. The pump dimensions:  $r_2 \approx 50$  mm,  $r_1 = 25$  mm,  $r_v = 12$  mm. The specific weight of the fluid  $\gamma = 918$  kgf/m<sup>3</sup>.

**Solution.** The pressure forces of the fluid on surfaces AB and CD cancel one another. Only the force of axial pressure on surface DE, i.e., on an annular surface bounded by circles of radii  $r_1$  and  $r_v$ , remains uncompensated. Consequently, the unknown force is directed from right to left and equals

$$P = 2\pi \int_{r_v}^{r_1} p \cdot r \cdot dr,$$

where, on the basis of (3.3) with  $p_2$  and  $r_2$  substituted for  $p_0$  and  $r_0$ , we have

$$p = p_2 - \gamma \frac{\omega_{zh}^2}{2g} (r_2^2 - r^2)$$

( $\omega_{zh}$  is the angular velocity of the fluid).

Hence

$$P = 2\pi \int_{r_0}^{r_1} \left[ p_2 - \gamma \frac{\omega_{zh}^2}{2g} (r_2^2 - r^2) \right] r dr = \pi (r_1^2 - r_0^2) \left[ p_2 - \gamma \frac{\omega_{zh}^2}{2g} \left( r_2^2 - \frac{r_1^2 + r_0^2}{2} \right) \right]$$

Substituting numerical values,

$$P = \pi (2.5^2 - 1.2^2) \left[ 2.981 - \frac{\pi \cdot 15500^2}{2 \cdot 30} \frac{1}{2 \cdot 981} \left( 5^2 - \frac{2.5^2 + 1.2^2}{2} \right) \right] = 460 \text{ kgf.}$$

### Symbol List

Manu- script page	Symbol	English equivalent
47	в v	shaft
48	ж zh	fluid

## C H A P T E R   I V

### THE FUNDAMENTAL EQUATIONS OF HYDRAULICS

#### §14. FUNDAMENTAL CONCEPTS

In turning to study of the problems of fluid motion, it must be noted that we shall first examine the motion of a so-called ideal fluid, i.e., an imaginary fluid that has no viscosity at all, and only then pass to a study of real flows. In such an inviscid fluid, as in real fluids at rest, only one form of stress is possible: the normal compressive stress, i.e., hydromechanical pressure or simply pressure.

In a moving ideal fluid, pressure has the same properties as in a stationary fluid, i.e., it is directed along inner normals on the outer surface of the fluid and is the same in all directions at any point inside the fluid.<sup>1</sup>

Fluid flow may be steady (stationary) or nonsteady (nonstationary).

Steady flow is flow that does not change in time, with the hydromechanical pressure and velocity functions only of the coordinates and not of time. Pressure and velocity may change as fluid particles move from one position to another, but at a given point that is stationary with respect to the channel, the pressure and velocity do not change in time during steady motion.

This can be written mathematically as follows:

<sup>1</sup>See page 74 for footnote.

$$p = f_1(x, y, z); v = f_2(x, y, z),$$

$$\frac{\partial p}{\partial t} = 0; \frac{\partial v_x}{\partial t} = 0; \frac{\partial v_y}{\partial t} = 0; \frac{\partial v_z}{\partial t} = 0,$$

NOT REPRODUCIBLE

where the velocity subscripts denote the projections of this velocity onto the corresponding axes, which are rigidly attached to the channel.

In a particular case, steady flow may be uniform, in which case the velocity of each particle does not change with a change in its coordinates.

In the general case of nonsteady flow, pressure and velocity depend on both the coordinates and time, i.e.,

$$p = f_1(x, y, z, t); v = f_2(x, y, z, t).$$

As examples of nonsteady fluid flow, we might cite the gradual drainage of a container through a hole in its bottom or motion of a fluid through the intake or delivery pipe of a simple piston pump whose piston executes reciprocating motion.

Examples of steady flow: outflow of fluid from a container in which constant level is maintained; motion of fluid in a closed pipe due to the action of a centrifugal pump turning at constant speed.

Investigation of steady flows is a much simpler matter than that of nonsteady flows. Below we shall be concerned chiefly with steady flows and only a few particular cases of nonsteady flow.

The trajectories of fluid particles in steady flow are curves that do not vary in time.

In nonsteady flow, the trajectories of different particles passing through a given point in space will have different shapes. Hence the concept of the streamline is introduced for purposes of examining flow patterns formed at particular points in time.

A streamline is a line in a moving fluid the tangent to which at any point coincides with the velocity vector of the particles on this line at the particular point in time (Fig. 22).

In steady flow, the streamline will obviously coincide with the trajectory and will not change shape with time.

If we take an elementary closed contour in a moving fluid and pass streamlines through all of its points, the result is a tubular surface known as a stream tube. The part of the flow enclosed within a stream tube is called a filament (Fig. 23).

As the transverse dimensions of a filament tend to zero, the filament becomes a streamline.

At any point on the lateral surface of a filament, i.e., on the stream tube, the velocity vectors are tangential and there are no velocity components normal to this surface; consequently, no fluid particle can escape the filament or enter it at any point on the stream tube. Thus, the stream tube is a kind of impenetrable wall, and the elementary filament is a kind of independent elementary flow.



Fig. 22. Streamline.

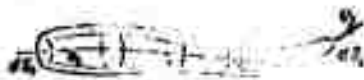


Fig. 23. Filament.

We shall at first regard flows of finite dimensions as aggregates of elementary filaments, i.e., we shall assume the flow to be filamentary. As a result of the velocity difference, adjacent filaments will slip on one another without mixing.

An effective section or simply a section of the flow is generally a surface inside the flow that passes normal to its streamlines. Usually, zones in which the filaments may be regarded as parallel and the effective sections, therefore, as plane are considered in the flows.

Ramming and nonramming fluid flows are distinguished. Ramming flows are flows in closed channels with no open surface, while nonramming flows are flows with a free surface. In ramming flows, the pressure is usually variable along the flow, while in nonramming flows it is constant (usually at atmospheric). Examples of ramming flows are flows in pipes with elevated (or lowered) pressure and flows in hydraulic machines and other hydraulic accessories. Nonramming flows occur in rivers, open channels, and millraces. In the present textbook, we shall be concerned almost exclusively with ramming flows.

#### §15. FLOW RATE. THE FLOW RATE EQUATION

The flow rate is the quantity of fluid that passes across the effective flow (filament) section per unit of time. This quantity can be measured in units of volume, weight, or mass, so that a distinction arises between the volumetric  $Q$ , gravimetric  $G$ , and mass  $M$  flow rates.

For an elementary filament that has infinitesimally small cross sections, we can regard the velocity  $v$  as the same at all points in each section. Consequently, the volume flow rate for an elementary filament will be

$$dG = v dS [m^3/s], \quad (4.1)$$

where  $dS$  is the sectional area of the filament; the gravimetric flow rate

$$dG = \gamma dQ \text{ [N/s] or [kgf/s]} \quad (4.2)$$

and the mass flow rate

$$dM = \rho dQ = \rho v dS \text{ [kg/s] or [kgf}\cdot\text{s/m]}. \quad (4.3)$$

For flows with finite dimensions, velocity is generally different at different points in a cross section; hence the flow rate must be computed as a sum of elementary filament flow rates, i.e.,

$$Q = \int v dS. \quad (4.4)$$

Usually, the velocity averaged over the cross section is introduced; it equals

$$v_{av} = \frac{Q}{S}, \quad (4.5')$$

from which

$$Q = v_{av} S. \quad (4.5)$$

On the basis of the law of conservation of matter, the hypothesis of continuity of the flow, and the above property of the stream tube, by which it is "impermeable," we can say for steady flow of an incompressible fluid that the flow rate is the same in all cross sections of an elementary filament (see Fig. 23), i.e.,

$$(4.6)$$

This equation is known as the flow rate equation for the elementary filament.

A similar equation can also be written for a flow of finite dimensions bounded by impermeable walls, except that average velocities must be introduced instead of the true ones; then

$$(4.7)$$

It follows from this last equation that the average velocities in a flow of incompressible fluid are inversely proportional to the cross-sectional areas, i.e.,

$$\frac{v_{av1}}{v_{av2}} = \frac{S_2}{S_1}. \quad (4.7')$$

Obviously, the flow rate equation is a particular case of the general law of conservation of matter, as well as a condition of flow continuity.

## §16. DERIVATION OF BERNOULLI EQUATION FOR A FILAMENT OF IDEAL FLUID

Let us examine steady flow of an ideal fluid acted upon only by a single mass force, gravity, and derive for this case the fundamental equation linking the pressure in the fluid with the velocity of its motion.

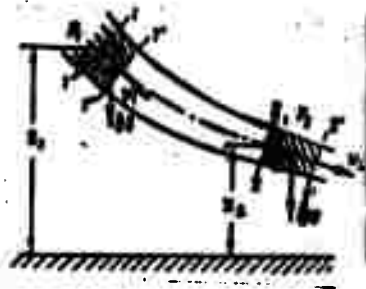


Fig. 24. Illustrating derivation of Bernoulli equation for a filament.

Let us take one of the filaments composing the flow and isolate a filament of arbitrary length from this filament with sections 1 and 2 (Fig. 24). Suppose that the area of the first section is  $dS_1$ , the velocity in it is  $v_1$ , the pressure is  $p_1$ , and the height of its center of gravity, reckoned from an arbitrary horizontal plane, is  $z_1$ . In the second section, we shall have  $dS_2$ ,  $v_2$ ,  $p_2$ , and  $z_2$ , respectively.

During an infinitesimal time segment  $dt$ , our segment of filament moves to position 1'-2' under the action of external forces.

To this segment of the filament, we apply the theorem from mechanics to the effect that the work done by the forces applied to the body is equal to the kinetic-energy increment of this body. In our case, these forces are pressure forces acting normal to the surface of the filament segment under consideration, and only one of the mass forces - gravity.

Let us calculate the work of the pressure forces and gravity and the kinetic-energy change of the filament segment during time  $dt$ .

The work of the pressure force will be positive in the first section, since the direction of the force coincides with the direction of motion, and it will be expressed as the product of the force ( $p_1 dS_1$ ) by the distance ( $v_1 dt$ ), i.e.,

$$p_1 dS_1 v_1 dt.$$

In the second section, the work of the pressure force will have the minus sign, since the force is directly opposed to the direction of motion; it will be expressed as follows:

$$-p_2 dS_2 v_2 dt.$$

The pressure forces acting on the sides of the filament segment will not perform work, since they are normal to this surface and, consequently, also normal to the displacements.

Thus, the work of the pressure forces will be

$$p_1 v_1 dS_1 dt - p_2 v_2 dS_2 dt. \quad (4.8)$$

The work of gravity is equal to the change in the position potential energy of the filament segment. We must therefore subtract the position energy of the fluid in volume 1'-2' from the position energy of the fluid in volume 1-2. In this subtraction, the position energy of the intermediate volume 1'-2 cancels out, leaving only the position-energy difference of filament segments 1-1' and 2-2'. If we use the flow equation (4.6), we see at once that the volumes and hence the weights of segments 1-1' and 2-2' are equal, i.e.,

$$\delta G = \gamma v_1 dS_1 dt = \gamma v_2 dS_2 dt. \quad (4.9)$$

Hence the work of gravity will be expressed as the product of the height difference by the weight  $\delta G$ :

$$(z_1 - z_2) \delta G. \quad (4.10)$$

To calculate the kinetic-energy increment of this filament segment during time  $dt$ , it is necessary to subtract the kinetic energy of volume 1-2 from that of volume 1'-2'. On subtraction, the kinetic energy of the intermediate volume 1'-2 cancels, leaving only the potential-energy difference of filament segments 2-2' and 1-1', each of which weighs  $\delta G$ .

We thus obtain the kinetic-energy increment, which will be

$$(v_2^2 - v_1^2) \frac{\delta G}{2g}. \quad (4.11)$$

Adding the work of the pressure forces (4.8) to the work of gravity (4.10) and equating this sum to the kinetic-energy increment (4.11), we obtain

$$p_1 dS_1 v_1 dt - p_2 dS_2 v_2 dt + (z_1 - z_2) \delta G = (v_2^2 - v_1^2) \frac{\delta G}{2g}. \quad (4.12')$$

Let us divide all terms of the equation by the weight  $\delta G$ . After appropriate cancelling,

$$\frac{p_1}{\gamma} - \frac{p_2}{\gamma} + z_1 - z_2 = \frac{v_2^2}{2g} - \frac{v_1^2}{2g}.$$

Grouping terms pertaining to the first section in the left member of the equation and the terms for the second section in the right member,

$$z_1 + \frac{p_1}{\gamma} = z_2 + \frac{p_2}{\gamma} + \frac{v_2^2}{2g} - \frac{v_1^2}{2g}. \quad (4.12)$$

NOT REPRODUCIBLE

where  $z$  is the levelling height or geometric head;  $p/\gamma$  is the piezometric height or piezometric head, and  $v^2/2g$  is the velocity height or velocity head.

The resulting equation is known as the Bernoulli equation for a filament of an ideal incompressible fluid. It was derived by Daniel Bernoulli in 1738.<sup>2</sup>

The terms of the Bernoulli equation in the form (4.12) have the dimensions of length.

The trinomial of the form

$$z + \frac{p}{\gamma} + \frac{v^2}{2g} = H$$

is known as the total head.

The Bernoulli equation (4.2) has been written for two arbitrarily chosen filament sections, the first and second, and expresses the equality of the total heads  $H$  in these sections. Since they were taken quite arbitrarily, the total head will have the same value for any other section of the same filament, i.e.,

$$z + \frac{p}{\gamma} + \frac{v^2}{2g} = H = \text{const (along a filament)}.$$

Thus, for an ideal moving fluid, the sum of three heights, levelling, piezometric, and velocity, is constant along a filament.

This statement is illustrated by the diagram in Fig. 25, which shows the variation of all three heights along a filament. The curve of piezometric heights is called the piezometric line; it can be regarded as the geometric locus of levels in piezometers set up along the filament.

It follows from the Bernoulli and flow rate equations that if the cross-sectional area of the filament decreases, i.e., the filament tapers, the fluid flow velocity increases and pressure decreases; conversely, if the filament expands, velocity diminishes and pressure rises.

By way of example, Fig. 25 shows a filament whose cross-sectional area decreases by a factor of 4 from section 1-1 to section 2-2, with the result that the velocity head increases by a factor of 16 and section 3-3 has the same area as 1-1. The dashed curve is the piezometric line for a flowrate increase by a factor of  $\sqrt{2}$ , with the result that the velocity heights increase by a factor of 2 and the pressure drops below atmospheric in the narrow section of the filament.

Let us examine the physical or, more precisely, energetic sense of the Bernoulli equation. Let us adopt the term specific

<sup>2</sup>See page 74 for footnote.

energy for the energy of the fluid per unit weight, i.e.,

$$c = \frac{E}{G}.$$

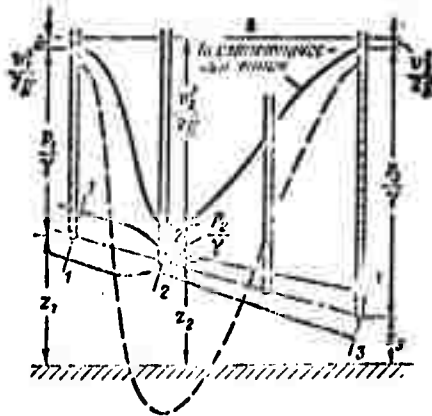


Fig. 25. Curve of variation of levelling, piezometric, and velocity heights along filament of ideal fluid.  
KEY: (a) piezometric line.

Specific energy has the dimensions of length, like the terms of the Bernoulli equation. It is easily shown that the terms of the Bernoulli equation are various forms of the fluid's specific mechanical energy, and namely:

$z$  is the specific position energy, since a fluid particle of weight  $\Delta G$  situated at height  $z$  has a position energy equal to  $\Delta Gz$  and, per unit weight,  $\Delta Gz/\Delta G = z$ ;

$p/\gamma$  is the specific pressure energy of the moving fluid, since a fluid particle weighing  $\Delta G$  and under a pressure  $p$  can rise through height  $p/\gamma$  and thereby acquire a position energy  $\Delta G(p/\gamma)$ ; on division by  $\Delta G$ , we obtain  $p/\gamma$ ;

$z + (p/\gamma)$  is the specific potential energy of the fluid;

$v^2/2g$  is the specific kinetic energy of the fluid, since the kinetic energy per unit weight of the same particle  $\Delta G$  is

$$\Delta G \frac{v^2}{2g} : \Delta G = \frac{v^2}{2g};$$

$H = z + \frac{p}{\gamma} + \frac{v^2}{2g}$  is the total specific energy of the moving fluid.<sup>3</sup>

<sup>3</sup>See page 74 for footnote.

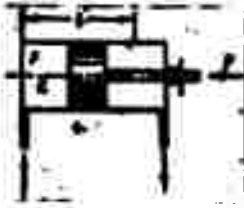


Fig. 26. Cylinder with piston and rod.

Thus, the energetic sense of the Bernoulli equation for an elementary filament of ideal fluid consists in constancy of the fluid's total specific energy along the filament. Consequently, the Bernoulli equation expresses the law of conservation of mechanical energy in an ideal fluid.

The mechanical energy of a moving fluid may take three forms: position, pressure, and kinetic energies. The first and third forms of mechanical energy are known from mechanics, and they are equally inherent to solids and fluids. As for the pressure energy, however, this form is specific for moving fluids.

During motion of an ideal fluid, one form of energy may be transformed into another, but the total specific energy, as follows from the Bernoulli equation, remains unchanged through this.

Pressure energy is easily transformed into mechanical work. An elementary device that brings this transformation about and is widely used on aircraft is the cylinder-and-piston group (Fig. 26). Let us show that in the transformation, the work per unit weight of fluid is numerically equal to the piezometric height.

Let us denote by  $S$  the piston area, by  $L$  its stroke, and by  $p$  the excess pressure admitted to the left chamber of the cylinder; the excess pressure on the other side of the piston is zero. Then the resultant pressure force of the fluid, which is equal to the force  $P$  that is overcome in moving the piston from the extreme left to the extreme right position, will be

$$P = pS,$$

and the work of this force

$$E = pSL.$$

The weight of fluid that must be supplied to the cylinder to perform this work is equal to the weight of fluid in the volume of the cylinder, i.e.,

$$G = SL\gamma.$$

Consequently, the work per kilogram will be

$$e = \frac{E}{G} = \frac{pSL}{SL\gamma} = \frac{p}{\gamma}.$$

The Bernoulli equation is often written differently. Multiplying all terms of (4.12) by  $\gamma$ , we obtain

$$z_1\gamma + p_1 + \gamma \frac{v_1^2}{2g} = z_2\gamma + p_2 + \gamma \frac{v_2^2}{2g}. \quad (4.13)$$

Now the terms of the Bernoulli equation have the dimensions of pressure:  $z\gamma$  is the weight pressure,  $p$  is the hydromechanical pressure (or simply the pressure), and  $\frac{\rho v^2}{2}$  is the dynamic pressure.\*

It is easily seen that the terms of (4.13) represent various forms of the fluid's mechanical energy per unit of its volume.

The Bernoulli equation for a filament of ideal fluid can also be derived easily by integrating the differential equations of motion of the ideal fluid.

#### §17. DERIVATION OF THE DIFFERENTIAL EQUATIONS OF MOTION OF AN IDEAL FLUID AND THEIR INTEGRATION

Let us take an arbitrary point  $M$  with the coordinates  $x, y, z$  (Fig. 27) in an ideal fluid and isolate an element of fluid at this point in the form of a rectangular parallelepiped with point  $M$  at one of its vertices. Let the sides of this parallelepiped be parallel to the coordinate axes and equal, respectively, to  $\delta x, \delta y,$  and  $\delta z$ .<sup>5</sup>

Let us write the equations of motion of this isolated fluid element, whose mass equals  $\rho\delta x\delta y\delta z$ .

As in our examination of the equilibrium of a similar fluid volume (see §6), we shall assume that the fluid in this volume is acted upon by a resultant mass force whose components, referred to the unit of mass, are  $X, Y,$  and  $Z$ . Then the mass forces acting on the isolated volume in the directions of the coordinate axes will be equal to these components multiplied by the mass of the isolated volume.

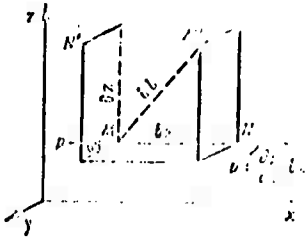


Fig. 27. Illustrating derivation of differential equations of motion of an ideal fluid.

If  $p$  is the pressure at point  $M$ , we find by reasoning similar to that in §6 that the difference between the pressure forces acting on the parallelepiped, e.g., in the direction of the  $x$ -axis, will be

$$-\frac{\partial p}{\partial x} \delta x \delta y \delta z.$$

The velocity of the fluid at point  $M$  will be denoted by  $\vec{v}$  and its components by  $v_x, v_y,$  and  $v_z$ . Then the projections of the acceleration with which the isolated volume is moving will be

$$\frac{dv_x}{dt}, \frac{dv_y}{dt}, \frac{dv_z}{dt}.$$

\*<sup>5</sup>See page 74 for footnotes.

NOT REPRODUCIBLE

and the forces that must be introduced into the equations of motion by the d'Alembert principle are determined as the products of these forces by the mass of the parallelepiped.

The equations of motion of the isolated fluid volume are now written as follows in the projections onto the coordinate axes:

$$\left. \begin{aligned} \rho \delta x \delta y \delta z \frac{dv_x}{dt} &= X \rho \delta x \delta y \delta z - \frac{\partial p}{\partial x} \delta x \delta y \delta z; \\ \rho \delta x \delta y \delta z \frac{dv_y}{dt} &= Y \rho \delta x \delta y \delta z - \frac{\partial p}{\partial y} \delta x \delta y \delta z; \\ \rho \delta x \delta y \delta z \frac{dv_z}{dt} &= Z \rho \delta x \delta y \delta z - \frac{\partial p}{\partial z} \delta x \delta y \delta z. \end{aligned} \right\}$$

We divide these equations term by term by the mass  $\rho \delta x \delta y \delta z$  of the element and pass to the limit, letting  $\delta x$ ,  $\delta y$ , and  $\delta z$  vanish simultaneously, i.e., letting the parallelepiped shrink to the original point M. Then at the limit we obtain the equations of motion of the fluid referred to point M:

$$\left. \begin{aligned} \frac{dv_x}{dt} &= X - \frac{1}{\rho} \frac{\partial p}{\partial x}; \\ \frac{dv_y}{dt} &= Y - \frac{1}{\rho} \frac{\partial p}{\partial y}; \\ \frac{dv_z}{dt} &= Z - \frac{1}{\rho} \frac{\partial p}{\partial z}. \end{aligned} \right\} \quad (4.14)$$

The equations of this system of differential equations of motion of the ideal fluid are known as the Euler equations. The terms of these equations represent the corresponding accelerations, and the sense of each of the equations is as follows: the total acceleration of a particle along a coordinate axis is composed of the acceleration of the mass forces and the acceleration of the pressure forces.

The Euler equations are valid in this form for both incompressible and compressible fluids, and for the case in which only gravity among the mass forces is in operation, and for the general case of relative motion of the fluid (see §44). Here the acceleration components of the translational (or rotational) motion must be introduced into the quantities X, Y, and Z. Since we did not impose the condition of steady motion in deriving Eqs. (4.14), they are also valid for nonsteady motion.

Considering steady motion of the fluid, let us multiply all equations of (4.14) by the corresponding projections of the elementary displacement, which equal

$$dx = v_x dt, \quad dy = v_y dt, \quad dz = v_z dt.$$

and add the equations. We have

$$X dx + Y dy + Z dz - \frac{1}{\rho} \left( \frac{\partial p}{\partial x} dx + \frac{\partial p}{\partial y} dy + \frac{\partial p}{\partial z} dz \right) = v_x dv_x + v_y dv_y + v_z dv_z. \quad (4.15')$$

Remembering that the expression in parentheses is the total differential of the pressure and that

$$v_x dv_x = d\left(\frac{v_x^2}{2}\right);$$

$$v_y dv_y = d\left(\frac{v_y^2}{2}\right);$$

$$v_z dv_z = d\left(\frac{v_z^2}{2}\right)$$

and

$$v_x^2 + v_y^2 + v_z^2 = v^2,$$

we can rewrite (4.15') in the form

$$Xdx + Ydy + Zdz = -\frac{1}{\rho} dp + d\left(\frac{v^2}{2}\right) \quad (4.15)$$

or

$$dU = -\frac{1}{\rho} dp + d\left(\frac{v^2}{2}\right),$$

where U is the force function with which we are already familiar (see §13).

We integrate this equation for the fundamental particular case of steady motion of an ideal fluid, when the fluid is acted upon only by a single mass force, gravity.

For this case, with the z-axis pointing vertically upward

$$X=0; Y=0; Z=-g.$$

Substituting these values into (4.15),

$$gdz + \frac{\rho}{\rho} dz + d\left(\frac{v^2}{2}\right) = 0$$

or

$$d\left(z + \frac{v^2}{2g}\right) = 0.$$

Since  $\gamma = \text{const}$  in the case of an incompressible fluid, the above equation can be rewritten

$$d\left(z + \frac{p}{\gamma} + \frac{v^2}{2g}\right) = 0.$$

This equation signifies that the increment in the sum of the three terms in the parentheses in displacement of a fluid particle along a streamline (trajectory) is zero. We infer from this that the above trinomial is a constant along a streamline, and hence also along an elementary filament, i.e.,

$$z + \frac{p}{\gamma} + \frac{v^2}{2g} = \text{const.}$$

NOT REPRODUCIBLE

Thus, we have arrived at the Bernoulli equation for a filament of ideal fluid, which we derived in the preceding section by another method.

If we write this equation for two sections of the filament, 1-1 and 2-2, it assumes the form already familiar to us (4.12).

#### §18. BERNOULLI EQUATION FOR VISCOUS-FLUID FLOW

On passing from the elementary filament of ideal fluid to a viscous-fluid flow that has finite dimensions and is bounded by walls, it will be necessary to remember, firstly, the nonuniformity of velocity distribution over the cross section and, secondly, the energy (head) losses. Both are consequences of the viscosity of the fluid.

In motion of a viscous fluid along a solid wall, as in a pipe, the flow is decelerated by viscosity and by the action of molecular cohesive forces between the fluid and the wall. As a result, velocity reaches its highest value at the center of the stream; as we approach the wall, velocity drops practically to zero. The result is a velocity distribution similar to that shown in Fig. 28.

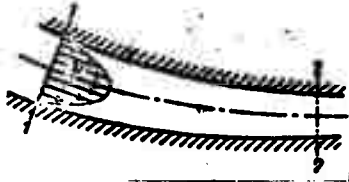


Fig. 28. Velocity distribution in stream.

Nonuniform velocity distribution implies slip (shear) of some layers or parts of the fluid with respect to others, giving rise to tangential stresses, i.e., frictional stresses. In addition, the motion of a viscous fluid is often accompanied by rotation of particles, eddy formation, and mixing. All of this requires expenditure of energy, so that the specific energy of a moving viscous fluid (its total head) does not remain constant, as in the case of the

ideal fluid, but is gradually expended in overcoming resistances and, consequently, decreases along the flow.

As a result of the nonuniform velocity distribution, it is necessary to introduce the velocity  $v_{sr}$  averaged over the cross section (see §15) and the average value of the fluid's specific energy in a given cross section.

Before turning to an examination of the Bernoulli equation for a flow of viscous fluid, we shall adopt the following assumption: within the flow cross sections under consideration, the fundamental law of hydrostatics is valid, for example, in the form of (2.3), i.e., the hydrostatic head is the same for all points in a section:

$$z + (p/\gamma) = \text{const (within the section).}$$

In so doing, we assume that individual filaments in the moving fluid exert the same pressure on one another in the transverse direction as layers of the fluid do at rest. This is realistic, and can be demonstrated theoretically in the case of parallel-filament flow in the cross sections under consideration. We shall therefore be examining precisely these cross sections (or closely similar ones).

Let us introduce the concept of flow power. The flow power in a given cross section is the total energy that the stream carries through this section per unit of time. Since the fluid particles have different energies at different points in the flow cross section, we shall first express the elementary power, i.e., the power of an elementary filament, as the product of the total specific energy of the fluid at the particular point by the elementary gravimetric flow rate:

$$dN = \rho v \left( z + \frac{v^2}{2g} + \frac{p}{\rho g} \right) dS$$

The power of the entire flow is found as the integral of this expression over the entire area S, i.e.,

$$N = \rho \int_S \left( z + \frac{v^2}{2g} + \frac{p}{\rho g} \right) v dS,$$

or, applying our assumption,

$$N = \rho \left( z + \frac{V^2}{2g} + \frac{p}{\rho g} \right) \int_S v dS = \rho Q \left( z + \frac{V^2}{2g} + \frac{p}{\rho g} \right)$$

Let us find the average total fluid specific energy over the cross section by dividing the total flow power by the gravimetric flow rate. Applying (4.4),

$$H_{\text{av}} = \frac{N}{Q} = z + \frac{V^2}{2g} + \frac{1}{2g} \frac{\int_S v^2 dS}{\int_S v dS}$$

Multiplying and dividing the last term by  $v_{\text{sr}}^2$ , we obtain

$$H_{\text{av}} = z + \frac{V^2}{2g} + \frac{\int_S v^2 dS}{v_{\text{sr}}^2 \int_S v dS} = z + \frac{V^2}{2g} + \alpha \frac{v_{\text{sr}}^2}{2g}, \quad (4.16)$$

where  $\alpha$  is a dimensionless coefficient that takes account of the velocity-distribution nonuniformity and equals

$$\alpha = \frac{\int_S v^2 dS}{v_{\text{sr}}^2 \int_S v dS} \quad (4.17)$$

If we multiply the numerator and denominator of (4.17) by  $\rho/2$ , we shall see at once that the coefficient  $\alpha$  is the ratio of

the actual flow kinetic energy in the given cross section to the kinetic energy of the same flow in the same section, but with a uniform velocity distribution.

For the usual type of velocity distribution (see Fig. 28), the coefficient  $\alpha$  is always greater than unity,<sup>6</sup> but it is unity for a uniform velocity distribution.

Let us take two sections through a real flow - first and second - and denote the average specific energy values (total heads) of the fluid in these sections by  $H_{sp1}$  and  $H_{sp2}$ , respectively; then

$$H_{sp1} = H_{sp2} + \sum h, \quad (4.18')$$

where  $\sum h$  is the total loss of specific energy (head) on the segments between these sections.

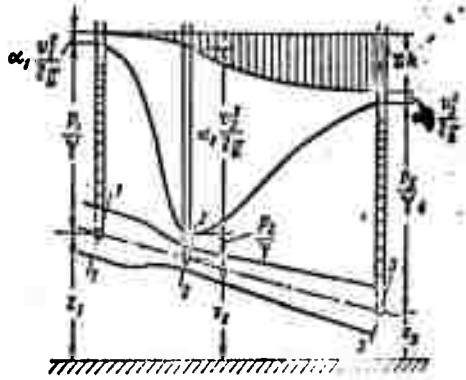


Fig. 29. Graphical illustration of Bernoulli equation for a real flow.

Applying (4.16), we can rewrite the above equation as follows:

$$z_1 + \frac{p_1}{\gamma} + \alpha_1 \frac{v_{cp1}^2}{2g} = z_2 + \frac{p_2}{\gamma} + \alpha_2 \frac{v_{cp2}^2}{2g} + \sum h. \quad (4.18)$$

This is the Bernoulli equation for viscous-fluid flow. It differs from its analogue for an elementary filament of ideal fluid in the term representing the specific-energy (head) loss and the coefficient that takes account of velocity-distribution nonuniformity. In addition, the velocities that appear in this equation are averages over the sections.

<sup>6</sup>See page 74 for footnote.

The Bernoulli equation (4.18) is applicable not only for liquids, but also for gases, assuming that their velocities are considerably below that of sound.

This equation can be represented graphically in much the same way as was done for the ideal fluid, but with consideration of the head loss. The latter also represents a certain height, which increases steadily along the flow (Fig. 29).

While the Bernoulli equation represents the law of conservation of mechanical energy for a filament of ideal fluid, it is an energy-balance equation with consideration of losses for the real flow. The energy lost by the fluid on the segment of flow under consideration does not, of course, vanish without a trace, but is simply converted into another form: heat. The thermal energy is, of course, continually being dissipated, so that the temperature rise is often hardly noticeable in practice. This process of conversion of mechanical energy into heat is irreversible, i.e., one that cannot reverse its course (with conversion of heat to mechanical energy).

The decrease in the average total specific energy of fluid flow along the stream, referred to unit stream length, is known as the hydraulic gradient. The change in specific potential energy of the fluid per unit length is called the piezometric gradient. Obviously, these gradients are the same in a pipe of constant diameter with constant velocity distribution.

#### §19. HYDRAULIC LOSSES (IN GENERAL)

Specific-energy (head) losses or, as they are commonly called, hydraulic losses, depend on the shape, dimensions, and roughness of the channel, flow velocity, and the viscosity of the fluid, but are practically independent of the absolute pressure in the fluid. Although it is the root cause of all hydraulic losses, fluid viscosity by itself influences the losses substantially in far from all cases. This will be discussed in greater detail below.

Experiments have shown that the hydraulic losses are in many cases approximately proportional to the square of velocity, and for this reason hydraulics has long made use of the following general method of expressing hydraulic total-head losses in linear units:

$$h = \zeta \frac{v_{cp}^2}{2g} \quad (4.19')$$

or in pressure units

$$\Delta p = h \gamma = \zeta \frac{v_{cp}^2}{2g} \gamma = \zeta \rho \frac{v_{cp}^2}{2}$$

This expression is convenient in that it incorporates the dimensionless proportionality factor  $\zeta$ , which is known as the

coefficient of resistance, and the velocity head, which appears in the Bernoulli equation.

Thus, the coefficient of resistance  $\zeta$  is the ratio of the lost head to the velocity head.

Hydraulic losses are usually classified into two forms: local and frictional.

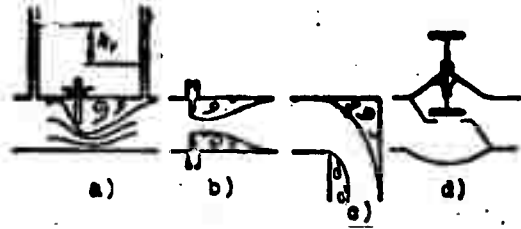


Fig. 30. Diagrams of local hydraulic resistances.

Local energy losses are governed by the so-called local hydraulic resistances, i.e., local changes in the shape and dimensions of the channel, which cause deformation of the stream. During passage of the fluid through local resistances, its velocity changes and eddies usually form.

The devices shown in Fig. 30 may serve as examples of local resistances: the check (a), diaphragm (b), elbow (c), and valve (d).

The local energy losses are determined by Formula (4.19')

$$h_m = \zeta_m \frac{v^2}{2g} \quad (4.19)$$

or

$$\Delta p_m = \zeta_m \frac{v^2}{2g} \gamma = \zeta_m \rho \frac{v^2}{2}.$$

This last equation is often referred to as the Weissbach formula.

In it,  $v$  is the average velocity over the cross section in the pipe in which the particular local resistance has been installed. If, on the other hand, the pipe diameter and, consequently, the velocity in it vary lengthwise, it is more convenient to take the higher of the velocities as the working velocity - i.e., the one that corresponds to the smaller pipe diameter. Each local resistance is characterized by its own resistance coefficient  $\zeta_m$ , which in many cases can be assumed approximately constant for a given local-resistance shape. Local hydraulic resistances will be examined more closely in Chapter VIII.

See page 75 for footnotes.

The frictional losses or length losses are energy losses that arise in pure form in straight constant-section pipes, i.e., in uniform flow, and increase in proportion to pipe length (Fig. 31). Losses of this type are governed by internal friction in the fluid, and therefore occur in pipes no matter how smooth their walls are.

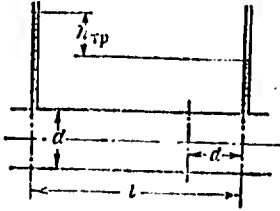


Fig. 31. Frictional loss of head in pipe.

The frictional loss of head can be expressed by the general formula for hydraulic losses (4.19'), i.e.,

$$h_{tr} = \zeta_{tr} \frac{v^2}{2g}, \quad (4.20')$$

but it will be more convenient to relate the coefficient  $\zeta_{tr}$  to the relative pipe length  $l/d$ .

Let us take a segment of round pipe whose length is equal to its diameter and denote by  $\lambda$  its coefficient of resistance, which appears in Formula (4.20'). Then the resistance coefficient for the entire pipe of length  $l$  and diameter  $d$  (see Fig. 31) will be larger by a factor of  $l/d$ , i.e.,

$$\zeta_{tr} = \lambda \frac{l}{d}$$

and Formula (4.20') becomes

$$h_{tr} = \lambda \frac{l}{d} \frac{v^2}{2g} \quad (4.20)$$

or

$$\Delta p_{tr} = \lambda \frac{l}{d} \frac{\rho v^2}{2g} \gamma. \quad (4.21)$$

Formula (4.20) is usually known as the Darcy formula.

The dimensionless coefficient  $\lambda$  will be referred to here as the coefficient of frictional loss or the coefficient of frictional resistance. It can be regarded as a coefficient of proportionality between the frictional head loss on the one hand and the product of relative pipe length by velocity head on the other.

We can easily establish the physical significance of the coefficient  $\lambda$  by examining the condition of uniform motion in a cylindrical pipe of length  $l$  and diameter  $d$ , i.e., zero sum of two forces acting on the volume: the pressure and friction forces. This equality takes the form

$$\frac{\pi d^2}{4} \Delta p_{tr} - \pi d l \tau_0 = 0,$$

where  $\tau_0$  is the frictional stress on the pipe wall.

From this, applying (4.21), we quickly obtain

$$\lambda = \frac{4\tau_0}{\gamma \frac{v^2}{2g}} = \frac{4\tau_0}{\rho \frac{v^2}{2}}, \quad (4.22)$$

i.e., the coefficient  $\lambda$  is proportional to the ratio of the frictional stress on the pipe wall to the dynamic pressure, the latter calculated from the average velocity.

In rammed flows (see §14), hydraulic losses occur owing to a decrease in the specific potential energy of the fluid ( $z + [p/\gamma]$ ) along the stream. Here, even if the specific kinetic energy of the fluid ( $v^2/2g$ ) changes along the stream at a given flow rate, this is not due to energy losses, but results from changes in the cross-sectional dimensions of the channel, since it depends only on velocity and velocity is determined by flow rate and sectional area:

$$v = \frac{Q}{S}.$$

On a constant-cross-section pipe, therefore, the average velocity and specific kinetic energy remain strictly constant despite the presence of hydraulic resistances and head losses. In this case, the head loss is determined as the difference between the readings of two piezometers (Figs. 30 and 31).

Calculation of hydraulic losses for various specific cases represents one of the basic problems of hydraulics. The next two chapters are devoted to this problem.

## §20. EXAMPLES OF APPLICATION OF THE BERNOULLI EQUATION IN ENGINEERING

The Bernoulli equation, which we derived in the preceding sections, is a fundamental law of steady-state fluid motion. It enables us to analyze and understand the operation of a number of devices whose action is based on utilization of this important law. Let us consider these devices.

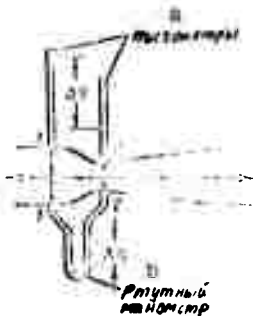


Fig. 32. Diagram of choke-type flowmeter.  
KEY: (a) piezometers;  
(b) mercury manometer.

1. The choke-type flowmeter, or Venturi flowmeter, is a device that is installed in pipelines and restricts or chokes the flow (Fig. 32). The flowmeter consists of two sections: a smoothly tapered section (the nozzle) and a progressively expanding section (diffuser). The flow velocity increases in the narrow section, and pressure drops. The result is a pressure difference (gradient), which is measured by a pair of piezometers or a U-tube differential manometer and is related in a definite manner to flow rate. Let us find this relationship.

Suppose that we have velocity  $v_1$ , pressure  $p_1$ , and sectional area  $S_1$  in section 1-1 of the flow immediately ahead of the constriction and  $v_2$ ,  $p_2$ , and  $S_2$ , respectively, in section 2-2, i.e., at the narrowest point of the flow.

Let us write the Bernoulli and flow-rate equations for the first and second flow sections (assuming the velocity distribution to be uniform):

$$\frac{p_1}{\gamma} + \frac{v_1^2}{2g} = \frac{p_2}{\gamma} + \frac{v_2^2}{2g} + h_m;$$

$$v_1 S_1 = v_2 S_2,$$

where  $h_m$  is the head loss between sections 1-1 and 2-2.

Remembering that

$$h_m = \zeta \frac{v_2^2}{2g} \quad \text{and} \quad \frac{p_1 - p_2}{\gamma} = \Delta H,$$

where  $\Delta H$  is the difference between the readings of the piezometers connected to these sections. From this equation system, we find one of the velocities, e.g.,  $v_2$ :

$$v_2 = \sqrt{\frac{2g\Delta H}{1 - \left(\frac{S_2}{S_1}\right)^2 + \zeta}}.$$

Hence the volume flow rate is

$$Q = v_2 S_2 = S_2 \sqrt{\frac{2g\Delta H}{1 - \left(\frac{S_2}{S_1}\right)^2 + \zeta}} \quad (4.23)$$

or

$$Q = C \sqrt{\Delta H}, \quad (4.23')$$

where  $C$  is a constant for a given flowmeter:

$$C = S_2 \sqrt{\frac{2g}{1 - \left(\frac{S_2}{S_1}\right)^2 + \zeta}}.$$

Knowing  $C$  and watching the piezometer readings, we can easily determine the flow rate in the pipe at any point in time by Formula (4.23'). The constant  $C$  can be calculated theoretically, but it is found more accurately from experiment, i.e., by calibrating the flowmeter.

The relation between  $\Delta H$  and  $Q$  is found to be parabolic. If we plot the square of flow rate along the axis of abscissas, the graph of this relationship will be a straight line.

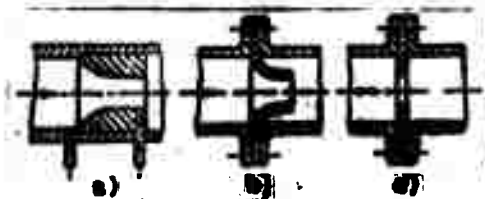


Fig. 33. Diagrams of metering nozzles and diaphragms.

Quite frequently, a differential mercury manometer (see Fig. 32) is used instead of the pair of piezometers to measure the pressure gradient in a flowmeter. Since the same fluid with its specific weight  $\gamma$  occupies the tubes above the mercury, we can write

$$\Delta H = \Delta h \frac{\gamma_p - \gamma}{\gamma}$$

It should be noted that the choke flowmeter can be made with the nozzle alone, which may be press-fitted into the pipe (Fig. 33a) or clamped between flanges (Fig. 33b). In this case, the same smooth constriction of the flow as in Fig. 32 will result, but the expansion of the flow beyond the nozzle will occur spontaneously and be accompanied by eddying. Hence the resistance of such a nozzle is higher than that of a nozzle fitted with a diffuser.

Flowmeters can also be made in the form of diaphragms (Fig. 33c). It must be remembered here that the smallest section of the flow will be to the right of the diaphragm plane owing to the additional constriction and will be somewhat smaller than the hole in the diaphragm.

Formula (4.21') also applies for these devices, but with certain correction factors, which can be found in the appropriate handbooks for the standard flowmeter forms.

These choke-type flowmeters are the most accurate types and are used to calibrate (test) aircraft flowmeters.

2. The carburetor of the piston-type internal-combustion engine has the function of aspirating gasoline and mixing it with a stream of air (Fig. 34). The stream of air drawn into the engine narrows at the exact position of the gasoline jet (at the cut end of the tube). In this cross section, the velocity of the air rises and the pressure drops in accordance with the Bernoulli law. The vacuum also draws gasoline through the jet into the air stream.

Let us find the relation between the gravimetric flow rates of the gasoline  $G_b$  and air  $G_v$  for given dimensions ( $D$  and  $d$ ) and

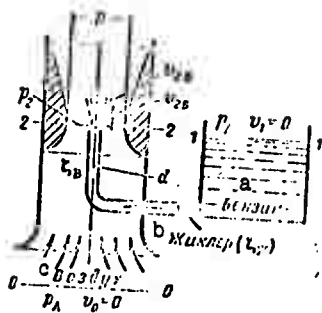


Fig. 34. Diagram of carburetor.  
KEY: (a) gasoline; (b) jet ( $\zeta_{zh}$ ); (c) air.

resistance coefficients of the air intake (upstream of section 2-2),  $\zeta_v$ , and the jet  $\zeta_{zh}$  (disregarding the resistance of the gasoline line).

Writing the Bernoulli equation for the air stream (section 0-0 and 2-2) and then for the gasoline stream (section 1-1 and 2-2), we obtain (for  $z_1 = z_2$  and  $\alpha = 1$ )

$$\frac{P_A}{\gamma_a} = \frac{P_2}{\gamma_a} - \frac{v_2^2}{2g} + \zeta_v \frac{v_2^2}{2g};$$

$$\frac{P_A}{\gamma_g} = \frac{P_2}{\gamma_g} - \frac{v_2^2}{2g} - \zeta_{zh} \frac{v_2^2}{2g}.$$

from which

$$\gamma_a \frac{v_2^2}{2g} (1 + \zeta_v) = \gamma_g \frac{v_2^2}{2g} (1 + \zeta_{zh}).$$

Remembering that the gravimetric flow rates equal

$$G_a = \frac{\pi D^2}{4} v_2 \gamma_a \quad \text{and} \quad G_g = \frac{\pi d^2}{4} v_2 \gamma_g.$$

we obtain

$$\frac{G_g}{G_a} = \left( \frac{d}{D} \right)^2 \sqrt{\frac{\gamma_a (1 + \zeta_v)}{\gamma_g (1 + \zeta_{zh})}}.$$

3. The jet pump (ejector pump) consists of a smoothly narrowing mouthpiece A (Fig. 35), which constricts the flow, and a progressively expanding pipe C, which is set up at a certain distance from the mouthpiece in chamber B. Owing to the flow-velocity increase the pressures in the jet and throughout chamber B are lowered considerably. In the expanding pipe, velocity decreases, and pressure rises to about atmospheric (if the fluid is flowing out into the atmosphere); consequently, the pressure in chamber B will normally be below atmospheric, i.e., a vacuum will be produced.

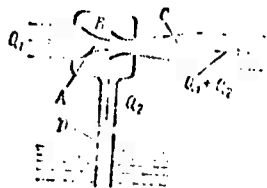


Fig. 35. Diagram of ejector pump.

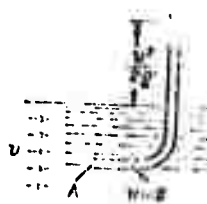


Fig. 36. Diagram of Pitot tube.

NOT REPRODUCIBLE



Fig. 37. Diagram of aircraft speed-indicator head.

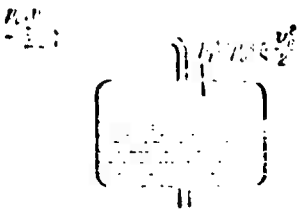


Fig. 38. Diagram of velocity pressurization.

This vacuum draws fluid from the tank at the bottom through line D into chamber B, where the two flows merge and then mix.

As a result, the fluid flow rate in pipe C is found to be equal to the sum of the flow rates  $Q_1$  in mouthpiece A and  $Q_2$  in induction pipe D. Ejectors are used in liquid rocket engines [LRE] (ЖРД), and in various other branches of engineering.

4. The Pitot tube can be used to measure flow velocity. Suppose that a fluid is moving in an open channel at velocity  $v$  (Fig. 36). If a pipe bent at a right angle is inserted in a stream with its orifice A facing into it, the fluid in this pipe will rise to a height equal to the velocity head above the free surface. The explanation for this is that the velocity of the fluid particles entering the orifice of the pipe drops to zero, so that the pressure is increased by an amount equal to the velocity head. The flow velocity is easily determined by measuring the height to which the fluid has risen in the pipe.

Aircraft airspeed indicators are built on the same principle. Figure 37 shows a diagram of an aircraft velocity tube (head) for low flight speeds (low by comparison with that of sound).

Let us write the Bernoulli equation for an elementary filament that enters the tube along its axis and then spreads out over its surface. Taking sections 0-0 (free stream) and 1-1 (where  $v = 0$ ), we have

$$p_0 + \frac{\rho v^2}{2} = p_1$$

Since the side-facing holes of the tube sense the approximate pressure of the free stream, we have  $p_2 \approx p_0$ ; consequently, the above yields

$$v = \sqrt{\frac{2(p_1 - p_2)}{\rho}}$$

5. Velocity pressurization (Fig. 38) is extensively used on aircraft to pressurize fuel and other tanks. At low flight speeds, the excess pressure in the tank is approximately equal to the dynamic pressure calculated from airspeed and air density.

## Footnotes

Manu-  
script  
page

- 50       <sup>1</sup>This last statement is proven in much the same way as for the stationary fluid (see §4): the equations of motion of an elementary tetrahedron are written with consideration of the d'Alembert forces, which are then allowed to vanish together with the mass forces as the tetrahedron shrinks to a point.
- 56       <sup>2</sup>Daniel Bernoulli (1700-1782), son of Johann and nephew of Jacob Bernoulli, the famous Swiss scientists, mathematicians, and mechanics. D. Bernoulli also worked in the fields of mathematics and mechanics; in his work entitled "Hydrodynamics" (1738), he laid the theoretical foundations of hydraulics as a science. D. Bernoulli spent a considerable part of his life at St. Petersburg as an active and, later, an honorary member of the Russian Academy of Sciences.
- 57       <sup>3</sup>It must be remembered that internal energy, which is characterized by the temperature of the fluid and does not change along a stream of ideal incompressible fluid, is not incorporated here into the concept of the total specific energy  $H$  of a fluid.
- 59       <sup>4</sup>It must be remembered that the pressure  $p$  is the only really existing pressure in the stream, i.e., the only stress of normal surface force. However, the other two quantities ( $zy$  and  $\rho(v^2/2)$ ) can easily be converted to corresponding pressures  $p$  and for this reason are also referred to conventionally as pressures.
- 59       <sup>5</sup>These arbitrary elementary segments should not be confused with the projections of the elementary displacements  $dx$ ,  $dy$ , and  $dz$ .
- 64       <sup>6</sup>This can be proven by expressing the velocity  $\underline{v}$  in Formula (4.17) as the sum  $v = v_{sr} + \Delta v$ , breaking the integral up into four integrals, and analyzing the numerical value of each of them.

Manu-  
script  
page

66       <sup>7</sup>The structure of these formulas can be obtained by dimensional analysis.

66       <sup>8</sup>From now on, the subscript "sr" to the symbol y will be used only when the average velocity might be confused with the local velocity.

### Symbol List

Manu- script page	Symbol		English equivalent
53	cp	sr	average
66	m	m	local
67	tp	tr	friction
71	x	zh	jet (carburetor)
71	b	v	air
71	o	b	gasoline

## C H A P T E R V

### FLUID FLOW IN PIPES. HYDRODYNAMIC SIMILARITY

#### §21. FLOWS OF FLUIDS IN PIPES

Experiments have shown that there are two possible regimes or two forms of liquid (and gas) flows in pipes: laminar and turbulent.

Laminar flow<sup>1</sup> is layered flow without mixing of fluid particles and without velocity pulsations. In such flows, all streamlines are fully determined by the shape of the channel through which the fluid is flowing. In laminar flow of a fluid in a straight pipe of constant cross section, all streamlines are parallel to the pipe axis, i.e., straight; there are no lateral movements of fluid particles and hence no mixing of the fluid as it flows. A piezometer connected to a pipe with a steady laminar flow indicates a constant pressure (and velocity) and the absence of oscillations (pulsations). Thus, a laminar flow is a fully ordered and, at constant head, strictly steady-state flow (although it may also be nonsteady in the general case).

However, a laminar flow cannot be regarded as irrotational, because even though it does not contain distinct eddies, the translational motion is accompanied by a simultaneous ordered rotational motion of the individual fluid particles around their instantaneous centers at quite definite angular velocities.

<sup>1</sup>See page 92 for footnote.

Turbulent flow<sup>2</sup> is flow accompanied by vigorous mixing of the fluid and by velocity and pressure pulsations. In a turbulent flow, the streamlines are determined only approximately by the shape of the channel. The motions of the individual particles are disordered, and the trajectories sometimes take the form of intricate curves. This is explained by the fact that in a turbulent flow, the fundamental longitudinal fluid displacement along the channel is accompanied by transverse displacements and rotational motions of individual fluid volumes.

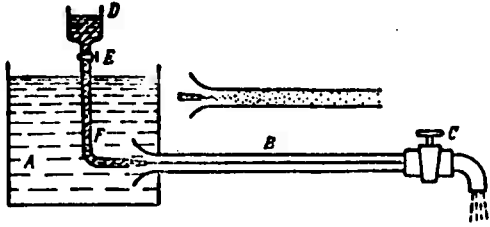


Fig. 39. Diagram of device used to demonstrate flow regimes.

These fluid-flow regimes can be observed in the apparatus shown above (Fig. 39). It consists of water tank A, from which is run a glass tube B with a cock C at its end, and a container D with an aqueous solution of a dye, which can be fed through tube F into glass tubes B in a thin filament.

If cock C is cracked open, allowing water to flow slowly through the tube, and cock E is then opened to admit the dye into the stream of water, we see that the dye introduced into the tube does not mix with the water stream. The dye filament will be clearly visible down the entire length of the glass tube, indicating that the fluid flow is laminar and that there is no mixing. This is the laminar flow regime.

As cock C is opened further, the water flow velocity in the tube increases, but the flow pattern does not change immediately; only at a certain flow velocity does a rapid change in the flow regime take place. The filament of dye exiting from the tube begins to oscillate, and then fades and mixes with the stream of water, with noticeable eddying and rotational motion of the fluid. The flow regime has become turbulent (see Fig. 39, top).

Laminar flow can be restored by lowering the flow velocity again.

The flow regime of this fluid in the tube changes at a definite flow velocity, which is known as the critical velocity ( $v_{kr}$ ). Experiments have shown that this velocity is directly proportional to the kinematic coefficient of viscosity ( $\nu$ ) and

<sup>2</sup>See page 92 for footnote.

inversely proportional to tube diameter ( $d$ ), i.e.,

$$v_{kp} = k \frac{v}{d}.$$

We find that the dimensionless proportionality coefficient  $k$  that appears here has a universal value, i.e., it is the same for all liquids and gases and all tube diameters.

This means that the flow regime changes at a quite definite relationship between viscosity, diameter, and the viscosity  $\nu$ ; it is

$$k = \frac{v_{kp} d}{\nu}.$$

This dimensionless number is known as the critical Reynolds number after the English scientist who established this criterion, and is denoted by

$$Re_{cr} = \frac{v_{kp} d}{\nu}. \quad (5.1)$$

Experiment has shown that the critical Reynolds number is approximately 2300.

However, we may speak not only of the critical number  $Re_{kr}$ , which corresponds to the change of regime, but also of the actual Reynolds number for any particular flow, expressing it in terms of the actual velocity, i.e.,

$$Re = \frac{v d}{\nu}. \quad (5.2)$$

Thus, we obtain a criterion by which we can judge the fluid-flow regimes in pipes. The flow is laminar for  $Re < Re_{kr}$  and usually turbulent for  $Re > Re_{kr}$ .

Knowing the fluid flow velocity, the tube diameter, and the fluid's viscosity, we can calculate the fluid-flow regime; this is highly important for later hydraulic calculations.

In practice, laminar flows are encountered when highly viscous fluids, such as lubricating oils, glycerin mixtures, etc., move through pipes.

Turbulent flow usually occurs in water lines and in pipes carrying gasoline, kerosene, alcohols, and acids. Thus, both laminar and turbulent fluid-flow regimes in pipes must be dealt with on aircraft; the flows are most often laminar in aircraft oil and hydraulic systems and turbulent in fuel systems.

The change in flow regimes on reaching  $Re_{kr}$  is explained by the fact that one flow regime loses stability, while the other

acquires it. For  $Re < Re_{kr}$ , the laminar regime is quite stable; all types of artificial turbulization of the flow and disturbances to it (shaking of the pipe, insertion of vibrating bodies into the flow, etc.) are damped by the effects of viscosity and laminar flow is restored. The turbulent regime is unstable under these conditions.

At  $Re > Re_{kr}$ , on the other hand, the turbulent regime is stable and laminar flow is unstable.

As a result, the critical number  $Re_{kr}$ , which corresponds to the transition from laminar to turbulent flow, may prove to be somewhat larger than the  $Re_{kr}$  for the reverse transition. Under special laboratory conditions, in the total absence of factors that contribute to flow turbulization, it is possible to obtain laminar flow at  $Re$  substantially larger than  $Re_{kr}$ . But in these cases the laminar flow is so unstable that, for example, a slight jolt is sufficient to transform the laminar flow quickly into a turbulent flow. In practice, and particularly in aircraft pipelines, we usually have conditions that promote turbulization - vibration of the pipes, local hydraulic resistances, nonuniformity (pulsations) of flow rate, etc., so that the above fact is of fundamental rather than practical importance in hydraulics.<sup>3</sup>

The question as to the stability of laminar flow and the turbulization mechanism has not yet been fully resolved theoretically. However, research has shown that such factors as distance from the wall, velocity, and its transverse gradient  $dv/dy$  tend to promote turbulization in a given section through a cylindrical pipe. The greatest wall distance and the highest velocity occur at the center of the stream, but the gradient  $dv/dy$  is zero there. At the wall, on the other hand, the velocity gradient is greatest, but the velocity and distance  $y$  are minimal or even zero. As a result, the initial turbulization of a laminar fluid in a straight pipe of constant cross section intervenes somewhere between the pipe axis and the wall, but closer to the wall.

Flow turbulization does not occur in the same way in variable-section pipes as in the cylindrical pipe. In expanding pipes, we observe deceleration of the flow and an increased tendency to transverse mixing, and  $Re_{kr}$  becomes smaller. In tapering pipes, flow is accelerated and the velocities are equalized over the cross section, there is less tendency to mix, and  $Re_{kr}$  increases.

## §22. HYDRODYNAMIC SIMILARITY

The Reynolds number derived in the preceding section is of great importance in hydraulics, and also in aerodynamics, since it is one of the basic criteria of hydrodynamic similarity.

<sup>3</sup>See page 92 for footnote.

Hydrodynamic similarity is similarity of incompressible-fluid flows and incorporates geometrical, kinematic, and dynamic similarities.

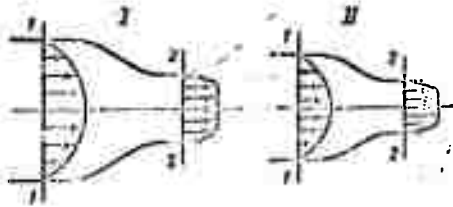


Fig. 40. Similar flows.

Geometrical similarity, as we know from geometry, means proportionality of corresponding dimensions and equality of corresponding angles. In hydraulics, we shall take geometrical similarity to mean similarity of the surfaces that bound the fluid flows, i.e., similarity of the channels (Fig. 40).

Kinematic similarity is similarity of streamlines and proportionality of corresponding velocities. Obviously, geometrical similarity of the channels is required for kinematic similarity of flows.

Dynamic similarity means proportionality of the forces acting on corresponding elements of kinematically similar flows and equality of the angles characterizing the directions of these forces.

A variety of forces are usually in operation in fluid flows — pressure, viscosity (friction), gravitational, and other forces. Observance of proportionality of all these miscellaneous forces signifies what is known as complete hydrodynamic similarity.

For example, proportionality of the forces of pressure  $P$  and friction  $T$  acting on corresponding volumes in flows I and II can be written

$$\left(\frac{P}{T}\right)_I = \left(\frac{P}{T}\right)_{II}.$$

It is extremely difficult to bring about complete hydrodynamic similarity in practice, and we therefore usually deal with partial (incomplete) similarity, in which proportionality of only the principal and basic forces is observed. For ramming flows in closed channels, i.e., flows in pipes, hydraulic machines, etc., calculations indicate that these principal forces are the forces of pressure, friction, and their resultants, i.e., forces of inertia. As can be shown for similar flows, the latter are proportional to the product of dynamic pressure  $\rho v^2/2$  by the characteristic area  $S$ .

Actually, for a fluid particle one of whose dimensions is  $\Delta l$ , the force is equal to the product of its mass by its acceleration, i.e.,

$$\Delta F = \rho (\Delta l)^3 \frac{dv}{dt} = k \rho (\Delta l)^3 \frac{dv}{ds} \frac{ds}{dt} = k \rho (\Delta l)^3 v \frac{dv}{ds},$$

where  $k$  is a dimensionless proportionality coefficient that depends on particle shape and  $ds$  is an element of the particle's path.

Let us multiply and divide the last expression by  $l^2$  and  $v_{sr}^2$ , i.e., introduce, in addition to the quantities that pertain to the particle, similarly named quantities that characterize the flow as a whole; we shall have

$$\Delta F = k \frac{\Delta l}{ds} \left( \frac{\Delta l}{l} \right)^2 \frac{v}{v_{sr}} d \left( \frac{v}{v_{sr}} \right) \rho v_{sr}^2 l^2.$$

The five dimensionless multipliers in the expression for  $\Delta F$  have the same values for geometrically and kinematically similar flows and similar particles. Consequently, by substituting the proportionality sign for the equals sign, we can write for these flows

$$\Delta F \sim \rho v_{sr}^2 l^2,$$

or, since  $l^2 \sim S$  and  $\Delta F \sim F$ , we finally obtain

$$F \sim \rho v_{sr}^2 S. \quad (5.3)$$

For similar flows I and II,

$$\frac{F_I}{F_{II}} = \left( \frac{v_{sr}^2 S}{v_{sr}^2 S} \right)_I,$$

or

$$\left( \frac{F}{\rho v_{sr}^2 S} \right)_I = \left( \frac{F}{\rho v_{sr}^2 S} \right)_{II}.$$

The latter ratio, which is the same for similar flows, is known as the Newton number and denoted by  $Ne$ .

We note in passing that the forces that the flow exerts (or could exert) on obstacles such as solid walls, vanes of hydraulic machines, bodies washed by the flow, etc., are proportional in similar flows to this same product  $\rho v_{sr}^2 S$ . Thus, if a fluid flow strikes an infinite wall (Fig. 41) that has been erected normal to it and changes direction by  $90^\circ$  as it spreads out over the wall, the momentum theorem of mechanics tells us that the per-second impulse of the force equals

$$P = \rho Q v = \rho v^2 S. \quad (5.4)$$

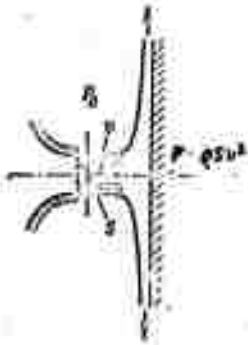


Fig. 41. Action of flow on obstacle.

This is the force that acts on the obstacle. If the wall is set at a different angle or has different shape and dimensions, the proportionality coefficient will be other than unity.

Let us examine the simplest case first - that of rammed flow of an ideal fluid, i.e., a motion in which there are no viscous forces and the action of gravity is manifested in pressure.

For this case, the Bernoulli equation for sections 1-1 and 2-2 (see Fig. 40) takes the form

$$\frac{p_1}{\gamma} + \frac{v_1^2}{2g} = \frac{p_2}{\gamma} + \frac{v_2^2}{2g},$$

or

$$\frac{p_1 - p_2}{\gamma \frac{v_2^2}{2}} = 1 - \frac{S_1^2}{S_2^2}.$$

For two geometrically similar flows, the right member of the equation has the same value; consequently, the left members are also the same, i.e., the pressure differences are proportional to the dynamic pressures:

$$\left(\frac{\Delta p}{\rho v^2}\right)_I = \left(\frac{\Delta p}{\rho v^2}\right)_{II}. \quad (5.5)$$

Thus, geometrical similarity alone is sufficient to ensure hydrodynamic similarity for rammed motions of an ideal incompressible fluid. The dimensionless quantity that represents the ratio of the pressure difference to the dynamic pressure (or of the piezometric-head difference to the velocity head) is known as the pressure coefficient or Euler number and is denoted by Eu.

Let us see what condition must be met by the same geometrically and kinematically similar flows to ensure their hydrodynamic similarity in the presence of viscosity forces and, consequently, energy losses - i.e., the condition for which the Eu will be the same for these rammed flows.

The Bernoulli equation will now take the form

$$\frac{p_1}{\gamma} + a_1 \frac{v_1^2}{2g} = \frac{p_2}{\gamma} + a_2 \frac{v_2^2}{2g} + \zeta \frac{v_2^2}{2g}.$$

or

$$\frac{2(p_1 - p_2)}{\rho v_2^2} = Eu = a_2 - a_1 \frac{v_1^2}{v_2^2} + \zeta. \quad (5.6)$$

As we see from (5.6), Eu will be the same for these flows and the flows will be similar to one another hydrodynamically if the resistance coefficients  $\zeta$  are equal (equality of the coefficients  $\alpha_1$  and  $\alpha_2$  for corresponding sections of the two flows follows from their kinematic similarity). Thus, the coefficients  $\zeta$  must be the same in similar flows, and this means that the head losses for corresponding segments (see Fig. 40) are proportional to the velocity heads, i.e.,

$$\left( \frac{h_{1-2}}{v_2^2} \right)_I = \left( \frac{h_{1-2}}{v_2^2} \right)_{II}$$

Let us consider a case of fluid motion that is very important in hydraulics - motion with friction in a cylindrical pipe, for which (see §19)

$$\zeta = \lambda \frac{l}{d}$$

The ratios  $l/d$  are the same for geometrically similar flows, and, consequently, identical values of the coefficient  $\lambda$  for these flows is a hydrodynamic-similarity condition in this case. On the basis of (4.22), this coefficient is expressed in terms of the frictional stress  $\tau_0$  at the wall and the dynamic pressure, as follows:

$$\lambda = \frac{4\tau_0}{\rho \frac{v^2}{2}}$$

Consequently, we can write for two similar flows I and II

$$\left( \frac{\tau_0}{\rho v^2} \right)_I = \left( \frac{\tau_0}{\rho v^2} \right)_{II} = k, \quad (5.7)$$

i.e., the frictional stresses are proportional to the dynamic pressures.

If we apply the third law of Newton and consider that  $v = v_{sr}$  in (5.7), the above ratios, denoted by the letter  $k$ , can be expressed as follows:

$$k = \mu \left( \frac{dv}{dy} \right)_{y=0} : \rho v_{cp}^2$$

where the subscript  $y = 0$  indicates that the derivative is taken at  $y = 0$ , i.e., at the pipe wall.<sup>4</sup>

After multiplying and dividing by the pipe diameter  $d$  and regrouping factors, we obtain

$$k = \left( \frac{dv}{dy} \right)_{y=0} \frac{d}{v_{cp}} \frac{\mu}{\rho} \frac{1}{e} \frac{1}{v_{cp} d} \dots \left[ \frac{d(v/v_{cp})}{d(y/d)} \right]_{y=0} \frac{v}{v_{cp} d} = c \frac{\nu}{v_{cp} d}$$

<sup>4</sup>See page 92 for footnote.

Here  $\underline{c}$  denotes the expression in the square brackets, which represents the dimensionless velocity gradient at the wall. The quantity  $\underline{c}$  is the same for kinematically similar flows, so that after cancelling the  $\underline{c}$ , the dynamic similarity condition for the flows (5.7) will be rewritten

$$\left(\frac{v}{v_0}\right)_I = \left(\frac{v}{v_0}\right)_{II}$$

or, converting to the reciprocals,

$$Re_I = Re_{II} \quad (5.8)$$

NOT REPRODUCIBLE

This is the import of the Reynolds similarity law, which can be stated as follows: with consideration of viscosity forces, equality of the Reynolds numbers calculated for any pair of corresponding sections through geometrically similar flows is required for hydrodynamic similarity of these flows.

It now becomes understandable why the transition from one flow regime to the other takes place at a definite  $Re$ , and the physical significance of this number for pipe flows has also been clarified, i.e.,  $Re$  is proportional to the ratio of the dynamic pressure to the frictional stress  $\sigma$ , which is the same thing, to the ratio of the inertial to the viscosity forces. The higher the velocity and the larger the transverse dimensions of the flow and the lower the viscosity of the fluid, the greater will  $Re$  become.  $Re$  is infinite for ideal-fluid flow, since the viscosity  $\nu = 0$ .

In nonramming flows (§14), the similarity question is complicated by the difference between levelling heights, since it is necessary to introduce one more similarity criterion - the Froude number, which takes account of the influence of gravity on fluid flow. But for the overwhelming majority of the problems that interest us in the field of aviation engineering, this criterion is unimportant and we shall not dwell upon it.

In similar flows, therefore, we have equality of the dimensionless coefficients, the numbers  $\alpha$ ,  $\zeta$ ,  $\lambda$ ,  $Eu$ ,  $Ne$ ,  $Re$ , and certain others that will be introduced and examined below. A change in  $Re$  signifies that the relationships among the principal forces in the flow have changed, with the result that these coefficients may also change. Thus, all of these coefficients must be regarded in the general case as functions of  $Re$  (although they may remain constant in certain  $Re$  ranges).

**Example.** Determine the flow regime of AMG-10 fluid in an aircraft hydraulic line with a diameter  $d = 12$  mm if the flow rate  $Q = 0.25$  l/s and the fluid temperature is  $0^\circ\text{C}$  (see Table 1 on page 12). At what temperature does the flow regime change?

**Solution.** 1. From Table 1 we find  $\nu = 42$  cSt =  $0.42$  cm<sup>2</sup>/s.

2. We determine the Reynolds number:

$$Re = \frac{v d}{\nu} = \frac{4Q}{\pi d^2 \nu} = \frac{4 \cdot 250}{\pi \cdot 3.02} = 632$$

The flow regime is laminar.

3. We find the viscosity corresponding to the flow-regime change:

$$\nu_{sp} = \frac{4Q}{\pi d Re_{sp}} = \frac{4 \cdot 250}{\pi \cdot 3.02 \cdot 2300} = 0.115 \text{ cm}^2/\text{s}.$$

4. Using the data in Table 1 for AMG-10 fluid, we plot a graph of the coefficient  $\nu$  as a function of temperature and use it to find  $t_{kr} = 40^\circ\text{C}$ .

### §23. CAVITATIONAL FLOW REGIMES

In certain cases, phenomena associated with changes in the physical state of the fluid, i.e., with its vaporization and with liberation of dissolved gases from the fluid, occur as fluids move in closed channels.

For example, in flow of a fluid through a local constriction in a pipe, velocity increases and pressure falls. If the absolute pressure reaches a value equal to the saturation vapor pressure of this fluid at the particular temperature, intensive vaporization and liberation of gases, i.e., local boiling of the fluid, begins at this point in the flow. In the expanding part of the flow, velocity decreases, pressure rises, and the boiling stops; the vapor that has been released is partially or totally condensed and the gases are gradually dissolved.

This local bumping of the fluid, which is governed by the local pressure drop in the flow with the subsequent condensation of vapor in a zone of higher pressure, is known as cavitation.



Fig. 42. Diagram of pipe for demonstrating cavitation.

KEY: (a) cavitation.

This phenomenon can be demonstrated impressively with a simple device (Fig. 42). Water or some other fluid is fed to regulating cock (valve) A at a pressure of several atmospheres and then allowed to flow through the glass tube, which first constricts the flow smoothly and then allows it to expand more smoothly until it discharges into the atmosphere through cock B.

When the regulating valve is cracked open and, consequently, the flow rates and velocities are low, the pressure drop at the throat of the tube is insignificant, the stream is quite transparent, and there is no cavitation. As cock A is progressively opened, velocity increases and the absolute pressure drops in the tube.

At  $p_{\text{abs}} = p_t$ , where  $p_t$  is the saturation vapor pressure, a distinct cavitation zone appears in the tube, and its dimensions increase as the valve is opened further.

Cavitation is accompanied by a characteristic noise, and, if it continues long enough, also by erosion damage to metal walls. The latter is explained by the fact that the vapor bubbles condense rather rapidly and the fluid particles filling the cavity of the condensing bubble rush toward its center, creating a local hydraulic shock as condensation culminates, i.e., a substantial local pressure increase. In cavitation, the material is damaged not where the bubbles are formed, but where they condense.

Cavitation is usually an undesirable effect and cannot be permitted in pipelines and other hydraulic systems. Cavitation causes a considerable increase in the resistance of the pipelines and, consequently, diminishes their throughput.

Cavitation may arise in any device in which the flow undergoes local constriction with subsequent expansion, e.g., in locks, valves, gates, diaphragms, nozzle jets, etc. In some cases, cavitation can occur even without expansion of the flow after the constriction, or in constant-section pipes on an increase in level height and hydraulic losses.

Cavitation can occur in hydraulic machines (pumps and hydraulic turbines) and on the blades of high-speed waterscrews. In these cases, it results in a sharp drop in the efficiency of the machine and then gradual destruction of the parts subject to cavitation.

In aircraft hydraulic systems, cavitation may arise as a result of a decrease in the external pressure as the airplane climbs. In this case, the cavitation region extends through a considerable part of the low-pressure pipeline (induction line) or even over its entire length. The result is a two-phased flow in the pipe, with liquid and vapor phases.

In the initial stage of vapor evolution, the vapor phase may take the form of minute bubbles distributed approximately uniformly through the volume of the moving fluid (Fig. 43a). On further release of vapor, the vapor phase increases and the bubbles grow, moving preferentially along the top of a horizontal pipe (Fig. 43b). Finally, the vapor and liquid phases may separate completely and move in independent streams: the former along the top of the line and the latter along the bottom (Fig. 43c).

Formation of vapor locks and motion of the phases in alternating slugs (Fig. 43d) are possibilities in small-diameter pipes.



Fig. 43. Diagrams of fluid-and-air flows.

Obviously, the throughput of the line is reduced substantially as the vapor phase increases. Condensation of the liberated vapor (partial or complete) takes place in pumps, where the pressure is increased substantially, and in the delivery pipes through which the fluid moves under high pressure from the pump to the appliance.

The cavitation phenomenon unfolds differently in single-component (simple) and multicomponent (complex) fluids. For a single-component fluid, the pressure corresponding to the onset of cavitation is fully determined by the saturation vapor pressure, which depends only on temperature, and cavitation proceeds in the manner described above.

A multicomponent fluid consists of so-called light and heavy fractions. The former have higher vapor pressures than the latter, so that the light fractions boil out first on cavitation, and then the heavy ones. Condensation of the vapor, on the other hand, takes place in the reverse order: the heavy fractions first, and then the light fractions.

In the presence of light fractions, multicomponent fluids have a stronger tendency to cavitation and their vapor phases persist longer, but the cavitation process is less conspicuous than in single-component fluids.

A dimensionless number known as the cavitation number is used to characterize flow regimes in respect to cavitation; it equals

$$\sigma = \frac{p - p_v}{\rho v^2 / 2}$$

where  $p$  and  $v$  are the absolute pressure and velocity of the flow, respectively.

The sense of the cavitation number is obviously similar to that of  $Eu$  (see §22). However, it is sometimes more convenient to use a slightly different expression for the cavitation number, i.e.,

$$\sigma = \sigma + 1 = \frac{p - p_v + \rho v^2 / 2}{\rho v^2 / 2} = \frac{p \gamma - p_v}{\rho v^2 / 2}$$

where  $H$  is the total head of the flow ( $z = 0$ ).

It is clear from the above exposition that  $\kappa = 0$  and  $\sigma = 1$  where cavitation arises. However, the cavitation number  $\kappa$  (or  $\sigma$ ) is usually determined at the entry into the unit in which cavitation is a possibility.

The value of  $\kappa$  (or  $\sigma$ ) at which cavitation begins in the unit is known as the critical cavitation number. For  $\kappa > \kappa_{kr}$ , the resistance coefficient  $\zeta$  of the unit does not depend on  $\kappa$ , but when  $\kappa < \kappa_{kr}$ ,  $\zeta$  increases with decreasing  $\kappa$ .

An effort is usually made to prevent cavitation in hydraulic systems. Sometimes, however, this phenomenon may be useful. For example, it is utilized in the so-called cavitation flow rate regulators.

The operating principle of such a regulator can be appreciated from the diagram of Fig. 42. Suppose that the pressure in section 1-1 ( $p_1$ ) is constant (the percentage opening of cock A is constant), and that the pressure in section 3-3 ( $p_3$ ) is gradually lowered by increasing the percentage opening of cock B. The result is that the flow rate through the pipe increases and the pressure in the throat section 2-2 ( $p_2$ ) decreases.

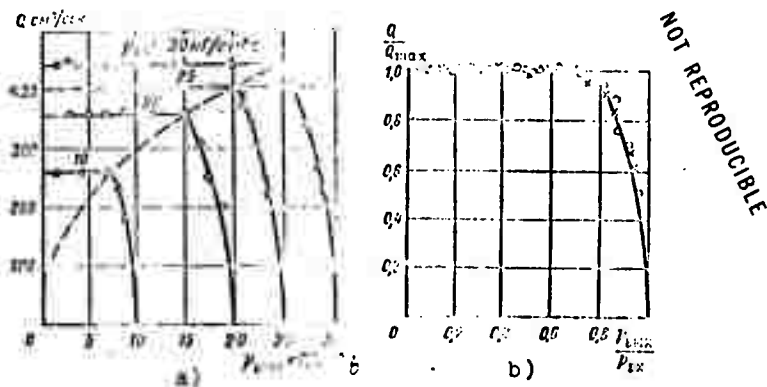


Fig. 44. Flow rate through cavitation pipe as a function of pressures at entrance and exit.

KEY: (a)  $\text{cm}^3/\text{s}$ ; (b)  $\text{kgf}/\text{cm}^2$ .

This will be the situation until the pressure  $p_2$  is made equal to the saturation vapor pressure  $p_t$  and cavitation begins in section 2-2. When cock B is opened further, the region of cavitation in the throat of the pipe will become larger and pressure  $p_2$  will become equal to  $p_t$ . The flow rate will remain constant through this despite the drop in pressure  $p_3$ .

This makes it possible to stabilize the fluid-flow rate through the regulator under conditions of variation of the back pressure  $p_2$  from critical  $(p_2)_{KR}$ , which corresponds to the onset of cavitation, to zero.

Figure 44 shows results of tests of a cavitation flow rate regulator made in the form of a Venturi tube with an axisymmetric throttle needle for adjustment of the throat-section area.<sup>5</sup>

Figure 44a shows curves of flow rate  $Q$  as a function of exit pressure  $p_2 = p_{vykh}$  for various entrance pressures  $p_1 = p_{vkh}$  and one regulating-needle position, while Fig. 44b shows the same curves replotted in dimensionless coordinates  $Q/Q_{max} = f(p_{vykh}/p_{vkh})$ , which yields a single curve.

The diagrams indicate that the precision of flow rate stabilization is very high.

The value of the critical pressure ratio, which corresponds to the onset of stabilization, is easily found from the following equations (we shall assume  $\alpha_1 = \alpha_2 = \alpha_3 = 1$ ).

- 1) The Bernoulli equation for sections 1-1 and 2-2

$$\frac{p_1}{\gamma} + \frac{v_1^2}{2g} = \frac{p_2}{\gamma} + \frac{v_2^2}{2g} + \zeta_c \frac{v_2^2}{2g}$$

- 2) Bernoulli equation for sections 1-1 and 3-3

$$\frac{p_1}{\gamma} + \frac{v_1^2}{2g} = \frac{p_3}{\gamma} + \frac{v_3^2}{2g} + (\zeta_s + \zeta_d) \frac{v_3^2}{2g}$$

- 3) The flow rate equation

$$v_1 S_1 = v_3 S_3$$

Here  $\zeta_s$  and  $\zeta_d$  are the respective resistance coefficients of the nozzle (segment 1-2) and the diffuser (segment 2-3).

Simultaneous solution of these equations on the assumption that  $p_2 = p_c$  and  $v_1 = v_3$  yields

$$\left(\frac{p_3}{p_1}\right)_{1,p} = \left(\frac{p_{vkh}}{p_{vkh}}\right)_{v,p} = 1 - \frac{\zeta_c + \zeta_d}{1 + \zeta_c + \kappa' - S_2^2/S_1^2}$$

where  $\kappa' = 2g\rho_1/\gamma v_2^2$ .

For the tested regulator, we can assume  $S_2^2/S_1^2 = 0$ ; moreover,  $\kappa' \approx 0$ , since the tests were run on cold water ( $p_c \approx 0$ ).

Since the regulator has a diffuser cone angle  $\alpha = 10^\circ$ , the diagram of Fig. 72 indicates  $\zeta_d = 0.19$ , while  $\zeta_s$  was found  
<sup>5</sup>See page 92 for footnote.

from the tests to be 0.07, which corresponds to the data in §4c.

Substituting these values into our formula, we find

$$\left(\frac{P_{\text{max}}}{P_{\text{at}}}\right)_{\text{sp}} = 1 - \frac{0.06 + 0.19}{1 + 0.06} = 0.765,$$

which agrees with the test results.

This stabilization of flow rate through cavitation is similar to the effects observed when a gas flows out through a hole or mouthpiece and the outflow velocity is made equal to the local speed of sound (see §77).

## Footnotes

Manu-  
script  
page

- 77      <sup>1</sup>From the Latin for layered.
- 78      <sup>2</sup>From the Latin for stormy, agitated.
- 80      <sup>3</sup>More precisely, turbulent flow in pipes is fully developed at  $Re > Re_{kr} = 4000$ , and a transitional critical region occurs at  $Re = 2300-4000$ .
- 84      <sup>4</sup>Newton's law of friction is applicable only for laminar flow. As will be shown below (see §28 and 29), however, a thin laminar layer within which Newton's law of friction is valid usually forms near the wall in turbulent pipe flows. Hence the frictional stress  $\tau_0$  at the wall can also be determined by this law for turbulent flow.
- 90      <sup>5</sup>The regulator was tested by B.L. Dzhikayev.

### Symbol List

Manu- script page	Symbol		English equivalent
78	кр	kr	critical
82	ср	sr	average
87	абс	abs	absolute
89	вх	vkh	entry
89	вых	vykh	exit
90	с	s	nozzle
90	д	d	diffuser

## CHAPTER VI

### LAMINAR FLOW

#### §24. THEORY OF LAMINAR FLUID FLOWS IN A ROUND PIPE

As we noted in §21, laminar flow is a strictly ordered layered flow without agitation of the fluid; it is subject to the Newtonian law of friction (see §3) and is fully defined by this law. Hence the theory of laminar fluid flow is based on Newton's law of friction.



Fig. 45. Illustrating theory of laminar fluid flow in a pipe.

Let us consider a steady-state laminar fluid flow in a straight circular-cylindrical pipe with an inside diameter  $d = 2r$ . To exclude the influence of gravity and thereby simplify the derivation, we shall use a horizontal pipe. At a sufficient distance from the entrance, we isolate a flow segment of length  $l$  between sections 1-1 and 2-2 (Fig. 45).

Let the pressure be  $p_1$  in the first section and  $p_2$  in the second. Owing to the constancy of pipe diameter, the velocity and the coefficient  $\alpha$  will be constant along the flow, so that the Bernoulli equation for the selected sections takes the form

$$\frac{p_1}{\gamma} = \frac{p_2}{\gamma} + h_{tr},$$

where  $h_{tr}$  is the frictional loss of head.

From this,

$$h_{tr} = \frac{p_1 - p_2}{\gamma} = \frac{F \Delta p}{\gamma},$$

which is indicated by piezometers attached at the sections.

In the fluid flow, we isolate a cylindrical volume of radius  $r$  coaxial with the pipe and having its bases in the chosen sections.

We write the equation of uniform motion of the isolated fluid volume in the pipe, i.e., we set the sum of the two forces acting on the volume - pressure and resistance - equal to zero. Using  $\tau$  to denote the tangential stress on the side of the cylinder, we obtain

$$(p_1 - p_2)\pi r^2 - 2\pi r l \tau = 0,$$

whence

$$\tau = \frac{p_1 p r}{2l}.$$

We see from the formula that the tangential stresses in a cross section of the pipe vary linearly as functions of radius. A diagram of tangential stress appears at the left in Fig. 45.

Let us express the tangential stress  $\tau$  in accordance with Newton's law of friction in terms of the viscosity coefficient and the transverse velocity gradient [Formula (1.14)]; here we substitute the present radius  $r$  for the variable  $y$  (distance from the wall):

$$\tau = \mu \left( \frac{dv}{dy} \right) = -\mu \frac{dv}{dr}.$$

The minus sign is due to the fact that the measuring direction for  $r$  (from the axis toward the wall) is the opposite of that in which  $y$  is reckoned (from the wall).

Substituting the values of  $\tau$  into the above equation,

$$\frac{F \mu r}{2l} = -\mu \frac{dv}{dr}.$$

From this, we find the velocity increment  $dv$ :

$$dv = -\frac{p_{tr}}{2\mu} r dr.$$

A negative increment (i.e., a decrease) in velocity corresponds to a positive radius increment, in agreement with the velocity profile shown in Fig. 45.

Integrating, we obtain

$$v = -\frac{p_{tr}}{4\mu} \frac{r^2}{2} + C.$$

We find the constant of integration C from conditions given at the pipe wall, where  $v = 0$  at  $r = r_0$ :

$$C = \frac{p_{tr}}{4\mu} r_0^2.$$

The velocity on a circle of radius  $r$  is

$$v = \frac{p_{tr}}{4\mu} (r_0^2 - r^2). \quad (6.1)$$

This is the law of velocity distribution across a circular pipe section in laminar flow. The curve representing the velocity diagram is a second-degree parabola.

The maximum velocity at the section center (at  $r = 0$ ) is

$$v_{max} = \frac{p_{tr}}{4\mu} r_0^2. \quad (6.2)$$

The ratio  $p_{tr}/\mu$  that appears in (6.1) represents, as we see from Fig. 45, the hydraulic (piezometric) gradient multiplied by  $\gamma$ . This quantity is constant along a straight pipe of constant diameter.

Let us apply the velocity-distribution law that we have derived (6.1) to compute flow rate. For this purpose, we first express the elementary flow rate across an infinitesimally small area  $dS$ :

$$dQ = v dS.$$

Here,  $v$  is a function of the radius that is determined by (6.1), and it is expedient to take the area  $dS$  in the form of a ring of radius  $r$  and width  $dr$ ; then

$$dQ = \frac{p_{tr}}{4\mu} (r_0^2 - r^2) 2\pi r dr.$$

On integration over the entire cross-sectional area, i.e., from  $r = 0$  to  $r = r_0$ , we have

$$Q = \frac{\pi p_{1p}}{2\mu l} \int_0^{r_0} (r_0^2 - r^2) r dr = \frac{\pi p_{1p}}{8\mu l} r_0^4. \quad (6.3)$$

We find the velocity averaged over the cross section by dividing the flow rate by the area:

$$v_{cp} = \frac{Q}{\pi r_0^2} = \frac{\pi p_{1p} r_0^4}{8\mu l r_0^2} = \frac{p_{1p}}{8\mu l} r_0^2. \quad (6.4)$$

Comparing this expression with (6.2), we conclude that the average velocity is half the maximum in laminar flow, i.e., that

$$v_{cp} = \frac{1}{2} v_{max}.$$

To obtain the law of resistance, i.e., an expression for the frictional head loss  $h_{tr}$  in terms of flow rate and pipe dimensions, we determine  $p_{tr}$  from (6.3):

$$p_{1p} = \frac{8\mu l Q}{\pi r_0^4}.$$

Dividing the equation by  $\gamma$ , we obtain the head loss:

$$h_{1p} = \frac{p_{1p}}{\gamma} = \frac{8\mu l Q}{\pi r_0^4 \gamma}.$$

Substituting  $\nu_0$  for  $\mu$  and  $g_0$  for  $\gamma$  and passing from  $r_0$  to  $d = 2r_0$ , we obtain finally

$$h_{1p} = \frac{160\nu_0 Q}{\pi g_0 d^4}. \quad (6.5)$$

This law of resistance indicates that in laminar flows in round pipes, the frictional head loss is proportional to the first powers of flow rate (velocity) and viscosity and inversely proportional to the fourth power of diameter. This law, which is frequently referred to as the Poiseuille-Hagen law, is used in calculations for pipelines in which flow is laminar.

Earlier (§19), we adopted the convention of expressing frictional head losses in terms of average velocity by Formula (4.18). Let us bring the law of resistance (6.5) to the form

$$l_{1p} = \lambda \frac{l}{d} \frac{v_{cp}^2}{g_0}.$$

To do so, we substitute the product  $\pi d^2 v_{sr} / 4$  for the flow rate in Formula (6.5); after cancelling,

$$p_{1p} = \frac{32\nu_0 v_{sr}}{g_0 d^3}.$$

Multiplying and dividing the right side of the equation by  $2v_{sr}$ , we obtain after regrouping factors

$$h_{1p} = \frac{64\nu}{v_{cp}d} \frac{l}{d} \frac{v_{cp}^2}{2g} = \frac{64}{Re} \frac{l}{d} \frac{v_{cp}^2}{2g},$$

or, reducing to the form of (4.20), finally

$$h_{1p} = \lambda_a \frac{l}{d} \frac{v_{cp}^2}{2g}, \quad (6.6)$$

where

$$\lambda_a = \frac{64}{Re}. \quad (6.7)$$

The subscript "1" to the  $\lambda$  stresses that we are speaking of laminar flow.

It must be remembered that the frictional head loss in laminar flow is proportional to the first power of velocity. Nor should it be forgotten that the square of velocity in Formula (6.6) for laminar flow was obtained by artificial multiplication and division by  $v_{sr}$ , and that the coefficient  $\lambda_{\underline{1}}$  is inversely proportional to  $Re$  and hence to the velocity  $v_{sr}$ .

Knowing the law of velocity distribution over the pipe cross section (6.1) and the relation between average velocity and head loss (6.4), it is easy to determine the value of the coefficient  $\alpha$ , which takes account of the velocity-distribution nonuniformity in the Bernoulli equation for the case of a stabilized laminar fluid flow in a round pipe.

In Expression (4.17), let us substitute the velocity according to (6.1) and the average velocity according to (6.4), remembering also that

$$S = \pi r_0^2$$

and

$$dS = 2\pi r dr.$$

After cancelling,

$$\alpha = \frac{1}{v_{cp}^2 S} \int_0^{r_0} v^3 dS = 16 \int_0^{r_0} \left(1 - \frac{r^2}{r_0^2}\right)^3 \frac{r dr}{r_0^2}.$$

Substituting the variable

$$1 - \frac{r^2}{r_0^2} = z,$$

we obtain

$$\alpha = \dots \int_1^0 z^2 / z = 2 \Big|_1^0 = 2. \quad (6.8)$$

Thus, the true kinetic energy of a laminar flow with a parabolic velocity distribution is twice that of the same flow when the velocities are uniformly distributed.

We can therefore show that the per-second momentum of a laminar flow with a parabolic velocity distribution is  $\beta$  times greater than the momentum of the same flow with uniform velocity distribution, and that the coefficient  $\beta$  is constant:

$$\beta = \int_0^R v^2 \cdot 2\pi r \cdot dr = \frac{4}{3}.$$

In general, the above theory of laminar fluid flow in a round pipe is nicely confirmed by experiment, and the resistance and velocity-distribution laws derived normally require no correction, except in the following cases.

1. For the flow at the start of the pipe, where the parabolic velocity profile is gradually established. The resistance is found to be higher on this segment than on those that follow it. However, this fact is taken into account only in calculations for very short pipes. This problem will be set forth in greater detail in the next section.

2. In flows with considerable heat transfer, i.e., when the fluid is heated or cooled while in motion (see §27).

3. For very high pressure gradients (see §27).

#### §25. THE INITIAL SEGMENT OF LAMINAR FLOW

If fluid runs from a tank into a straight constant-diameter pipe and thence along the pipe in a laminar flow, the velocity



Fig. 46. Shaping of parabolic velocity profile.

distribution is found to be practically uniform at first, especially if the entrance has rounded edges (Fig. 46). But then, under the action of viscous forces, the velocities are redistributed over the cross sections as follows: the layers of fluid next to the wall are slowed down, while the center (nucleus) of the flow, where the uniform velocity distribution still persists,

moves with an acceleration owing to the necessity of passing a definite flow rate through the constant area. Here the thickness of the decelerated fluid layers gradually increases until it becomes equal to the tube radius, i.e., until the layers on opposite walls meet at the axis of the pipe. Only then is the parabolic velocity profile characteristic of laminar flow established.

The distance from the beginning of the pipe at which the parabolic velocity profile is established (stabilized) is known as the initial flow segment ( $l_{nach}$ ). Beyond the initial segment, we have a stabilized laminar flow; the parabolic velocity profile remains unchanged no matter how long the pipe, provided that it remains straight and its section remains constant. The laminar-flow theory set forth above is valid for precisely this stabilized laminar flow and does not apply to the initial segment.

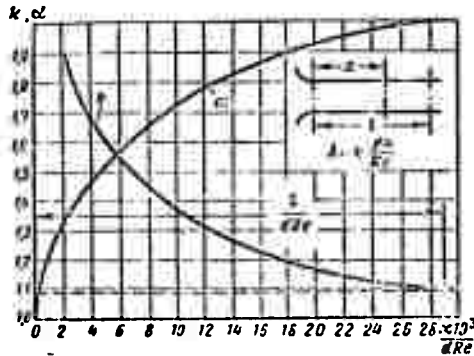


Fig. 47. Diagram showing variation of the coefficients  $K$  and  $\alpha$ .

To determine the initial-segment length, we can use the approximate Shiller formula, which expresses this length, referred to pipe diameter, as a function of Reynolds number:

$$\frac{l_{max}}{d} = 0,029 Re. \quad (6.9)$$

Substituting  $Re_{kr} = 2300$  into (6.9), we obtain the maximum possible length of the initial segment at 66.5 diameters.

As we noted above, the resistance is found to be higher on the initial segment of the pipe than on later segments. This is because the derivative  $dv/dy$  at the wall of the tube is larger on the initial segment than on the segments with stabilized flow, so that the tangential stresses defined by Newton's law are also larger and increase the closer the section under examination is to the beginning of the pipe, i.e., the smaller the  $x$ -coordinate.

The head loss on a segment of pipe whose length  $l \leq l_{\text{nach}}$  is determined by Formula (6.5) or by (6.6) and (6.7), but with a correction factor  $K$  greater than unity. The values of this coefficient can be found from the diagram (Fig. 47), in which the coefficient  $K$  is represented as a function of the dimensionless parameter  $(x/\text{Re } d) \cdot 10^3$ . As this parameter increases, the coefficient  $K$  becomes smaller, and at

$$\frac{x}{\text{Re } d} = \frac{l_{\text{nach}}}{\text{Re } d} = 0,029,$$

i.e., at  $x = l_{\text{nach}}$ , becomes equal to 1.09. Consequently, the resistance of the entire initial segment of the pipe is 9% higher than the resistance of the same length of pipe taken in the region of stabilized laminar flow.

For short pipes, as we see from the diagram, the correction factor  $K$  differs very greatly from unity.

When the pipe length  $l$  is greater than the initial-segment length  $l_{\text{nach}}$ , the head losses will be composed of the losses on the initial segment and the losses on the stabilized-flow segment, i.e.,

$$h_{\text{TP}} = \left[ 1,09 \lambda_a \frac{l_{\text{nach}}}{d} + \lambda_a \frac{(l - l_{\text{nach}})}{d} \right] \frac{\rho v^2}{2g}.$$

Applying (6.7) and (6.8) rearranging, and solving, we obtain finally

$$h_{\text{TP}} = \left( 0,165 + \frac{61}{\text{Re}} \frac{l}{d} \right) \frac{\rho v^2}{2g}. \quad (6.10)$$

If the pipeline length ratio  $l/d$  is large enough, the additional term 0.165 in the parentheses is small enough to be disregarded. However, this term should be taken into account in precision calculations for pipes whose length is comparable with  $l_{\text{nach}}$ .

For the initial segment of a tube with a flared entry, the coefficient  $\alpha$  rises from 1 to 2 (see Fig. 47).

## §26. LAMINAR FLUID FLOW IN GAPS

Let us consider laminar flow in a gap formed by two parallel flat walls separated by a distance  $a$  (Fig. 48). We shall place the coordinate origin at the center of the gap and direct the  $ox$ -axis along the flow and the  $oy$ -axis normal to the walls.

Let us take two normal cross sections of the flow at a distance  $l$  from one another and examine a unit flow width. We isolate a volume of fluid in the form of a right parallelepiped positioned symmetrically with respect to the  $ox$ -axis between the selected flow cross sections and having the side dimensions  $l \times 2y \times 1$ . We write the condition of uniform motion of this

volume along the ox-axis:

$$2y p_{tr} = -\rho \frac{dv}{dy} 2l,$$

where  $p_{tr} = p_1 - p_2$  is the pressure difference between these sections.

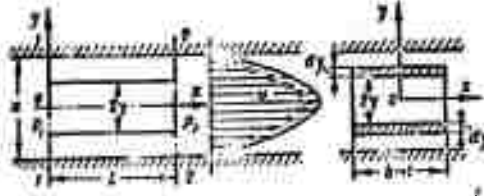


Fig. 48. Illustrating theory of laminar flow in gap.

The minus sign appears because the derivative  $dv/dy$  is negative.

From the above, we find the velocity increment  $dv$  corresponding to a coordinate increment  $dy$ :

$$dv = -\frac{p_{tr}}{\mu l} y dy.$$

Integration yields

$$v = -\frac{p_{tr}}{2\mu l} y^2 + C.$$

Since  $v = 0$  at  $y = a/2$ , we have  $C = \frac{p_{tr}}{2\mu l} \frac{a^2}{4}$ , from which, finally,

$$v = \frac{p_{tr}}{2\mu l} \left( \frac{a^2}{4} - y^2 \right). \quad (6.11)$$

Now let us calculate the flow rate per unit width by taking two elementary  $l \times dy$  areas symmetrically about the  $oz$ -axis and expressing the elementary flow rate

$$dQ = v dS = \frac{p_{tr}}{2\mu l} \left( \frac{a^2}{4} - y^2 \right) 2dy,$$

whence

$$Q = \frac{p_{tr}}{\mu l} \int_0^{\frac{a}{2}} \left( \frac{a^2}{4} - y^2 \right) dy = \frac{p_{tr} a^3}{12\mu l}. \quad (6.12)$$

From the above, we express the pressure loss in terms of the average velocity  $v_{sr} = Q/a$ :

$$P_{TP} = \frac{12\mu Ucy}{a^3} \quad (6.13)$$

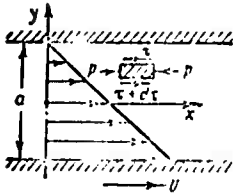


Fig. 49. Velocity profile in gap with moving wall.

When one of the walls forming the gap is in motion parallel to the other and the pressure in the gap is constant over its length, the moving wall will draw fluid with it, giving rise to what is known as nonramming frictional motion. Let us isolate an element from such a flow, as shown in Fig. 49, and examine the forces acting on it. Since the pressures  $p$  applied to the left and right faces of the element are the same, equilibrium of forces requires that the tangential stresses on the lower and upper faces also be the same. This implies that  $d\tau = 0$  and  $\tau = C$ , where  $C$  is a constant.

Using Newton's law of friction, we obtain

$$\tau = -\mu \frac{dv}{dy} = C$$

(the minus sign is taken because  $dv < 0$  when  $dy > 0$ ), and, after integration,

$$v = -\frac{C}{\mu} y + C_1$$

We find the constants  $C$  and  $C_1$  from the condition on the boundaries of the flow:  $v = 0$  at  $y = a/2$  and  $v = U$  for  $y = -a/2$ , where  $U$  is the speed of the wall. From this,

$$C = \frac{3\mu U}{a} \quad \text{and} \quad C_1 = \frac{U}{2}$$

After substitution into the integral, we finally obtain the linear velocity distribution law

$$v = \left(\frac{1}{2} - \frac{3y}{a}\right)U \quad (6.14)$$

The fluid flow rate per unit gap width is determined from the average velocity  $\frac{1}{2}U$ , i.e.,

$$Q = \frac{U}{2}a \quad (6.15)$$

If, however, this displacement of the wall takes place in the presence of a pressure gradient in the fluid filling the gap, the velocity distribution law in the gap will be found as the sum (or difference, depending on the direction of wall motion) of Expressions (6.11) and (6.14), i.e.,

$$v = \frac{P_{12}}{2\mu l} \left( \frac{a^2}{4} - y^2 \right) \pm \left( \frac{1}{2} - \frac{y}{a} \right) U.$$

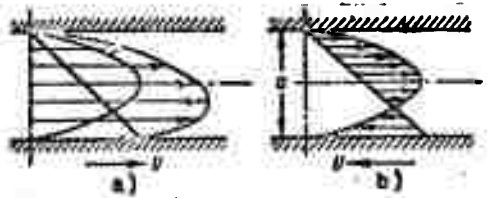


Fig. 50. Velocity profile in gap with moving wall and pressure gradient.

Two variants of the velocity distribution in a gap appear in Fig. 50: one in which the direction of wall motion coincides with the direction of fluid motion under the influence of the pressure

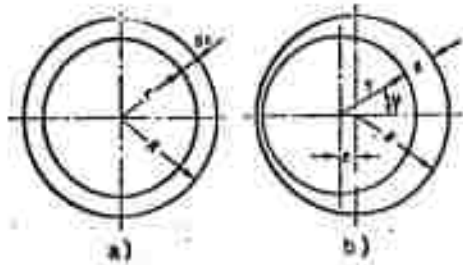


Fig. 51. Diagrams of concentric and eccentric gaps.

gradient (a), and one in which the direction of wall motion is opposite to the fluid flow (b).

In this case, the fluid flow rate through the gap will be determined as the sum of the flow rates expressed by Formulas (6.12) and (6.15), i.e.,

$$Q = \frac{P_{12} a^3}{12\mu l} \pm \frac{U}{2} a.$$

The first term in this formula is known as the ram flow rate and the second as the frictional flow rate.

These expressions can also be used when the gap is formed by two cylindrical surfaces, e.g., a piston and cylinder, provided that the gap between them is small by comparison with the

diameters of the surfaces and the surfaces are coaxial (Fig. 51a).

If the piston has a certain eccentricity  $e$  in the cylinder (Fig. 51b), the gap  $a$  between them will be variable, and it is easily seen that

$$a = R + e \cos \varphi - r = a_0 (1 + \epsilon \cos \varphi),$$

where  $a_0 = R - r$  and  $\epsilon = e/a_0$ .

Regarding an element of the gap of width  $rd\varphi$  as a plane slot, we obtain the following expression for the elementary flow rate:

$$dQ = \frac{p_1 \omega^3}{12\eta l} r d\varphi = \frac{p_1 \omega^3}{12\eta l} (1 + \epsilon \cos \varphi)^3 d\varphi.$$

Integrating around the circle, we obtain

$$Q = \frac{p_1 \omega^3}{12\eta l} \int_0^{2\pi} (1 + \epsilon \cos \varphi)^3 d\varphi = Q_0 \left( 1 + \frac{3}{2} \epsilon^2 \right),$$

where  $Q_0 = \frac{2\pi r \omega^3 a_0^3}{12\eta l}$  is the flow rate for the coaxial piston and cylinder.

It follows from the expression obtained for  $Q$  that at maximum eccentricity, i.e.,  $\epsilon = 1$ ,

$$Q = 2.5 Q_0.$$

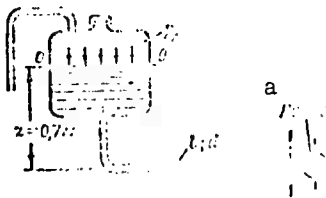


Fig. 52. Diagram of oil line.

KEY: (a) pump.

**Example.** To check out the altitude capability of an oil system, determine the absolute pressure at the entry into the pump in mmHg in level flight at 16 000 m of altitude ( $p_A / \gamma_{rt} = 77.1$  mmHg). The length of the intake oil line  $l = 2$  m,  $d = 18$  mm, the oil level in the tank is at a height  $z = 0.7$  m above the pump, and the pressure in the oil tank is atmospheric (Fig. 52). The required oil delivery rate, found from the amount of heat that must be dissipated into

the oil at maximum engine power, is  $Q = 16$  l/min; the viscosity of the MK-8 oil is  $\nu = 0.11$  cm<sup>2</sup>/s,  $\gamma_m = 900$  kgf/m<sup>3</sup>, and head losses in local resistances need not be taken into account.

**Solution.** 1. The velocity of the oil in the line is

$$v = \frac{4Q}{\pi d^2} = \frac{4 \cdot 16 \cdot 10^{-3}}{\pi \cdot 1.8^2 \cdot 10^{-4}} = 100 \text{ cm/s}.$$

2. The Reynolds number

$$Re = \frac{vd}{\nu} = \frac{105 \cdot 1,8}{0,11} = 1720.$$

3. The frictional loss of head in the intake pipe is

$$h_{rp} = \lambda_s \frac{l}{d} \cdot \frac{v^2}{2g} = \frac{64}{1720} \cdot \frac{200}{1,8} \cdot \frac{105^2}{2 \cdot 981} = 23,2 \text{ cm.}$$

4. We find the pressure at the pump entrance from the Bernoulli equation for sections 0-0 and 1-1:

$$z + \frac{pA}{\gamma_m} = \frac{p_1}{\gamma_m} + \alpha \frac{v^2}{2g} + h_{rp},$$

whence

$$\frac{p_1}{\gamma_m} = z + \frac{pA}{\gamma_m} - \alpha \frac{v^2}{2g} - h_{rp} = 70 + 7,71 \frac{13,6}{0,9} - \frac{2 \cdot 105^2}{2 \cdot 981} - 23,2 = 152 \text{ cm}$$

or

$$h_{pr} = 152 \frac{0,9}{13,6} = 10 \text{ cm} = 100 \text{ mmHg.}$$

## §27. SPECIAL CASES OF LAMINAR FLOW

### 1. Flow with Heat Transfer

In the cases of laminar flow considered above, no consideration whatsoever was given to temperature variation or, consequently, to viscosity changes either within the cross sections or along the flow, i.e., constancy of temperature at all points of the flow was assumed. Such flows are said to be isothermal, as distinct from flows accompanied by change in fluid temperature.

If a pipeline carries a fluid whose temperature is substantially higher than that of the environment, the flow will be accompanied by dissipation of heat through the pipe wall into the environment and, consequently, cooling of the fluid. If, on the other hand, the moving fluid is cooler than the environment, there will be an influx of heat through the pipe wall and the fluid will be heated as it flows.

In both of these cases, fluid flow is accompanied by exchange of heat with the environment and, consequently, the temperature and viscosity of the fluid are no longer constant and the flow is nonisothermal.

Formulas (6.5) and (6.13), which we derived above on the assumption of constant velocity over the flow cross section, require correction for flow with heat transfer.

In flow accompanied by cooling of the fluid, the layers of fluid directly adjacent to the wall are cooler and more viscous than those in the main nucleus of the flow. The results are

sharper deceleration of the wall layers of fluid and a drop in the velocity gradient at the wall.

On the other hand, if the flow is accompanied by heating of the fluid, the heat influx through the wall heats the wall layers of fluid and lowers their viscosity, so that the velocity gradient rises at the wall.

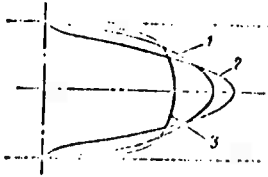


Fig. 53. Velocity distributions in isothermal and non-isothermal flows.

Thus, the normal parabolic velocity distribution is disturbed as a result of heat exchange through the pipe wall between the fluid and the environment. Figure 53 shows the velocity distribution in isothermal flow (1), in a flow in which the fluid is cooled (2), and in one in which it is heated (3). As we see from the figure, cooling of the fluid results in increased nonuniformity of the velocity distribution ( $\alpha > 2$ ), while heating reduces this nonuniformity ( $\alpha < 2$ ) by comparison with the ordinary parabolic velocity distribution ( $\alpha = 2$ ).

The change in the velocity profile in nonisothermal flow causes a change in the law of resistance.

Exact solution of problems of fluid flow with heat transfer is extremely complex, since it is necessary to consider the variability of fluid temperature and viscosity over the cross section and along the pipe, and to analyze the heat flows in various sections of the pipe.

For laminar flow of viscous fluids in pipes with dissipation of heat (cooling), the resistance is found to be higher than in isothermal flow, but it is smaller for flows with heat influx (heating). The basic reason for this is that the viscosity of the fluid in the layers next to the wall differs from the average fluid viscosity in the cross section.

This can be taken into account approximately by the following formula for the frictional loss coefficient  $\lambda_1$  in Formula (6.6). The expression

$$\lambda_1 = \frac{c}{Re_{zh}} \sqrt{\frac{\nu_{zh}}{\nu_{st}}}$$

is recommended instead of (6.7); here,  $Re_{zh}$  is the Reynolds number computed for the average fluid viscosity,  $\nu_{zh}$  is the fluid's average viscosity, and  $\nu_{st}$  is the fluid viscosity corresponding to the average wall temperature.

For more accurate calculations for small Reynolds numbers, it is necessary to use a formula due to Academician M.A. Mikheyev,

which is presented in [19].

## 2. Obliteration

A phenomenon that cannot be explained by the laws of hydraulics is sometimes observed when fluid flows through capillaries and small gaps. In this phenomenon, the flow rate of the fluid through the capillary or gap decreases with time despite the fact that the pressure gradient under which the fluid is moving and the physical properties of the fluid have not changed. Its cause is to be sought in a kind of plugging or coating of the channel by solid particles under certain conditions. Clearances and capillaries smaller than 0.01 mm may be clogged completely and the flow rates reduced to zero. This process is known as obliteration and consists in a so-called adsorption process that takes place on the interface between the solid and fluid under the action of molecular and electromagnetic forces that arise between the wall and the fluid, i.e., condensation of the fluid to a practically solid condition on the surface of the wall.

The extent of obliteration depends on the molecular structure of the fluid, and it is more conspicuous in complex, macromolecular fluids. This is the precise nature of the kerosene-based fluid mixtures used in aircraft hydraulic systems.

The thickness of the absorption layer is several microns for these fluids. Thus this layer can substantially reduce the cross-sectional area of the passage in flow through capillaries and small gaps, and even block it completely.

The intensity of adsorption and hence of obliteration decreases with rising temperature. On the other hand, an increase in the pressure gradient under which the fluid is moving through the gap or capillary increases the extent of obliteration.

If one of the walls forming the gap is set in motion, i.e., if shear occurs, previously formed absorption layers are broken up, obliteration is corrected, and the original flow rate of fluid through the gap is restored. However, this shear usually requires considerable effort. In general, obliteration does not occur in clearances between moving and stationary walls.

To prevent obliteration in nozzle jets and chokes, the holes should be made no smaller than 0.2-0.4 mm. Sometimes a reciprocating rod is passed through the choking orifice to provide for automatic clearing of the orifice and destruction of the adsorbed layers.

## 3. Laminar Flow at High Pressure Gradients

Experience has shown that the head loss along the stream is substantially nonlinear in laminar flows through small gaps and capillaries under the influence of large pressure gradients of the order of several hundred atmospheres, and that Poiseuille's law gives a rather large error.

This is because the fluid flow rate  $Q$  is proportional in laminar flow to the pressure gradient  $\Delta p$ , while the energy loss, which equals the product  $Q\Delta p$ , is proportional to the square of the pressure gradient. Hence the energy loss per unit of fluid flow rate increases in proportion to the pressure gradient. This results in heating of the fluid at high pressure gradients and a decrease in its viscosity; the influence of this factor will become stronger along the stream of fluid.

On the other hand, since fluid viscosity rises with increasing pressure, the viscosity at the beginning of the flow will be higher, but it will diminish along the flow as a result of the pressure drop. Thus, fluid viscosity becomes a variable along the flow and, as a result of the simultaneous operation of these two factors, the longitudinal pressure gradient  $dp/dx$ , which is governed by friction, will be larger at the beginning of the flow and smaller at the end than would follow from Poiseuille's law.

As for flow rate, a rise in temperature tends to increase it, and a high pressure in the fluid decreases it below the value obtained from Poiseuille's law, i.e., these two factors influence flow rate in opposite directions. However, total compensation is not normally the case, especially when there is a substantial amount of heat being dissipated through the wall and, consequently, the temperature increase is small.

This form of laminar flow is encountered particularly often in high-pressure hydraulic machines, in which a viscous fluid flows through small clearances under large pressure gradients.

Let us examine the problem of laminar flow in a gap of span  $a$ , length  $l$ , and width  $b$ , with consideration of viscosity as it varies with pressure and temperature. Here we shall assume that the density of the fluid does not depend on pressure or temperature and that the dimension ratio of the gap  $a/b \rightarrow 0$ .

To take the effects of pressure and temperature on fluid viscosity into account simultaneously, we shall use the following relationship in accordance with (1.17) and (1.18):

$$\mu = \mu_1 e^{(\alpha - \beta_1) - \lambda(\theta - \theta_1)} \quad (6.16)$$

Here the subscript 1 is attached to the quantities at the origin of the stream. Values of  $\alpha$  and  $\lambda$  were given in §3.

Placing the coordinate origin in the initial flow cross section (Fig. 54), we isolate an elementary fluid volume in the form of a rectangular parallelepiped positioned symmetrically about the  $x$ -axis and having the dimensions  $2y \times l \times dx$ , where the unit dimension is much smaller than the gap width  $b$ .

If the pressure acting on the left face of this volume is denoted by  $p$ , the right face will be acted upon by a pressure

$$p + dp$$

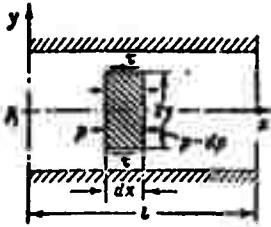


Fig. 54. Illustrating the theory of laminar fluid flow with variable viscosity.

The upper and lower faces will be acted upon by tangential stresses equal to

$$\tau = \mu \frac{dv}{dy}$$

and opposed to the motion.

The tangential stresses on the front and rear faces are zero, because velocity does not vary in the direction normal to the xoy-plane and, consequently, there is no velocity gradient.

Hence the equilibrium equation of our selected volume will be written

$$[p - (p - dp)] 2y - 2\mu \frac{dv}{dy} dx = 0$$

or

$$\frac{dv}{dy} = \frac{1}{\mu} \frac{dp}{dx} y.$$

It must be remembered that both of the derivatives are negative, since negative increments  $dp$  and  $dv$  correspond to positive increments  $dx$  and  $dy$ .

Integrating the equation within a flow cross section, and hence considering  $dp/dx$  and  $\mu$  to be constants, we obtain

$$v = -\frac{dp}{dx} \frac{1}{2\mu} y^2 + C.$$

Since  $V = 0$  at  $y = a/2$ , we have

$$C = -\frac{a^2 dp}{8\mu dx}$$

and, therefore,

$$v = \frac{1}{2\mu} \frac{dp}{dx} \left( y^2 - \frac{a^2}{4} \right). \quad (6.17)$$

We determine the flow rate per unit gap width by proceeding in much the same way as in the preceding section. Applying (6.17),

$$Q = \int_S v dS = -\frac{dp}{dx} \frac{1}{\mu} \int_0^{\frac{a}{2}} \left( \frac{a^2}{4} - y^2 \right) dy = -\frac{a^3}{12\mu} \frac{dp}{dx}. \quad (6.18)$$

This expression differs from (6.12) in that  $dp/dx$  and  $\mu$  are in this case variables that depend on  $x$ . Here, if  $Q = \text{const}$  (the fluid is absolutely incompressible), either variable is proportional to the other.

Let us now write the energy equation, i.e., set the frictional energy losses in the form of heat equal to the fluid's heat-energy increase per unit of time:

$$Q_0 c (t - t_1) = k (p_1 - p) Q. \quad (6.19)$$

Here  $c$  is the heat capacity of the fluid in SI units, i.e., in J/kg·deg;  $p$  is the pressure in N/m<sup>2</sup>;  $k$  is a coefficient that takes account of the fraction of the work of viscous forces that goes into heating the fluid.

For  $k = 1$ , no heat is dissipated through the wall and all of the work of viscous forces goes to heat the fluid. At  $k = 0$ , we have intensive dissipation of heat through the wall, and the fluid temperature is not raised (isothermal flow).

From the above, we have

$$t - t_1 = \frac{k}{c} (p_1 - p),$$

which yields, on substitution into (6.16),

$$\mu = \mu_1 e^{(p-p_1) \left(1 + \frac{k}{c}\right)}. \quad (6.20)$$

We use the relation obtained between  $\mu$  and  $p$  (6.20) to integrate (6.18).

On separation of variables, we have instead of (6.18)

$$\frac{12Q_0}{a^3} dx = - \frac{dp}{\mu}$$

or

$$\frac{12Q_0}{a^3} dx = - \int e^{(p_1-p) \left(1 + \frac{k}{c}\right)} dp.$$

After integration,

$$\frac{12Q_0 x}{a^3} = - \frac{1}{\alpha + \frac{k}{c}} e^{(\alpha + \frac{k}{c})(p_1 - p)} + C. \quad (6.21')$$

We find the constant of integration from the conditions in the initial flow cross section, where  $p = p_1$  at  $x = 0$  and, consequently,

$$C = \frac{1}{\alpha + \frac{k}{c}}.$$

In the final flow section at  $x = l$ ,  $p = p_{12b} = 0$ . Thus we finally obtain

$$Q = \frac{c^3}{12\mu_1 a^3} \left[ e^{\alpha \left( \frac{p_1}{c} \right)} - 1 \right]. \quad (6.21)$$

It must be remembered that the  $\mu_1$  that appears here is the viscosity in the initial flow cross section, i.e., that at  $p = p_1$  and  $t = t_0$ ; it can be expressed in terms of  $\mu_0$ , the viscosity at  $p = p_{1zb} = 0$  and  $t = t_0$ , in accordance with (6.16):

$$\mu_1 = \mu_0 e^{\alpha p_1}. \quad (6.22)$$

In the particular case of isothermal flow, it is necessary to set  $k = 0$  in (6.21). With consideration of the above, we then obtain

$$Q = \frac{c^3}{12\mu_0 a^3} (1 - e^{-\alpha p_1}). \quad (6.23)$$

We find the relative flow rate  $Q_0$ , which equals the ratio of the flow rate with variable viscosity to the flow rate at  $\mu = \mu_0 = \text{const.}$  For this purpose, we divide Eq. (6.21) by

$$Q_0 = \frac{Q}{Q_0} = \frac{e^{\alpha p_1} - 1}{\alpha p_1}.$$

NOT REPRODUCIBLE

We shall have

$$\bar{Q} = \frac{Q}{Q_0} = \frac{e^{\alpha p_1} - 1}{\alpha p_1} \left[ e^{\alpha \left( \frac{p_1}{c} \right)} - 1 \right] \quad (6.24)$$

Calculations were made by Formula (6.24) for a series of pressure values  $p_1$  from 0 to 800 kgf/cm<sup>2</sup> (7840 N/cm<sup>2</sup>) with the following values of the constants:  $\alpha = 1/430$  cm<sup>2</sup>/kgf (1/4210 cm<sup>2</sup>/N),  $\lambda = 1/36$  deg<sup>-1</sup>,  $c = 0.5$  kcal/kgf·deg (2.1 kJ/kg·deg), and  $\gamma = 850$  kgf/m<sup>3</sup> (8330 N/m<sup>3</sup>).

The results are presented in Fig. 55 as curves of  $\bar{Q}$  as a function of  $p_1$  for two values of  $k$ :  $k = 1$  (no heat exchange) and  $k = 0$  (isothermal flow).

As we see from the diagram, the curves corresponding to the two extreme conditions diverge quite widely. Real processes would be reflected by curves running somewhere between these extreme curves. Since the fluid flow velocities in gaps are very high at such high pressure gradients and the stay time of each particle in the gap is very short, the flow regime in which  $k \rightarrow 0$ , i.e., heat transfer is a minor factor, appears more probable.

But it must be remembered that with increasing relative gap length  $l/a$ , Reynolds number, and Prandtl number, the latter equal to

$$Pr = \frac{c_p \mu}{\lambda},$$

( $c$  is heat capacity and  $\lambda$  is the coefficient of thermal conductivity), the importance of heat transfer increases and the flow process may approach isothermal.

If Eq. (6.21') is divided, with the value found for the constant  $C$ , by Eq. (6.21), we obtain a formula linking the relative coordinate  $x/l$  and the pressures  $p$  and  $p_1$ .

By assigning various values to  $p$  at constant  $p_1$ , we can calculate the corresponding values of  $x/l$  and construct a diagram of the pressure along the gap for a series of constant pressure values  $p_1$  at the beginning of the gap.

The results of calculations of this kind are shown in Fig. 56 in the form of curves of  $p/p_1$  versus  $x/l$  for three constant  $p_1$  and  $k = 1$ .<sup>1</sup>

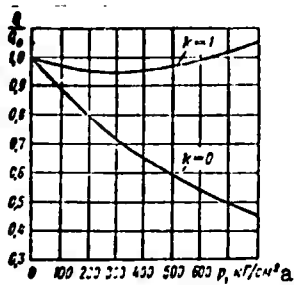


Fig. 55. Influence of variable viscosity on flow rate.  
KEY: (a) kgf/cm<sup>2</sup>.

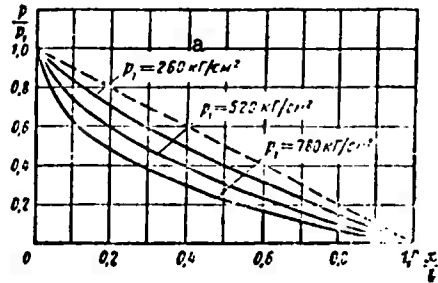


Fig. 56 Diagram of pressure along gap with consideration of variable viscosity and density.  
KEY: (a) kgf/cm<sup>2</sup>.

<sup>1</sup>See page 114 for footnote.

Footnote

Manu-  
script  
page

113

<sup>1</sup>Calculations performed by V.N. Prokof'yev and B.P. Borisov on the basis of their solution of the problem of laminar flow in a gap with consideration of viscosity and density variation.

### Symbol List

Manu- script page	Symbol		English equivalent
95	тр	tr	friction
97	ср	sr	average
98	л	l	laminar
100	нач	nach	initial
105	м	m	oil
105	рт	rt	mercury
107	ж	zh	fluid
107	ст	st	wall
111	изб	izb	excess

## CHAPTER VII

### TURBULENT FLOW

#### §28. TURBULENT FLOW OF FLUID IN SMOOTH PIPES

We said in §21 that turbulent flow is characterized by mixing of the fluid and by velocity and pressure pulsations during the flow process. If we were to use a highly sensitive automatic recording instrument to measure and register the pulsation of, for example, velocity as a function of time, we would obtain a pattern similar to that shown in Fig. 57. The velocity oscillates chaotically about a certain time-average value  $v_{osr}$ , which in this case remains constant.

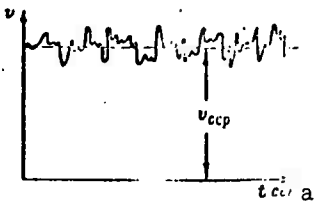


Fig. 57. Velocity pulsations in turbulent flow.  
KEY: (a) seconds.



Fig. 58. Nature of streamlines in turbulent flow.

The trajectories of particles passing through a given fixed point in space are represented for different points in time by

curved lines with different configurations, even though the pipe is straight. The nature of the streamlines in the pipe at a given point in time is also characterized by a great deal of variety (Fig. 58). Strictly speaking, therefore, turbulent flow is a nonsteady flow, since the velocities and pressures vary in time along with the particle trajectories. However, such flows may be regarded as steady in calculations provided that the time-averaged values of the velocity and pressure and the total flow rate of the flow do not vary with time. Such fluid flows are quite often encountered in practice.



Fig. 59. Velocity profiles in laminar and turbulent flows.  
KEY: (a) turbulent;  
(b) laminar.



Fig. 60. Diagram of coefficient  $\alpha$  as function of  $Re$ .

Since turbulent flows are not layered and the fluid mixes, the Newtonian law of friction is inapplicable. Because of the agitation of the fluid and the continual lateral transfer of momentum, the tangential stress on the pipe wall is substantially higher in turbulent than in laminar flow for identical values of  $Re$  and the dynamic pressure, as calculated from the average flow velocity.

The (time-averaged) velocity distribution in a cross section through a turbulent flow differs markedly from the characteristic distribution in laminar flow.

If we compare the velocity distribution curves in the same pipe and at the same flow rate (the same average velocity), but for laminar and turbulent flows, the difference in these curves will be quite substantial (Fig. 59). Under turbulent conditions, the velocity distribution is more uniform, and the velocity rise toward the wall is steeper than in laminar flow, for which, as we know, a parabolic velocity law is characteristic.

Thus, the coefficient  $\alpha$ , which takes account of the velocity distribution nonuniformity in the Bernoulli equation (see §18), is much smaller in turbulent than in laminar flow. In contrast to the laminar regime, where  $\alpha$  does not depend on  $Re$  (see §25), the coefficient  $\alpha$  is a function of  $Re$  in this case, diminishing with increasing Reynolds number from 1.18 at  $Re = Re_{kr}$  to 1.025 at  $Re = 3 \cdot 10^6$ . As we see from the diagram of Fig. 60, the curve of  $\alpha$  vs.  $Re$  makes an asymptotic approach to unity.<sup>1</sup> In

<sup>1</sup>See page 136 for footnote.

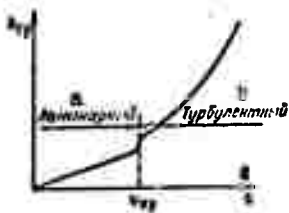


Fig. 61. Diagram of  $h_{tr}$  as function of

$v$  and  $Q$ .

KEY: (a) laminar;  
(b) turbulent.

of flow rate), transition to turbulent flow is accompanied by a certain discontinuity of resistance and then by a steeper increase in  $h_{tr}$  along a curve closely approximating a second-degree parabola (Fig. 61).

In view of the complexity of turbulent flow and the difficulty encountered in its analytical investigation, we do not yet have a sufficiently rigorous and exact theory of this flow. Instead, there are the so-called semiempirical, approximate turbulence theories of Prandtl, Karman, and others, one of which will be examined in the next section.

In most cases, purely experimental data that have been codified on the basis of hydrodynamic similarity theory are used for practical calculations involving turbulent fluid flows in pipes.

The basic working formula for turbulent flow in round pipes is the universal formula (4.20) derived above, which follows directly from similarity considerations and takes the form

$$h_{tr} = \lambda_t \frac{l}{d} \frac{v^2}{2g}$$

or

$$h_{tr} = \lambda_t \frac{l}{d} \frac{16Q^2}{2g\pi^2 d^5}$$

where  $\lambda_t$  is the coefficient of frictional loss in the turbulent regime.

This fundamental formula is applicable to both turbulent and laminar flows (see §24); the difference consists in the values of the coefficient  $\lambda$ .

Since the frictional head loss in turbulent flow is approximately proportional to the square of velocity (and the square of flow rate), the frictional-loss coefficient in Formula (4.20) may be regarded as constant in first approximation for a given pipe.

most cases, we can assume  $\alpha = 1$  for turbulent flows.

The energy losses in turbulent fluid flow in constant-section pipes (i.e., the frictional head losses) are also different from those in laminar flow. In turbulent flow, the frictional head losses are substantially larger than in laminar flows with the same dimensions, flow rates, and viscosities.

This increase in losses is caused by eddying, mixing, and the curvature of the trajectories. While the frictional head loss increases in laminar flow in proportion to the first power of velocity (and

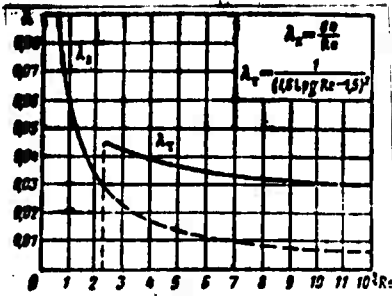


Fig. 62. Diagram of  $\lambda_1$  and  $\lambda_t$  as functions of  $Re$ .

But it follows from the law of hydrodynamic similarity (§22) that, like  $\lambda_1$ , the coefficient  $\lambda_t$  must be a function of the fundamental similarity criterion, i.e., the Reynolds number, which incorporates velocity, diameter, and viscosity, i.e.,

$$\lambda_t = f(Re) = f\left(\frac{vd}{\nu}\right).$$

There are a number of empirical and semiempirical formulas that express this function for turbulent flow in smooth pipes; one of the most convenient and widely used is that of P.K. Konakov, which takes the form

$$\lambda_t = \frac{1}{(1.81 \lg Re - 1.5)^2} \quad (7.1)$$

and is applicable from  $Re = Re_{kr}$  to  $Re$  ranging into the millions.

The old Blasius formula

$$\lambda_t = \frac{0.3161}{\sqrt[5]{Re}} \quad (7.2)$$

can also be used for Reynolds numbers in the range  $2300 < Re < 10^5$ .

We see from this that the coefficient  $\lambda_t$  decreases with increasing  $Re$ , but that this decrease is much less substantial than in laminar flow (Fig. 62).

This difference in the curves of  $\lambda$  results from the fact that the direct influence of fluid viscosity on resistance is much weaker in turbulent than in laminar flow. While the frictional head loss in laminar flow is directly proportional to viscosity (see §24), these losses are proportional to the  $1/4$  power of viscosity in turbulent flow, as follows from Formulas (4.20) and (7.2). As a matter of fact, mixing and momentum transfer are the basic factors in turbulent flow.

The above formulas (7.1) and (7.2) for determination of the coefficient of frictional loss  $\lambda_t$  in terms of  $Re$  are valid for the so-called technically smooth pipes, i.e., for pipes whose roughness is so slight that it has practically no influence on resistance. Seamless pipes drawn from nonferrous metals (including aluminum alloys) and carefully made seamless steel pipes can be classified as technically smooth without incurring any major error. Thus, the pipes used as fuel lines and for hydraulic transmissions (hydraulic systems) on aircraft can, under normal conditions, be regarded as smooth, and calculations for them can be made by the above formulas. Steel and cast-iron water pipes,

on the other hand, cannot be regarded as smooth, since they usually offer higher resistance, and Formulas (7.1) and (7.2) do not apply for them.

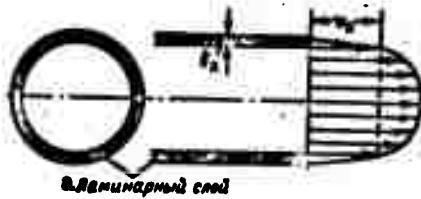


Fig. 63. Laminar layer at wall of pipe in turbulent flow.  
KEY: (a) laminar layer.

The resistance of rough-walled pipes is a problem that will be examined later (see §30).

As follows from similarity theory, and as the experiments of a number of investigators (I.I. Nikuradze, G.G. Gurzhiyenko, Reichardt, and others) indicate, turbulent flow of fluid in pipes is usually accompanied by a so-called laminar layer directly at the pipe wall (Fig. 63). This is a very thin layer of fluid in which the motion is slowest, stratified, and without mixing, i.e., laminar.

In this laminar layer, velocity rises steeply from zero at the wall to a certain finite value  $v_1$  at the layer boundary. The thickness  $\delta_1$  of the laminar layer is extremely small, and we find that the Reynolds number  $Re$ , calculated from the dimension  $\delta_1$ , the velocity  $v_1$ , and the kinematic viscosity coefficient  $\nu$ , is a constant, i.e.,

$$\frac{v_1 \delta_1}{\nu} = \text{const.} \quad (7.3)$$

This is a universal constant, like the critical Reynolds number  $Re$  for pipe flows. Thus, on an increase in flow velocity and, consequently, in  $Re$ , the velocity  $v_1$  also increases, while the thickness  $\delta_1$  of the laminar layer decreases. The laminar layer practically vanishes at large  $Re$ .

## §29. FUNDAMENTALS OF SEMIEMPIRICAL THEORY OF TURBULENT PIPE FLOW

It follows from the description of turbulent flow given in the preceding section that the true local velocity at a given point in time in a turbulent flow must be regarded as the sum of the time-averaged velocity and a certain positive or negative increment known as the pulsation velocity (see Fig. 57). As a

convention, we shall denote time-averaged quantities by the over-bar and pulsation velocities by the prime; we can then write for the component of local velocity along the pipe axis (the  $x$ -axis)

$$v_x = \bar{v}_x + v'_x,$$

where

$$\bar{v}_x = \bar{v} = \frac{1}{t} \int_0^t v_x dt.$$

$t$  is the time segment over which the velocity is averaged.

Since there is no averaged flow along the  $y$ - and  $z$ -axes in a straight pipe of constant section,  $\bar{v}_y = \bar{v}_z = 0$  and  $v_y = v'_y$ ,  $v_z = v'_z$ . Obviously, the averaged value of the pulsation velocities, obtained by the same method over an adequate length of time, will be zero, i.e.,

$$\bar{v}'_y = \bar{v}'_z = \bar{v}'_x = 0.$$

To find the relation between tangential stress in a turbulent flow and the pulsation velocities, let us take an elementary area  $dS$  of the flow that lies parallel to the pipe wall (Fig. 64). Owing to the presence of the pulsation velocity  $v'_y$ , a mass of liquid equal to

$$dm = \rho v'_y dS dt.$$

passes through area  $dS$  during time  $dt$ .

Since at the same time this mass acquires an additional velocity  $v'_x$  along the stream, the corresponding momentum increment will be

$$v'_x dm = \rho v'_x v'_y dS dt.$$

As a result of transport of this momentum through area  $dS$  from one layer into another, a tangential force  $\tau_t dS$  whose impulse over time  $dt$  is equal to the transferred momentum, i.e.,

$$\tau_t dS dt = \rho v'_x v'_y dS dt,$$

arises along this area.

After cancelling, this yields the absolute value of the local tangential stress due to turbulent mixing at a given time:

$$\tau_t = \rho v'_x v'_y.$$

The tangential stress averaged over time interval  $\tau$  is found as follows:

$$\bar{v}_x = \frac{\rho}{l} \int v_x' v_x' dl$$

or

$$\bar{v}_x = \rho \overline{v_x' v_x'} \quad (7.4)$$

where  $\overline{v_x' v_x'}$  is the averaged value of the pulsation-velocity product.

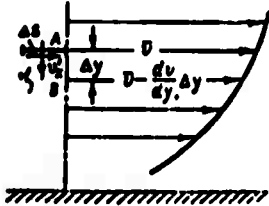


Fig. 64. Illustrating theory of turbulent mixing.

To convert from the pulsation velocities  $v_x'$  and  $v_y'$  to the averaged velocities ( $\overline{v_x} = \bar{v}$ ) and thereby render the above formula suitable for practical use, we reason as follows. Let a fluid particle be displaced transversely as a result of turbulent mixing from layer A, where the averaged velocity is  $\bar{v}$ , into layer B (see Fig. 64).<sup>2</sup> If the distance between layers A and B is denoted by  $\Delta y$ , the averaged velocity of layer B will be

$$\bar{v} + \Delta y \frac{d\bar{v}}{dy}$$

(we have omitted the subscript  $x$  to the average velocities).

Carrying the velocity excess  $\Delta y \frac{d\bar{v}}{dy}$  with it into layer B, the particle will cause a pulsation  $v_y'$ , as well as a  $v_x'$ .

We can assume that these pulsation velocities are proportional to the indicated velocity excess, i.e.,

$$v_x' \sim \Delta y \frac{d\bar{v}}{dy} \quad \text{and} \quad v_y' \sim \Delta y \frac{d\bar{v}}{dy}$$

(here  $\sim$  is the proportionality sign).

Applying (7.4), therefore, we can write

$$\tau_x \sim (\Delta y)^2 \left( \frac{d\bar{v}}{dy} \right)^2 \quad (7.5')$$

or, incorporating the proportionality factor in a certain linear quantity  $l$ ,

$$\tau_x = \rho l^2 \left( \frac{d\bar{v}}{dy} \right)^2 \quad (7.5)$$

This expression is named after L. Prandtl<sup>3</sup> and is a law of turbulent flow that is used in turbulent-flow theory in the same way as Newton's law of friction is used in laminar-flow theory.

<sup>2,3</sup>See page 136 for footnotes.

The quantity  $l$ , which is known as the "mixing length," is proportional to the time-averaged particle displacement in the transverse direction. The mixing length may be regarded as a notion that is to a certain degree analogous to the concept of molecular free path in the kinetic theory of gases (it must be remembered that turbulent mixing involves the displacement not of individual molecules, but of fluid particles consisting of large numbers of molecules).

Obviously,  $l$  takes different values at different points in the pipe cross section. At the wall of the pipe and within the laminar layer, where there are no transverse particle displacements,  $l$  is zero.

As we move away from the wall (more precisely, from the boundary of the laminar layer), the possibility of transverse particle displacements increases, turbulent mixing becomes more vigorous, and the mixing length  $l$  increases.

L. Prandtl proposed that  $l$  should be regarded as increasing linearly with the distance  $y$  from the wall, i.e.,

$$l = \kappa y, \quad (7.6)$$

where  $\kappa$  is a proportionality coefficient, which experiment indicates to be the same for all cases of turbulent flow (of the order of 0.4), and which is therefore known as the universal constant of turbulent flow.

Then, in an analysis of flow along an infinite plane, Prandtl set the tangential stress in the turbulent flow constant and equal to the stress  $\tau_0$  at the wall.

With these assumptions, we obtain from (7.15) [sic]

$$dv = - \int \frac{\sqrt{\frac{\tau_0}{\rho}}}{\kappa y} dy,$$

and, after integrating,

$$v = - \frac{1}{\kappa} \sqrt{\frac{\tau_0}{\rho}} \ln y + C \quad (7.7')$$

(here, and from now on, we shall omit the average bar on the velocities).

According to the Prandtl theory, therefore, the law of velocity distribution in turbulent flows is found to be logarithmic.

Formula (7.7') can be brought by simple modification to the dimensionless form

$$\frac{v}{v_*} = \frac{1}{\kappa} \ln \frac{v_* y}{\nu} + \text{const}$$

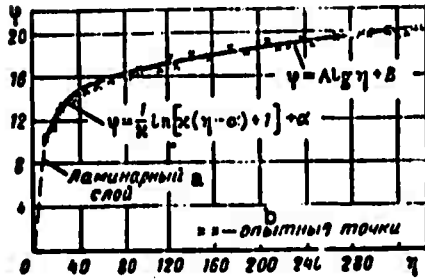


Fig. 65. Universal law of velocity distribution in turbulent flow.  
KEY: (a) laminar layer;  
(b) experimental points.

or

$$\varphi = A \lg \eta + B, \quad (7.7)$$

where  $v_* = \sqrt{\frac{\tau_0}{\rho}}$  is a quantity with the dimensions of velocity;

$\varphi = \frac{\bar{v}}{v_*}$  is dimensionless velocity;  $\eta = \frac{Kv_*}{\nu}$  is the dimensionless distance

from the wall, which is expressed in the same way as the Reynolds number; A and B are constant coefficients whose numerical values, on the basis of I.I. Nikuradze's experiments,<sup>4</sup> are A = 5.75 and B = 5.5.

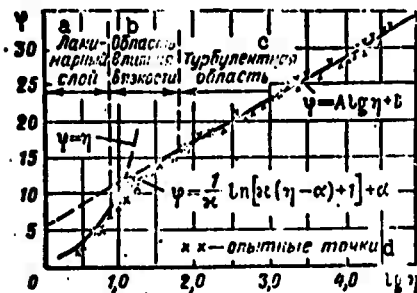


Fig. 66. Universal law of velocity distribution in semi-logarithmic coordinates.  
KEY: (a) laminar layer; (b) region of viscosity influence; (c) turbulent region; (d) experimental points.

In the form of (7.7), the velocity distribution law is said to be universal, since experimental points obtained in various pipes at various Re lie on the same  $\phi = \phi(\eta)$  curve (Fig. 65). The diagram of  $\phi$  as a function of  $\log \eta$  (Fig. 66), where most of Nikuradze and Reichardt's experimental points<sup>5</sup> lie along the straight line corresponding to Formula (7.7), is even more indicative. Deviation from linearity is noted only for small  $\eta$ , i.e., near the laminar layer, where viscosity makes itself felt, and inside it, where a totally different law of friction, that of Newton, applies.

<sup>4,5</sup> See page 136 for footnotes.

On the basis of the above results of Prandtl theory, let us derive the law of resistance for turbulent flow in round pipes, i.e., obtain a theoretical relation for the frictional loss coefficient  $\lambda_t$  as a function of Reynolds number.

The following expression is easily derived from (4.22):

$$\frac{v_{cp}}{v_0} = \varphi_{cp} = 2 \sqrt{\frac{2}{\lambda_t}}, \quad (7.8)$$

and we shall henceforth make use of it.

I.I. Nikuradze found experimentally that

$$\frac{v_{max} - v_{cp}}{v_0} = \varphi_{max} - \varphi_{cp} = 4.03, \quad (7.9')$$

and we have found theoretically<sup>6</sup> that while this quantity is a function of Re, it equals for large Re

$$\frac{v_{max} - v_{cp}}{v_0} = \frac{3}{2\kappa}. \quad (7.9)$$

Let us now apply (7.7) to points on the pipe axis:

$$\varphi_{max} = A \lg \eta_{max} + B$$

or

$$\frac{v_{max}}{v_0} = A \lg \frac{v_{cp}}{v_0} + B$$

and then replace  $\phi_{max}$  by its expression in terms of  $\phi_{sr}$  according to (7.9). We then apply (7.8) after replacing  $\phi_{sr}$  by its expression in terms of  $\lambda_t$ , and multiply and divide by  $2v_{sr}$  the quantity  $\eta_{max}$  under the logarithm sign.

We have

$$2 \sqrt{\frac{2}{\lambda_t}} + \frac{3}{2\kappa} = A \lg \left( \kappa \frac{v_{cp}}{v_0} \frac{v_0}{v_{cp}} \right) + B$$

or, after rearranging and taking the constant factor outside the logarithm sign,

$$\frac{1}{\sqrt{\lambda_t}} = A' \lg (\kappa \sqrt{2} \frac{v_{cp}}{v_0}) + B', \quad (7.10)$$

where  $A'$  and  $B'$  are constants determined by the values of  $\kappa$ ,  $A$ , and  $B$  and improved on the basis of Nikuradze's experiments:  $A = 2$ ,  $B = -0.8$ .

Formula (7.10) is not conveniently put to practical use, since it gives the unknown coefficient in implicit form. In

<sup>6</sup>See page 136 for footnote.

practice, therefore, the  $\lambda_t$  formulas given in the preceding section are preferred. However, Formula (7.10) is of fundamental interest as the first theoretically founded relation between  $\lambda_t$  and Re.

The Prandtl semiempirical turbulent-flow theory set forth above does not take account of the laminar layer at the wall or the viscosity tangential stress in the turbulent flow, and, as a result, the velocity-distribution law (7.7) or (7.7') is invalid near the wall (see Fig. 65) and does not satisfy the boundary condition at the wall. At  $y = 0$ , Formula (7.7) gives  $v = -\infty$ , which makes no sense. Moreover, the resistance law (7.10) yields a certain error for small Re.

The Prandtl theory can be improved by consideration of viscosity and the laminar layer.<sup>7</sup>

To do so, let us apply instead of (7.6) the following expression for the mixing length:

$$l = \kappa(y - \delta), \quad (7.11)$$

which provides for zero mixing length at  $y = \delta$ , i.e., at the laminar-layer boundary.

Then the total tangential stress in the turbulent flow will be regarded as the sum of viscosity and turbulence stresses, with the former expressed in accordance with Newton's law and the latter by the Prandtl law (7.5) with consideration of Expression (7.11). We shall have

$$\tau = \mu \frac{dv}{dy} + \rho \kappa^2 (y - \delta)^2 \left( \frac{dv}{dy} \right)^2. \quad (7.12)$$

Needless to say, this expression is valid only in the turbulent-flow zone, i.e., outside the laminar layer.

Converting to the already familiar dimensionless quantities and considering  $\tau = \tau_0 = \text{const}$  as before, we obtain

NOT REPRODUCIBLE

$$\kappa^2 (\eta - c)^2 \left( \frac{d\eta}{d\eta} \right)^2 + \frac{d\eta}{d\eta} - 1 = 0, \quad (7.12) \quad [\text{sic}]$$

where  $a = \frac{\delta_0 v_0}{\nu}$  is the dimensionless thickness of the laminar layer or the universal constant introduced by T. Karman. Solution of the quadratic equation (7.12) for  $d\eta/d\eta$ , followed by integration, gives

$$\eta = \frac{1}{\kappa} \ln \left[ \sqrt{4\kappa^2 (\eta - c)^2 + 1} + 2\kappa (\eta - c) \right] - \frac{2(\eta - c)}{1 + \sqrt{4\kappa^2 (\eta - c)^2 + 1}} + c. \quad (7.13)$$

<sup>7</sup>See page 136 for footnote.

The constant of integration is found from the conditions at the boundary of the laminar layer, where for  $\eta = \alpha$

$$\varphi = \frac{v_1}{v_0}$$

Assuming a linear velocity distribution inside the laminar layer and applying Newton's law and the expression for  $\alpha$ , we obtain

$$\tau_0 = \mu \frac{v_1}{\delta_L} \quad \text{or} \quad \frac{v_1}{v_0} = \frac{\delta_L v_0}{\nu}$$

Hence  $\phi = \eta$  for the laminar layer, and  $\phi = \alpha$  for its boundary. Consequently, the integration constant in (7.13) equals  $C = \alpha$ .

For large  $\eta$ , i.e., at a sufficient distance from the wall and large enough  $Re$ , Formula (7.13) reduces to the Prandtl velocity distribution law (7.7), where

$$A = \frac{2.303}{\kappa}; \quad B = \frac{2.303}{\kappa} \ln 4 - \frac{1}{\kappa} - \alpha$$

With the approach to the wall and at small  $Re$ , the quantity  $\eta$  approaches closer and closer to  $\alpha$ , so that the velocity effect increases and Formula (7.13) diverges increasingly from the Prandtl law.

By solving (7.12) approximately, we can obtain a simplified form of the law of velocity distribution in turbulent flow with consideration of the laminar layer and viscosity:

$$\varphi = \frac{1}{\kappa} \ln [\kappa(\eta - \alpha) + 1] + \alpha \quad (7.14)$$

Like (7.13), Eq. (7.14) satisfies the boundary condition for  $\eta = \alpha$  and agrees well with Reichardt's results of experimental velocity measurement near the wall (see Fig. 66). However, this equation is much simpler and more convenient to use than the result of exact solution (7.13).

Let us apply Eq. (7.13) to the center of the pipe section and use (7.8) and (7.9) in the same way as in deriving (7.10). Here, we disregard the units under the radicals and in the denominator of the second term in (7.13), so that this term reverts to  $1/\kappa$ .

Simple modifications yield an improved resistance law in the form

$$\frac{1}{\sqrt{\lambda_r}} = \frac{1}{2\sqrt{2\kappa}} \ln [Re]^{1/\sqrt{\lambda_r}} - \frac{1}{\sqrt{2\kappa}} + C, \quad (7.15)$$

where

$$C = \frac{a + b \left( \frac{v}{\nu} \right)^{-1/2}}{2 \gamma^2 k}$$

At large  $Re$ , Formula (7.15) becomes the Prandtl resistance law (7.10), but for small  $Re$  it gives values of  $\lambda$  that are somewhat on the high side owing to the direct viscosity effect.

Thus, the constant coefficients in (7.13) and (7.15) (velocity-distribution and resistance laws) are expressed in terms of the two universal constants  $\kappa$  and  $a$ , determinations of which from velocity-distribution and resistance experiments yields practically identical results, namely: from the velocity distribution  $\kappa = 0.401$  and  $a = 6.82$ , and from resistance  $\kappa = 0.407$  and  $a = 6.93$ .

Thus, consideration of viscosity and the laminar layer in the Prandtl theory has made it possible to obtain improved laws of velocity distribution and resistance, has made the velocity-distribution law satisfy the boundary condition near the wall, and has enabled us to express all constant coefficients in terms of the two universal constants  $\kappa$  and  $a$ .

### §30. TURBULENT FLOW IN ROUGH-WALLED PIPES

While the frictional-loss coefficient is fully determined by  $Re$  for smooth pipes, the  $\lambda_t$  of rough pipes also depends on the roughness of the pipe's internal surface. What is important here

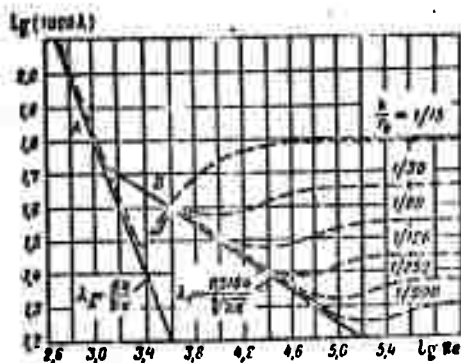


Fig. 67. Dependence of  $\log(1000\lambda)$  on  $\log Re$  for artificially roughened pipes according to I.I. Nikuradze's experiments.

is not the absolute dimension  $k$  of the roughness peaks, but the ratio of this dimension to pipe radius, i.e., the so-called roughness ratio  $k/r_0$ . A given absolute roughness may have no effect at all on resistance in a large-diameter pipe, but be

capable of increasing it substantially in a small-diameter pipe. Further, resistance is influenced by the nature of the roughness: distance between peaks, height nonuniformity, etc. The simplest case would be that in which all roughness peaks had the same dimension  $k$  and the same shape, i.e., the case of so-called uniformly distributed granular roughness.

In the case of uniformly distributed granular roughness, therefore, the coefficient  $\lambda_t$  will depend on both  $Re$  and the ratio  $k/r_0$ , i.e.,

$$\lambda_t = f(Re; \frac{k}{r_0}).$$

The manner in which these two parameters influence pipe resistance is distinctly evident from a diagram representing the experimental results of I.I. Nikuradze (Fig. 67), who tested a series of pipes with artificially created roughness for resistance. Uniformly distributed roughness was obtained by gluing grains of sand of uniform size to the inside walls of the pipes.

The pipes were tested in a broad range of relative roughnesses ( $k/r_0 = 1/500$  to  $1/15$ ) and Reynolds numbers ( $Re = 500-10^6$ ). The test results are plotted on a logarithmic diagram in the form of curves of  $\log(1000\lambda)$  as a function of  $\log Re$  for a series of  $k/r_0$ .

The inclined straight lines A and B correspond to the resistance laws of smooth pipes, i.e., to Formulas (6.7) and (7.2). On multiplying by 1000 and taking logarithms, we obtain the equations of the lines in  $\log(1000\lambda) = f(\log Re)$  coordinates:

$$\lg(1000\lambda_A) = \lg 64000 - \lg Re$$

and

$$\lg(1000\lambda_B) = \lg 316,4 - \frac{1}{4} \lg Re.$$

The curves for pipes with various roughness ratios are dashed.

The following basic conclusions can be drawn from analysis of the diagram:

1. In laminar flow, roughness does not influence resistance; the dashed curves corresponding to various roughnesses practically coincide with line A.

2. The critical  $Re$  is practically independent of roughness. The dashed curves deviate from line A at about the same  $Re$ .

3. In the turbulent-flow range, but at moderate  $Re$  and  $k/r_0$ , roughness does not influence resistance; the dashed lines coincide with line B on certain segments. As  $Re$  increases, however, this influence begins to make itself felt, and the curves for rough pipes begin to deviate from the line corresponding to the resistance law for smooth pipes.

4. At large  $Re$  and large relative roughnesses, the coefficient  $\lambda_t$  ceases to depend on  $Re$  and becomes constant for a given roughness ratio. This corresponds to the segments of the dashed curves on which, after rising slightly, they run parallel to the axis of abscissas.

Thus, we can discern the following three ranges of  $Re$  and  $k/r_0$ , which differ from one another in the way in which the coefficient  $\lambda_t$  varies, for each of the curves corresponding to rough pipes in turbulent flow.

The first range, the range of small  $Re$  and  $k/r_0$ , in which the coefficient  $\lambda_t$  is independent of roughness and is determined only by  $Re$ , as in the case of smooth pipes. This region does not appear for the largest roughness values in I.I. Nikuradze's experiments.

A second region, where the coefficient  $\lambda_t$  depends on two parameters simultaneously:  $Re$  and surface roughness.

A third region of large  $Re$  and  $k/r_0$ , in which the coefficient  $\lambda_t$  does not depend on  $Re$  and is determined only by roughness ratio. This region is known as the self-similarity region or the square-law resistance zone, since a  $\lambda_t$  that is independent of  $Re$  signifies that the head loss is exactly proportional to the square of velocity [see Formula (4.20)].

For better understanding of these resistance properties of rough pipes, it is necessary to take account of the presence of the laminar layer (see §28).

As we noted above, the thickness  $\delta_1$  of the laminar layer decreases with increasing  $Re$ . For this reason, when we have a turbulent flow in a rough pipe, the laminar-layer thickness at small  $Re$  is greater than the roughness-peak height, the peaks are inside the laminar layer and are washed smoothly (without separation), and hence do not affect resistance. With increasing  $Re$ , the thickness  $\delta_1$  decreases, and the roughness heights begin to project outside the layer and influence resistance. At large  $Re$ , the laminar-layer thickness becomes vanishingly small, and the roughness peaks are washed by the turbulent flow with separation and eddying at each peak; this explains the square-law resistance curve that applies in this region.

I.I. Nikuradze's diagram can be used to construct an approximate Reynolds-number curve of the so-called acceptable roughness, i.e., of the maximum value of  $k/r_0$  at which the roughness of the pipe still does not influence its resistance. For this purpose, it is necessary to select the points on the diagram (see Fig. 67) at which the rough-pipe curves begin to deviate from line B for

smooth pipes. Obviously, the acceptable roughness figure becomes smaller with increasing Re.

I.I. Nikuradze ran his experiments on pipes lined with an artificial, uniformly distributed granular roughness. For natural rough pipes, the variation of  $\lambda_t$  with Re is found to be somewhat different, without the rise in the curves after their deviation from the smooth-pipe law. Figure 68 presents the results of very careful experiments conducted by G.A. Murin at the All-Union Institute of Technology.

On this diagram, the coefficient  $\lambda_t$  for natural rough pipes is given as a function of Re for various values of  $d/k_e$ , where  $k_e$  is an absolute roughness equivalent to the granular roughness in Nikuradze's experiments. G.A. Murin recommends  $k_e = 0.06$  for new steel pipes and  $k_e = 0.2$  mm for used pipes.

The difference in the character of the Nikuradze and Murin curves is explained by the fact that the roughness peaks in a natural pipe have varying heights and, as Re is increased, begin to project outside the laminar layer not simultaneously, but at different Re. As a result, the transition from the curve corre-

TABLE 2

а - Материал трубы	b $10^3 k'$ мм
с Стекло	0,0
d Тянутые трубы из латуни, свинца, меди	0,0
e Бесшовные стальные трубы тщательного изготовления	0,6—2,0
f Стальные трубы	3—10
g Чугунные асфальтированные трубы	10—25
h Чугунные трубы	25—50

KEY: (a) pipe material; (b)  $10^3 k'$ , mm; (c) glass; (d) brass, lead, or copper seamless pipes; (e) carefully made seamless steel pipes; (f) steel pipes; (g) asphalted cast-iron pipes; (h) cast-iron pipes.

sponding to the resistance of smooth pipes to the horizontal lines corresponding to the square law takes place more smoothly for natural pipes, without the trough in the typical curves of the Nikuradze diagram. The boundary of the square-law resistance range is indicated on the diagram (see Fig. 68) by the dashed line; this boundary is determined by the limiting Reynolds number, which is larger the smaller  $k_e/d$ .

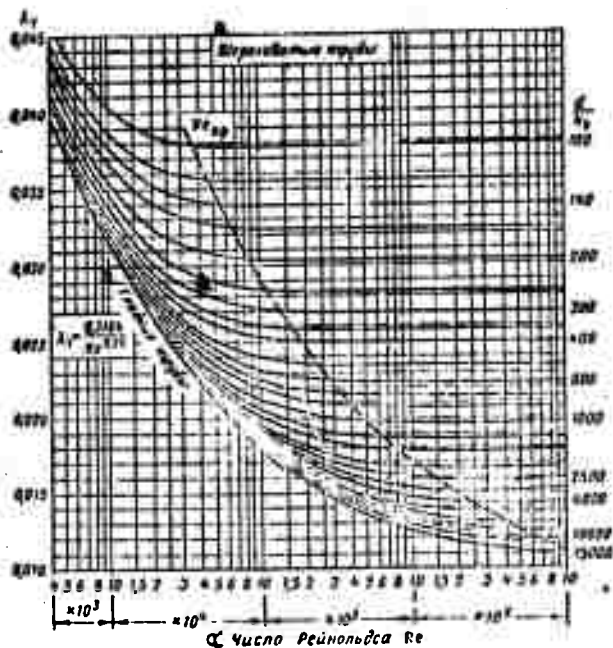


Fig. 68. Diagram of  $\lambda_t$  as a function of  $Re$  for naturally rough pipes according to G.A. Murin's experiments. KEY: (a) rough pipes; (b) smooth pipes; (c) Reynolds number  $Re$ .

For practical calculations to determine the resistance of real rough pipes, we might also recommend the following new universal formula of A.D. Al'tshul' [5]:

$$\frac{1}{\sqrt{\lambda}} = 1,8 \lg \frac{Re}{Re \frac{k'}{d} + 7}, \quad (7.16)$$

where  $d$  is the pipe diameter and  $k'$  is a dimension proportional to the absolute roughness.

The limiting values of  $k'$  for various pipes are listed in Table 2.

For values of  $Re \frac{k'}{d}$  smaller than 7, Formula (7.16) becomes the Konakov formula (7.1) given earlier for smooth pipes, while at large  $Re \frac{k'}{d}$ , it becomes the formula for fully roughened pipes, i.e., for the square-law resistance mode (self-similarity):

$$\frac{1}{\sqrt{\lambda}} = 1.8 \lg \frac{d}{\nu}. \quad (7.17)$$

Thus, by comparing the numerical value of the product  $Re \frac{\lambda}{d}$  with 7, we can establish the boundaries of the above regions (regimes) of turbulent flow in rough pipes.

### §31. TURBULENT FLOW IN NONCIRCULAR PIPES

We have now considered turbulent flow in pipes of round cross section. However, it is sometimes necessary to deal with turbulent flow in nonround pipes, such as are used, for example, in cooling devices.

Let us consider calculation of frictional losses for turbulent flow in a pipe with a cross section of arbitrary shape.

The resultant frictional force acting on the outer surface of a stream of length  $l$  can be expressed as follows:

$$T = \Pi \tau_0,$$

where  $\Pi$  is the section perimeter;  $\tau_0$  is the tangential stress at the wall, which depends basically on dynamic pressure, i.e., on the average flow velocity and density of the fluid (see §17 and 25).

At a given cross-sectional area and a given fluid flow rate (and hence at a given average velocity), therefore, the friction is proportional to section perimeter. Thus, to reduce friction and the energy lost on friction, it is necessary to make the section perimeter smaller. The smallest perimeter for a given area is the circular section, which is therefore optimal from the standpoint of minimizing energy (head) losses due to friction in the pipe.

The so-called hydraulic radius  $R_g$ , which is equal to the ratio of the pipe's sectional area to its perimeter, is introduced into the calculation for quantitative evaluation of the effect of sectional shape on head loss:<sup>8</sup>

$$R_g = \frac{S}{\Pi}. \quad (7.18)$$

The hydraulic radius can be figured for any cross section. For example, we have for a circular section

$$R_g = \frac{\pi d^2}{4\pi d} = \frac{d}{4},$$

from which

$$d = 4R_g. \quad (7.19)$$

<sup>8</sup>See page 136 for footnote.

for a rectangular cross section with sides  $a \times b$

$$R_r = \frac{ab}{2(a+b)},$$

and for a square with side  $a$

$$R_r = \frac{a}{4}.$$

For a gap of dimension  $a$ , we obtain from the above (regarding  $a$  as very small by comparison with  $b$ ):

$$R_r = \frac{a}{2}.$$

Substituting the hydraulic radius (7.19) for the geometrical diameter  $d$  in the basic formula for frictional head loss (4.20), we obtain

$$h_{sp} = \lambda \frac{l}{4R_r} \frac{v^2}{2g}. \quad (7.20)$$

Since this formula is a more general expression of the loss law (4.18), it should be valid not only for round, but also for nonround pipes.

Experiment has confirmed the validity of (7.20) for pipes with any cross-section formula. The coefficient  $\lambda$  is calculated from the same formulas (7.1) or (7.2), but the Reynolds number is expressed in terms of  $R_g$ , i.e.,

$$Re = \frac{4R_r v_{cp}}{\nu}. \quad (7.21)$$

**Example.** Determine the frictional pressure loss in the cylindrical part of the combustion-chamber cooling jacket of the "Rheintochter" liquid rocket engine [LRE] (ЖРД) [25]. The jacket takes the form of an annular gap with  $\delta = 2$  mm and length  $l = 500$  mm; the inner circle diameter is  $D = 155$  mm. The coolant (nitric acid) flow rate is  $G = 10$  kgf/s, and the specific weight  $\gamma_k = 1510$  kgf/m<sup>3</sup>.

Assume that the acid temperature is constant in this zone and averages  $t_{sr} = 80^\circ\text{C}$  ( $\nu = 0.25$  cSt).

**Solution.** 1) The flow velocity in the gap

$$v = \frac{G}{\gamma_k D \delta} = \frac{10}{1510 \cdot \pi \cdot 0.155 \cdot 0.002} = 6.8 \text{ m/s}.$$

2) The hydraulic radius of the jacket is

$$R_r = \frac{\pi [(D+2\delta)^2 - D^2]}{4\pi(D+2\delta+D)} = \frac{\delta}{2} = 1 \text{ mm}.$$

3) The Reynolds number

$$Re = \frac{4R_r v}{\nu} = \frac{4 \cdot 0,1 \cdot 680}{0,0025} = 110000.$$

4) The pressure loss due to friction

$$\begin{aligned} p_{r,p} &= \lambda_r \frac{l}{4R_r} \cdot \frac{\rho v^2}{2g} \gamma = \frac{1}{(1,8 \lg Re - 1,5)^2} \frac{500}{4 \cdot 1} \cdot \frac{6,8^2}{2 \cdot 9,8} 1510 \cdot 10^{-4} = \\ &= 0,8 \text{ kgf/cm}^2 = 78\,500 \text{ N/m}^2. \end{aligned}$$

The pressure losses in the conical segments of the cooling passage are much larger, but their calculation is more complex, since it is necessary to carry out an integration.

## Footnotes

Manu-  
script  
page

- 117 <sup>1</sup>See the author's paper "O sootnoshenii skorostei i koeffitsiyente Koriolisa pri turbulentnom techenii v trubakh" (Velocity and Coriolis coefficient relationships in turbulent pipe flows) (Trudy VVIA im. N.Ye. Zhukovskogo [Transactions of the N.Ye. Zhukovskiy Air Force Engineering Academy], 1944, No. 104), where the Re curve of  $\alpha$  was obtained theoretically.
- 122 <sup>2</sup>It will be understood that we can speak only conventionally of layers in turbulent flow.
- 122 <sup>3</sup>Ludwig Prandtl (1875-1953) was a noted German scientist in the fields of aerohydropneumatics, meteorology, and elasticity theory and a professor at Göttingen University.
- 124 <sup>4</sup>I.I. Nikuradze was a colleague of Prof. L. Prandtl and, at Göttingen, carried out a series of meticulous experimental studies of fluid flow in pipes the results of which have won wide recognition (see also §30).
- 124 <sup>5</sup>ZAMM, Vol. 20, No. 6, 1940.
- 125 <sup>6</sup>See footnote to page 117.
- 126 <sup>7</sup>The author's results are cited below.
- 133 <sup>8</sup>The notion of the hydraulic diameter, which equals  $D_g = 4R_g$ , is also in use.

### Symbol List

Manu- script page	Symbol		English equivalent
116	ocp	osr	averaged
117	кp	kr	critical
118	тp	tr	friction
118	т	t	turbulent
119	л	l	laminar
125	cp	sr	average
131	э	e	equivalent
133	г	g	hydraulic
134	к	k	acid

## C H A P T E R VIII

### LOCAL HYDRAULIC RESISTANCES

#### §32. LOCAL RESISTANCES IN GENERAL. ABRUPT EXPANSION OF THE CHANNEL

It was stated above (§19) that hydraulic energy losses are classified into two categories: local losses and losses to friction. We have already considered frictional losses in straight constant-section pipes for laminar (Chapter VI) and turbulent (Chapter VII) flow regimes. Let us now examine the losses governed by the so-called local hydraulic resistances, i.e., those elements of the pipelines in which flow velocity changes and eddies usually form as a result of changes in the dimensions or configuration of the channel.

In §19, we cited examples of certain local resistances and gave a general method for expressing them based on experimental data (4.19), namely:

$$h_{\text{л}} = \zeta_{\text{л}} \frac{v^2}{2g} = \zeta_{\text{л}} \cdot \frac{16Q^2}{2g\pi^2 d^4}.$$

The problem is now to find a way to determine the  $\zeta_{\text{л}}$  coefficients for various types of local resistances.

Elementary local hydraulic resistances can be classified into the following groups and subgroups:

- 1) expansion of the channel - abrupt, smooth;

- 2) constriction of the channel - abrupt, smooth;
- 3) turning of the channel - abrupt, smooth.

More complex cases of local resistance are combinations of the elementary forms listed above. Thus, the fluid flows through a gate valve (see Fig. 30d), the stream curves, changes direction, narrows, and, finally, expands to its original size; this is accompanied by intensive eddying.

Let us examine the elementary local resistances for turbulent flow in the order in which they are listed above. It should be noted that the coefficients  $\zeta_m$  are determined almost exclusively in turbulent flows by the shape of the local resistances and change very little with changes in channel dimensions, stream velocity, or fluid viscosity, i.e., with changes in  $Re$ . They are therefore usually assumed to be independent of  $Re$ , which signifies a square-law resistance curve or self-similarity. We shall touch upon local resistances in laminar flow at the end of the chapter.



Fig. 69. Abrupt expansion of channel.

Values of the local-resistance coefficients  $\zeta$  are usually obtained by experiment and then used in experimental formulas or graphs.

However, the head loss can be found accurately enough by a purely theoretical route for the case of abrupt expansion of the channel in turbulent flow.

Figure 69 shows a sudden channel (pipe) expansion and the flow pattern that corresponds to it.

The flow does not detach at the corner and expand abruptly, like the channel, but does so gradually, with formation of eddies in the annular space between the stream and the pipe wall; it is these eddies that cause the loss of energy in this case.

Observations have shown that there is a continuous exchange of fluid particles between the main stream and the rotational zone of the flow.

Let us take two sections through the flow: 1-1 in the plane of the pipe expansion and 2-2 where the stream, after expanding, has filled the entire section of the wider pipe. Since the stream expands between these sections, its velocity decreases, while the pressure rises. As a result, the second piezometer indicates a height  $\Delta H$  greater than the first; however, if there were no head losses at this point, the second piezometer would indicate a still greater height. The "missing" height  $h$  is the local head loss due to expansion.

Let us denote the pressure, velocity, and sectional area of the stream in section 1-1 by  $p_1$ ,  $v_1$ , and  $S_1$ , respectively, and those in section 2-2 by  $p_2$ ,  $v_2$ , and  $S_2$ . We write the Bernoulli equation for these sections on the assumption that the distribution of velocity over the sections is uniform, i.e., setting  $\alpha_1 = \alpha_2 = 1$ .

We obtain

$$\frac{p_1}{\gamma} + \frac{v_1^2}{2g} = \frac{p_2}{\gamma} + \frac{v_2^2}{2g} + h_{\text{расш.}}$$

We then apply the momentum-change theorem of mechanics to the cylindrical volume enclosed between sections 1-1 and 2-2. For this, we determine the impulse of the external forces acting on this volume in the direction of motion, assuming zero tangential stresses on the side of the cylinder. Remembering that the left and right bases of the cylinder have the same area  $S_2$  and assuming that the pressure  $p_1$  in section 1-1 acts on the entire area  $S_2$ , we obtain the per-second force impulse in the form

$$(p_1 - p_2)S_2.$$

The change in momentum corresponding to this impulse is found as the difference between the per-second momenta: that transferred out of the volume under consideration and that transferred into it; with a uniform velocity distribution over the sections, this difference equals

$$QQ(v_2 - v_1).$$

Equating the two,

$$(p_1 - p_2)S_2 = \frac{Q\gamma}{g}(v_2 - v_1).$$

We divide the equation by  $S_2\gamma$ , remembering that  $Q = S_2v_2$ , and rearrange the right member:

$$\frac{p_1 - p_2}{\gamma} = \frac{v_2}{g}(v_2 - v_1) = \frac{v_2^2}{2g} + \frac{v_1^2}{2g} - \frac{2v_1v_2}{2g} + \frac{v_1^2}{2g} - \frac{v_1^2}{2g}.$$

Grouping terms, we obtain

$$\frac{p_1}{\gamma} + \frac{v_1^2}{2g} = \frac{p_2}{\gamma} + \frac{v_2^2}{2g} + \frac{(v_1 - v_2)^2}{2g}.$$

Comparing the resulting equation with the Bernoulli equation that we wrote earlier, we see that they are quite analogous; from this we can conclude that

$$h_{\text{расш.}} = \frac{(v_1 - v_2)^2}{2g}, \quad (8.1)$$

i.e., that the head (specific energy) loss on an abrupt channel

expansion is equal to the velocity head calculated from the velocity difference. This statement is often referred to as the Borda-Carnot theorem after two French scientists - one a hydraulicist and the other a mathematician.

If we take into consideration that, according to the flow rate equation,

$$v_1 S_1 = v_2 S_2,$$

the result obtained can be written in still another form corresponding to the general method of expressing local losses:

$$h_{p.a.c.m} = \left(1 - \frac{S_1}{S_2}\right)^2 \frac{v_1^2}{2g} = \zeta \frac{v_1^2}{2g}, \quad (8.1')$$

Consequently, the resistance coefficient for the case of a sudden channel expansion equals

$$\zeta = \left(1 - \frac{S_1}{S_2}\right)^2 \quad (8.1'')$$

As we should expect with the assumptions adopted, the theorem that has been proven agrees well with experiment for turbulent flow and is used extensively in calculations.

In the particular case in which the area  $S_2$  is very large by comparison with  $S_1$  and, consequently, velocity  $v_2$  can be set equal to zero, the expansion loss equals

$$h_{p.a.c.m} = \frac{v_1^2}{2g},$$

i.e., the entire velocity head and all of the kinetic energy of the fluid is lost; in this case, the resistance coefficient  $\zeta = 1$ . One such case is that of fluid running through a pipe into a sufficiently large reservoir.

It must be stressed that this head (energy) loss on an abrupt channel expansion can be thought of as going entirely into formation of the eddies associated with flow separation from the walls, i.e., into maintenance of the continuous rotational motion of the fluid masses and their continuous replenishment (exchange). For this reason, energy losses of this type, which are proportional to the square of velocity (flow rate), are known as eddy-ing losses.

They are also often called impact losses, since we have here a rather sharp velocity decrease, a kind of impact of rapidly moving fluid on fluid that is moving slowly or not at all.

### §33. DIFFUSERS

A progressively expanding pipe is called a diffuser. Fluid flow in a diffuser is accompanied by a decrease in velocity and

an increase in pressure. Particles of the moving fluid overcome the increasing pressure at the expense of their kinetic energy, but the latter diminishes along the diffuser and in the direction from the axis to the wall. The fluid layers next to the wall have so little kinetic energy that they are often unable to overcome the elevated pressure; they stand still or even begin to move backward. The main stream comes up against these back currents, eddies form, the the flow separates from the wall (Fig. 70). The intensity of these effects increases with increasing expansion angle of the diffuser, and the eddying losses in the diffuser increase concurrently. In addition, the diffuser is subject to the usual frictional losses, which resemble those that arise in constant-section pipes.

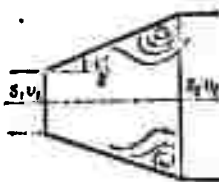


Fig. 70. Eddying in a diffuser.

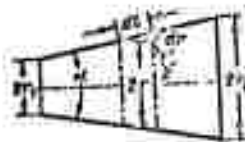


Fig. 71. Diagram of diffuser used in calculations.

The total head loss  $h_{dif}$  in a diffuser will be regarded conventionally here as the sum of two terms:

$$h_{dif} = h_{tr} + h_{p.rash} \quad (8.2)$$

where  $h_{tr}$  is the head loss due to friction and  $h_{rash}$  is the head loss due to expansion (formation of eddies).

The frictional head loss can be calculated approximately as follows. Take a circular-section diffuser with a straight generatrix and an angle  $\alpha$  at its vertex. Let the radius of the diffuser entry orifice be  $r_1$ , and its exit radius  $r_2$  (Fig. 71). Since the section radius and the velocity of fluid motion are variable along the diffuser, it is necessary to take an elementary segment of the diffuser of length  $dl$  along the generatrix and express the elementary frictional head loss for it by the basic formula (4.18):

$$dh_{tr} = \lambda \frac{dl}{2r} \frac{v^2}{2g}$$

where  $v$  is the average velocity in an arbitrarily chosen section of radius  $r$ .

It follows from the elementary triangle that

$$dl = \frac{dr}{\sin \frac{\alpha}{2}}$$

We can then write on the basis of the flow rate equation

$$v = v_1 \left( \frac{r_1}{r} \right)^2,$$

where  $v_1$  is the velocity at the beginning of the diffuser.

Let us substitute these expressions into the formula for  $dh_{tr}$  and integrate from  $r_1$  to  $r_2$ , i.e., over the entire length of the diffuser, on the assumption that the coefficient  $\lambda_t$  is constant:

$$dh_{tr} = \lambda_t \frac{dr}{2r \sin \frac{\alpha}{2}} \left( \frac{r_1}{r} \right)^4 \frac{v_1^2}{2g},$$

from which

$$h_{tr} = \frac{\lambda_t}{2 \sin \frac{\alpha}{2}} \frac{v_1^2}{2g} r_1^4 \int_{r_1}^{r_2} \frac{dr}{r^5} = \frac{\lambda_t}{8 \sin \frac{\alpha}{2}} \left[ 1 - \left( \frac{r_1}{r_2} \right)^4 \right] \frac{v_1^2}{2g},$$

or, finally,

$$h_{tr} = \frac{\lambda_t}{8 \sin \frac{\alpha}{2}} \left( 1 - \frac{1}{n^2} \right) \frac{v_1^2}{2g}, \quad (8.3)$$

where  $n = \frac{S_2}{S_1} = \left( \frac{r_1}{r_2} \right)^2$  is the so-called expansion ratio of the diffuser.

The second term, the expansion (eddy) head loss, is of the same nature in a diffuser as in an abrupt expansion, but is smaller and is therefore usually expressed by the same formula (8.1) or (8.1'), but with a correction factor  $k$  that is smaller than unity, i.e.,

$$h_{pacw} = k \frac{(v_1 - v_2)^2}{2g} = k \left( 1 - \frac{S_1}{S_2} \right)^2 \frac{v_1^2}{2g} = k \left( 1 - \frac{1}{n} \right)^2 \frac{v_1^2}{2g}. \quad (8.4)$$

Since the impact is "softer" in a diffuser than in an abrupt expansion, the coefficient  $k$  is often referred to as the impact softening coefficient. The numerical value of this coefficient for diffusers with taper angles  $\alpha$  of the order of 5-20° can be determined by the following experimental formula of I.Ye. Idel'-chik:

$$k = 3.2 \lg \frac{\alpha}{2} \sqrt[4]{\lg \frac{\alpha}{2}}. \quad (8.5)$$

or from the approximate Fligner formula

$$k = \sin \alpha. \quad (8.6)$$

Using Formulas (8.3) and (8.4), we can rewrite the original expression (8.2) in the form

$$h_{\text{diff}} = \left[ \frac{\lambda_v}{8 \sin \frac{\alpha}{2}} \left(1 - \frac{1}{n^2}\right) + k \left(1 - \frac{1}{n}\right)^2 \right] \frac{v_1^2}{2g} = \zeta_{\text{diff}} \frac{v_1^2}{2g}, \quad (8.7)$$

and the diffuser's resistance coefficient can finally be expressed as follows:

$$\zeta_{\text{diff}} = \frac{\lambda_v}{8 \sin \frac{\alpha}{2}} \left(1 - \frac{1}{n^2}\right) + k \left(1 - \frac{1}{n}\right)^2. \quad (8.8)$$

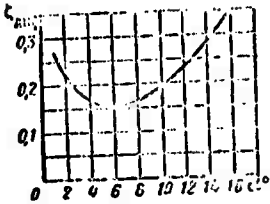


Fig. 72. Diagram of  $\zeta_{\text{diff}}$  as a function of angle  $\alpha$ .

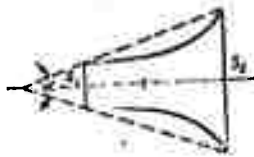


Fig. 73. Diffuser with constant pressure gradient.

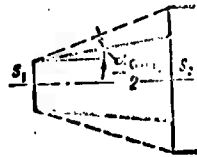


Fig. 74. Stepped diffuser.

From this we see that the coefficient  $\zeta_{\text{diff}}$  depends on the angle  $\alpha$ , the coefficient  $\zeta_t$ , and the expansion ratio  $\underline{n}$ .

It is important to ascertain the manner in which  $\zeta_{\text{diff}}$  depends on  $\alpha$ . With increasing angle  $\alpha$ , the first term in Formula (8.8), which is governed by friction, decreases for given  $\lambda_t$  and  $\underline{n}$ , since the diffuser is made shorter and the second term, which is governed by eddying and flow detachment, increases.

On the other hand, when  $\alpha$  becomes smaller, eddying decreases but friction increases, since for a given expansion ratio  $\underline{n}$ , the diffuser becomes longer and its friction surface larger.

The function  $\zeta_{\text{diff}} = f(\alpha)$  has a minimum at a certain optimum angle  $\alpha$  (Fig. 72).

The value of this angle can be found in approximation from Formula (8.8) after replacing  $\sin \frac{\alpha}{2}$  by  $\frac{1}{2} \sin \alpha$ , as follows: differentiate Expression (8.8) with respect to  $\alpha$  with consideration of (8.6), equate to zero and solve for  $\alpha$ :

$$\frac{d\lambda_t}{d\alpha} = -\frac{\lambda_t}{4} \left( 1 - \frac{1}{n^2} \right) \frac{\cos \alpha}{\sin^2 \alpha} + \cos \alpha \left( 1 - \frac{1}{n} \right)^2 = 0.$$

whence

$$\alpha_{opt} = \arcsin \sqrt{\frac{n+1}{n-1} \frac{\lambda_t}{4}}.$$

When a frictional-loss coefficient of the order of  $\lambda_t = 0.015-0.025$  and area ratios in the range  $n = 2-4$  are substituted into this formula, we obtain an average of about  $6^\circ$  for the optimum diffuser angle; this agrees with experimental data.

In practice, somewhat larger angles  $\alpha$  ( $\alpha = 7-9^\circ$ ) are usually used to shorten the diffuser at a given  $n$ . The same  $\alpha$  values can also be recommended for square diffusers.

For rectangular diffusers with expansion in one plane (flat diffusers), the optimum angle is larger than for the round and square diffusers, amounting to  $10-12^\circ$ .

If near-optimum angles  $\alpha$  cannot be used because of bulk considerations, it is advisable to abandon the straight-generatrix diffuser with  $\alpha > 15-25^\circ$  and go over to one of the special diffusers, e.g., a diffuser that provides for a constant pressure gradient along the axis ( $dp/dx = \text{const}$ ).<sup>1</sup> The approximate outlines of such a diffuser are shown in Fig. 73.

The decrease in energy loss in these diffusers by comparison with the straight-generatrix types is larger the larger the angle  $\alpha$ , and ranges up to 40% at  $\alpha$  of the order of  $40-60^\circ$ . In addition, the flow in a curvilinear diffuser is more stable.

Good results are also obtained with the stepped diffuser, which consists of an ordinary diffuser with the optimum angle in series with an abrupt expansion (Fig. 74). The latter does not give rise to large energy losses, since the velocities are comparatively low at its position. The total resistance of such a diffuser is considerably smaller than that of an ordinary diffuser of the same length and expansion ratio. More detailed information on special diffusers will be found in [12].

#### §34. CONSTRICTION OF CHANNEL

An abrupt constriction of the channel (pipe) (Fig. 75) usually causes a smaller energy loss than an abrupt expansion with the same area ratio. In this case, the loss is due, firstly, to friction at the entrance into the narrow pipe and, secondly, to eddying losses. The latter occur because the stream does not wash the entrance corner, but detaches from it and tapers; the annular space around the constricted section of the flow is filled with sluggish eddying fluid.

<sup>1</sup>See page 157 for footnote.

Subsequent expansion of the stream is accompanied by a head loss that can be determined by the theorem for abrupt pipe expansion. Consequently, the total head loss equals

$$h_{\text{сум}} = \zeta_0 \frac{v_x^2}{2g} + \frac{(v_x - v_2)^2}{2g} = \zeta_{\text{сум}} \frac{v_x^2}{2g}, \quad (8.9)$$

where  $\zeta_0$  is the resistance coefficient governed by the friction of the stream as it enters the narrow pipe and  $v_x$  is the velocity at the constriction.

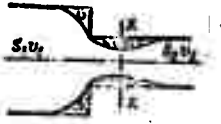


Fig. 75. Abrupt constriction of pipe.

The resistance coefficient of an abrupt constriction depends on the constriction ratio, i.e., on  $n = S_1/S_2$ , and can be determined from the following semiempirical formula, which was proposed by I.Ye. Idel'chik:

$$\zeta_{\text{сум}} = \frac{1}{2} \left( 1 - \frac{S_2}{S_1} \right) = \frac{1}{2} \left( 1 - \frac{1}{n} \right). \quad (8.10)$$

It follows from this formula that in the particular case in which we may set  $S_2/S_1 = 0$ , i.e., when the pipe empties into a large enough reservoir and the entrance corner is not rounded, the resistance coefficient is

$$\zeta_{\text{сум}} = \zeta_{\text{вх}} = 0.5.$$

The head loss at entry into the pipe can be lowered substantially by rounding the entry corner (entry edge).

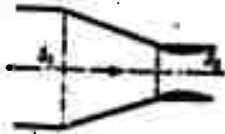


Fig. 76. Confuser.

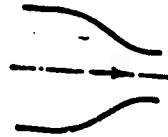


Fig. 77. Nozzle.

A gradual constriction of a pipe, i.e., a converging conical pipe, is called a confuser (Fig. 76). The fluid flow in a confuser is accompanied by a velocity increase and a pressure decrease; the fluid moves from higher to lower pressure, so that there is no cause for the formation of eddies or flow detachment (as was the case in the diffuser). The confuser has only friction losses. Accordingly, the resistance of a confuser is always smaller than that of the identical diffuser.

The pressure loss to friction in a confuser can be calculated in the same way as for the diffuser, i.e., the loss is first written for an elementary segment, and this is followed by integration. This yields the formula

$$K_{vp} = \frac{1}{8 \sin \frac{\alpha}{2}} \left( 1 - \frac{1}{n^2} \right) \frac{v_2^2}{2g} \quad (8.11)$$

where  $n$  is the constriction ratio.

Minor eddying and flow separation from the wall with simultaneous constriction of the stream occur only at the exit from the confuser, at the point at which the conical pipe joins the cylindrical pipe. To eliminate this vorticity and the associated losses, it is recommended that the conical segment be coordinated smoothly with the cylinder or that it be replaced by a curvilinear segment that merges smoothly into the cylinder (Fig. 77). This solution yields a very large constriction ratio on a short axial length and very modest losses.

The resistance coefficient of a smooth constriction of this type, which is known as a nozzle, varies in the approximate range  $\zeta = 0.03-0.10$ , depending on constriction ratio, smoothness, and  $Re$  (small values of  $\zeta$  correspond to larger  $Re$  and vice versa).

### §35. TURNS IN THE CHANNEL

An abrupt turn in the channel (pipe) or unrounded elbow (Fig. 78) usually produces considerable energy losses, since flow separation and eddying take place in it; these losses are larger the larger the angle  $\delta$ . The resistance coefficient  $\zeta_{kol}$  of a circular-section elbow increases very steeply with increasing  $\delta$  (Fig. 79) and reaches 1.0 at  $\delta = 90^\circ$ .

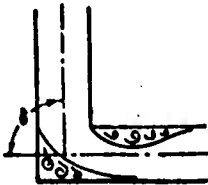


Fig. 78. Elbow.

In view of the large head losses of unrounded elbows, it is not recommended that they be used in pipelines.

A smooth turn in the pipe, or rounded elbow (Fig. 80), is also known as a bend. The smoothness of the turn reduces the scale of the eddying substantially and, consequently, also lowers the resistance of the bend by comparison with the elbow. This decrease will be larger the larger the relative radius of curvature  $R/d$  of the bend, and flow detachment and the associated eddying will be eliminated altogether if it is made large enough. The resistance coefficient of the bend depends on the ratio  $R/d$ , the angle  $\delta$ , and the cross-sectional shape of the pipe.

The following experimental formula can be used for circular-section bends with the angle  $\delta = 90^\circ$  and  $R/d \geq 1$ :

$$\zeta_{in} = 0.051 + 0.19 \frac{d}{R} \quad (8.12)$$

For angles  $\delta \leq 70^\circ$ , the resistance coefficient equals

$$\zeta_{otv} = 0,9 \sin \delta \zeta'_{otv} \quad (8.13)$$

and for  $\delta \geq 100^\circ$

$$\zeta_{otv} = \left(0,7 + \frac{\delta}{90} 0,35\right) \zeta'_{otv} \quad (8.14)$$

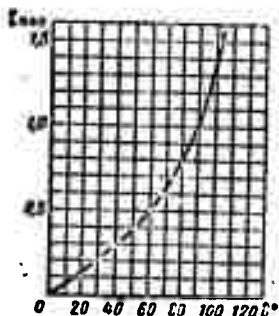


Fig. 79.  $\zeta_{kol}$  as a function of angle  $\delta$ .

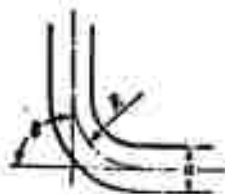


Fig. 80. Smooth turn in pipe (bend).

It must be remembered that the head loss defined by these coefficients  $\zeta_{otv}$ , i.e.,

$$h = \zeta_{otv} \frac{v^2}{2g}$$

is the difference between the total head loss in the bend and the frictional losses in a straight pipe whose length is equal to that of the bend, i.e., the coefficient  $\zeta_{otv}$  takes account only of the additional resistance due to the curvature of the channel. In the design of pipelines containing bends, therefore, the lengths of these bends must be included in the total length of the pipeline, which is used to figure the frictional losses, and then the additional loss due to curvature, which is determined by the coefficient  $\zeta_{otv}$ , must be added to this frictional loss.

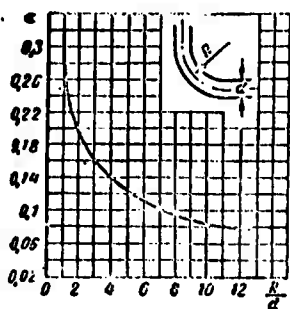


Fig. 81. Diagram of  $a$  as a function of  $R/d$ .

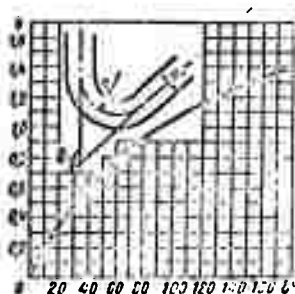


Fig. 82. Diagram of  $b$  as a function of  $\delta$ .

We have based the above formulas (8.12), (8.13), and (8.14) on diagrams plotted by Prof. G.N. Abramovich, who reduced a large

compilation of the most reliable experimental studies of the resistance of bends and proposed the following expression for the resistance coefficient:

$$\zeta_{\text{bend}} = 0,73 \zeta_{\text{a}} \zeta_{\text{b}} \zeta_{\text{c}} \quad (8.15)$$

where  $\zeta_{\text{a}}$  is a function of the relative radius of curvature and is given by a curve of  $\zeta_{\text{a}} = f_1(R/d)$  (Fig. 81);  $\zeta_{\text{b}}$  is a function of the turn angle, which is given by the  $\zeta_{\text{b}} = f_2(\delta)$  curve (Fig. 82) and equals unity at  $\delta = 90^\circ$ ;  $\zeta_{\text{c}}$  is a function of the pipe's cross-sectional shape, equals unity for round and square sections, and is given by a  $\zeta_{\text{c}} = f_3(e/d)$  curve for rectangular sections with sides  $\underline{e}$  and  $\underline{d}$  (side  $\underline{e}$  is parallel to the axis of curvature) (Fig. 83).

We see from this last diagram that the function  $\zeta_{\text{c}}$  has a minimum when the sides of the rectangle are related as  $e/d = 2.5$ . This is because a so-called "paired vortex" forms in the rectangle as the stream turns in it. The reason for this is that centrifugal forces act on all particles of the fluid as it moves through the curved channel. But since the velocity distribution is not uniform over the cross section (the velocities are higher at the center and lower at the walls), the centrifugal force, which is proportional to the square of velocity, will be considerably larger at the center of the stream than at the walls. As a result, centrifugal-force moments arise about the axes  $O_1$  and  $O_2$  (Fig. 84) and set the fluid in rotation. At the center of the stream, fluid is displaced from the inner wall toward the outer wall, i.e., along the radius of curvature, while the fluid at the lateral walls moves in the opposite direction. The pair of vortices is formed in this way. The stream divides into two helical flows as a result of addition of the circular motion of the fluid to its translational motion.

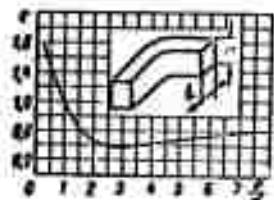


Fig. 83. Diagram of  $\zeta_{\text{c}}$  as a function of  $e/d$ .

other cases, the vortices will be flattened in one direction or the other.

Thus, while the circular pipe cross section is the optimum shape from the standpoint of reducing frictional losses, the rectangular section with a 2.5 sides ratio (longer side parallel to the axis of curvature of the bend) is most advantageous for

the purpose of minimizing  $\zeta_{otv}$ . The resistance coefficient of a bend with this sectional shape is

$$\zeta = 0.4\zeta_{otv}$$

where  $\zeta_{otv}$  is the resistance coefficient of a circular-section bend with the same  $R/d$  and  $\delta$ .

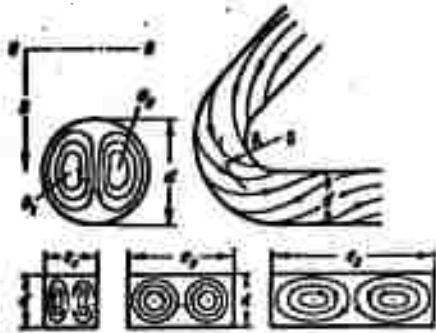


Fig. 84. Diagram showing formation of vortex pair.



Fig. 85. Vaned elbows.

Thus, the curvature losses can be reduced by a factor of 2.5 below those of the circular cross section by using the optimum channel-section shape at the turn.

In certain critical cases, when it is particularly important to minimize losses, it is advisable to

use this special section shape, and this is done, for example, in the air intakes of certain aviation engines.

In addition, guide vanes are sometimes installed in large elbows (as in wind tunnels) to reduce resistance. Installation of unprofiled vanes that have been bent along circular arcs (Fig. 85a) lowers the resistance coefficient of the elbow to  $\zeta = 0.4$ ; profiled vanes (Fig. 85b) reduce  $\zeta$  even further, to  $\zeta = 0.25$ . More detailed information on vaned elbows can be found in the specialized literature [12].

### §36. LOCAL RESISTANCES IN LAMINAR FLOW

All material set forth in preceding sections of this chapter pertains to local hydraulic losses in turbulent flow. As concerns laminar flow: firstly, the local resistances are usually unimportant here by comparison with friction and, secondly, the law of resistance is more complex in this case and has not been investigated as thoroughly as for turbulent flow.

While the local head losses can be considered proportional to the square of velocity (flow rate) in turbulent flow, and the resistance coefficients  $\zeta$  are determined basically by the shape of the resistance and are practically independent of  $Re$ , the head loss  $h_m$  in laminar flow must be regarded as the sum

$$h_m = h_{tr} + h_{vikhr}, \quad (8.16)$$

where  $h_{tr}$  is the head loss due directly to friction (viscosity) at the particular local resistance, and is proportional to the first power of fluid viscosity and velocity;  $h_{vikhr}$  is the loss due to flow separation and eddying in the local resistance itself or downstream of it, and is proportional to the square of velocity.

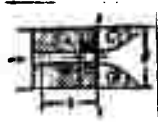


Fig. 86. Diagram of jet tube.

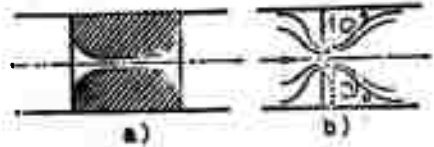


Fig. 87. Two types of local resistance.

Thus, for example, in flow through a jet tube (Fig. 86), a frictional head loss occurs to the left of section 1-1, and an eddying loss to its right.

Applying the law of resistance for laminar flow (6.6) and (6.7) with a correction for the initial segment, and Formula (4.19), we can write the same sum in the form

$$h_m = \frac{A}{Re} \frac{v^2}{2g} + B \frac{v^2}{2g}, \quad (8.16')$$

where A and B are dimensionless constants that depend on the shape of the local resistance.

After dividing (8.16') by the velocity head, we obtain a general expression for the coefficient of local resistance in laminar flow:

$$\zeta_m = \frac{A}{Re} + B. \quad (8.17)$$

The relation between the first and second terms in Formulas (8.16) and (8.17) depends on the shape of the local resistance and on Reynolds number.

In local resistances where there is a narrow passage whose length is considerably greater than its transverse dimension and which has smooth entry and exit outlines, as shown in Fig. 87a, and the  $Re$  are small, the head loss is determined basically by friction and the resistance law is close to linear. In this case, the second term in Formulas (8.16) and (8.17) is zero or very small by comparison with the first.

If, on the other hand, friction has been minimized in the local resistance, e.g., by providing a sharp edge (Fig. 87b),

and flow separation and eddying occur, and the Re are quite large, then the head losses are approximately proportional to the squared velocity (and flow rate).

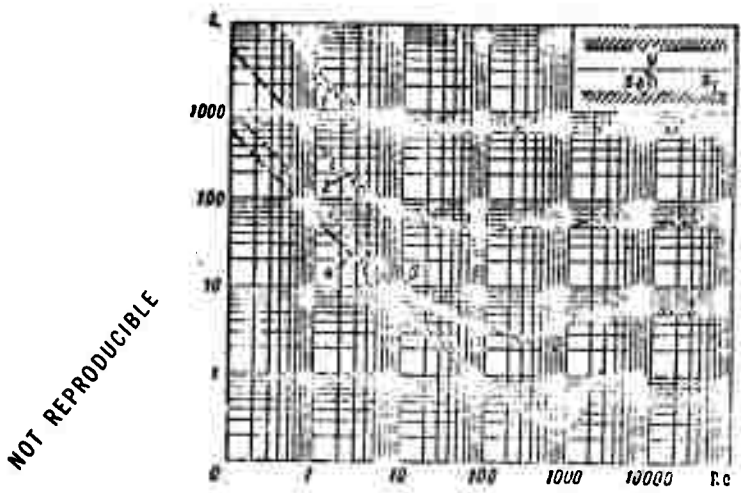


Fig. 88. Diagram showing  $\zeta$  of diaphragms as functions of Re:

$$1 - \frac{S_0}{S_1} = 0,05; \quad 2 - \frac{S_0}{S_1} = 0,16;$$

$$3 - \frac{S_0}{S_1} = 0,43; \quad 4 - \frac{S_0}{S_1} = 0,61.$$

When Re varies widely in a given local resistance, both linear (at small Re) and square-law (at large Re) resistance curves are possible; there may also be a transitional resistance range between them at moderate Re. Figure 88, which shows the results of tests on four diaphragms in logarithmic coordinates, represents a typical  $\zeta$ -Re relationship for a broad Re range of this type.<sup>2</sup> The sloping lines correspond to linear resistance variation (coefficient  $\zeta$  inversely proportional to Re), the curving segments represent the transitional range, and the horizontal straight lines the square law or self-similarity (coefficient  $\zeta$  independent of Re). Diagrams of this type are usually plotted on the basis of experimental data for specific local resistances.

Occasionally, the binomial form of the expression for local hydraulic losses is replaced by a power monomial of the form

$$h_x = kQ^m,$$

where  $k$  is a dimensional quantity;  $m$ , the exponent, depends on

<sup>2</sup>See page 157 for footnote.

the shape of the local resistance and Reynolds number and varies from 1 to 2.

For local resistances and Re for which the resistance law is nearly linear, the local hydraulic losses are often expressed in terms of equivalent pipe lengths, i.e., the actual pipe length is increased by the length whose resistance is equivalent to the local resistance. Thus, we have

$$l_{\text{pacu}} = l_{\text{факт}} + l_{\text{экв}} \quad \} \quad (8.18)$$

and

$$\sum h = \frac{64 l_{\text{pacu}}}{\text{Re}} \frac{v^2}{d} = \frac{128 v l_{\text{pacu}} Q}{\pi g d^4} \quad (8.19)$$

The numerical values of the equivalent lengths (referred to pipe diameter) are usually found experimentally for the various local resistances.

The theorem of head loss on an abrupt expansion of the channel that was proven in §32 for the case of turbulent flow is invalid for laminar flow. This is because the assumptions made in proving this theorem, namely, the hypotheses of uniform velocity distribution in sections 1-1 and 2-2, constant pressure over the entire area  $S_2$  in section 1-1, and zero tangential stresses (see Fig. 69) are no longer admissible in this case.

Very recent experimental studies have shown that at very small Re ( $\text{Re} < 9$ ), the abrupt-expansion resistance coefficient depends little on the area ratio and is determined basically by Re in a relation of the form

$$\zeta = \frac{A}{\text{Re}}$$

This means that the flow is nonseparating, and the expansion losses are proportional to the first power of velocity. For  $9 < \text{Re} < 3500$ , the resistance coefficient depends on both the Reynolds number and the area ratio. For  $\text{Re} > 3500$ , we may regard the Borda-Carnot theorem, i.e., Formula (8.1), as completely valid.

When the pipe conducts fluid at velocity  $v_1$  to a large tank ( $v_2 = 0$ ), we can assume loss of all of the fluid's specific kinetic energy, which equals

$$h = \alpha_2 \frac{v_1^2}{2g} = \frac{v_1^2}{g}$$

for stabilized laminar flow in a round pipe.

If, on the other hand, the flow is not stabilized, i.e., if the pipe length  $l < l_{\text{нач}}$ , the coefficient  $\alpha$  should be taken from the diagram (Fig. 47).

**Example.** Find the resistance coefficient of a jet tube of diameter  $d_{zh} = 1$  mm and length  $l = 5$  mm as a function of  $Re$  when it is installed in a pipe of diameter  $d = 6$  mm (see Fig. 86).

**Solution.** Regarding the jet tube as the initial segment of the pipe and assuming that all kinetic energy is lost as the jet expands, we represent the head loss in the jet tube as the sum (disregarding the constriction losses)

$$h_x = h_{tp} + h_{pacm} = \left( k \frac{64}{Re_x} \cdot \frac{l}{d} + \alpha \right) \frac{v_x^2}{2g}$$

Converting from the velocity  $v_{zh}$  in the jet tube to the velocity  $v$  in the pipe, we find the resistance coefficient of the jet tube:

NOT REPRODUCIBLE

$$\zeta_x = \frac{2gh_x}{v^2} = \left( k \frac{64}{Re_x} \cdot \frac{l}{d} + \alpha \right) \frac{d^4}{d_x^4}$$

Assigning a series of values to  $Re$  in the pipe, we find the Reynolds number  $Re_{zh}$  in the jet tube from the relation

$$Re_x = \frac{v_x d_x}{\nu} = \frac{4Q}{\pi d_x v} \cdot \frac{d}{d} = Re \frac{d}{d_x}$$

We then use the diagram (see Fig. 47) to find the coefficients  $k$  and  $\alpha$  and, carrying out the calculations, we enter the results in the following table:

TABLE 3

$Re$	10	100	200	300	400	500
$\zeta_x$	9500	3140	2500	2200	2030	1885

### §37. LOCAL RESISTANCES IN AIRCRAFT HYDRAULIC SYSTEMS

Aircraft hydraulic systems (hydraulic transmissions) usually have local hydraulic resistances in the form of filters, cocks, gate valves, elbows, and other units and pieces with a wide variety of geometrical shapes. The flow of fluid through these resistances may be either laminar or turbulent, depending on fluid velocity and temperature (viscosity); the Reynolds numbers vary over a rather broad range, which may even include  $Re_{kr}$ . As a result, the coefficients  $\zeta_m$  of these resistances must be regarded as functions of  $Re$ .

Figure 89 shows curves of the coefficient  $\zeta_m$  as a function of  $Re$  in logarithmic coordinates for the most typical local resistances of aircraft hydraulic systems, as obtained in experimental studies by N.V. Levkoyeva [Moscow Aviation Institute (MAI)].

The Reynolds numbers  $Re$  and the coefficients  $\zeta_m$  were calculated from the velocity in the pipe and its diameter.

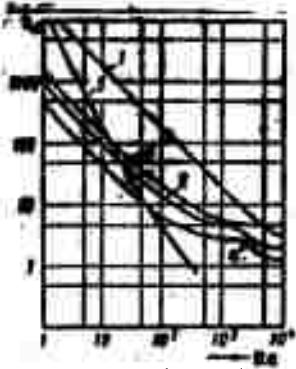


Fig. 89. Diagram of  $\zeta$  as a function of  $Re$  for the following units: 1) felt filter; 2) shutoff valve; 3) split valve; 4) 90° elbow; 5) check valve.

Our attention is drawn to the  $Re$  curve of the  $\zeta_m$  for the felt filter, which is linear all the way up to  $Re = 5000$ . This is explained by the fact that there is quite a great deal of friction in laminar flow through the pores of felt, and practically no eddying. The linear segments are much shorter for the petcock, valve, and elbow; they are followed by a long transitional segment and, finally, by a range of square-law resistance or self-similarity ( $\zeta_m = \text{const}$ ).

The steeper curve for the check valve as compared to the other resistances is explained by the fact that the opening of the valve increases with increasing  $Re$  owing to the increased flow velocity, i.e., its geometrical characteristic changes.

In aircraft fuel lines, the  $Re$  are usually considerably larger than in hydraulic systems. It can therefore be

TABLE 4

Вид сопротивления	$\zeta_m$
б Гибкое соединение труб	0,3
с Стандартный угольник 90° (кернус сверлений)	1,2-1,3
д Тройник-отставление	3,5
е Кран топливный	1-2,5
г Обратный клапан	2,0
ф Фильтр сетчатый	1,5-2,5
ж Датчик расходомера:	
и при вращающейся крыльчатке	7,0
и при заторможенной крыльчатке	11-12
к Вход в трубу (выход из бака)	0,5-1,0
л Выход из трубы (вход в бак)	1,0

KEY: (a) type of resistance; (b) flexible pipe joint; (c) standard 90° elbow (drilled body); (d) tee branch; (e) fuel valve; (f) check valve; (g) felt filter; (h) flowmeter sender; (i) impeller turning; (j) impeller arrested; (k) pipe entrance (pickup from tank); (l) pipe exit (feed into tank).

assumed without incurring any major error that the local-resistance coefficients of fuel lines are independent of  $Re$ .

Table 4 shows values of the coefficients  $\zeta_m$  for self-similar flows in the most commonly used hardware components of fuel lines [11]. The  $\zeta_m$  values are referred to the velocity head in the entry pipe of the unit (part).

### Footnotes

Manu-  
script  
page

- 145      <sup>1</sup>The pressure gradient in a straight-generatrix diffuser varies along the axis, with its maximum in the initial cross section.
- 152      <sup>2</sup>According to the experiments of N.V. Levkoyeva [18].

### Symbol List

Manu- script page	Symbol		English equivalent
138	м	m	local
140	расш	rassh	expansion
142	диф	dif	diffuser
142	тр	tr	friction
143	т	t	turbulent
145	опт	opt	optimum
146	суж	suzh	constriction
146	вх	vkh	entrance
147	кол	kol	elbow
148	отв	otv	bend
151	вихр	vikhr	eddying
152	д	d	diaphragm
153	расч	rasch	calculation
153	факт	fakt	actual
153	экв	ekv	equivalent
153	л	l	laminar
153	нач	nach	initial
154	ж	zh	jet

## C H A P T E R IX

### OUTFLOW OF FLUID THROUGH HOLES AND MOUTHPIECES

#### §38. HOLE IN THIN WALL

In this chapter, we shall examine various cases of fluid outflow from reservoirs, boiler tanks, holes, and mouthpieces (short pipes of various shapes) into the atmosphere or, in general, into a space filled by gas or by the same fluid. It is characteristic of this case of fluid motion that the potential-energy reserve of the fluid in the tank is converted, with some degree of loss, into the kinetic energy of a free jet or drop during the outflow process.

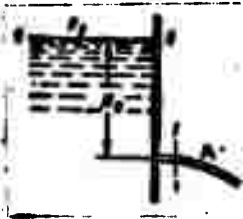


Fig. 90. Outflow from reservoir through small hole.

In aeronautical engineering, fluid outflows must be dealt with in analysis of fuel feed into the combustion chambers of gas-turbine and liquid-rocket engines. The shock-damping processes when an airplane lands or fires cannon also take place basically by expression of fluid through small holes.

Moreover, the flow of fluid through the various jet tubes and nozzles used in fuel and other systems is essentially a case of outflow through holes or mouthpieces.

The basic problem in which we shall be interested in this case is that of determining the outflow velocity and flow rate

of the fluid for the various hole and mouthpiece shapes.

Let us take a large storage tank containing fluid under a pressure  $p_0$  and having a small hole in its wall at a rather great depth  $H_0$  below the exposed surface (Fig. 90). Fluid flows out through this hole into an air (gas) space with a pressure  $p_1$ .

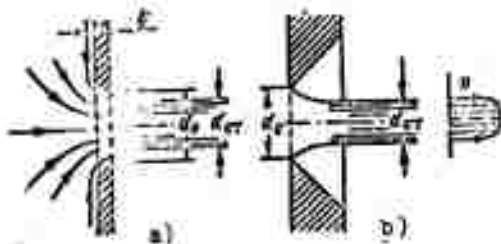


Fig. 91. Outflow through round hole. a) in thin wall; b) with sharp edge.

Let the hole have the shape shown in Fig. 83a, i.e., let it be drilled in the thin wall without finishing of the entrance edge, or let it have the shape shown in Fig. 91b, i.e., let it be made in a thick wall, but with the entrance edge countersunk sharp from the outside. The conditions of fluid outflow will be quite identical in these two cases: fluid particles approach the hole from the entire communicating volume, moving with acceleration along various smooth trajectories (Fig. 91a); the jet separates from the wall at the edge of the hole and then contracts slightly. The jet acquires a cylindrical shape at a distance of approximately one hole diameter. The contraction of the jet is due to the necessity of smooth transition from the various directions of motion of the fluid particles in the tank, including those moving along the wall in a radial direction, to the axial direction of motion in the jet.

Since the hole dimension is assumed small by comparison with the head  $H_0$  and the dimensions of the tank and, consequently, the side walls of the tank and the exposed fluid surface do not affect the inflow of fluid to the hole, we observe what is known as perfect contraction of the jet, i.e., the greatest degree of contraction, as opposed to imperfect contraction, which will be examined later.

The degree of contraction is evaluated in terms of the contraction coefficient  $\epsilon$ , which equals the ratio of the jet cross-sectional area to the area of the hole, i.e.,

$$\epsilon = \frac{S_c}{S_0} = \left( \frac{r_c}{r_0} \right)^2. \quad (9.1)$$

Let us write the Bernoulli equation for motion of the fluid from its free surface in the tank (section 0-0 in Fig. 90), where the pressure is  $p_0$  and velocity can be set equal to zero, to one of the jet cross sections (1-1) in the zone in which the jet has already become cylindrical, so that the pressure in it has reached  $p_1$ . Assuming uniform velocity distribution in the jet,

$$H_0 + \frac{p_0}{\gamma} = \frac{p_1}{\gamma} + \frac{v^2}{2g} + \zeta \frac{v^2}{2g},$$

where  $\zeta$  is the resistance coefficient of the hole.

Introducing the theoretical head  $H$ , we obtain

$$H = \frac{v^2}{2g} (1 + \zeta),$$

where

$$H = H_0 + \frac{p_0 - p_1}{\gamma}.$$

Using the above, we write for the outflow velocity

$$v = \frac{1}{\sqrt{1 + \zeta}} \sqrt{2gH} = \varphi \sqrt{2gH}, \quad (9.2)$$

Here  $\varphi$  is the so-called velocity coefficient, which equals

$$\varphi = \frac{1}{\sqrt{1 + \zeta}}. \quad (9.3)$$

In the case of outflow of an ideal fluid,  $\zeta = 0$ , so that  $\varphi = 1$  and the theoretical outflow velocity is

$$v_t = \sqrt{2gH}. \quad (9.4)$$

Thus, we can conclude from analysis of (9.2) that the velocity coefficient  $\varphi$  is the ratio of the actual to the theoretical outflow velocity:

$$\varphi = \frac{v}{\sqrt{2gH}} = \frac{v}{v_t}. \quad (9.5)$$

The actual outflow velocity  $v$  is always somewhat smaller than theoretical because of resistance, and hence the velocity coefficient is always smaller than unity.

It must be remembered that the velocities are uniformly distributed over the jet cross section only at its center (at the core of the jet); the outer fluid layer is slowed down slightly because of friction against the wall (see Fig. 91b). Experiments have shown that the velocity in the nucleus of the jet is practically equal to the theoretical velocity ( $v_t = \sqrt{2gH}$ ) so that our velocity coefficient  $\varphi$  should be regarded as an average-velocity

coefficient. If the fluid flows out into the atmosphere, the pressure is equal to atmospheric over the entire cross section of a cylindrical jet; this is also confirmed by experiments.

Let us now figure the fluid flow rate as the product of the actual outflow velocity by the actual jet cross sectional area, and then apply (9.1) and (9.2):

$$Q = S_c \phi \sqrt{2gH} \quad (9.6')$$

The product of the coefficients  $\epsilon$  and  $\phi$  is usually denoted by  $\mu$  and called the flow rate coefficient, i.e.,

$$\mu = \epsilon \phi.$$

Then Formula (9.6') is written finally in the form

or

NOT REPRODUCIBLE

$$\left. \begin{aligned} Q &= \mu S_0 \sqrt{2gH} \\ Q &= \mu S_0 \sqrt{2g \frac{p_0}{\gamma}} \end{aligned} \right\} \quad (9.6)$$

where  $p$  is the calculated outflow pressure.

Expression (9.6) is the basic one for this section, since it solves the basic problem - that of determining flow rate; it is applicable for all cases of outflow. The difficulty of using this expression consists in determining the flow rate coefficient  $\mu$  accurately enough.

It follows from Eq. (9.6) that

$$\mu = \frac{Q}{S_0 \sqrt{2gH}} = \frac{Q}{Q_t}$$

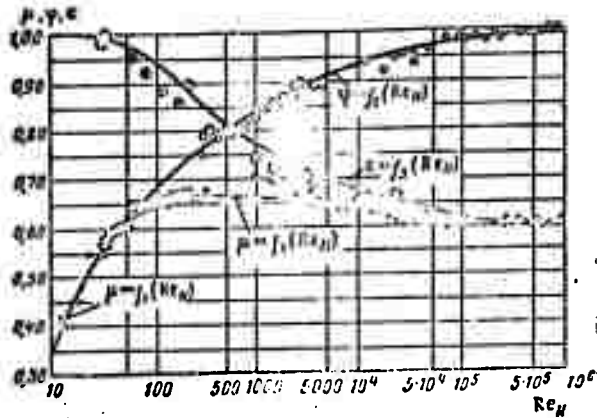
This means that the flow rate coefficient is the ratio of the actual to the theoretical flow rate, i.e., to the flow rate ( $Q_t$ ) that would be the case in the absence of jet contraction and resistance. It must be remembered that the theoretical flow rate  $Q_t = S_0 \sqrt{2gH}$  is not the flow rate for outflow of an ideal fluid, since the jet would contract even in the absence of hydraulic losses.

Since the actual flow rate is always smaller than theory, the flow rate coefficient  $\mu$  is always smaller than unity because of two factors: jet contraction and resistance. The former predominates in some cases and the latter in others.

The contraction ( $\epsilon$ ), resistance ( $\zeta$ ), velocity ( $\phi$ ), and flow rate ( $\mu$ ) coefficients that we have introduced are primarily functions of the type of hole or mouthpiece and, like all of the dimensionless coefficients of hydraulics, of the fundamental criterion of hydrodynamic similarity,  $Re$ .

Figure 92 shows a diagram<sup>1</sup> of the coefficients  $\phi$ ,  $\epsilon$ , and  $\mu$  of a round hole as functions of Reynolds number, which was calculated from the theoretical outflow velocity, i.e.,

$$Re_t = \frac{v_t d_0}{\nu} = \frac{d_0 v_t \sqrt{2.22}}{\nu} = Re_H$$



NOT REPRODUCIBLE

Fig. 92. Diagram of  $\epsilon$ ,  $\phi$ , and  $\mu$  as functions of  $Re_t$  for a round hole in a thin wall.

We see from the diagram that with increasing  $Re_t$ , i.e., with decreasing influence of viscosity forces, the coefficient  $\phi$  increases owing to a decrease in the resistance coefficient  $\zeta$ , while the coefficient  $\epsilon$  decreases as a result of faster flow at the edge of the hole and the increase in the radii of curvature of the jet surface on the segment from the edge to the beginning of the cylindrical part. Both coefficients ( $\phi$  and  $\epsilon$ ) approach asymptotically to the values corresponding to ideal-fluid outflow, i.e., as  $Re_t \rightarrow \infty$ ,  $\phi \rightarrow 1$ ; here, the contraction coefficient  $\epsilon$  tends to the value 0.61, which can be arrived at theoretically for an ideal fluid.

The flow rate coefficient  $\mu$ , which is determined by the product of  $\epsilon$  and  $\phi$ , first increases with increasing  $Re_t$  because of the steep rise of  $\phi$  and then, after reaching a maximum ( $\mu_{\max} = 0.69$  at  $Re_t \approx 350$ ), diminishes because of the substantial decrease in  $\epsilon$  and becomes practically constant at  $\mu = 0.59-0.60$  for large  $Re_t$ .

<sup>1</sup>See page 197 for footnote.

In the region of very small  $Re_t$  ( $Re_t < 15$ ), the importance of viscosity is so great and the deceleration at the edge so considerable that the jet does not contract ( $\epsilon = 1$ ) and  $\phi = \mu$ . The flow rate  $Q$  in this range is proportional to the first power of head loss, so that the flow rate coefficient is approximately proportional to  $Re_t$ . In this case, the following theoretical formula, which has been confirmed by experiments [4], is more accurate:

$$\mu = \varphi = \frac{Re_t}{25 + \mu Re_t}. \quad (9.7)$$

The formula of A.D. Al'tshul' is recommended for  $Re_t > 10^4$ :

$$\mu = 0.59 + \frac{5.5}{\sqrt{Re_t}}. \quad (9.8)$$

For high-viscosity fluids (water, gasoline, kerosene, etc.), outflow usually takes place at rather large  $Re$ , so that the outflow coefficients vary in narrow ranges; the following averaged values are usually taken in calculations:

$$\epsilon = 0.63; \varphi = 0.97; \mu = 0.61; \zeta = 0.065.$$

In outflow of low-viscosity fluids through round holes in a thin wall, there is considerable contraction of the jet and very little resistance. Hence the flow rate coefficient  $\mu$  is found to be substantially smaller than unity, chiefly owing to the influence of jet contraction.

### §39. IMPERFECT CONTRACTION OF JET. OUTFLOW BELOW LEVEL

Imperfect contraction of the jet occurs when the outflow of fluid through the hole and shaping of the jet are influenced by the proximity of the tank's lateral walls and the hole is situated at equal distances from these walls, i.e., on the axis of symmetry of the tank (Fig. 93). Since the side walls give some direction to the fluid motion as it approaches the hole, the jet contracts to a lesser degree on issuing from the hole than in the case of outflow from an unbounded tank, as it was examined above for perfect contraction.

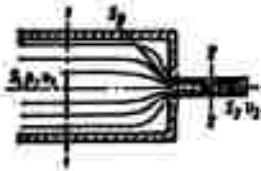


Fig. 93. Diagram of imperfect contraction of jet.

Owing to the reduced contraction of the jet, the contraction coefficient increases and, consequently, so does the flow rate coefficient. The theoretical solution to the problem of ideal-fluid outflow from a flat reservoir of finite width and infinite length through a slit hole in its end wall, i.e., the solution for the case of imperfect contraction in plane flow, was found as early as 1890 by Prof. N.Ye. Zhukovskiy.

When low-viscosity fluids flow out of a cylindrical circular-section tank through a round hole in the center of the end wall, the contraction coefficient  $\epsilon_1$  can be found from the following empirical formula as a fraction of the contraction coefficient  $\epsilon$  for perfect contraction:

$$\frac{\epsilon_1}{\epsilon} = 1 + \frac{0.37}{\epsilon} n^2, \quad (9.9)$$

where  $n = S_0/S_1$  is the ratio of the hole area to the cross-sectional area of the reservoir.

The resistance coefficient  $\zeta$  of the hole and the velocity coefficient  $\phi$  in imperfect contraction may be regarded as independent of the area ratio  $n$  (provided, of course, that  $n$  is not too close to unity) at the following approximate values for low-viscosity fluids:

$$\zeta = 0.065 \quad \text{and} \quad \phi = 0.97.$$

Hence the flow rate coefficient  $\mu_1$  is easily found from the relationship

$$\mu_1 = \epsilon_1 \phi,$$

and the flow rate is determined from the formula

$$Q = \mu_1 S_0 \sqrt{2gH}.$$

However, when this formula is used in the case of imperfect contraction, it must be remembered that the theoretical head  $H$  that appears in the formula represents the total head, which equals

$$H = \frac{p_1 - p_2}{\gamma} + \frac{v_1^2}{2g}.$$

This means that the velocity head in the tank must be taken into account in addition to the hydrostatic head. But since the velocity head is usually also unknown when the flow rate is being determined, it is desirable to have a formula that expresses the flow rate for imperfect contraction not in terms of the total head  $H$ , but in terms of the hydrostatic head.

This formula is easily obtained by writing the Bernoulli and flow rate equations for sections 1-1 and 2-2 (see Fig. 93), i.e.,

$$\frac{p_1}{\gamma} + \frac{v_1^2}{2g} = \frac{p_2}{\gamma} + \frac{v_2^2}{2g} + \zeta \frac{v_2^2}{2g};$$

$$v_2 S_2 = v_1 S_1.$$

This yields

$$v_2 = \frac{1}{\sqrt{1 + \zeta - \epsilon_1^2 n^2}} \sqrt{2g \frac{p_1 - p_2}{\gamma}}$$

and then

$$Q = \frac{\epsilon_1}{\sqrt{1 + \zeta - \epsilon_1^2 n^2}} S_0 \sqrt{2g \frac{\Delta p}{\gamma}} = \mu_1 S_0 \sqrt{2g \frac{\Delta p}{\gamma}}, \quad (9.10)$$

where

$$\mu_1 = \frac{\epsilon_1}{\sqrt{1 + \zeta - \epsilon_1^2 n^2}}. \quad (9.11)$$

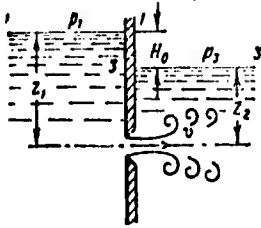


Fig. 94. Outflow below level.

It is often necessary to deal with outflow of fluid not into the atmosphere, but into a space that is filled with the same fluid (Fig. 94). This case is known as outflow below level or outflow through a submerged hole.

In this case, all of the jet's kinetic energy is lost to eddying, as in the case of abrupt expansion. Hence the Bernoulli equation for sections 1-1 and 3-3 (where we assume the velocities to equal zero) is written in the form

$$z_1 + \frac{p_1}{\gamma} = z_2 + \frac{p_3}{\gamma} + \sum h = z_2 + \frac{p_3}{\gamma} + \zeta \frac{v^2}{2g} + \frac{v^2}{2g}$$

or

$$H = H_0 + \frac{p_1 - p_3}{\gamma} = (\zeta + 1) \frac{v^2}{2g},$$

where  $H$  is the theoretical head,  $v$  is the outflow velocity in the compressed section of the jet, and  $\zeta$  is the resistance coefficient of the hole, which has about the same value as in outflow into the atmosphere. From this,

$$v = \frac{1}{\sqrt{1 + \zeta}} \sqrt{2gH} = \varphi \sqrt{2gH}$$

and

$$Q = v S_c = \epsilon \varphi S_0 \sqrt{2gH} = \mu S_0 \sqrt{2gH}.$$

Thus, we have the same working formulas as for outflow into air (gas), except that the head  $H$  represents in this case the difference between the hydrostatic heads on the two sides of the wall, i.e., velocity and outflow do not depend on the height of the hole in the wall.

The contraction and flow rate coefficients in below-level outflow can be assumed to be the same as for outflow into the air.

#### §40. OUTFLOW THROUGH MOUTHPIECES

A short pipe whose length is a few times its diameter [ $l = (2-6)d$ ] and whose entry edge is not rounded is known as an external cylindrical mouthpiece (Fig. 95a). In practice, such mouthpieces are often formed when a hole is drilled in a thick wall and its entry edge is not ground (Fig. 95b).

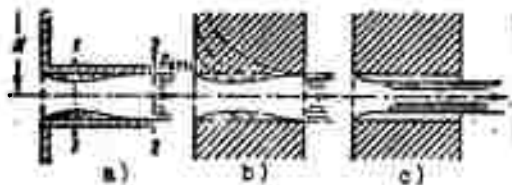


Fig. 95. Diagram of outflow through cylindrical mouthpiece.

Either of two outflow regimes may be observed in outflow through such a mouthpiece into a gaseous medium. The flow diagram corresponding to the first regime appears in Fig. 95, a and b. On entering the mouthpiece, the jet is compressed for approximately the same reason as in outflow through a hole in a thick wall. Then, since the compressed part of the jet is surrounded by eddying fluid, the jet gradually expands to the size of the hole and emerges full-section from the mouthpiece.

Since the jet diameter is equal to the hole diameter as it emerges from the mouthpiece, we have  $\epsilon = 1$  and hence  $\mu = \phi$ .

The flow rate coefficient of an external cylindrical mouthpiece in the first outflow regime depends on the relative length  $l/d$  of the mouthpiece and on  $Re$ . An experimental graph illustrating this relationship appears in Fig. 96 [4].

The averaged coefficient values for this outflow condition are as follows for low-viscosity fluids (large  $Re$ ):

$$\mu = \phi = 0.80 \text{ and } \zeta = 0.55.$$

Comparison with the hole in the thin wall indicates that in outflow through a cylindrical mouthpiece (first regime), the flow rate is higher than in outflow through the hole because of the lack of compression at the exit from the mouthpiece; the velocity, on the other hand, is lower owing to the substantially higher resistance.

Let a fluid flow out under a pressure  $p_0$  into a gaseous medium at pressure  $p_2$ , e.g., into a liquid rocket engine [LRE] (ЖРД) combustion chamber. In this case, the theoretical head for perfect contraction equals

$$H = \frac{p_0 - p_1}{\gamma}$$

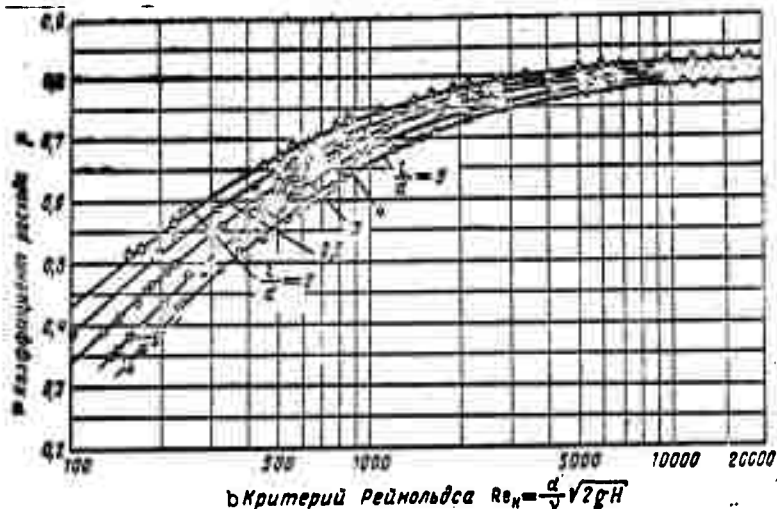


Fig. 96. Flow rate coefficient of cylindrical mouthpiece as a function of Re.  
KEY: (a) flow rate coefficient; (b) Reynolds number.

Since the pressure in the jet is  $p_2$  at the exit from the mouthpiece, the pressure  $p_1$  in the constricted zone of the jet inside the mouthpiece, where the velocity is elevated, is lower than  $p_2$ . Here, the larger the head under which outflow occurs and, consequently, the greater the flow rate through the mouthpiece, the smaller will be the absolute pressure in the contraction inside the mouthpiece. The pressure difference  $p_2 - p_1$  increases in proportion to the head  $H$ . We can demonstrate this by writing the Bernoulli equation for sections 1-1 and 2-2 (see Fig. 95a):

$$\frac{p_1}{\gamma} + \frac{v_1^2}{2g} = \frac{p_2}{\gamma} + \frac{v_2^2}{2g} + \frac{(v_1 - v_2)^2}{2g}$$

Here the last term represents the head loss on stream expansion, which takes place in approximately the same way here as in an abrupt channel expansion and, consequently, is determined by Formula (8.1). The contraction of the jet inside the mouthpiece is evaluated by the same contraction coefficient  $\epsilon$  as in the case of the hole, so that we can write on the basis of the flow rate equation

$$\frac{v_1}{v_2} = \frac{1}{\epsilon}$$

Using this relation to exclude the velocity  $v_1$  from the above Bernoulli equation and replacing the velocity  $v_2$  by its expression in terms of the mouthpiece velocity coefficient  $v_2 = \phi\sqrt{2gH}$ , we find the pressure drop inside the mouthpiece, i.e.,

$$p_2 - p_1 = \varphi^2 \left[ \frac{1}{\epsilon^2} - 1 \cdot \left( \frac{1}{\epsilon} - 1 \right)^2 \right] H \gamma. \quad (9.13)$$

Substituting  $\phi = 0.80$  and  $\epsilon = 0.63$  in the above,

$$p_2 - p_1 = 0.75 H \gamma. \quad (9.13')$$

At a certain critical head ( $H_{kr}$ ), the absolute pressure inside the mouthpiece (section 1-1) vanishes (or, more precisely, becomes equal to the vaporization pressure), and

$$H_{kr} = \frac{P_v}{0.75 \gamma}. \quad (9.14)$$

With  $H > H_{kr}$ , therefore, the pressure  $p_1$  would have to be negative, but since negative pressures do not usually occur in a fluid, the first outflow regime with  $H > H_{kr}$  becomes impossible. Experiment confirms this, indicating that an abrupt change in outflow regime and a transition from the first regime to the second take place at  $H \approx H_{kr}$  (see Fig. 95c).

The second outflow regime is characterized by a jet that no longer expands after contracting, but remains cylindrical and flows out of the mouthpiece without touching its walls. The outflow becomes identical to that from a hole in a thin wall, with the same outflow-coefficient values. On transition from the first outflow regime to the second, therefore, velocity increases and flow rate diminishes owing to compression of the jet.

If water flows out through this mouthpiece into the atmosphere,

$$H_{kr} = \frac{P_v}{0.75 \gamma} = \frac{1.23}{0.75 \cdot 9.8} \approx 16 \text{ m.}$$

If the saturation vapor pressure  $p_v$  of the outflowing fluid is comparable with the pressure  $p_2$  in the medium into which it is flowing, it is necessary to set  $p_1 = p_v$  in Formula (9.13) and obtain for the critical head instead of (9.14)

$$H_{kr} = \frac{P_v - p_2}{0.75 \gamma}.$$

The second outflow regime is also possible at  $H < H_{kr}$ , i.e., when either the first or the second outflow regime is realized in accordance with the conditions under which the outflow begins.

In below-level outflow through a cylindrical mouthpiece, the first flow regime will not differ from the above description. But when the absolute pressure inside the mouthpiece drops to the saturation vapor pressure as a result of an increase in  $H$ , cavitation outflow begins; flow rate ceases to depend on the pressure  $P_2$ , i.e., the effect is to stabilize flow rate as described in §23.

Thus, an external cylindrical mouthpiece has substantial deficiencies: high resistance and inadequate flow rate coefficients in the first regime and a very low flow rate coefficient in the second. Another shortcoming of this mouthpiece is the two possible regimes of outflow into a gas at  $H < H_{kr}$  and, consequently, the two-valued flow rate at a given  $H$  and the possibility of cavitation in outflow below level.

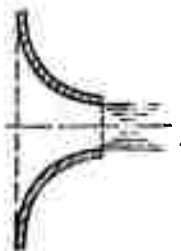


Fig. 97. Nozzle.



Fig. 98. Diffuser mouthpiece.  
KEY: (a) cavitation.

When cylindrical mouthpieces (holes drilled in a thick wall) are used, for example, as jet tubes, chokes, or nozzles (see example), these deficiencies must be taken into account. This mouthpiece can be improved substantially by rounding the entry edge (see dashed line in Fig. 95b). The greater the rounding, the larger will be the flow rate coefficient and the smaller the resistance coefficient. In the limit, at a radius of curvature equal to the wall thickness, the cylindrical mouthpiece approximates the so-called conoidal mouthpiece or nozzle.

The conoidal mouthpiece or nozzle (Fig. 97) has an outline that approximates the shape of a naturally contracting jet, and this ensures nonseparation of the flow inside the mouthpiece and a parallel jet in the exit cross section. This mouthpiece is used very extensively because it has a flow rate coefficient near unity, very small losses, a contraction coefficient  $\epsilon = 1$ , and stable outflow conditions without cavitation.

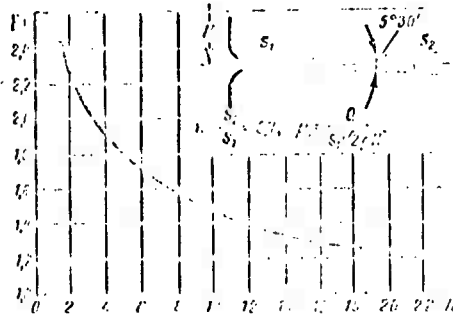
The resistance-coefficient values are the same as those given for the smooth contraction (§34), i.e.,  $\zeta = 0.03-0.10$  (small  $\zeta$  correspond to larger  $Re$  and vice versa). Accordingly,  $\mu = \phi = 0.99-0.96$ .

The diffuser nozzle represents a combination of a nozzle and a diffuser (Fig. 98). Attaching the diffuser to the nozzle lowers the pressure in the throat of the mouthpiece and, consequently, increases the velocity and flow rate of the fluid through it. The diffuser mouthpiece may deliver a substantially higher flow rate than the nozzle (by a factor of up to 2.5) at the same throat diameter as the nozzle and the same head.

Mouthpieces of this type are used when the throat-section diameter and head are specified and it is necessary to obtain the highest possible flow rate. However, the diffuser mouthpiece can be used only at very modest heads ( $H = 1-4$  m), since otherwise cavitation arises in the mouthpiece throat. Cavitation results in increased resistance and lowered throughput of the mouthpiece.

Figure 99 shows the drop in flow rate coefficient of a diffuser mouthpiece with increasing head owing to cavitation initiated in the throat of the mouthpiece (flow rate coefficient referred to throat section area).

This curve was obtained by testing a diffuser mouthpiece with the optimum angle and expansion ratio, i.e., those that ensure the largest possible flow rate coefficient (author's experiments).



NOT REPRODUCIBLE

Fig. 99. Diagram of flow rate coefficient as a function of head.

**Example.** So-called jet nozzles, i.e., simple drilled passages, are used to supply propellants into the combustion chambers of certain liquid rocket engines. Determine the necessary number  $z$  of these nozzles for oxidizer supply to the rocket engine if  $G = 1.6$  kgf/s, the pressure drop across the nozzle  $\Delta p = 6$  kgf/cm<sup>2</sup>, the chamber pressure  $p_2 = 25$  kgf/cm<sup>2</sup>, the hole diameter  $d_0 = 1.5$  mm, and the ratio of wall thickness to hole diameter  $\delta/d_0 = 0.5$ . The oxidizer is nitric acid with a specific weight  $\gamma = 1510$  kgf/m<sup>3</sup> and a viscosity coefficient  $\nu = 0.02$  cm<sup>2</sup>/s.

How many nozzles would be required if  $\delta/d_0 = 2.5$ ?

Solution. 1. The theoretical outflow velocity

$$v_t = \sqrt{2g \frac{\Delta p}{\gamma}} = \sqrt{2 \cdot 9.81 \frac{6 \cdot 10^4}{1510}} = 28 \text{ m/s.}$$

2. The Reynolds number

$$Re_t = \frac{v_t d_0}{\nu} = \frac{2800 \cdot 0.15}{0.02} = 21000.$$

3. We refer to the diagram (Fig. 92) to find the flow rate coefficient  $\mu = 0.62$  from the  $Re_t$ .

4. We determine the total hole area  $S_0$  of all nozzles from the equation

$$S_0 = \frac{G}{\gamma \mu v_t} = \frac{1.6 \cdot 10^4}{1.51 \cdot 0.62 \cdot 2800} = 0.61 \text{ cm}^2.$$

5. The number of nozzles is

$$z = \frac{4S_0}{\pi d_0^2} = \frac{4 \cdot 0.61}{\pi \cdot 0.15^2} = 35.$$

6. If the hole had a ratio  $\delta/d_0 = 2.5$ , fuel outflow would take place as from an external cylindrical mouthpiece.

To determine the outflow regime, we find  $\Delta p_{kr}$  from (9.13'):

$$\Delta p_{kr} = \frac{2\gamma}{0.7G} = 33.5 \text{ kgf/cm}^2.$$

Since  $\Delta p_{kr} > \Delta p$ , we shall have the first outflow regime with a flow rate coefficient  $\mu = 0.82$ . Hence the number of nozzles is

$$z_1 = z \frac{\mu}{\mu_1} = 35 \frac{0.62}{0.82} = 27.$$

#### §41. OUTFLOW UNDER VARIABLE HEAD (DRAINAGE OF CONTAINERS)

Let us consider the process in which an arbitrarily shaped container that communicates with the atmosphere is drained through a hole or mouthpiece in its bottom that has a flow rate coefficient  $\mu$  (Fig. 100). In this case, we have outflow under a variable and progressively decreasing head, i.e., the flow is, strictly speaking, nonsteady.

However, if the head and, consequently, the outflow velocity vary slowly, the motion can be regarded as steady for any particular point in time and the Bernoulli equation can be used to solve the problem.



Fig. 100. Drainage of container.

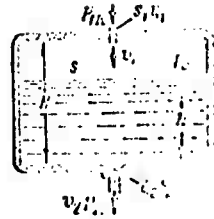


Fig. 101. Drainage of vented tank.

Denoting by  $h$  the variable height of the liquid level in the container as measured from the bottom, by  $S$  the cross sectional area of the tank at this level, and by  $S_0$  the area of the hole, and taking an infinitesimally short time segment  $dt$ , we can write the following equation of volumes:

$$S dh = -Q dt \quad (9.15)$$

or

$$S dh = -\mu S_0 \sqrt{2gh} dt,$$

where  $dh$  is the drop in fluid level in the container during time  $dt$ .

The minus sign appears because a negative increment  $dh$  corresponds to a positive increment  $dt$ .

Hence the time for complete drainage of a container of height  $H$  (assuming  $\mu = \text{const}$ ) is

$$t = \frac{1}{\mu S_0 \sqrt{2g}} \int_0^H \frac{S dh}{\sqrt{h}} \quad (9.16)$$

The integral can be evaluated if we know the law of variation of the area  $S$  versus height  $h$ . For a prismatic container,  $S = \text{const}$ , so that

$$t = \frac{1}{\mu S_0 \sqrt{2g}} \int_0^H \frac{S dh}{\sqrt{h}}$$

or

$$t = \frac{2S}{\mu S_0 \sqrt{2g}} \sqrt{H} = \frac{2S \sqrt{H}}{\mu S_0 \sqrt{2g}} \quad (9.17)$$

The numerator in this formula is equal to twice the container volume, while the denominator represents the flow rate at the beginning of drainage, i.e., at head  $H$ . Consequently, the total draining time of the container is twice the time for outflow of

the same volume of fluid at a head that remains constant at the initial value.

Formula (9.16) and (9.17) can also be used to determine the times to fill containers under variable heads that decrease from  $h = H$  to  $h = 0$  as the tank is filled.

In aviation practice, it is necessary to deal with drainage of sealed containers (tanks) that communicate with the atmosphere only through a small-diameter hole, mouthpiece, or drainage pipe (Fig. 101). In this case, atmospheric air flows into the container, in which a partial vacuum is set up, as the fluid flows out of it. Drainage of the container is therefore retarded, and to a greater degree the more difficult it is for air to get into it.

Let us determine the time to drain such a container, for which we write two Bernoulli equations: one for the motion of air from a stationary atmosphere into the container, and another for the motion of fluid from the upper surface to the exit into the atmosphere. Using the nomenclature of Fig. 101, we write

NOT REPRODUCIBLE

$$\frac{p_{A_1}}{\gamma_{\text{air}}} - \frac{p_0}{\gamma_{\text{air}}} + (1 + \zeta_1) \frac{v_1^2}{2g};$$

$$h + \frac{p_0}{\gamma_{\text{fl}}} - \frac{p_A}{\gamma_{\text{fl}}} + (1 + \zeta_2) \frac{v_2^2}{2g}.$$

The compressibility of the air can be disregarded in this case; hence the volume flow rates of air and fluid can be set equal to one another, i.e.,

$$Q = v_1 S_1 = v_2 S_2$$

(if the jet contracts, it is also necessary to introduce the coefficient  $\epsilon_1$ ).

The above equations will now be rewritten

$$p_A = p_0 + (1 + \zeta_1) \frac{Q^2}{2g S_1^2} \gamma_{\text{air}};$$

$$h \gamma_{\text{fl}} + p_0 = p_A + (1 + \zeta_2) \frac{Q^2}{2g S_2^2} \gamma_{\text{fl}}.$$

Adding these equations and determining the flow rate, we obtain

$$Q = \sqrt{\frac{2gh\gamma_{\text{fl}}}{\frac{1 + \zeta_1}{S_1^2} \gamma_{\text{air}} + \frac{1 + \zeta_2}{S_2^2} \gamma_{\text{fl}}}} \quad (9.18)$$

Substituting Expression (9.18) into the equation of volumes (9.15), determining  $dt$  from that equation, and then integrating with  $h = H$  and  $h = 0$  as limits, we have

$$t = \frac{2SH}{\sqrt{2gH\gamma_k}} \sqrt{\frac{1 + \zeta_1}{S_1^2 V_{\text{res}} + \frac{1 + \zeta_2}{S_2^2 V_k}}}. \quad (9.19)$$

This formula can also be used when air enters the tank and fluid leaves it through pipes, but then the corresponding coefficient  $\zeta$  must be replaced by

$$\zeta = \lambda \frac{l}{d} \left( \frac{v}{c} \right)^2 \zeta_m$$

where  $l$  and  $d$  are the length and diameter of the pipe and  $\sum \zeta_m$  is the sum of the local resistance coefficients in the pipe.

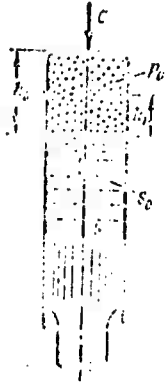


Fig. 102. Diagram of undercarriage shock-absorber strut.

The process of shock absorption when an airplane touches down can serve as another example of fluid outflow under the action of a variable head. The top of an air-oil undercarriage shock absorber (Fig. 102) contains compressed air, which is under a pressure  $p_0$  in flight. On contact of the airplane's wheels with the ground, fluid flows through holes of area  $S_0$  with a flow rate coefficient  $\mu$ , and the air cushion is compressed to pressure  $p_1$ . The height of the air cushion is reduced in this process from  $h_0$  to  $h_1$ .

To simplify the actual shock-absorbing process, let us assume that a constant force  $G$  is abruptly applied to the shock absorber and that the air is isothermally compressed. Let us find the time of the shock-absorbing process, i.e., the fluid-flow time to establishment of equilibrium.

We again have Eq. (9.15):

$$S dh = Q dt,$$

NOT REPRODUCIBLE

where  $S$  is the piston area and  $dh$  is the compression of the cylinder during time  $dt$ .

The flow rate through the holes is

$$Q = \mu S_0 \sqrt{2g \frac{p_1}{\gamma} \left( \frac{p_0}{p_1} \right)^{\frac{1}{k}}}$$

Here  $p_1$  is the constant pressure over the piston, which equals  $p_1 = G/S$ , and  $p$  is the variable air pressure, which is determined by the isotherm equation  $p (h_0 + h_1) \frac{1}{k} = p_1 h_1$ .

On substituting the expressions for  $p_1$  and  $p$  into (9.15), we have

$$t = \frac{S \sqrt{\gamma}}{\mu S_0 \sqrt{2g (p_1 + p_A)}} \int \sqrt{\frac{h}{h-h_1}} dh,$$

where

$$h_1 = \frac{p_0 + p_A}{p_1 + p_A} h_0.$$

Integrating from  $h = h_0$  to  $h = h_1$  gives us the unknown time  $t$ .

## §42. FUNDAMENTALS OF HYDRAULIC AUTOMATION

A variety of hydraulic devices and systems whose operation is automatically controlled are used extensively in aviation engineering and other machine-building fields.

Such systems and devices are usually controlled by regulating fluid flow, i.e., by adjusting the pressure, flow rate, or direction of motion of fluid.

Here we shall examine only the simplest control devices, those that are the basic elements of more complex hydraulic-automation components and systems. Some of the more complex control devices, which consist of a number of elements, will be considered later in §72 as elements of aircraft hydraulic power systems.

Control devices are classified on the basis of function as pressure regulators, flow rate regulators, and distributors; the latter act to change the direction of motion of a fluid.

These control devices can be subclassified as chokes and valves on the basis of operating principle. Both present local hydraulic resistances that are deliberately inserted into the path of the fluid to throttle it. Throttling is a process in which the fluid's pressure (head) is reduced as it moves through a local hydraulic resistance.

The difference between a choke and a valve consists in the following. The geometrical characteristics of a choke, i.e., the dimensions of its ports (holes), in which the throttling takes place, do not change under the influence of the fluid flow rate passing through it. The geometrical characteristics of a valve, on the other hand, do change under the influence of flow rate.

Both chokes and valves can be made adjustable and nonadjustable. This means that in the former case their geometrical characteristics can be varied by external manipulation during their operation, while in the latter case such external adjustments are not possible.

The jet tube examined in §36 (Fig. 86) can be taken as an example of the simplest type of nonadjustable choke, while any cock, valve, slide, or flap whose aperture can be regulated manually or automatically is an adjustable choke. The adjustable

choke can be used to vary the flow variables of a fluid (its flow rate, pressure), but there is no back effect of the flow on the choke that can cause a change in its geometry.

The elementary valve (see Fig. 106) is usually pressed against its seat by a spring or under its own weight, and opens when it is acted upon by a fluid-pressure drop. Here the opening of any valve is always determined by equilibrium, i.e., equality of the force (or torque) that the fluid exerts on the valve, which tends to open it further, to the force that resists opening of the valve.

If the force resisting opening of the valve is constant (e.g., the valve's own weight), or if it increases on a certain curve with valve opening (for example, a spring force), the valve or nonadjustable. If, on the other hand, some sort of device acts on the valve from the outside during its operation and changes the force that resists its opening (for example, if the spring is loaded or some other additional force is applied) and the valve opening changes as a result, the valve is adjustable.

Let us examine the geometrical shapes and hydraulic properties of chokes and valves.

A choke is a local resistance that consists in the simplest case of a more or less smooth or abrupt constriction of the channel and a narrow passage beyond which there is usually a sudden expansion.

The hydraulic properties of a choke are determined by the dependence of the local head loss  $h_m$  on flow rate  $Q$ . As we have already stated in §36, this relationship is linear for small Reynolds numbers and a great enough relative length of the choke's narrow passage, because the head loss is basically due to friction in laminar flow. In this case, we speak of a linear choke. It must be remembered that the head loss in the choke varies in direct proportion to fluid viscosity and, consequently, the hydraulic characteristic of such a choke depends on fluid temperature, i.e., is not stable.

When the length of the choke's narrow passage is minimized and the Reynolds numbers are large enough, the head loss in the choke is determined basically by eddying on the abrupt expansion, and the curve of  $h_m$  as a function of  $Q$  is practically quadratic. The device is known as a square-law choke; its hydraulic characteristic is more stable, i.e., practically independent of fluid viscosity.

In this case, the optimum shape for the throttling orifice is that of a circular hole in a thin wall (see Fig. 91). For technological reasons, however, drilled passages with length ratios  $l/d = 1-3$ , i.e., external cylindrical mouthpieces, are used more often.

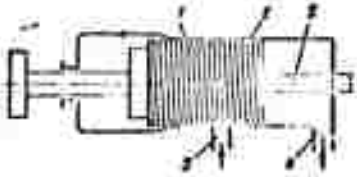


Fig. 103. Diagram of linear choke with screw-type throttling valve.



Fig. 104. Diagram of multistage choke.

Very often, a choke is called upon to produce a large pressure drop, i.e., a very substantial head loss. And this requires a very small throttling orifice, which is undesirable in view of the possibility of plugging or obliteration (see §27). In these cases, therefore, recourse is taken to chokes with extended throttling passages (in the case of the linear choke) or several throttling orifices are placed in sequence (for the square-law choke).

In one practical linear choke (Fig. 103), the throttling passage is the helical groove of screw 1, which is tightly fitted to case 2.

Fluid enters the choke through hole 3, runs along the helical groove, and exits through hole 4. The length of the throttling passage and, consequently, the resistance of the choke are easily regulated during operation (or adjusted when idle) by turning screw 1 either into or out of internal screw 5. The resistance of such a choke varies in direct proportion to the turn angle of the screw. Since the characteristic of a linear choke depends on viscosity and hence on fluid temperature, it is especially important to be able to regulate it.

The diagram shown in Fig. 104 represents a typical nonadjustable square-law choke designed for a large pressure drop. The version shown is a multistage type, since in it the fluid passes through several elementary chokes that have been set up in series. It is recommended that the throttling-orifice diameter  $d$  be made no smaller than 0.5-1.5 mm, the wall thickness  $(1-2)d$ , and the distance between the walls  $(3-5)d$ . The holes should be placed not opposite one another on the axis of the choke, but at diametrically opposite points, so that the path of the fluid will be labyrinthine.

Tests run on such multistage chokes by V.V. Vakina<sup>2</sup> indicate that the resistance coefficient of a choke with  $n$  stages is smaller than that of a single-stage choke multiplied by  $n$ , and that the flow rate coefficient  $\mu$  is accordingly larger. The results of these tests appear in Fig. 105, where the flow rate coefficient, referred to the area of the throttling orifice, is given

<sup>2</sup>See page 197 for footnote.

as a function of Reynolds number for  $n = 1, 2, 7,$  and  $10$  stages. The dashed curves on the same figure were constructed on the assumption that the stages do not influence one another, i.e., by the formula

$$C = \frac{\zeta_1 \mu_1}{\sqrt{n}} \cdot \frac{1}{\sqrt{n_1}}$$

where  $\zeta_1$  and  $\mu_1$  are the resistance and flow rate coefficients of the single-stage choke, respectively, and  $C$  is the calculated flow rate coefficient of the  $n$ -stage choke.

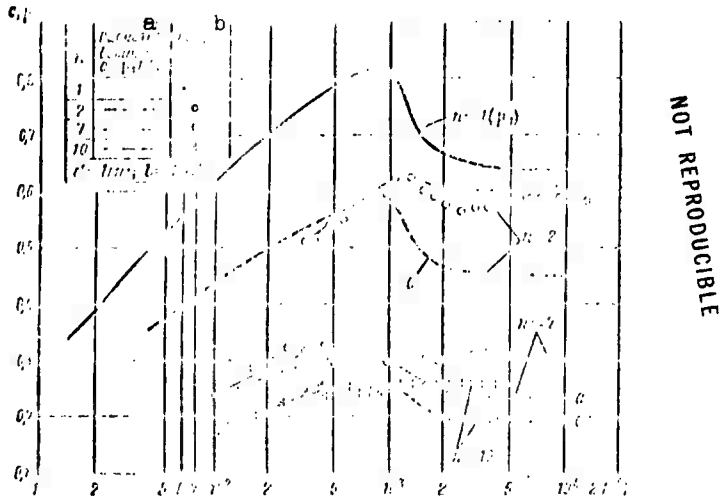


Fig. 105. Results of tests of multistage chokes.  
KEY: (a) calculated value of  $C$ ; (b) experimental results.

The experiments were run using AMG-10 fluid with chokes having orifice diameters  $d = 1$  mm, wall thicknesses  $\delta = 1.5$  mm, and wall separations of 5 mm. The pressure drop was varied from 0.25 to 170 kgf/cm<sup>2</sup>.

The disagreement between experiment and calculation is explained by the reciprocal effects between stages, which consist in less than total extinction of the outflow velocity in the spaces between chokes.

We see from the diagram that the greater the number of stages  $n$ , the more stable is the flow rate coefficient with Reynolds-number variation and, consequently, the more precisely will the choke follow the square-law resistance curve. This is because the transition from nonseparating outflow to separating outflow in the throttling orifices, which takes place in the same

way as in a cylindrical mouthpiece (see §40), does not occur simultaneously in all of the choke orifices. The outflow-regime change takes place first in the last orifice on the path of the fluid, where the absolute pressure is lowest. As the pressure drop across the choke increases further, and flow rate and Reynolds number increase with it, the outflow regime changes in the next-to-last orifice, and so forth.

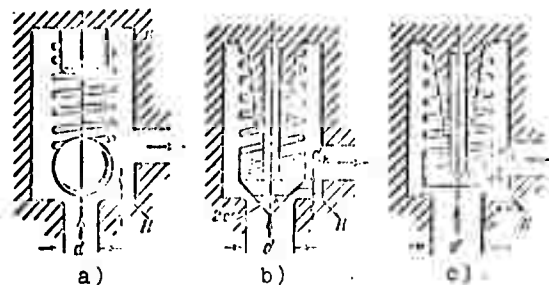


Fig. 106. Varieties of the valve.

The following expression, which defines the flow rate coefficient of an  $n$ -stage choke, can be used in practical mathematical design of multistage chokes similar to those tested:

$$F_n = k \cdot \frac{\mu_1}{\sqrt{n}}$$

where  $k$  is the stage interference coefficient, which can be set equal to 1.27.

Valves are used in the following three basic design configurations, which are shown schematically in Fig. 106: ball, cone, and poppet or mushroom.

The ball valve (a) is simplest in design and manufacture, but is usually used only for low pressures and not in continuous duty.

The cone (b) and poppet (c) valves are the most reliable and can be used at high pressures and flow rates.

The diameter of a valve is usually

$$d_n = (1.15 - 1.25) d,$$

where  $d$  is the diameter of the port at the seat; the ratio  $d_n/d$  is larger for poppet than for cone valves.

The hydraulic characteristics of valves, i.e., their coefficients of resistance  $\zeta$  and flow rate  $\mu$ , can be determined in two ways: by taking as the working area and velocity either the

constant area of the port and the variable velocity in it or the variable area of the slit under the valve and the approximately constant (for a given pressure drop across the valve) velocity of outflow through this slit.

In the latter case, we have for the valve's flow rate coefficient in accordance with the fundamental formula (9.6)

$$K = \frac{Q}{S \sqrt{2gH}}$$

where for a poppet valve

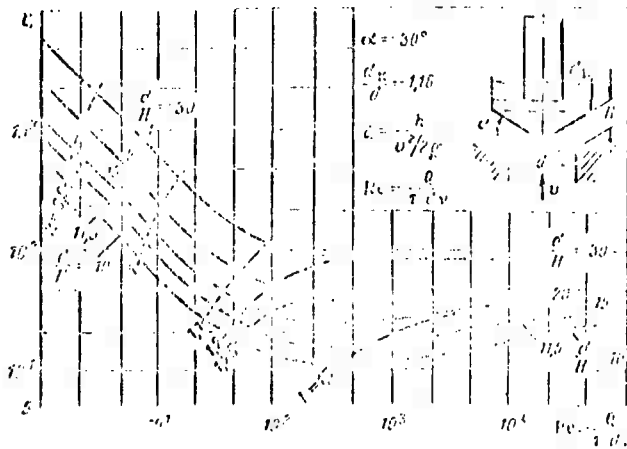
$$S = a d H,$$

and for a cone valve with a cone angle of  $2\alpha$ ,

$$S = a d H \sin \alpha,$$

(here H is the height to which the valve is lifted).

When this notation is used, the flow rate coefficient can be considered independent of valve lift (if it is not lifted too high). However, this coefficient does depend on Reynolds number.



NOT REPRODUCIBLE

Fig. 107. Results of tests on cone valve.

For large enough  $Re$ , i.e., for

$$Re = \frac{\rho v d}{\mu} > (1 - 3) 10^3,$$

the regimes of outflow through valves can be considered square-law. In these cases, it is recommended that the flow rate coefficients of cone and ball valves be set equal to 0.52-0.56, and

those for poppet valves to 0.58-0.62 [6].

At smaller Reynolds numbers, it is necessary to resort to appropriate experimental data. Thus, Figs. 107 and 108 show test results for cone and poppet valves in a broad Reynolds-number range from linear to quadratic resistance laws.<sup>3</sup> The vertical axis is marked off for the resistance coefficients of the valves, which equal

$$\zeta = \frac{2R\Delta p}{\gamma v^2} = \frac{2R h_{k1}}{v^2},$$

(where  $v$  is the velocity in the port and  $h_{k1}$  is the head loss in the valve), while the horizontal coordinate is the Reynolds number computed by the formula

$$Re' = \frac{Q}{\pi d v}.$$

The curves were plotted for various valve lifts referred to the port diameter  $d$ . The same diagrams have a line of constant load coefficient  $k$ , which is equal to

$$k = \frac{\Delta p \pi d^2}{4P} = \frac{h_{k1} \gamma \pi d^2}{4P},$$

where  $P$  is the force exerted by the fluid flow on the valve.

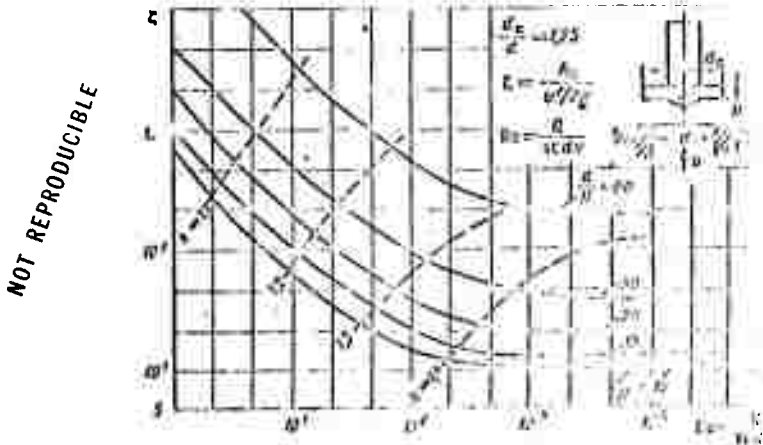


Fig. 108. Results of tests on poppet valve.

These diagrams enable us to solve, for example, the following practically important problem. The dimensions of the loaded valve and spring and the properties of the fluid ( $\gamma$  and  $v$ ) are given. Construct the characteristic of the valve, i.e., the  
<sup>3</sup>See page 197 for footnote.

relation

$$h_{k1} = f(Q).$$

Let the spring force  $P_{pr}$  increase in proportion to its deformation, i.e., in proportion to the valve lift  $H$ , so that it equals

$$P_{pr} = P_{pr0} + CH,$$

where  $P_{pr0}$  is the spring force with the valve closed and  $C$  is a constant of the spring that can be calculated from the diameter of the spring stock, the coil radius, the number of coils, and the shear modulus.

Let us take the basic expression for the head loss in the valve in the form

$$h_{k1} = \zeta \frac{v^2}{2g}$$

replace  $h_{k1}$  by its expression in terms of the above coefficient  $\zeta$ , and express  $v$  in terms of the flow rate:

$$\frac{4P_{pr}f}{\pi d^2 \gamma} = \zeta \frac{16Q^2}{2g\pi^2 d^5}$$

Cancelling and substituting the expression for  $P_{pr}$  in terms of  $H$ , we solve the equation for  $Q$ :

$$Q = \sqrt{\frac{P_{pr0} + CH}{\zeta \gamma}}$$

On the other hand,

$$h_{k1} = \frac{\zeta (P_{pr0} + CH)}{\gamma}$$

The two equations obtained can be used to make the calculations needed to plot the desired curve, but since the Reynolds numbers are not known in advance, the problem must be solved by successive approximations. We might, for example, first assign a square-law regime, take the  $H/d$  from the diagram, and find  $H$ ,  $\zeta$ , and  $k$  for them. Then the resulting formulas would be used to determine the  $Q$  and  $h_{k1}$  for each of the  $H/d$  values, i.e., to obtain the first-approximation curve of the valve. Then  $Re$  can be calculated for each value of  $Q$ , the same diagram again consulted to find  $\zeta$  and  $k$ , followed by use of the same formulas to determine  $Q$  and  $h_{k1}$  in the second approximation. In the case of a substantial disagreement with the first approximation, the calculation should be continued with the same procedure.

NOT REPRODUCIBLE

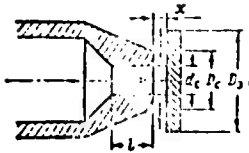


Fig. 109. Diagram of flap nozzle.

The flap nozzle (Fig. 109) is a combination of two elements: a nozzle, which usually consists of conical and short cylindrical segments, and a flap - a round plate that is hinged on an arm long enough so that its motions relative to the nozzle can be considered translational.

Some kind of external force is usually applied to the flap and, together with the fluid pressure force, determines the degree of opening of the nozzle, i.e., the distance of the flap from the nozzle exit plane. By its operating principle, therefore, the flap nozzle is an adjustable valve.

Devices of this type are widely used in the automatic control systems of aviation-type pumps (§68), in automatic-pilot servosystems, etc.

The device is usually quite small: nozzle diameter  $d_s$  of the order of 1 mm, diameter of outer circle of nozzle exit plane  $D_s = (1.2-1.5)d_s$ , flap diameter  $D_z = (3-4)d_s$ , length of nozzle cylindrical section  $l = (1-2)d_s$ .

When such a unit is used in hydraulic automation systems, it is necessary to determine its throughput (fluid flow rate) and the force that the fluid exerts on the flap at various pressures and various flap-to-nozzle distances.

Research has shown that the following modes of fluid outflow through a flap nozzle are possible: separating, nonseparating, and transitional. The separating regime (Fig. 110a) occurs at large enough distances  $x$  from the nozzle exit plane to the flap and is characterized by pressure equal to ambient in the jet at the nozzle exit plane; the fluid does not contact the nozzle exit plane, but impinges on the flap, spreading out over it in the radial directions. The thickness of the fluid layer is smaller than the distance  $x$ .

NOT REPRODUCIBLE

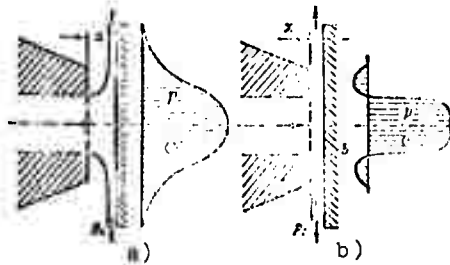


Fig. 110. Diagrams of outflow regimes through flap nozzle.

The nonseparating outflow regime (Fig. 110b) usually occurs when the distance  $x$  from the nozzle to the flap is short; in it, the fluid characteristically moves in a gap-type flow between the nozzle exit plane and the flap, filling the volume of this gap completely. As the flow makes its right-angle turn, local separation occurs and an eddying region  $b$  forms, but then the flow broadens and has a thickness equal to the distance  $x$  when it emerges into the environment.

The best way to judge the probability of a given outflow regime through a nozzle flap is to compare the area of the nozzle orifice ( $\pi d_s^2/4$ ) with the areas of the cylindrical gap sections directly after the turning of the flow ( $\pi d_s x$ ) and at the exit into the environment ( $\pi D_s x$ ). With

$$x < \frac{d_s^2}{4D_s}$$

NOT REPRODUCIBLE

the gap sectional area at the exit is smaller than the area of the nozzle orifice and nonseparating outflow is more probable. With

$$x > \frac{d_s^2}{4D_s}$$

the nozzle orifice area is smaller than the gap sectional area immediately after the turning of the flow, and a separating or transitional outflow mode is more likely.

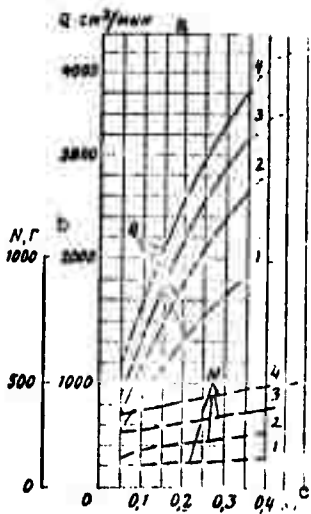
The outflow mode observed is also influenced by the pressure drop  $\Delta p$  under which outflow takes place and by the absolute pressure  $p_0$  in the environment into which the fluid is flowing.

Since the flow constricts slightly in nonseparating outflow immediately after the turn, its velocity rises and its pressure drops. During the subsequent radial flow in the gap, velocity decreases and pressure rises (as in a diffuser) to the value  $p_0$  at the exit. Thus we obtain a phenomenon similar to that observed in an external cylindrical or diffuser mouthpiece with nonseparating outflow.

Just as in these mouthpieces, therefore, the larger the drop  $\Delta p$  and the lower the absolute pressure  $p_0$ , the more will conditions favor the appearance of separating outflow.

In addition to the distinct separating and nonseparating outflow regimes, a flap nozzle can also develop outflow with partial flow separation, i.e., with separation on the part of the annular area bounded by circles of diameters  $D_s$  and  $d_s$ , i.e., a transitional regime.

The transition from nonseparating to separating flow as  $x$  increases takes place gradually, passing through a regime of partial separation, and not all at once.



- 1)  $\Delta p = 10 \text{ kgf/cm}^2$
- 2)  $\Delta p = 20 \text{ kgf/cm}^2$
- 3)  $\Delta p = 30 \text{ kgf/cm}^2$
- 4)  $\Delta p = 40 \text{ kgf/cm}^2$

Fig. 111. Results of tests on flap nozzle.  
KEY: (a)  $Q$ ,  $\text{cm}^3/\text{min}$ ; (b)  $N$ ,  $\text{gf}$ ; (c)  $x$ ,  $\text{mm}$ .

The results of tests on flap nozzles are usually presented in the form of curves of the flow rate  $Q$  and the force  $N$  exerted by the fluid on the flap as functions of the flap displacement  $x$ . The results of tests on a flap nozzle with the dimensions  $d_s = 1 \text{ mm}$ ,  $D_s = 1.5 \text{ mm}$ , cylindrical-section length  $l = 2 \text{ mm}$ , and a  $50^\circ$  angle before it can be cited as an example of such a diagram (Fig. 111).

At small  $x$ , the flow rate  $Q$  increases for a given  $\Delta p$  in proportion to  $x$ . This is because of the increase in the gap area, which is  $\pi D_s x$  in the exit section. On a further increase in  $x$ , the relation becomes increasingly nonlinear owing to the appearance of local separation, and, finally, the curve runs parallel to the axis of abscissas when separating flow has intervened over the entire area.

When flow is completely separated, flow rate does not depend on gap size, which should be quite obvious.

The force  $N$  increases with  $x$ , not from zero, but from an  $N_0$  equal to

$$N_0 = \frac{1}{4} \pi d_c^2 \Delta p,$$

which corresponds to a nozzle orifice completely closed by the flap.

With large  $x$ , i.e., with separating outflow, the force  $N_0$  ceases to depend on  $x$ , which should also come as no surprise.

In the separating regime, the force  $N$  can be found from the momentum equation written for the direction of the jet. Assuming that the pressure in the jet is equal to the ambient pressure and that the outflow velocity has the theoretical value

$$v = \sqrt{2g \frac{\Delta p}{\gamma}},$$

we obtain [see also Formula (5.4) and Fig. 4.1]

$$N_{\max} = QQv = \frac{1}{4} \pi d_c^2 \Delta p \sqrt{2g \frac{\Delta p}{\gamma}} = \frac{1}{4} \pi d_c^2 \Delta p \sqrt{2g \frac{\Delta p}{\gamma}}$$

NOT REPRODUCIBLE

Thus, the maximum force acting on the flap is only twice the minimum. In occasional cases with large  $D_s/d_s$  and small  $\Delta p$ , it is possible to obtain a force  $N$  that is smaller than  $N_0$  owing to partial vacuum in the gap (see pressure diagram in Fig. 110b).

We express the flow rate through the flap nozzle by the usual formula

$$Q = \mu'_{s-z} S_z \sqrt{2g \frac{\Delta p}{\gamma}}, \quad \text{NOT REPRODUCIBLE}$$

where  $\mu'_{s-z}$  is the flow rate coefficient of the flap nozzle, referred to the area  $S_z$ ;  $S_z = \pi D_s x$  is the gap sectional area at the exit into the environment.

Generally speaking, the coefficient  $\mu'_{s-z}$  is a function of  $Re$ , but, for example, for the test results in Fig. 111 it can be regarded as practically constant at  $\mu'_{s-z} = 0.54$  in the linear range.

Multiplying and dividing the flow rate formula by  $S_0 \sqrt{2g \frac{\Delta p}{\gamma}}$  we rewrite it as follows:

$$Q = \mu_{s-z} A \frac{D_s^2}{d_s^2} S_0 \sqrt{2g \frac{\Delta p}{\gamma}} = \mu_{s-z} S_0 \sqrt{2g \frac{\Delta p}{\gamma}},$$

where  $\mu_{s-z} = \mu'_{s-z} \frac{A D_s^2}{d_s^2 S_0}$  is the flow rate coefficient of the flap nozzle referred to the constant nozzle-orifice area.

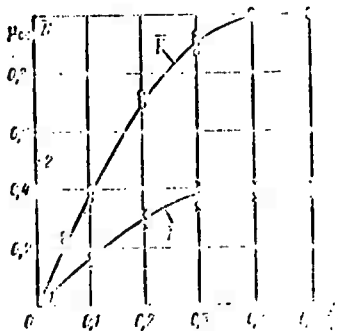


Fig. 112. Universal characteristics of flap nozzle.

rate coefficient

Thus, the flow rate coefficient  $\mu_{s-z}$  of the flap nozzle is equal to the product of a practically constant quantity by the gap ratio  $x/d$ , i.e.,  $\mu_{s-z}$  is directly proportional to  $x/d$  for the nonseparating regime.

In the transitional regime, this proportionality is violated, and with full separation, the coefficient  $\mu_{s-z}$  ceases to depend on  $x/d$  and becomes equal to the flow rate coefficient  $\mu_s$  of the nozzle without the flap.

The coefficient  $\mu_s$  varies just as little with  $Re$  as does  $\mu_{s-z}$ . Consequently, introducing a relative flow

$$\mu_{s-z} = \frac{Q}{S_0 \sqrt{2g \frac{\Delta p}{\gamma}}}$$

we obtain a quantity that is practically independent of  $Re$  and is determined only by the gap ratio  $x/d$ .

If we plot a diagram of  $\mu_{s-z}$  as a function of  $x/d$ , we obtain a practically universal flow rate characteristic for the flap nozzle (Fig. 112), one that is valid for various viscosity values and even for different flap nozzles.

Similarly, a practically universal force characteristic can be obtained for flap nozzles by plotting the force ratio

$$\bar{N} = \frac{IN}{N_0},$$

as a function of the gap ratio  $x/d$ .

It is clear from the above that as  $x/d$  increases from zero to  $x/d = 0.3-0.5$ , the values at which complete flow separation intervenes,  $\bar{N}$  increases from 1 nearly to 2 (see Fig. 112).

#### §43. SPRAY NOZZLES (INJECTORS)

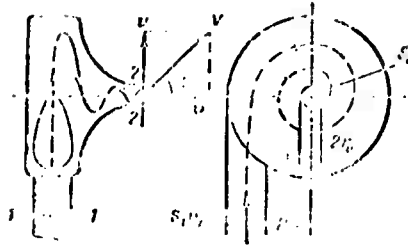
A spray nozzle is a special mouthpiece that atomizes fluid, i.e., expels it in such a way that on emerging into the atmosphere (or into a space at elevated gas pressure), the jet is immediately broken up into minute drops.

So-called centrifugal or swirl nozzles are used extensively in aviation gas-turbine engines and in liquid-fuel rockets to spray fuel into combustion chambers.

The working principle of such a nozzle is as follows: the fluid flow is first twisted and then compressed (Fig. 113). The angular momentum (twist) set up by tangential inflow of the fluid remains approximately constant as the fluid moves through the nozzle; as the flow constricts, therefore, the circumferential velocity component  $u$  rises considerably, and large centrifugal forces appear and press the flow against the walls to form a thin film, which breaks up into minute drops when it emerges from the nozzle. This is accompanied by formation of an air (gas) vortex along the axis of the nozzle, with nearly atmospheric surface pressure (for outflow into the atmosphere). This air vortex is quite similar to the vortex funnel (Fig. 114) that forms when a container is drained through a hole in its bottom, except that it is considerably stronger in the nozzle.

Thus, the fluid flow does not fill the entire exit orifice of a nozzle of diameter  $2r_0$ ; it is annular in cross section, with the center filled by an air vortex of diameter  $2r_v$  (Fig. 115). As a result, the contraction coefficient  $\epsilon$  of a nozzle is usually much smaller than unity.

Because of this and the fact that the resultant outflow velocity  $V$  from the nozzle (see Fig. 113) is directed not normal to



NOT REPRODUCIBLE

Fig. 113. Diagram of centrifugal nozzle.



Fig. 114. Vortex funnel (whirlpool).



Fig. 115. Cross section through vortex in nozzle.

the plane of the orifice, but at a certain angle  $\alpha$  whose tangent is equal to the ratio of the circumferential velocity component  $\underline{u}$  to the axial component  $\underline{v}$ , the flow rate coefficient of a nozzle is always substantially smaller than unity and varies widely depending on the shape and dimensional relationships of the nozzle.

To determine the throughput of a nozzle from the basic equation (9.6)

$$Q = \mu S_0 \sqrt{2gH} / \gamma$$

it is necessary to know the flow rate coefficient  $\mu$  quite accurately.

The theory of the nozzle developed by Prof. G.N. Abramovich [1] enables us to find the coefficient  $\mu$  from the dimensions and shape of the nozzle. We set forth this theory briefly for the case of an ideal fluid, for which we write the following three starting equations:

1) the Bernoulli equation for sections 1-1 and 2-2 (see Fig. 113):

$$\frac{p_1}{\gamma} + \frac{V_1^2}{2g} + \frac{V_1^2}{2g} = \frac{p_2}{\gamma} + \frac{V_2^2}{2g} + \frac{V_2^2}{2g}$$

or

$$H = \frac{v^2 + u_v^2}{2g},$$

where H is the theoretical head, which equals  $H = \frac{2\pi \rho \int_0^R v^2}{\gamma} + \frac{v^2}{2g}$ ; v and  $u_v$  are the axial and circumferential components of the velocity V in section 2-2 at the surface of the air vortex;

2) the equation of constant angular momentum of the fluid about the nozzle axis for the same sections:

$$QcRv_1 = QcRv_2,$$

or

$$u_v = v_1 \frac{R}{r_v},$$

where  $r_v$  is the radius of the air vortex in section 2-2;

3) the flow rate equation for the same sections\*

$$v_1 S_1 = v_2 S_2$$

or

$$v_1 = \frac{S_2 v_2}{S_1},$$

where

$$\epsilon = \frac{S_2 v_2}{S_1 v_1} = 1 - \frac{r_v^2}{r_0^2}.$$

We have from this last expression

$$r_v = r_0 \sqrt{1 - \epsilon},$$

which gives on substitution into the second equation

$$u_v = v_1 \frac{R}{r_0 \sqrt{1 - \epsilon}}.$$

Applying the third equation, we obtain

$$u_v = \frac{S_2 R}{S_1 r_0 \sqrt{1 - \epsilon}} = A \frac{v_2}{\sqrt{1 - \epsilon}},$$

where  $A = \frac{S_2 R}{S_1 r_0}$  is a parameter characterizing nozzle shape.

Substituting the expression found for  $u_v$  into the Bernoulli equation (the first equation),

\*See page 197 for footnote.

$$H = \frac{v^2}{2g} \left( 1 + A \frac{v^2}{1-v^2} \right),$$

NOT REPRODUCIBLE

from which

$$v = \frac{1}{\sqrt{1 + A^2 \frac{v^2}{1-v^2}}} \sqrt{2gH}.$$

We can now express the flow rate as the product of velocity by the annular area of the flow in the nozzle exit section, i.e.,

$$Q = v S_0 = \frac{1}{\sqrt{1 + A^2 \frac{v^2}{1-v^2}}} S_0 \sqrt{2gH}.$$

Thus, the flow rate coefficient of the nozzle is

$$\mu = \frac{1}{\sqrt{1 + A^2 \frac{v^2}{1-v^2}}} \sqrt{\frac{1}{2} \frac{v^2}{1-v^2}} \quad (9.20)$$

But we do not know the coefficient  $\epsilon$ , i.e., we do not know the size of the air vortex (the radius  $r_v$  for the given  $r_0$  and  $A$ ), and it will be necessary to adopt some additional condition in order to determine it.

For this condition, G.N. Abramovich proposed the following hypothesis, which was subsequently confirmed by experiment: a stable vortex size is that which ensures the maximum flow rate  $Q$  at a given head  $H$  or, in other words, the establishment of the outflow regime requiring the smallest head to obtain a given flow rate.

Let us find the  $\epsilon$  that corresponds to the maximum flow rate coefficient  $\mu$ ; to do so, we differentiate the radicand in (9.20) with respect to  $\epsilon$  and equate the derivative to zero. We shall have

$$-\frac{2}{\epsilon^3} + \frac{A^2}{(1-\epsilon)^2} = 0,$$

from which

$$A = \sqrt{\frac{2}{\epsilon^3} (1-\epsilon)}. \quad (9.21)$$

This formula enables us to plot a diagram of  $\epsilon$  as a function of  $A$  (Fig. 116), which can be used with (9.20) to calculate values of  $\mu$  for a series of values of the parameter  $A$  and plot a curve of  $\mu$  as a function of  $A$ .

As we see from the diagram, the coefficient  $\mu$  decreases with increasing  $A$ . The physical explanation for this is that an increase in  $A$  means an increase in the twist of the flow at the nozzle exit, i.e., a continuing increase in the circumferential velocity  $u$  as compared with the entry velocity  $v_1$  and, consequently, increased vorticity in the nozzle. As a result, the

diameter of the vortex increases, the flow cross section decreases, and an increasingly large part of the available energy H is expended in creating the fluid's circumferential velocity. For  $A = 0$  ( $R = 0$ ),  $\mu = 1$ , i.e., the flow is not twisted and the injector is functioning as a simple nozzle.

With the above formulas, it is easy to determine the fluid spray angle (the angle of the spray cone)  $\alpha$ . With increasing A, the angle  $\alpha$  becomes larger and the flow rate coefficient diminishes. In the design of nozzles, therefore, the parameter A is so selected as to provide a large enough angle  $\alpha$  (up to  $60^\circ$ ) in combination with a large enough coefficient  $\mu$ .

This theory of the spray nozzle was constructed for an ideal fluid. The effect of fluid viscosity in flow through an injector is to make the angular momentum decrease toward the exit from the nozzle instead of remaining constant.

As a result, the circumferential velocity components in the exit section are found to be smaller and the flow rates larger than in ideal-fluid outflow; at first glance, this is somewhat paradoxical.

We can reduce the viscosity effect to a certain decrease in the parameter A and use an equivalent parameter  $A_e$  expressed by the following formula, which was proposed by L.A. Plyachko:

NOT REPRODUCIBLE

$$A_e = \frac{A}{1 + \frac{\lambda_f}{2} \left( \frac{2A^2}{S_1} - A \right)}$$

where  $\lambda_f$  is the coefficient of friction in the nozzle, which can be taken from Table 5 as a function of the Reynolds number calculated from the orifice diameter and nozzle entrance velocity.

TABLE 5

$Re_1$	$1,5 \cdot 10^3$	$3 \cdot 10^3$	$5 \cdot 10^3$	$1 \cdot 10^4$	$2 \cdot 10^4$	$5 \cdot 10^4$
$\lambda_f$	0,22	0,11	0,077	0,055	0,01	0,03

Using the equivalent nozzle parameter  $A_e$  calculated in this way, we determine the flow rate coefficient  $\mu$  and the angle  $\alpha$  with consideration of fluid viscosity by reference to the same diagram of G.N. Abramovich, where  $A_e$  is taken instead of A. Since normally  $A_e < A$ , the coefficient  $\mu$  is found to be slightly larger when viscosity is considered, while the angle  $\alpha$  is smaller.



Fig. 116. Diagram of  $\epsilon$ ,  $\mu$ , and  $\alpha$  as functions of  $A$  for spray nozzle.



Fig. 117. Diagram of spray nozzle with helical swirl vanes.

Instead of tangential fluid inflow, so-called helical swirl vanes, i.e., two- or three-start screws inserted into the injectors, are often used in liquid rocket engines to swirl injector flow. The fluid passes through the helical grooves of the vane insert and acquires the necessary twist in the process (Fig. 117).

The spray-nozzle theory introduced above is also valid in this case, except that the coefficient  $A$  must be calculated by the formula

$$A = \frac{S_n^2 \cos^2 \phi}{S_{nrr_0}} \quad (9.22)$$

where  $r_{sr}$  is the mean radius of the helical thread,  $S_n$  is the area of the normal effective section of the helical groove,  $n$  is the number of screw starts, and  $\phi$  is the spiral angle of the helix.

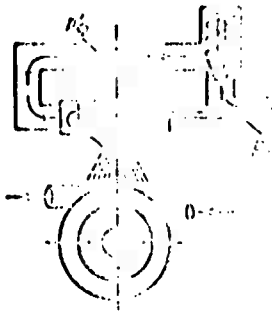


Fig. 118. Diagram of two-nozzle injector.

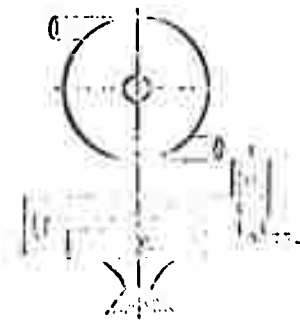


Fig. 119. Diagram of two-stage injector.

NOT REPRODUCIBLE

Contemporary gas-turbine engines usually use adjustable centrifugal nozzles whose flow rate coefficients (or exit-orifice areas) are automatically varied by fuel pressure. Use of these nozzles makes it possible to broaden the range of fuel flow rates with a given pressure range and to maintain the required spray efficiency.

The adjustable-injector types that have come into use include two-hole burners, two-stage nozzles, and spill burners. They have in common a valving device that opens (or closes) an auxiliary passage on an increase in pressure, and thereby increases the flow rate coefficient or the exit-orifice area.

In the two-nozzle or two-hole injector (Fig. 118), what we have is essentially two nozzles, one inside the other. At low pressures, the valve is closed and the primary (internal) nozzle operates; on an increase in the pressure  $p_f$ , the valve is lifted and the secondary goes into operation at a pressure  $p_f'$ . Fuel supply rises steeply.

In the two-stage burner (Fig. 119), we have one nozzle and a common swirl chamber, but two entry passages. At low pressures, fuel is fed through one of the passages, and at high pressures through both. As a result, the parameter  $A$  decreases and the coefficient  $\mu$  increases.

The spill burner (Fig. 120) is provided with a drainage line in which a valve is inserted. The valve opens wider the lower the fuel pressure, and closes the drain line completely at maximum pressure. Thus, an increased entry velocity is obtained at low pressures; this is equivalent to reducing the entry area and this means an increase in the equivalent parameter  $A_e$  and a smaller  $\mu$ . This is what is needed to broaden the flow rate range.

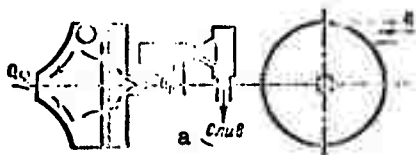


Fig. 120. Diagram of spill burner.  
KEY: (a) drain.

Calculations for these adjustable injectors can be made on the basis of the same Abramovich formula, but this requires taking account of the peculiarities of each type (see examples).

Example 1. Construct the hydraulic characteristic of the two-hole burner described above (see Fig. 118), i.e., a curve of the relation between flow rate and the pressure drop across the

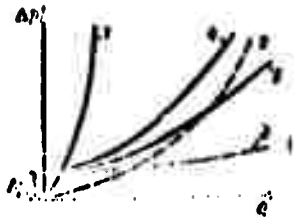


Fig. 121. Characteristics of (two-hole) burner.

nozzle, if the secondary hole (secondary passage) goes into operation at a pressure drop of  $\Delta p_0$ . The geometrical characteristics of both burner passages (dimensions and parameters  $A_1$  and  $A_2$ ) and the hydraulic characteristic of the regulating valve are given. Solve the problem in general form.

Solution. 1. From the values given for  $A_1$  and  $A_2$ , consult the diagram (Fig. 116) to find  $\mu_1$  and  $\mu_2$ .

2. Applying the formulas

$$Q_1 = \mu_1 A_1 \sqrt{2g \frac{h_p}{\gamma}}, \text{ and } Q_2 = \mu_2 A_2 \sqrt{2g \frac{h_p}{\gamma}},$$

we construct the characteristics of the primary and secondary burner passages (curves 1 and 2 in Fig. 121).

3. We add the characteristics of the regulating valve 3 and the nozzle's secondary passage. In adding, it must be remembered that the pressure drop  $\Delta p$  across the nozzle is expended in the second passage both in the nozzle itself and in the valve. In adding the characteristics, therefore, it is necessary to sum the ordinates  $\Delta p$  for given flow rate values. The result is curve 4.

4. To obtain the over-all hydraulic characteristic 5 of the burner, we add the characteristics of the primary and the secondary with the valve by adding the flow rates (see Fig. 121).

Example 2. Find an expression for the parameter  $A_1$  of a centrifugal spill burner if the total fuel feed to the burner  $Q = Q_f + Q_n$ , where  $Q_f$  is the flow rate through the burner orifice and  $Q_n$  is the spill rate (see Fig. 120).

Solution. 1. We introduce the spill coefficient  $k_n$ , which equals

$$k_n = 1 + \frac{Q_n}{Q_f} = \frac{Q}{Q_f}$$

2. The fuel supply to the nozzle through the entry passages is

$$Q = k_n Q_f = c_1 S_1$$

3. The amount of fuel that has passed through the burner hole

$$Q_f = c_2 S_2$$

Consequently,

$$c_1 S_1 = k_n c_2 S_2$$

NOT REPRODUCIBLE

from which

$$v_1 = \frac{K_n S_0 v}{S_1}$$

5. Substituting the value found for  $v_1$  into the angular-momentum equation and then into the Bernoulli equation, we find the velocity  $v$  in much the same way as we did previously, i.e.,

$$v = \frac{1}{\sqrt{1 + K_n^2 A^2 \frac{1}{1-\epsilon}}} \sqrt{2gH}$$

6. The fuel supply  $Q_f$  through the burner is determined by the formula

$$Q_f = S_0 v = \frac{S_0}{\sqrt{1 + K_n^2 A^2 \frac{1}{1-\epsilon}}} \sqrt{2gH}$$

7. Comparing this formula with (9.20), we find that

$$A_1 = K_n A$$

NOT REPRODUCIBLE

### Footnotes

Manu-  
script  
page

- 163      <sup>1</sup>The diagram was plotted by A.D. Al'tshul' [4] on the basis of experiments of a number of authors.
- 178      <sup>2</sup>Tests conducted at Kiev Civil Aviation Institute.
- 182      <sup>3</sup>Tests conducted by K.N. Popov at the Bauman Moscow Higher Engineering School.
- 190      <sup>4</sup>We assume uniform distribution of the axial velocities over the annular flow section at the exit from the nozzle. This proposition can be proven theoretically; see [1], or [7].

### Symbol List

Manu- script page	Symbol		English equivalent
160	ст	st	wall
160	с	s	jet
161	т	t	theoretical
167	атм	atm	atmospheric
169	кр	kr	critical
174	воз	voz	air
174	ж	zh	fluid
175	м	m	local
180	к	k	valve
182	кл	kl	valve
183	пр	pr	spring
184	с	s	nozzle
184	з	z	flap
187	с-з	s-z	flap nozzle
190	в	v	vortex
192	э	e	equivalent
192	ф	f	injector, burner
193	ср	sr	mean

## CHAPTER X

### RELATIVE AND NONSTEADY MOTION OF FLUID IN PIPES

#### §44. BERNOULLI EQUATION FOR RELATIVE MOTION. MOTION UNDER CONDITIONS OF WEIGHTLESSNESS

The Bernoulli equation in the form of (4.12) or (4.16) is valid in those cases of steady fluid flow when gravity is the only mass force acting on the fluid. In aviation and rocket engineering, however, we encounter flows in the calculation of which it is necessary to take into account the inertia forces of translational motion in addition to gravity. Cases in point are those in which the channel (for example, a pipeline) along which the fluid is moving is itself moving in space with a certain acceleration. If the inertial force that results is constant in time, the flow of the fluid relative to the channel walls may be steady, and the Bernoulli equation for it can be derived in the same way as in §16. The difference will be that we must add the work of the inertial force acting on a filament of weight  $dG$  as it moves from section 1-1 to section 2-2 to the work of the pressure and gravity forces (see Fig. 24). Then we divide all terms of (4.12) by  $dG$ , i.e., we refer it to unit weight and, obtaining a certain head, transpose it to the right member of the equation. This will be the Bernoulli equation for relative motion, which assumes the following form in the case of a real flow:

$$z_1 + \frac{p_1}{\gamma} + \alpha_1 \frac{v_1^2}{2g} + \Delta H_{in} = z_2 + \frac{p_2}{\gamma} + \alpha_2 \frac{v_2^2}{2g} + \Delta H_{fr} + \Delta H_{loc} \quad (10.1)$$

where  $\Delta H_{in}$  is the so-called inertia head, which is the work of the inertial forces per unit weight, taken with the opposite

sign. The sign reversal is accounted for by the fact that we transposed this work from the left to the right member of the equation.

Let us determine the inertia head for the following basic cases of relative fluid motion.



Fig. 122. Flow in channel moving with acceleration.

Fig. 122. Flow in channel moving with acceleration.

**Straight-line uniformly accelerated motion of channel.** If the channel through which the fluid is flowing moves in a straight line with a constant acceleration  $\underline{a}$  (Fig. 122), all fluid particles moving through this channel are acted upon by the same time-constant inertial force of translational motion, which may work either with or against the flow.

Referred to unit mass, this force is equal to the corresponding acceleration  $\underline{a}$  and is opposed to the acceleration; each unit weight of fluid will be acted upon by an inertial force

$$\frac{1}{g} \cdot a.$$

The work done by this force in moving fluid from the first section to the second (like the work of gravity) does not depend on the shape of the path, but is determined only by the difference between the coordinates measured in the direction of the acceleration  $\underline{a}$ ; it therefore equals

$$\Delta H_{in} = \frac{a}{g} \cdot l_a, \quad (10.2)$$

where  $l_a$  is the projection of the channel segment under consideration onto the direction of the acceleration  $\underline{a}$ .

To avoid giving  $\Delta H_{in}$  the wrong sign in the right member of the Bernoulli equation, we can hold to the following rule, which proceeds directly from the physics of the phenomenon.

If the acceleration  $\underline{a}$  is directed from section 1-1 to section 2-2 and the inertial force in the opposite direction, this force will work against flow of the fluid and the inertia head must be given the plus sign. In this case, the inertia head will lower the pressure in the second section by comparison with the first and, consequently, will have an effect similar to that of the hydraulic losses  $\Sigma h$ , which always appear in the right side of the Bernoulli equation with the plus sign.

If, on the other hand, the acceleration  $\underline{a}$  is directed from the second section toward the first, the inertia force assists the flow and the inertia head must be given the minus sign. In

this case, the inertia head will raise the pressure in the second section, i.e., it will have an effect opposite to that of the hydraulic losses.

The Bernoulli equation for this case of relative ideal-fluid motion can also be obtained by integrating differential equation (4.15). We have in this case

$$X = a_x; Y = a_y; Z = a_z - g,$$

where  $a_x$ ,  $a_y$ , and  $a_z$  are the projections of the unit inertia force of translational motion onto the coordinate axes.

Equation (4.15) can be written

$$a_x dx + a_y dy + (a_z - g) dz + \frac{1}{\rho} dp + d\left(\frac{v^2}{2g}\right),$$

or

$$dz + \frac{dp}{\gamma} + d\left(\frac{v^2}{2g}\right) = -\frac{1}{\gamma} (a_x dx + a_y dy + a_z dz) = -\frac{1}{\gamma} dU_a,$$

where  $dU_a$  is the increment of the force function of the inertia force (the potential of this force with the opposite sign) and equals (see §13)

$$dU_a = -adl \cos(\alpha, \hat{a}'),$$

On integrating the differential equation in the range from section 1-1 to 2-2, we obtain

$$z_2 - z_1 + \frac{p_2}{\gamma} - \frac{p_1}{\gamma} + \frac{v_2^2}{2g} - \frac{v_1^2}{2g} = -\frac{a}{g} \int_0^l \cos(\alpha, \hat{a}') dl = -\frac{a}{g} l_a,$$

or

$$z_1 + \frac{p_1}{\gamma} + \frac{v_1^2}{2g} = z_2 + \frac{p_2}{\gamma} + \frac{v_2^2}{2g} - \Delta h_{in}.$$

Thus we have obtained the same inertia-head expression as before. The minus sign appears before  $\Delta h_{in}$  because the value of  $\cos(\alpha, \hat{a}')$  was assumed positive for integration, i.e., force  $\underline{a}$  was assumed to coincide with the flow direction projected onto this force, and this means that the force  $\underline{a}$  assists the flow. The sign obtained conforms to the sign rule given above.

**Rotation of channel about vertical axis.** Let the channel through which the fluid is moving be in rotation around a vertical axis at constant angular velocity  $\omega$  (Fig. 123). The fluid will then be acted upon by an inertia force of rotational motion, which is a function of radius. It will therefore be necessary to integrate in order to obtain the work of this force or the change in potential energy due to its action.

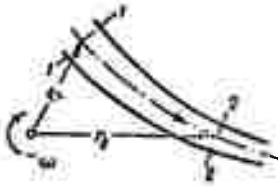


Fig. 123. Flow in rotating channel.

A unit weight will be acted upon by an inertia force equal to

$$\frac{\omega^2}{g} r.$$

The work of this force in radial displacement through a distance  $dr$  will be

$$\frac{\omega^2}{g} r dr,$$

and for motion from radius  $r_1$  to radius  $r_2$  (along any curve), the work will be found by integrating this expression with  $r_1$  and  $r_2$  as limits. We find the magnitude of the inertia head by integrating, but the sign must be reversed (as we noted earlier, this term is transferred from the left to the right member in deriving the Bernoulli equation).

We finally obtain

$$\Delta H_{in} = -\frac{\omega^2}{g} \int_{r_1}^{r_2} r dr = -\frac{\omega^2}{2g} (r_1^2 - r_2^2). \quad (10.3)$$

The sign of the inertia head obtained with this formula conforms to our sign rule. We obtain the same result by integrating differential equation (4.15).

If the Z-axis is aligned with the axis of channel rotation and pointed upward,

$$X = \omega^2 x; \quad Y = -\omega^2 y; \quad Z = -g$$

and (4.15) becomes

$$\omega^2 x dx + \omega^2 y dy - g dz = \frac{1}{\rho} dp + d\left(\frac{v^2}{2}\right).$$

Since  $x^2 + y^2 = r^2$ ,

$$\omega^2 d\left(\frac{r^2}{2}\right) - g dz = \frac{1}{\rho} dp + d\left(\frac{v^2}{2}\right).$$

Integrating and transposing,

$$z + \frac{p}{\gamma} + \frac{v^2}{2g} - \frac{\omega^2 r^2}{2g} = \text{const}$$

or

$$z_1 + \frac{p_1}{\gamma} + \frac{v_1^2}{2g} = z_2 + \frac{p_2}{\gamma} + \frac{v_2^2}{2g} + \Delta H_{in},$$

where

$$\Delta H_{in} = \frac{t^2}{2} (v_1^2 - v_2^2).$$

Fluid motion under conditions of weightlessness is characterized first of all by the fact that the resultant mass force acting on each fluid particle is zero, because gravity is offset by the inertial force of translational motion. In the Bernoulli equation (10.1) written for two flow sections in a pipe, therefore, we must set  $z_1 - z_2 = \Delta H_{in}$ .

In weightlessness, fluid is unable to form a free interface of the usual form with the gaseous medium. Fluid and gas mix in a tank and form a two-phase medium (a liquid-and-gas suspension). It is also possible for the gas to become concentrated at the center of the tank in the form of a spherical nucleus, while the (wetting) fluid envelops the entire inside surface of the tank. This requires preventing contact between the fluid and gas in hydraulic systems that must function under conditions of weightlessness. As in an accumulator (see Fig. 223), a separator in the form of a spring- or gas-loaded moving piston or an elastic diaphragm (membrane) must be placed between the fluid and the gas.

In the absence of fluid-gas contact, the flow of fluid through the pipelines under the pump, gas, or spring pressure gradient  $\Delta p$  under weightless conditions will differ from the flow under ordinary conditions only in that the levelling-height difference  $\Delta z$  will have no influence. And, in the cases of large pressure gradients  $\Delta p$  and flow in sealed pipelines (§51), there will be no difference at all between the weightless and ordinary flows.

Nor will there be anything particularly different about weightless fluid flows into a gaseous medium through holes and mouthpieces under large enough heads until the fluid jet loses its kinetic energy. Outflow through injectors and atomization of fluids will take place as usual.

The behavior of a fluid that does not have a head and comes into contact with air (gas) will be quite different under conditions of weightlessness. In this case, surface-tension forces become the decisive factor.

While we know (see §3) that under "ground" conditions, these forces cause fluid to rise or drop in capillaries by a height inversely proportional to tube diameter and dependent on the nature of the fluid, surface-tension forces cause continuous motion of a weightless fluid in a pipe one end of which is immersed in the fluid. Theoretical analyses have shown that the fluid flow velocity first rises until friction becomes equal to surface tension. Then the flow velocity begins to decrease gradually because the friction in the pipe is continuing to increase.

Thus, a simple pipe can, under weightless conditions, perform the function of a small pump, for which it makes no difference in

which direction the fluid-supply pipe is pointed.

**Example.** Determine the absolute pressure at the intake into the pump of the aircraft oil system considered in the example in Chapter VI (see Fig. 52) as the airplane goes into a dive with negative g-factor  $n_y$ . The inertia force is directed upward and is twice gravity.

**Solution.** The unit inertia force is (see §11)

$$a = -2g.$$

and the inertia head

$$\Delta H_{in} = -\frac{a}{g} z = +2z.$$

We have from the Bernoulli equation for relative motion

$$\frac{p_1}{\gamma_n} = z + \frac{pA}{\gamma_n} - a \frac{v^2}{2g} - h_{fp} - \Delta H_{in} = 152 - 140 = 12 \text{ cm.}$$

or

$$h_1 = 12 \frac{0.9}{13.6} 10 = 6 \text{ mmHg.}$$

This low pump intake pressure is not acceptable; measures must therefore be taken to improve the altitude performance of the oil system.

#### §45. NONSTEADY FLUID FLOW IN PIPES

Since nonsteady fluid flows are generally quite complex, we shall limit ourselves to the basic particular cases encountered in aviation engineering - those of nonsteady fluid flows in constant-section pipes and in pipelines composed of sequences of pipes with differing diameters.

Take a pipe of length  $l$  and diameter  $d$  with an arbitrary orientation in space (Fig. 124) and denote by  $z_1$  and  $z_2$  the levelling heights of the initial (1-1) and final (2-2) sections of this pipe, respectively. Let a fluid move in this pipe with an acceleration that can, in the general case, vary in time:

$$j = \frac{dv}{dt}.$$

At a given point in time, the velocity  $v$  and acceleration  $j$  are obviously the same for all cross sections through the pipe.

For the time being, we shall disregard frictional energy losses and assume that the velocities are distributed uniformly over the sections.

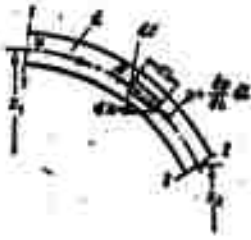


Fig. 124. Diagram of nonsteady pipe flow.

Isolating an elementary cylindrical volume of length  $dl$  and base area  $dS$  from the total moving volume of fluid in the pipe, we write its equation of motion.

Projecting the forces of pressure and gravity onto the tangent to the pipe axis, we obtain

$$p dS - \left( p + \frac{\partial p}{\partial l} dl \right) dS + \gamma dS dl \cos \alpha = \frac{\gamma}{g} dS dl \frac{dv}{dt},$$

or

$$\frac{\partial p}{\partial l} dl + \gamma \cos \alpha dl = \frac{\gamma}{g} \frac{dv}{dt} dl.$$

Since

$$\cos \alpha = - \frac{\partial z}{\partial l},$$

we have

$$- \frac{\partial p}{\partial l} dl - \gamma \frac{\partial z}{\partial l} dl = \frac{\gamma}{g} j dl,$$

(It must be remembered that  $p$  is a function not only of  $l$ , but also of  $t$ .)

On integrating over the length of the pipe for a certain point in time,

$$\frac{p_1}{\gamma} + z_1 - z_2 = \frac{j}{g} l,$$

or

$$z_1 + \frac{p_1}{\gamma} - z_2 + \frac{p_2}{\gamma} = h_{in}, \quad (10.4)$$

where

$$h_{in} = \frac{j}{g} l.$$

This equation resembles the Bernoulli equation for relative motion, and the term  $h_{in}$  is also called the inertia head, but  $h_{in}$  should not be confused with  $\Delta H_{in}$ , since their meanings are different. As we see from (10.4),  $h_{in}$  represents the difference between the fluid specific energies in sections 1-1 and 2-2 at a particular point in time, a difference governed by the acceleration (or deceleration) of the fluid flow in the pipe. This difference is positive for acceleration, i.e., the fluid's specific energy decreases downstream, but it is negative for deceleration, which means an increase in fluid specific energy from the first to the second section.

In the presence of hydraulic energy losses in the pipe (local and frictional), they must also, by analogy with the

Bernoulli equation for steady flow, also appear in the right member of (10.4), i.e.,

$$z_1 + \frac{P_1}{\gamma} = z_2 + \frac{P_2}{\gamma} + \sum h + h_{in} \quad (10.5)$$

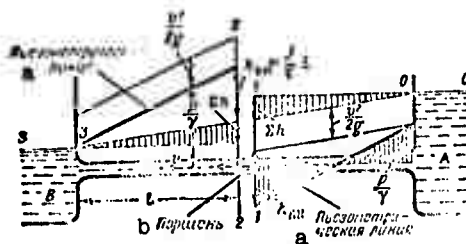


Fig. 125. Construction of piezometric line for nonsteady pipe flow.  
KEY: (a) piezometric line; (b) piston.

It should not be forgotten that Eq. (10.5) is valid only for a constant-section pipe. If the pipeline consists of several segments with different sectional areas ( $S_1, S_2$ , etc.), the inertia head for the entire line must obviously be found as the sum of the inertia heads for each segment. Here, the corresponding accelerations are determined from the following equations, which are the result of time differentiation of the flow rate equation:

$$\frac{dQ}{dt} = S_1 j_1 = S_2 j_2 = S_3 j_3 = \dots$$

and so forth.

In addition, as follows from the energy considerations presented above, it is necessary to take account of the velocity heads in the initial and final cross sections of the pipeline.

Thus, the equation of nonsteady fluid flow between sections 1-1 and n-n assumes the form

$$z_1 + \frac{P_1}{\gamma} + a_1 \frac{v_1^2}{2g} = z_2 + \frac{P_2}{\gamma} + a_2 \frac{v_2^2}{2g} + \sum h + \sum h_{in} \quad (10.6)$$

This equation is used in calculations for the starting and transitional modes of aircraft hydraulic systems and especially of the fuel systems of liquid rockets.

We present the following example to illustrate this equation. Let a piston move to the left with a positive acceleration  $j$  (Fig. 125) in a pipe connected to tanks A and B. We apply Eq. (10.6) for sections 0-0 and 1-1 and then for sections 2-2 and 3-3, and construct the piezometric line for a particular point in time; we shall have

$$z_0 = \frac{p_0}{\gamma} - \frac{p_1}{\gamma} + \frac{v_0^2}{2g} + \lambda \frac{l}{d} \frac{v_0^2}{2g} + \frac{J}{g} \cdot l$$

and

$$\frac{p_1}{\gamma} = z_0 - \frac{p_0}{\gamma} + \lambda \frac{l}{d} \frac{v_0^2}{2g} + \frac{J}{g} \cdot l$$

In the former case, therefore, the inertia head, which adds to the head losses, causes an even greater pressure drop at the piston than that in uniform motion. A partial vacuum is formed in section 1-1, and the fluid may even separate from the piston. In the latter case, the inertia of the fluid column causes a pressure increase at the piston as a result of the same addition of  $h_{tr}$  and  $h_{in}$ .

With a negative acceleration  $j$ , i.e., when the fluid is decelerated, the inertia head is negative in both cases and, consequently, offsets the head loss to one degree or another and lowers the vacuum in the former case and the pressure increase in the latter.

#### §46. WATER HAMMER IN PIPES

Water hammer is an oscillatory process that takes place in a resilient pipe containing a nearly incompressible fluid when its velocity or pressure changes suddenly. This process is a very rapid one and is characterized by alternation of abrupt pressure increases and decreases. Here, the pressure variation is closely related to the elastic deformations of the fluid and pipe walls.

Water hammer is most frequently caused by the quick closing or opening of a valve or other flow-control device. There are also other causes.

The first theoretical and experimental study of water hammer in pipes was made by Prof. N.Ye. Zhukovskiy. In our explanation of this effect, we have used the basic premises of his fundamental work "O gidravlicheskom udare" [Water hammer], which appeared in 1899.

Suppose that valve A (Fig. 126a) at the end of a pipe through which fluid is moving at velocity  $v_0$  and pressure  $p_0$  has closed instantaneously. The fluid particles will stop on striking the valve, and their kinetic energy will be converted into the work of deforming the pipe walls and the fluid. The pipe walls come under tension and the fluid is compressed in accordance with the pressure increase  $\Delta p_{ud}$ .<sup>1</sup> The particles that have been stopped at the valve will be run onto by other neighboring particles, and the latter will also lose velocity, with the result that section n-n moves to the right with a velocity  $a$ , the shock-wave velocity; the actual transition region in which the pressure changes by  $\Delta p_{ud}$  is known as a shock wave.

<sup>1</sup>See page 217 for footnote.

When the shock wave reaches the tank, the fluid has been stopped and compressed over the entire length of the pipe, and the pipe walls have been stretched. The shock pressure increase  $\Delta p_{ud}$  has propagated the entire length of the pipe (Fig. 126b).

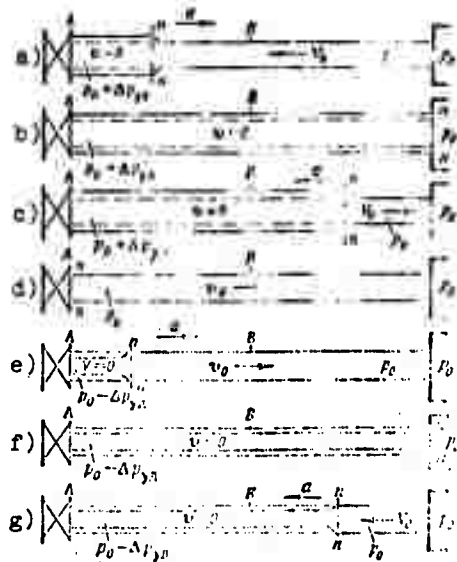


Fig. 126. Diagram of motion of shock wave in water hammer.

But this is not an equilibrium situation. Under the influence of the pressure drop  $\Delta p_{ud}$ , fluid rushes from the pipe into the tank, with this motion beginning at the section directly at the tank. Section n-n will now run back to the cock at velocity  $a$ , leaving the equalized pressure  $p_0$  behind it (Fig. 126c).

The fluid and pipe walls are assumed to be perfectly elastic, so that they return to their previous states corresponding to the pressure  $p_0$ . The work of deformation is converted entirely back into kinetic energy, and the fluid in the pipe acquires its original velocity  $v_0$ , but the latter is now directed the other way.

At this speed, the fluid column (Fig. 126d) will be repelled from the valve, with the result that a negative shock wave  $-\Delta p_{ud}$  is formed and travels from the valve to the tank at velocity  $a$ , leaving compressed pipe walls and expanded fluid behind it because of the pressure decrease  $-\Delta p_{ud}$  (Fig. 126e). The fluid's kinetic energy is again transformed into a work of deformation, but one of the opposite sign.

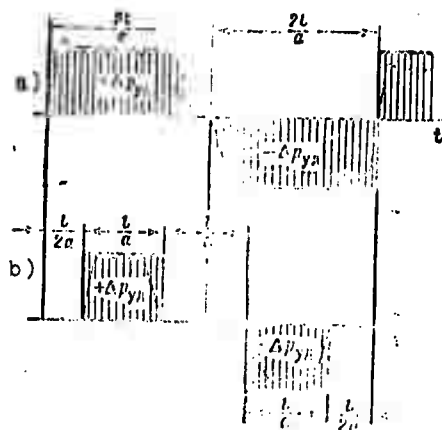


Fig. 127. Time variation of pressure at valve and at center of pipe.

Figure 126f shows the state of the pipe at the time of arrival of the negative shock wave at the tank. As in the case of Fig. 126b, it is not an equilibrium condition. Figure 126g shows the process of pressure equalization in the pipe and tank, which is accompanied by formation of velocity  $v_0$ .

Obviously, as soon as the shock wave  $-\Delta p_{ud}$  reflected from the tank reaches the valve, the situation that prevailed when the valve was closed is repeated. The entire water-hammer cycle is run through again.

In his experiments, N.Ye. Zhukovskiy registered 12 complete cycles with a progressive decrease in  $\Delta p_{ud}$  as a result of friction and loss of energy to the tank.

The time course of water hammer is illustrated by the diagram of Fig. 127.

The solid lines on the upper diagram indicate the theoretical pressure change  $\Delta p_{ud}$  at point A (in Fig. 126) directly at the valve (it is assumed that the valve closes instantaneously).

At point B, which is situated at the middle of the pipe, the shock pressure appears with a time delay  $l/2a$ . It persists during the time necessary for the shock wave to travel from point B to the tank and back, i.e., during a time  $l/a$ . Then pressure  $p_0$  is established at point B (i.e.,  $\Delta p_{ud} = 0$ ) and is maintained until the negative shock wave from the valve arrives at point B, after a time interval  $l/a$ .



Fig. 128. Pipe under tension.



Fig. 129. Diagram of fluid compression in pipe.

The broken lines on the same figure approximate the actual time variation of pressure. In reality, the pressure rises (and falls) steeply, but not instantaneously. Moreover, the pressure oscillations are damped, i.e., the amplitude values decrease as a result of energy dissipation.

Let us find the shock pressure  $\Delta p_{ud}$  on the assumption that the fluid's kinetic energy is converted into work of pipe-wall and fluid deformation. The kinetic energy of the fluid in a pipe of radius  $R$  equals

$$\frac{Mv_0^2}{2} = \frac{1}{2} \pi R^2 l \rho v_0^2.$$

The work of deformation is half the product of force by elongation. Expressing the work of pipe-wall deformation as the work of pressure forces on length  $\Delta R$  (Fig. 128), we obtain

$$\frac{1}{2} \Delta p_{yx}^2 \Delta R \pi R.$$

According to Hooke's law,

$$\frac{\Delta R}{R} E = \sigma, \quad (10.7)$$

where  $\sigma$  is the normal stress in the pipe-wall material and is related to the pressure  $\Delta p_{ud}$  and the wall thickness  $\delta$  by the familiar equation

$$\sigma = \frac{\Delta p_{yx} R}{\delta}. \quad (10.8)$$

Taking the expression for  $\Delta R$  from (10.7) and  $\sigma$  from (10.8), we obtain the work of deformation of the pipe walls:

$$\frac{\Delta p_{yx}^2 \pi R^3 l}{8E}.$$

The work of compression of a fluid volume  $W$  can be represented as the work of pressure forces on length  $\Delta l$  (Fig. 129),

i.e.,

$$\frac{1}{2} \Delta p_{y, \Delta l} = \frac{1}{2} \Delta p_{y, \Delta l}''.$$

In analogy to Hooke's law for linear elongation, the relative fluid-volume decrease  $\Delta W/W$  is related to pressure by

$$\frac{\Delta W}{W} K = \Delta p_{y, \Delta l}''.$$

where  $K$  is the bulk elastic modulus of the fluid (see §3).

Taking the volume of fluid in the pipe as  $W$ , we obtain an expression for the work of compression of the fluid:

$$\frac{1}{2} \frac{\Delta p_{y, \Delta l}'' R^2 l}{K}.$$

Thus, the kinetic-energy equation takes the form

$$\frac{1}{2} \pi R^2 \rho_0 v_0^2 = \frac{\pi R^2 \Delta p_{y, \Delta l}'' R^2 l}{2K} + \frac{\pi R^2 \Delta p_{y, \Delta l}'' R^2 l}{2K}.$$

Solving it for  $\Delta p_{y, \Delta l}''$ , we arrive at N.Ye. Zhukovskiy's formula:

$$\Delta p_{y, \Delta l}'' = \rho_0 v_0 \sqrt{\frac{1}{K} + \frac{2v_0^2}{E}}. \quad (10.9)$$

The quantity  $\sqrt{\frac{1}{K} + \frac{2v_0^2}{E}}$  has the dimensions of velocity. Its

physical significance can be ascertained by assuming that the pipe has absolutely rigid walls, i.e.,  $E = \infty$ . Then only  $\sqrt{K/\rho}$ , i.e., the speed of sound in a homogeneous elastic medium of density  $\rho$  and bulk modulus  $K$ , remains of the last expression (see §3).

This velocity is 1435 m/s for water, 1116 m/s for gasoline, and 1400 m/s for oil.

Since  $E \neq \infty$  in our case,

$$\sqrt{\frac{1}{K} + \frac{2v_0^2}{E}} = a$$

represents the velocity of propagation of a shock wave in fluid filling an elastic pipe. This can be proven by examining an elementary displacement  $dx$  of the shock wave during time  $dt$  and applying the momentum-change theorem to pipe element  $dx$  (Fig. 130):

$$[(p_0 + \Delta p_{y, \Delta l}'' - p_0) S dt] = (v_0 - 0) \rho S dx.$$

Hence the propagation velocity of the shock wave

$$a = \frac{dx}{dt} = \frac{\Delta p_{yA}}{\rho v_0}$$

or

$$\Delta p_{yA} = \rho v_0 a. \quad (10.10)$$

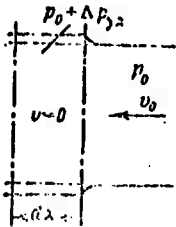


Fig. 130. Displacement of shock wave during time  $dt$ .

Comparing the resulting formula with (10.9), we see that the above statement was correct.

Thus, the Zhukovskiy formula (10.9) can be abbreviated into the form of (10.10). When the velocity in the pipe does not decrease to zero, but only to  $v$ , we have the so-called incomplete water hammer, and Zhukovskiy's formula becomes

$$\Delta p_{yA} = \rho a (v_0 - v).$$

This formula is valid for very quick closing of the valve or, more precisely, when the closing time

$$t_{zakr} < t_0 = \frac{2l}{a},$$

where the time  $t_0$  is known as the phase of the water hammer.

With this condition, we have a direct water hammer.

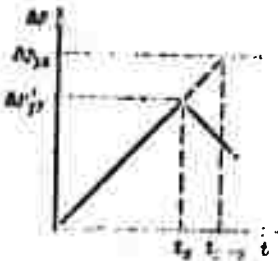


Fig. 131. Shock pressure rise with  $t_{zakr} > t_0$ .

When  $t_{zakr} > t_0$ , we have the so-called indirect water hammer, in which the shock wave reflected from the tank returns to the valve before it is completely closed. Obviously, the pressure increase  $\Delta p'_{ud}$  will be smaller in this case than  $\Delta p_{ud}$  for the direct hammer.

If we assume that the flow velocity decreases when the valve is closed and that pressure rises linearly with time, we can write (Fig. 131)

$$\frac{\Delta p'_{yA}}{\Delta p_{yA}} = \frac{t_0}{t_{zakr}}$$

From this,

$$\Delta p'_{yA} = \frac{t_0}{t_{zakr}} \Delta p_{yA} = \frac{2l}{a t_{zakr}} \rho v_0 a = \frac{2l v_0}{t_{zakr}}. \quad (10.11)$$

Thus, unlike  $\Delta p_{ud}$ , the quantity  $\Delta p'_{ud}$  depends on pipe length, but not on the velocity  $a$ .

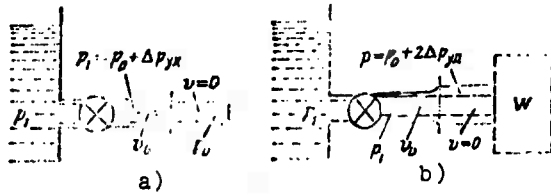


Fig. 132. Diagram of blind pipe.

It must be remembered that the shock pressure can be doubled in a so-called blind pipe. Let us explain this as follows with reference to Fig. 132. Suppose that a pipe with an initial low pressure  $p_0$  is cut off by a valve from a large tank (or pump) with a high pressure  $p_1$ . On instantaneous opening of the valve, the pressure at the beginning of the pipe rises suddenly by an amount  $\Delta p_{ud} = p_1 - p_0$ .

The resulting pressure wave moves at velocity  $a$  toward the end of the pipe (see Fig. 132a). The pressure behind the wave front differs from the pressure in front of it by  $\Delta p_{ud}$ , and the velocity of the fluid in the plane of the front increases from zero to the value  $v_0$  determined by Formula (10.10), i.e.,

$$v_0 = a \frac{\Delta p_{ud}}{c^2}$$

When the wave front arrives at the blind end, the fluid pressure has been raised by  $\Delta p_{ud}$  over the entire length of the pipe, and all of the fluid has acquired the velocity  $v_0$ . Since further motion of the fluid is impossible, the velocity of the entire fluid column drops to zero, in turn increasing the pressure by another  $\Delta p_{ud} = \rho v_0 a$ .

Thus, a new (reflected) pressure wave moves down the pipe toward the valve; behind it, the pressure has risen by  $2\Delta p_{ud}$  by comparison with the initial value, and the velocity of the fluid  $v = 0$  (see Fig. 132b).

If there is a fluid-filled volume  $W$  at the end of the pipe, e.g., a hydraulic power cylinder, this volume will have a damping action and the pressure will increase by less than two times. If volume  $W$  is very large, there will be practically no reflection. The volume of fluid in a hydraulic power cylinder is usually very small or even zero (piston in contact with cylinder head) when the high pressure is switched to it, so that the possibility of doubled pressure is quite a real one.

Formula (10.10) was derived with a number of simplifying assumptions: validity of Hooke's law for the deformation of the pipe and fluid, absence of friction in the fluid and of other forms of energy dissipation during the hammer process, uniform velocity distribution over the pipe section.

Experimental studies of water hammer made by Prof. I.F. Livurdov and others indicate that if the fluid contains no air and if the initial pressure  $p_0$  is moderate, the Zhukovskiy formula is confirmed quite well by experiment in spite of the above assumptions. It would appear that nonuniform velocity distribution and, consequently, nonuniform flow conditions in the pipe (laminar or turbulent) would have to influence  $\Delta p_{ud}$ , since the kinetic energy of the flow depends on it. However, this effect is practically absent. I.F. Livurdov's explanation for this is that the abrupt deceleration of the flow is accompanied by strong shearing between layers of fluid and a large energy loss to internal friction, which approximately offsets the kinetic-energy excess due to velocity nonuniformity. The loss of energy to friction and dissipation of energy during the subsequent course of the hydraulic hammer help to damp out the pressure oscillations.

It was found as a result of B.S. Rozhdestvenskiy's special studies [27] of water hammer in aircraft hydraulic-system pipelines that under real conditions with high enough initial pressures  $p_0$ , the quantity  $\Delta p_{ud}$  exceeds the theoretical value given by the Zhukovskiy formula by 10-20% and more. This is explained by a slight increase in the fluid's elastic modulus  $K$  with increasing pressure  $p_0$  (see §3), and, consequently, an increase in the velocity  $a$ . This means a certain deviation from Hooke's law, i.e., violation of the linear relation between deformation and pressure.

Owing to the high operating speeds of hydraulic-system controls (electromagnetic valves, etc.), which have very short response times (of the order of 0.008-0.002 s),  $\Delta p_{ud}$  ranges up to several tens and even hundreds of  $\text{kgf/cm}^2$  in the pressure lines of aircraft hydraulic systems. These sharp pressure rises may damage pipelines and other system components. Moreover, as they propagate throughout the entire piping system, water-hammer pressure pulses may cause some devices in the system to operate unexpectedly (pressure relays, hydraulic locks, etc.).

Countermeasures against water hammer in aircraft systems are matched to each specific case. The most effective method of lowering  $\Delta p_{ud}$  is to eliminate the possibility of direct water hammer, which reduces, for a given pipe, to increasing the operate times of valves and other devices. A similar effect is obtained by installing compensators in the form of adequate local fluid volumes or hydraulic accumulators in front of these devices. Shock pressure can also be lowered by lowering the velocity of the fluid in the pipes (increasing pipe diameter at a given flow rate) and shortening the runs of pipe (to obtain indirect hammer).

Sometimes, rather than lower the pressure  $\Delta p_{ud}$ , the designer prefers to increase the strength of weak links in the system.

Example. An appliance in an aircraft hydraulic system is shut off by means of an electromagnetic valve. The valve closes the line completely during a time  $t_{zakr} = 0.02$  s.

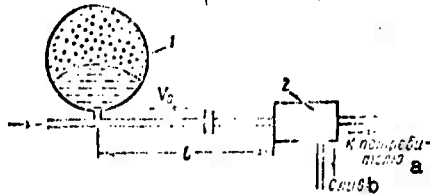


Fig. 133. Illustrating example:  
1) hydraulic accumulator; 2) electromagnetic valve.  
KEY: (a) to appliance; (b) drain.

Determine the pressure rise in front of the valve when the appliance is shut off, using the following data (Fig. 133).

The length of the pipeline from the valve to the accumulator in which the shock pressure is quenched is  $l = 4$  m, pipeline diameter 12 mm, pipe wall thickness  $\delta = 1$  mm, material steel ( $E = 2.2 \cdot 10^6$  kgf/cm<sup>2</sup>); bulk elastic modulus of AMG-10 fluid  $K = 13\,300$  kgf/cm<sup>2</sup>, fluid density  $\rho = 90$  kgf·s<sup>2</sup>/m<sup>4</sup>, flow velocity in pipe  $v_0 = 4.5$  m/s.

Solution. We determine the propagation velocity of the shock wave through a pipe filled with AMG-10 fluid:

$$\frac{1}{c} = \sqrt{\frac{e}{K} + \frac{2\lambda\rho}{E}} = \sqrt{\frac{90}{13300 \cdot 10^4} + \frac{2 \cdot 0.001 \cdot 90}{2.2 \cdot 10^6}} = \frac{1}{1170} \text{ s/m},$$

or

$$c = 1170 \text{ m/s}.$$

The full shock pressure with instantaneous closing of the valve would be

$$\Delta p = \rho \cdot c \cdot v_0 = 90 \cdot 1170 \cdot 4.5 = \frac{\text{kgf}}{\text{m}^2} = \frac{\text{kgf}}{\text{cm}^2}.$$

But we have indirect water hammer in this case, since the back-and-forth travel time of the shock wave is

$$t_0 = \frac{2l}{c} = \frac{2 \cdot 4}{1170} = 0.007 \text{ s},$$

i.e., it is shorter than the complete closing time  $t_{zakr}$  of the valve. Thus, the pressure rise in front of the valve is only

$$\Delta p_{ya}' = \Delta p_{ya} \frac{t_0}{t_{zakr}} = 47,3 \frac{0,0638}{0,02} = 16,2 \frac{\text{kgf}}{\text{cm}^2}.$$

## Footnotes

Manu-  
script  
page

207

<sup>1</sup>Here we cannot disregard the compressibility of the fluid, as is usually done in hydraulics problems, since it is the fluid's slight compressibility that causes the large but finite shock pressure  $\Delta p_{ud}$ .

### Symbol List

Manu- script page	Symbol		English equivalent
199	ин	in	inertia
207	тр	tr	friction
207	уд	ud	shock, hammer
212	закр	zacr	closing

## CHAPTER XI

### HYDRAULIC DESIGN OF PIPELINES

#### §47. THE SIMPLE CONSTANT-SECTION PIPELINE

All pipelines can be classified as simple or complex. We shall call an unbranched pipeline a simple pipeline and a pipeline with one or more branches a complex pipeline.

Fluid moves through a pipeline because its potential energy at the beginning of the line is greater than at its end. This gradient (difference) of potential-energy levels may be created by a variety of methods: operation of a pump, gas pressure, or a difference in fluid levels.

Aviation engineering deals chiefly with pipelines in which fluid motion is due to pump operation. Certain liquid-rocket and other systems use what is known as gas-pressure fluid feed. Fluid is allowed to flow under a level difference (levelling-height difference) chiefly in ground applications.

The pipeline working principles set forth in this section (and in §§49 and 50) apply equally to all three of these fluid-feed variations and are independent of the method by which the energy gradient is set up. Peculiarities of pumped fluid supply through pipelines are set forth in §51.

Let a simple constant-section pipeline, oriented arbitrarily in space (Fig. 134), have a total length  $l$  and a diameter  $d$  and contain a number of local resistances. In the initial section 1-1, we have levelling height  $z_1$ , and excess pressure  $p_1$ , and in

the final section 2-2,  $z_2$  and  $p_2$ , respectively. The flow velocities are the same in these sections because of the constant pipe diameter, and equal  $v$ . Let us write the Bernoulli equation for sections 1-1 and 2-2, setting  $\alpha_1 = \alpha_2$  and cancelling the velocity heads:

$$z_1 + \frac{p_1}{\gamma} = z_2 + \frac{p_2}{\gamma} + \sum h,$$

or

$$\frac{p_1}{\gamma} = z_2 - z_1 + \sum h + \frac{p_2}{\gamma} = \Delta z + \sum h.$$

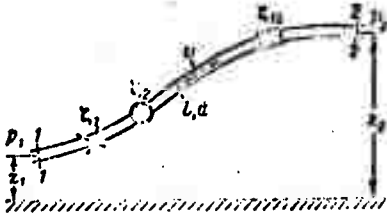


Fig. 134. Diagram of simple pipeline.

We shall call the piezometric height in the left member of the equation the required head  $H_{potr}$ .

If, however, this quantity is given, we shall call it the available head  $H_{расп}$ . As we see from the equation, this head is composed of the geometrical height  $\Delta z$  to which the fluid rises in motion along the pipeline, the piezometric height at the end of the line, and the sum of all hydraulic losses in the pipeline.

The sum of the first two terms  $\Delta z + p_2/\gamma$  is a static head; we can represent it as a certain equivalent geometrical fluid rise height  $\Delta z'$  and the last term  $\sum h$  as a power-law function of flow rate; then

$$H_{расп} = \Delta z' + \sum h = \Delta z' + kQ^m, \quad (11.1)$$

where  $k$  and the exponent  $m$  have different values depending on flow regime.

For laminar flow, we shall have on substitution of equivalent lengths for the local resistances in accordance with (6.5) and (8.19)

$$\sum h = \frac{128\nu(L + L_{\text{экв}})Q}{\pi d^4},$$

consequently,

$$k = \frac{128\nu(L + L_{\text{экв}})}{\pi d^4}, \text{ and } m = 1. \quad (11.2)$$

For turbulent flow, we obtain from (4.17) and (4.18), expressing velocity in terms of flow rate,

$$\sum h = \left( \sum \zeta + \lambda \frac{L}{d} \right) \frac{16Q^2}{2g\pi^5 d^5},$$

consequently,

$$k = \left( \sum_{i=1}^n \lambda_i \frac{l_i}{d} \right) \frac{8}{2.548} \text{ and } m = 2. \quad (11.3)$$

Formula (11.1), supplemented by Expressions (11.2) and (11.3), is the basis for mathematical design of simple pipelines. At the same time, this formula enables us to construct a required-head curve.

The latter is a diagram of the required head as a function of fluid flow rate in the pipe. The greater the flow rate that must be put through the line, the greater is the required head. In laminar flow, the required-head curve is a straight line (or nearly straight when the dependence of  $\lambda_{ekv}$  on Re is considered), and in turbulent flow it is a parabola of the second degree (for  $\lambda_t = \text{const}$ ) or of approximately the second degree (when the dependence of  $\lambda_t$  on Re is considered). The quantity  $\Delta z'$  is positive when the fluid rises from a lower to a greater height in its motion through the pipe or moves into a space at elevated pressure and negative when it flows downward or into a space with a partial vacuum.



Fig. 135. Required-head curves.

Various forms of required-head curves are shown in Fig. 135 for laminar (a) and turbulent (b) flows. The slope of the curve depends on the coefficient  $k$  and increases with increasing pipeline length, decreasing diameter, and increasing local hydraulic resistance coefficients in the pipe. In addition, the slope of the line varies in proportion to fluid viscosity in laminar flow.

The point at which the required-head curve intersects the axis of abscissas at  $\Delta z \neq 0$  (point A) determines the flow rate in motion of the fluid by gravity, i.e., owing to the levelling-height difference  $\Delta z$  alone. The required head is zero in this case, since the pressure is equal to atmospheric pressure  $p_A$  at the beginning and end of the pipe (we consider the free surface in the upper tank to be the beginning of the pipeline); we shall refer to such a pipeline as a gravity pipeline (Fig. 136). If fluid flows out into the atmosphere at the end of a gravity pipeline, a velocity head must be added to the head losses in the equation for required head (11.1).

Sometimes it is more convenient to use the so-called characteristics of the pipeline instead of the required-head curves.

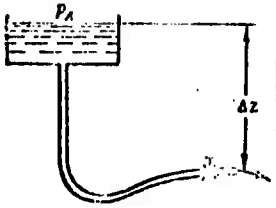


Fig. 136. Diagram of gravity pipeline.

The characteristic of a pipeline is a curve of its total head (or pressure) loss as a function of flow rate, i.e.,

$$\sum h = f(Q).$$

Thus, the characteristic of a pipeline represents the required-head curve shifted to the coordinate origin. The characteristic of a pipeline coincides with its required-head curve for  $\Delta z' = \Delta z + p_2/\gamma = 0$ , e.g., when the pipeline lies in the horizontal plane and there is no back pressure  $P_2$ .

Let us consider certain problems that might be encountered in calculations for a simple pipeline.

**Problem 1.** Given: flow rate  $Q$ , pressure  $p_2$ , properties of fluid ( $\gamma$  and  $\nu$ ), all dimensions of the pipeline, and the material and finish quality (roughness) of the pipe. Find the required head  $H_{\text{potr}}$ .

The solution procedure is as follows. From the flow rate and pipe diameter  $d$ , find the flow velocity  $v$ ; from  $v$ ,  $d$ , and  $\nu$ , determine  $Re$  and the flow regime. Then use appropriate formulas or experimental data to evaluate the local resistances ( $l_{\text{ekv}}/d$  or  $\zeta$  in laminar flow and  $\zeta$  in turbulent flow); from  $Re$  and the roughness, determine  $\lambda$ , and, finally, solve the basic equation (11.1) for  $H_{\text{potr}}$ .

Calculation of  $\lambda$  is not mandatory for laminar flow;  $k$  can be determined at once by Formula (11.2).

**Problem 2.** Given: available head  $H_{\text{расп}}$ , properties of fluid, all pipeline dimensions, and roughness. Find the flow rate  $Q$ .

The solutions for laminar and turbulent flow will differ substantially. For this reason, we assign a flow regime on the basis of fluid viscosity.<sup>1</sup>

1. The problem is easy to solve for laminar flow and with equivalent lengths substituted for local resistances: find the flow rate  $Q$  from (11.1) with consideration of (11.2); substitute  $H_{\text{расп}}$  for  $H_{\text{potr}}$  in this procedure.

2. In turbulent flow, the problem is solved by successive approximations or graphically.

In the former case, we have one equation (11.1) with the two unknowns  $Q$  and  $\lambda_t$ . To solve the problem, we assign a value to the coefficient  $\lambda_t$  with consideration of roughness. Since this

<sup>1</sup>See page 241 for footnote.

coefficient varies in a comparatively narrow range ( $\lambda_t = 0.015-0.04$ ), we do not incur any great error in so doing, the more so since the coefficient  $\lambda_t$  is under the radical in subsequent determination of  $Q$ .

By solving (11.1) with (11.3) for  $Q$ , we find the first-approximation flow rate. From the value found for  $Q$ , we determine  $Re$  in first approximation, and a more accurate value of  $\lambda_t$  from this  $Re$ . We again substitute the value obtained for  $\lambda_t$  into the same fundamental equation and solve it for  $Q$ . Having obtained the second-approximation flow rate, we find a greater or smaller discrepancy between it and the first approximation. If the disagreement is large, the calculation is repeated in the same order. The difference between each subsequent  $Q$  and the preceding one will become smaller and smaller. The calculation should be continued until the disagreement between successive values of  $Q$  is within the limits of acceptable error.

Usually, two or three approximations are quite adequate to obtain acceptable accuracy.

To solve the same problem graphically, we construct a required-head curve for the particular pipeline with consideration of the variability of  $\lambda_t$ , i.e., we compute  $Re$ ,  $\lambda_t$  and, finally,  $H_{potr}$  by Formula (11.1) for a series of  $Q$ -values. Then, plotting a curve of  $H_{potr}$  against  $Q$  and knowing the ordinate  $H_{potr} = H_{rasp}$ , we find the abscissa, i.e., the  $Q$ , that corresponds to it.

**Problem 3.** Given: flow rate  $Q$ , available head  $H_{rasp}$ , fluid properties, and all pipeline dimensions except the diameter. Find the diameter.

We begin the solution by assigning the flow regime on the basis of the fluid's properties ( $\nu$ ).<sup>2</sup>

In the case of laminar flow, the problem is solved simply on the basis of (11.1) with application of (11.2), namely:

$$d = \sqrt[4]{\frac{128 \nu (l + l_s) Q}{\pi g (H - \Delta z)}} \quad (11.4)$$

Having determined  $d$ , we choose the next larger standard diameter and use the same equation to improve the head value for the given  $Q$  or vice versa.

For turbulent flow, solution of (11.1) for  $d$  with consideration of (11.3) is best accomplished as follows: assign a series of standard values to  $d$  and calculate a series of  $H_{potr}$  for the given  $Q$ ; then construct a diagram of  $H_{potr}$  as a function of  $d$  and

<sup>2</sup>See page 241 for footnote.

refer to the curve to find  $d$  for the given  $H_{\text{resp}}$ , round this value off to the standard, and improve  $H_{\text{potr}}$ .

#### §48. THE SIPHON

A siphon is a simple gravity pipeline part of which is situated above the supplying tank (Fig. 137). Fluid moves through a siphon because of the difference in levels  $H$ , first rising to a height  $H_1$  above the free surface under atmospheric pressure and then dropping through height  $H_2$ .

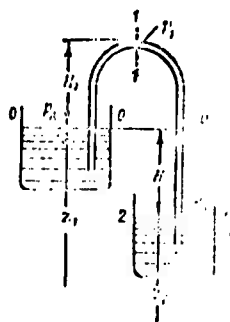


Fig. 137. Diagram of siphon pipeline.

A property of such a pipeline is that the fluid pressure is below atmospheric throughout the ascending line and in part of the descending line.

To start a siphon supplying fluid, it is necessary to fill its entire volume with fluid. If a small hose is being used as a siphon, it is easily filled by first immersing it in the fluid or suctioning the air out of its lower end.

pump (see §18).

If, on the other hand, the siphon is made in the form of a fixed metal pipe, it is necessary to provide a valve at its highest point for withdrawal of air. The air can be removed either by a displacement pump (see Chapter XIII) or by an ejector

Let us write the Bernoulli equation for sections 0-0 and 2-2 (see Fig. 137), where we shall regard the velocity as equal to zero, and the pressure as atmospheric:

$$z_1 + z_2 = \dots$$

or

$$\Delta z = kQ^n = H.$$

Thus, the flow rate through the siphon is determined by the level difference  $H$  and the resistance of the pipeline, and is independent of rise height  $H_1$ . However, this is true only within certain limits. With increasing height  $H_1$ , the absolute pressure  $p_1$  in the uppermost section 1-1 of the siphon decreases. When this pressure becomes equal to the saturation vapor pressure, cavitation begins and flow rate decreases; subsequently, vapor lock shuts off the fluid feed.

In designing a siphon, therefore, it is necessary to make sure that the pressure at the top point ( $p_1$ ) does not become too low. If the fluid flow rate through the siphon and all dimensions are known, the absolute pressure  $p_1$  can be found from the

Bernoulli equation for sections 0-0 and 1-1, which reads

$$\frac{P_A}{\gamma} + H_1 + \frac{P_1}{\gamma} + a \frac{v^2}{2g} + \sum h_0$$

If, on the other hand, the minimum permissible pressure  $p_1$  is known, then, knowing the flow rate, we can use the same equation to find the maximum permissible height  $H_1$ .

§49. SERIES- AND PARALLEL-CONNECTED PIPES.

Let us take several pipes, for example, 1, 2, and 3, which have different lengths and diameters and contain different local resistances, and connect them in series (Fig. 138). The result is a simple pipeline of variable cross section.

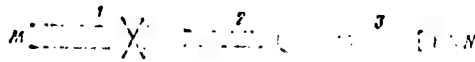


Fig. 138. Pipes connected in series.

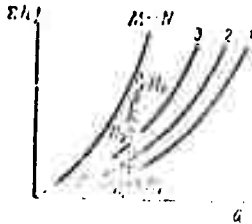


Fig. 139. Construction of characteristic for series-connected pipes.



Fig. 140. Parallel-connected pipes.

Quite obviously, when fluid is fed through such a pipeline, the flow rate will be the same in all of the series-connected pipes, and the total head loss between points M and N will be equal to the sum of the head losses in all of the series-connected pipes, i.e., we have the following fundamental equations:

$$\left. \begin{aligned} Q_1 &= Q_2 = Q_3 = Q \\ \sum h_{01} &= \sum h_{02} = \sum h_{03} = \sum h_0 \end{aligned} \right\} \quad (11.5)$$

These equations give a rule for construction of characteristics for series-connected pipes.

Suppose we have been given (or have ourselves constructed) characteristics (1, 2, 3) for the three pipelines (Fig. 139). To construct the characteristic M-N of the entire series unit, we must, according to equation system (11.5), add the head losses

for identical flow rates, i.e., add the ordinates of all three curves at each abscissas.

Since the velocities at the beginning (M) and end (N) of the pipe are different in the more general case under consideration, the expression for the head required for the entire pipeline M-N must, unlike Formula (11.1) contain the velocity-head difference between the end and beginning of the pipeline, i.e.,

$$H_{\text{not p}} = z_M - z_N + \frac{a_N v_N^2 - a_M v_M^2}{2g} + \sum h_{M-N} + \frac{p_N}{\gamma} \quad (11.6)$$

$$= \Delta z' + CQ^2 + kQ^n,$$

where

$$C = \frac{1}{2g} \left( \frac{a_N}{S_N^5} - \frac{a_M}{S_M^5} \right);$$

$$\Delta z' = z_M - z_N + \frac{p_N}{\gamma}.$$

Let us now consider several unlike pipelines (1, 2, 3), connected in parallel between points M and N (Fig. 140).

Let us denote the total heads at points M and N by  $H_M$  and  $H_N$ , respectively, the flow rate in the main line (i.e., before branching and after merging) by  $Q$ , and those in the parallel pipelines by  $Q_1$ ,  $Q_2$ , and  $Q_3$ , and the total head losses in these pipelines by  $\Sigma h_1$ ,  $\Sigma h_2$ , and  $\Sigma h_3$ .

We first write the following obvious equation:

$$Q = Q_1 + Q_2 + Q_3. \quad (11.7)$$

We then express the head loss in each of the pipelines in terms of the total heads at points M and N, i.e.,

$$\Sigma h_1 = H_M - H_N;$$

$$\Sigma h_2 = H_M - H_N;$$

$$\Sigma h_3 = H_M - H_N.$$

From this we draw the following important conclusion:

$$\Sigma h_1 = \Sigma h_2 = \Sigma h_3. \quad (11.8)$$

i.e., the head losses in parallel pipelines are equal to one another.

In general form, these losses can be expressed as follows in terms of the corresponding flow rates:

$$\sum h_1 = k_1 Q_1^m;$$

$$\sum h_2 = k_2 Q_2^m;$$

$$\sum h_3 = k_3 Q_3^m;$$

where the coefficient  $k$  and the exponent  $m$  are determined by Formulas (11.2) or (11.3), depending on flow regime.

To supplement (11.7), therefore, we obtain two more equations on the basis of (11.8):

$$k_1 Q_1^m = k_2 Q_2^m; \quad (11.9)$$

$$k_2 Q_2^m = k_3 Q_3^m. \quad (11.10)$$

Equation system (11.7), (11.9), and (11.10) enables us to solve, for example, the following typical problem: the flow rate  $Q$  in the main line and all pipeline dimensions are given; determine the flow rates  $Q_1$ ,  $Q_2$ , and  $Q_3$  in the parallel pipes.

Applying (11.7) and rule (11.8), we can always write as many equations as there are parallel pipelines between points M and N.

Problems of the following type must also be solved frequently in the design of aircraft fuel systems: the total flow rate and the lengths of the parallel pipelines are given; find the diameters of these pipelines that will ensure certain flow rates in each of them. The solution of such a problem is considered in an example.

The following important rule proceeds from (11.7) and (11.8): to construct the characteristic of several pipelines connected in parallel, it is necessary to add the abscissas of the characteristics of each of these pipes (the flow rates) at identical ordinates ( $\Sigma h$ ). An example of this construction is given in Fig. 141.

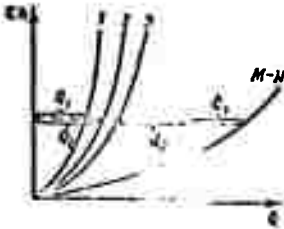


Fig. 141. Construction of characteristics for parallel-connected pipes.

These relationships and rules for parallel-connected pipes are, of course, also valid when pipes 1, 2, 3, etc. (see Fig. 140) do not meet at the same point N, but deliver fluid at various points at the same pressure and equal final-section levelling heights. If the latter condition is not met, however, these pipelines cannot be regarded as parallel, but must be assigned to the category of branched pipelines (see §50).

#### §50. BRANCHED PIPELINES. CALCULATIONS FOR THE COMPLEX PIPELINE IN THE GENERAL CASE

We shall use the term "branched pipeline" for a set of several pipes that have a common cross section - a point at which they branch or merge. Such pipelines are

usually encountered in aircraft fuel systems (service and fueling) and in hydraulic transmission systems, as well as in stationary fuel-handling systems at airports.

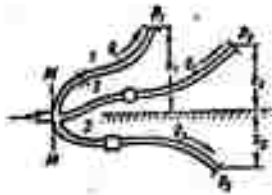


Fig. 142. Branched pipeline.

Let the main pipeline branch at section M-M, at which, for example, three pipes (1, 2, 3) with different diameters and different local resistances branch off (Fig. 142). Assume further that the leveling heights of the terminal sections ( $z_1$ ,  $z_2$ , and  $z_3$ ) and their pressures ( $p_1$ ,  $p_2$ , and  $p_3$ ) are also different. Let us find the relation between the pressure in section M-M ( $p_M$ ) and the flow rates in the pipes ( $Q_1$ ,  $Q_2$ , and  $Q_3$ ), assuming that the direction of flow in the pipes is given (see arrows).<sup>3</sup>

As for parallel pipelines, we have

$$Q_M = Q_1 + Q_2 + Q_3.$$

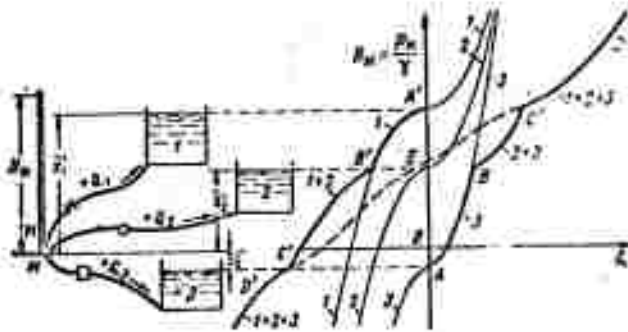


Fig. 143. Construction of required-head curve for branched pipeline.

Writing the Bernoulli equation for section M-M and for the final section, for example, of the first pipeline, we obtain (disregarding the velocity-head difference)

$$\frac{p_M}{\gamma} = z_1 + \frac{p_1}{\gamma} + \sum h_1.$$

Denoting by  $z_1'$  the sum of the first two terms in the right member of the equation and expressing the third term in terms of flow rate (as we did above),

$$\frac{p_M}{\gamma} = z_1' + k_1 Q_1^n.$$

<sup>3</sup>See page 241 for footnote.

Similarly, we can write for the other two pipes

$$\frac{p_M}{\gamma} = z'_2 + k_2 Q_2^m,$$

$$\frac{p_M}{\gamma} = z'_3 + k_3 Q_3^m.$$

Thus, we obtain a system of four equations with four unknowns:  $Q_1$ ,  $Q_2$ ,  $Q_3$ , and  $p_M$ . Graphical solution is convenient. For this purpose, we construct a curve of  $p_M/\gamma$  as a function of  $Q_M$  for each of the pipes from the equations given above, and then add them in the same way as we added the characteristics of the parallel-connected pipes, i.e., we add the abscissas ( $Q$ ) at identical ordinates ( $H_M = p_M/\gamma$ ) (Fig. 143). The resulting inflected curve ABCD is the required-head curve for the branched pipeline, and with it we can determine the flow rates from the pressures  $p_M$  or vice versa.

When the direction of the pipe flows is reversed, i.e., fluid moves from tanks 1, 2, and 3 to section M-M, the signs of the head losses in the above equations are reversed and, consequently, the losses are plotted from top to bottom in constructing the  $H_M = f(Q)$  curves. Regarding the rate of fluid flow from tanks 1, 2, and 3 to section M-M as negative, we carry out the construction in the same way as before, but along the left side of the axis of ordinates. The broken curve A'B'C'D' represents the required head in section M-M as a function of the total negative flow rate  $Q_M$  (see Fig. 143, where, for clarity, open tanks with fluid levels  $z' = z + p/\gamma$  are shown on the diagram of the pipelines at sections 1, 2, and 3, and a piezometer appears in section M-M).

Another possibility is the case in which there are no check valves in the pipelines and the flow can move in either direction. In this case, construction of the over-all curve, i.e., addition of abscissas at identical ordinates, must be performed with consideration of the signs of flow rate  $Q_1$ ,  $Q_2$ , and  $Q_3$ . Instead of two different curves, we obtain a single curve D'C'ECD, which relates the flow rate  $Q_M$  and head  $H_M$  and can be used to determine, for example, the flow rates  $Q_M$ ,  $Q_1$ ,  $Q_2$ , and  $Q_3$  with consideration of signs at a given  $H_M$  or to solve other problems. In the particular case with  $Q_M = 0$  at point E, we obtain the answer to the so-called three-tank problem, in which one tank is fed from the other two or two tanks from one.

The branched pipeline considered above, and pipelines composed of several parallel pipes, are variations of the complex pipeline. In the general case, as is clear from the definition (see §47), a complex pipeline may consist of series- and parallel-connected segments or branches.

Normally, calculations for both gravity and pump-fed complex pipelines are made by a graphoanalytical method, i.e., using required-head curves.

In the general case, calculation and construction of these curves for the complex pipeline proceeds as follows. The complex pipeline is broken up into a series of simple pipelines. Each of these simple pipelines is calculated and curves of  $H_{potr} = f(Q)$  are plotted as described above. Then these curves are added for the parallel segments for the elements of a branched pipeline by the rules set forth in §49. The result is a required-head curve for (one or more) parallel-connected pipes or the branched pipeline. This curve is then added to the curves for the series-connected segments in accordance with Formulas (11.5).

Guided by this rule, we can plot a required-head curve for any complex pipeline for either turbulent or laminar flow. When  $\Delta z' = \Delta z + p/\gamma = 0$ , pipeline characteristics are constructed instead of required-head curves.

An example of construction of a required-head curve for a complex pipeline is given at the end of this chapter.

#### §51. PIPELINE WITH PUMP DELIVERY OF FLUID

Up to this point, we have been concerned essentially only with isolated segments of simple and complex pipelines, and not with complete fluid-feed systems (other than the elementary gravity-flow type). And as we have noted, the basic method of fluid delivery in aviation engineering is forced pump feed. Let us consider the combined operation of a pipeline and a pump and the principle involved in mathematical design of pipelines with pumped fluid supply.

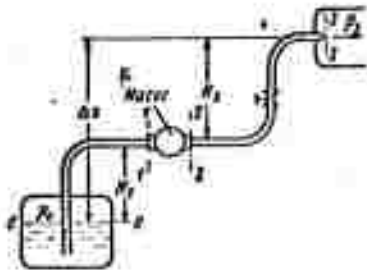


Fig. 144. Diagram of pump-fed pipeline.  
KEY: (a) pump.

A pump-delivery pipeline may be either open, i.e., one through which fluid is transferred from one point to another, or closed (circulating), with a constant amount of fluid circulating in it.

Let us first consider an open pipeline (Fig. 144) through which a pump transfers fluid, for example, from a lower tank at pressure  $p_0$  to some type of chamber - an engine combustion chamber at pressure  $p_3$ , or another tank.

The height of the pump axis relative to the lower level ( $H_1$ ) is known as the geometrical intake height, and the pipeline through which fluid flows to the pump as the intake pipeline or suction line. The height of the terminal section of the pipeline or the upper fluid level ( $H_2$ ) is known as the geometric delivery height

and the pipeline through which fluid moves from the pump as the delivery or pressure line.

We write the Bernoulli equation for the fluid flow in the intake pipeline (for sections 0-0 and 1-1):

$$\frac{p_0}{\gamma} = H_1 + \frac{p_1}{\gamma} + a_1 \frac{v^2}{2g} + \sum h_{0-1} \quad (11.11)$$

This equation indicates that the intake process, i.e., that of raising the fluid to height  $H_1$ , imparting kinetic energy to it, and overcoming all hydraulic resistances takes place with the pump utilizing pressure  $p_0$ . Since this pressure is usually quite low, it must be expended in such a way as to leave a certain pressure margin  $p_1$  in front of the entry into the pump, as necessary for normal cavitation-free operation of the pump. Calculations for intake lines must therefore be particularly meticulous and accurate.

Equation (11.11) is basic to the mathematical design of intake pipelines.

The following problems may be encountered in the design of intake pipes.

1. All dimensions and the flow rate are given. Find the absolute pressure before the entry into the pump.

The solution of this problem is a trial calculation of the intake line. The absolute pressure  $p_1$  found from (11.11) is compared with the minimum acceptable pressure for the particular case.

2. The minimum acceptable absolute pressure in front of the pump,  $p_{1\min}$ , is given. Find one of the following acceptable-limit values:  $H_{1\max}$ ,  $Q_{\max}$ ,  $d_{\min}$ , or  $p_{0\min}$ .

Determination of the last quantity is of particular importance for aircraft hydraulic systems for which  $p_0 = p_A + \Delta p$ .

Here  $\Delta p$  is the excess over atmospheric pressure provided by pressurization or by the pressure of an inert gas. The minimum acceptable atmospheric pressure  $p_{A\min}$  is found from  $p_{0\min}$ , and then the maximum permissible flight altitude of an airplane with the particular system, i.e., the altitude capability of the system, is found by referring to a standard-atmosphere table.

An increase in the pressure  $p_0$  increases the pressure throughout the entire intake line and, consequently, increases system altitude capability. However, high pressures in the supply tank are not admissible, since this requires making the tank stronger and, consequently, heavier. For this reason, still another method is usually used to increase the altitude capabilities of aircraft hydraulic systems: an auxiliary pump (booster pump)

is inserted at the beginning of the intake line to raise the pressure in that line and prevent cavitation in front of the entry into the main pump.

We write the Bernoulli equation for the motion of the fluid through the delivery line, i.e., for sections 2-2 and 3-3:

$$\frac{p_2}{\gamma} + \alpha_2 \frac{v_2^2}{2g} = H_2 + \frac{p_3}{\gamma} + \alpha_3 \frac{v_3^2}{2g} + \sum h_{2-3}. \quad (11.12)$$

If the delivery line terminates in a tank, there will be no velocity head in the right member of (11.12), but it will be necessary to take the expansion head loss into consideration.

The left side of (11.12) represents the specific energy of the fluid at the exit from the pump.

The fluid's specific energy before the pump entrance can be found from (11.11):

$$\frac{p_1}{\gamma} + \alpha_1 \frac{v_1^2}{2g} = \frac{p_0}{\gamma} - H_1 - \sum h_{0-1}.$$

Let us find the specific-energy increment of the fluid in the pump, i.e., determine the energy acquired by each unit weight of fluid as it passes through the pump. This energy is imparted to the fluid by the pump and is therefore referred to as the pump head and denoted by  $H_{\text{нас}}$ . To find  $H_{\text{нас}}$ , we subtract the last equation from (11.12):

$$\begin{aligned} H_{\text{нас}} &= \left( \frac{p_2}{\gamma} + \alpha_2 \frac{v_2^2}{2g} \right) - \left( \frac{p_1}{\gamma} + \alpha_1 \frac{v_1^2}{2g} \right) = \\ &= H_1 + H_2 + \frac{p_2 - p_0}{\gamma} + \alpha_3 \frac{v_3^2}{2g} + \sum h_{0-1} + \sum h_{2-3}, \end{aligned}$$

or

$$H_{\text{нас}} = \Delta z + \frac{p_2 - p_0}{\gamma} + CQ^2 + kQ^m, \quad (11.13)$$

where  $\Delta z$  is the total geometrical rise height of the fluid (see Fig. 144),  $CQ^2 = \alpha_3 \frac{v_3^2}{2g}$  is the velocity head in section 3-3, and  $kQ^m$  is the sum of the hydraulic losses in the intake and delivery lines.

If we add the piezometric-height difference  $(p_2 - p_0)/\gamma$  to the actual level difference  $\Delta z$ , we can work with a kind of augmented level difference equal to

$$\Delta z' = \Delta z + \frac{p_2 - p_0}{\gamma},$$

and rewrite (11.13) as follows:

$$H_{\text{нас}} = \Delta z' + CQ^2 + kQ^m.$$

Let us compare Expression (11.13) with the required-head formula (11.6). Obviously,

$$H_{\text{нас}} = H_{\text{потр}} \quad (11.14)$$

This equation can be extended to all cases of stable operation of the pump connected to the line and can be formulated in the form of a rule: with steady flow in the pipeline, the pump develops the required head. Only with this condition is stable pump operation possible. The condition is usually met automatically.

A method of calculation for pump-fed pipelines is based on (11.14) and consists in plotting two curves on the same scale and on the same diagram: a required-head curve  $H_{\text{потр}} = f_1(Q)$  and the pump characteristic  $H_{\text{нас}} = f_2(Q)$  and finding their point of intersection (Fig. 145).

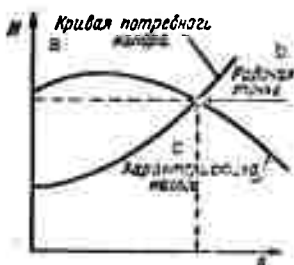


Fig. 145. Finding operating point graphically.  
KEY: (a) required-head curve; (b) operating point; (c) pump characteristic.

Pump characteristics will be discussed at some length later, in Chapters XII and XIII. For the moment, anticipating somewhat, we give only a definition: the characteristic of a pump is the curve of the head that it develops as a function of its delivery (flow rate) at constant speed.

At the point of intersection of the required-head curve and the pump characteristic we have equal required head and pump head, i.e., Equality (11.14). This point is called the operating point, since the pump operating mode corresponding to precisely this point is always established.

To obtain a different operating point, it is necessary either to change the opening of the regulating valve (gate, spool), i.e., to change the pipeline characteristic, or change the pump speed, of which we shall speak in greater detail below.

It should be noted, however, that this calculation of the operating point is applicable only when the speed of the pump drive is independent of the power taken by the pump, i.e., of the load on the pump shaft. This is the case, for example, when the pump is coupled to an ac motor or an aviation engine whose power is many times that of the pump.

If the pump is driven by an individual internal-combustion engine, or a special turbine whose power depends on pump shaft load, the calculation must be performed differently. In this case, it is necessary to construct required and available power

curves against rpm and determine the operating speed and power at their point of intersection.

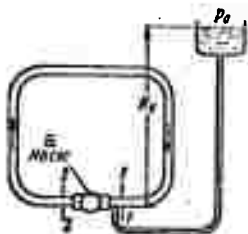
For a closed pipeline (Fig. 146), the geometrical fluid rise height is zero ( $\Delta z = 0$ ); consequently, for  $v_1 = v_2$

$$H_{\text{total}} = \sum h = \frac{P_2 - P_1}{\gamma} = H_{\text{net}}$$

i.e., the same equality applies between required head and pump head.

It must be remembered that a closed pipeline must in all cases be provided with a so-called expansion or compensation tank connected by a pipe to one of the sections of the pipeline, most frequently the section at the entrance to the pump, where the pressure is lowest. Without this tank, the absolute pressure

inside the closed pipeline would be indeterminate, and also variable because of temperature fluctuations and seepage.



With the expansion tank connected to the pipeline as shown in Fig. 146, the pressure before the pump entrance becomes quite definite at

$$p_1 = p_0 + H_0 \gamma$$

Fig. 146. Diagram of closed pipeline.  
KEY: (a) pump.

The pressure in any cross section of the closed pipeline can be computed from  $p_1$ . If the pressure  $p_0$  in the tank is changed by a certain amount, the pressure will change by the same amount at all points of the particular system. Consequently, Pascal's law of pressure transmission in a stationary fluid (see §5) is also valid here. A tank can also be connected into a closed pipeline as shown in Fig. 172.

**Example 1.** Determine the head required at the exit from an aircraft booster pump to feed T-1 fuel at a rate of  $G = 1200$  kgf/h from the service tank to the fuel pump at the engine if the length of the duralumin pipeline  $l = 5$  m, its diameter  $d = 15$  mm, the required pressure at the entrance into the fuel pump  $p_2 = 1.3$  kgf/cm<sup>2</sup>, the viscosity coefficient of the kerosene  $\nu = 0.045$  cm<sup>2</sup>/s, and its specific weight  $\gamma_k = 820$  kgf/m<sup>3</sup>. Figure 147 shows the local resistances inserted in the pipeline. Disregard the height of the fluid column in the tank.

**Solution.** 1. The velocity of flow in the line

$$v = \frac{4G}{3600 \pi d^2 \gamma_k} = \frac{4 \cdot 1200 \cdot 10^3}{3500 \cdot 3.14 \cdot 1.5^2 \cdot 0.82} = 210 \text{ cm/s.}$$

2. The Reynolds number

$$Re = \frac{vd}{\nu} = \frac{210 \cdot 1.5}{0.045} = 8000.$$

3. We determine the coefficient of frictional resistance  $\lambda_t$  by the Konakov formula:  $\lambda_t = 0.0328$ .

4. We take the values of the resistance coefficients for the filter, shutoff valve, flowmeter sender, and standard bends (elbows) from Table 2 (Chapter IX):

$$\zeta_b = 2; \zeta_{sp} = 1.5; \zeta_p = 7; \zeta_{vr} = 1.2$$

5. We compute the pressure loss in the line from the booster pump to the fuel pump by the formula

$$\begin{aligned} \sum p_{rp} &= \gamma_k \left( \lambda_t \frac{l}{d^5} + 3\zeta_{vr} + \zeta_p + \zeta_{sp} + \zeta_b \right) \frac{v^2}{2g} = \\ &= 820 \left( 0.0328 \frac{500}{1.5^5} + 3 \cdot 1.2 + 7 + 1.5 + 2 \right) \frac{2.4^2}{2 \cdot 9.81} = \\ &= 6000 \text{ kgf/m}^2 = 0.6 \text{ kgf/cm}^2 = 58 \text{ 800 N/m}^2. \end{aligned}$$

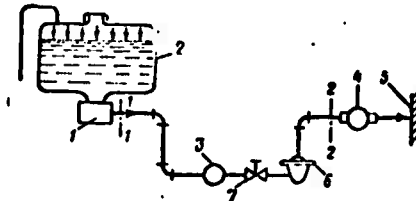


Fig. 147. Illustrating example 1. 1) booster pump; 2) service tank; 3) flowmeter sender; 4) main fuel pump; 5) engine; 6) filter; 7) shutoff valve.

6. Hence the pressure required at the exit from the booster pump is

$$p_1 = p_2 + \sum p_{rp} = 1.3 + 0.6 = 1.9 \frac{\text{kgf}}{\text{cm}^2} = 185400 \frac{\text{N}}{\text{m}^2}.$$

Example 2. T-1 fuel is supplied from two underwing tanks to the service tank of an airplane (Fig. 148) by an excess of pressure in these tanks over that in the service tank  $\Delta p = p_b - p_{r,b} = 0.2 \text{ kgf/cm}^2$ .

Determine the pipeline diameter  $d$ , remembering that the underwing tanks must be depleted simultaneously at a total fuel flow rate  $G = 1500 \text{ kgf/h}$ . Each underwing tank holds a volume  $W = 450 \text{ l}$ . Pipelines of length  $l = 7 \text{ m}$  are assembled from duralumin tubing. The viscosity coefficient of the kerosene  $\nu = 0.045 \text{ cm}^2/\text{s}$  and  $\gamma_k = 830 \text{ kgf/m}^3$ . Disregard the liquid column in the tanks.

Solution. 1. We find the engine running time to complete exhaustion of the kerosene in the underwing tanks:

$$t = \frac{2R^2 \gamma_k}{G} = \frac{2 \cdot 450 \cdot 0,83}{1500} = 0,5 \text{ h.}$$

2. We determine the fuel flow from each tank from the expression

$$Q = \frac{W}{t} = \frac{450}{0,5} = 900 \text{ l/h} = 0,25 \text{ l/s.}$$

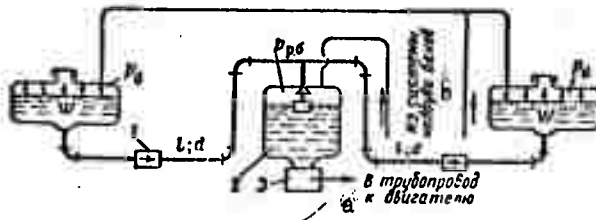


Fig. 148. Illustrating example 2. 1) check valve; 2) service tank; 3) booster pump. KEY: (a) to pipeline to engine; (b) from tank pressurization system.

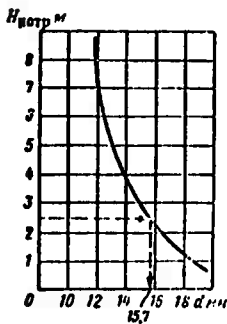


Fig. 149. Illustrating example 2.

3. We assign a series of values to the diameter  $\underline{d}$ : 12, 14, 16 and 18 mm.

4. We refer to Table 2 for the resistance coefficients at the entry into the pipeline  $\zeta_{vkh}$ , those of the check valve  $\zeta_{o.k}$ , the elbow  $\zeta_{kol}$ , and the tee  $\zeta_{tr}$ , and that at the exit from the line,  $\zeta_{vykh}$ . We calculate the coefficient  $\lambda_t$  by the Kona-kov formula for each  $\underline{d}$  after first determining Re.

5. We determine the head  $H_{potr}$  required for each  $\underline{d}$  by the formula

$$H_{potr} = \left( \zeta_{vkh} + \zeta_{o.k} + 3\zeta_{kol} + \zeta_{tr} + \zeta_{vykh} + \lambda_t \frac{l}{d} \right) \frac{16Q^2}{2g\pi^2 d^5}$$

and plot a curve of  $H_{potr} = f(d)$  (Fig. 149).

7. For the available head, which is found by dividing  $\Delta p$  by  $\gamma_k$ , we refer to the diagram to find the required diameter,  $d = 15,7 \text{ mm}$ .

We select the standard pipeline diameter  $d = 16 \text{ mm}$ , which provides for the necessary flow rate with simultaneous depletion of both tanks.

If the lengths of the pipelines were equal, their diameters would be different for this condition, and it would be necessary to construct an  $H_{potr} = f(d)$  curve for each pipeline.

**Example 3.** In centralized fueling of an airplane under pressure, all tanks must be filled and topped off simultaneously.

Figure 150 shows a schematic diagram of a centralized fueling system.

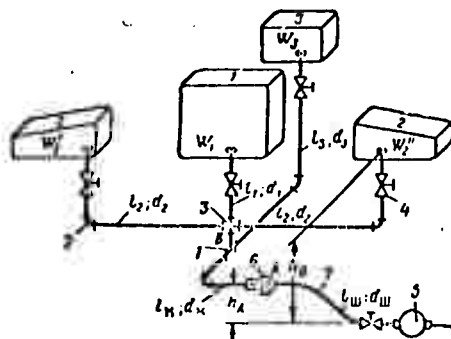


Fig. 150. Illustrating example 3. 1) tee; 2) elbow; 3) cross-pipe; 4) valve; 5) fuel-truck pump; 6) check valve; 7) hose.

Let all tanks with their volumes  $W_1$ ,  $W_2 = W_2''$ , and  $W_3$  lie in the same horizontal plane at a height  $h_b$  above the fuel-truck pump. The elevation of the main pipeline A-B above pump level is  $h_A$ . The characteristic of the fuel-truck pump, the length  $l_{sh}$  and diameter  $d_{sh}$  of the delivery hose, and the lengths of all pipelines and the tank capacities are given.

Disregarding the heights of the liquid columns in the tanks and their excess pressures, solve the following problems, which are likely to be encountered in practice:

I. Determine the fueling time  $t$  if the pipeline diameters are given.

II. Find the necessary pipeline diameters  $d_m$ ,  $d_1$ ,  $d_2$ , and  $d_3$  for simultaneous fueling of all tanks during time  $t$ .

I. The problem is solved graphoanalytically.

1. We construct the characteristic of the delivery hose from the pump to point A, the beginning of the main pipeline, with consideration of the height  $h_A$ .

2. We construct the characteristic of the main pipeline (from point A to point B).

3. We add the two characteristics in conformity to the rule for adding characteristics of series-connected pipes (Fig. 151).

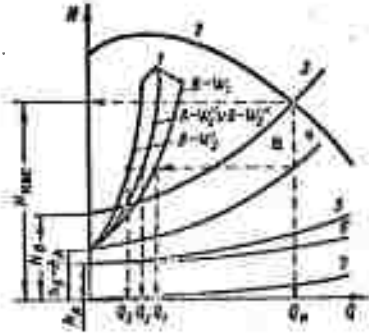


Fig. 151. Illustrating example 3. 1) characteristics of pipelines to tanks; 2) pump characteristics; 3) characteristic of complete pipeline; 4) resultant characteristic of pipelines to tanks; 5) resultant characteristic of hose and main A-B; 6) characteristic of hose; 7) characteristic of main line A-B.

KEY: (a)  $B-W_1'$  and  $B-W_2''$  .

4. We construct the characteristics of the pipelines from branch point B to the respective tanks with consideration of the height  $h_b - h_A$ .

5. We add the characteristics of the pipelines to tanks by the rule for addition of the characteristics of parallel pipelines.

6. Adding the characteristic of the pipeline from the pump to point B to the resulting over-all characteristic for the four parallel pipelines, we obtain the characteristic of the entire complex pipeline with consideration of the height  $h_b$ , i.e., the required-head curve.

7. From the point of intersection of this curve with the fuel-truck-pump characteristic, we can determine the head  $H_{nas}$  to be developed by the pump and its delivery rate  $Q_n$ .

8. The flow rates fed to each tank are determined as shown in Fig. 151.

9. The fueling time  $t$  (with simultaneous completion of fueling) will be

$$t = \frac{\sum W}{Q_n} = \frac{W_1}{Q_1} = \frac{W_2' + W_2''}{Q_2} = \frac{W_3}{Q_3}$$

II. The problem is solved graphoanalytically.

1. We determine the flow rate  $Q_n$  from the fuel-truck pump for filling of all tanks during time  $t$  by dividing the total tank volume by  $t$ .

2. On the pump characteristic at flow rate  $Q_n$  we find the operating point, i.e., the head  $H_{nas}$  to be developed by the pump. The calculation indicates that the pipeline diameters must be so

selected that the flow rate  $Q_n$  will be able to pass through the pipelines under a head  $H_{nas}$ .

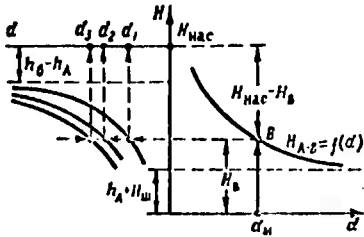


Fig. 152. Illustrating example 3.

3. The flow rates in the lines to the respective tanks can be found by dividing the volume of each tank by the time  $t$ .

4. The fueling-hose head loss  $H_{sh}$  is found with consideration of filler-checkvalve losses.

5. For the main line (between points A and B) we construct a curve of head loss vs. line diameter  $H_{A-B} = f(d)$ . For this purpose, we

assign a series of diameters and determine for each  $d$  the Reynolds number  $Re$ , the coefficient  $\lambda_t$ , and the head loss  $H_{A-B}$  with consideration of the levelling-height difference between the main line and the truck pump,  $h_A$ , and the delivery-hose losses  $H_{sh}$ .

6. We construct a curve of head loss as a function of diameter for each tank pipeline.

We construct these graphs in the same way as that of  $H_{A-B} = f(d)$ , but in a coordinate system whose origin is at  $H_{nas}$ , with the positive diameter axis on the left and the positive head axis pointing downward (Fig. 152). We add the height  $h_B - h_A$  to the head losses.

This somewhat unusual arrangement of the coordinate axes and the  $H_1 = \phi(d_1)$  curves for the pipelines to the tanks makes it easier to find the unknown diameters.

We assign a diameter  $d_m$  to the main pipeline and, referring to our graphs, find the diameters  $d_1$ ,  $d_2$ , and  $d_3$  as indicated by the arrows in Fig. 152.

The diameters can be determined from the graph in several variations, of which the most rational can be selected for use.

Point B on the  $H_{A-B} = f(d)$  curve indicates the amount of head ( $H_B$ ) lost on the path from the pump to the branching point of the pipelines. The rest of the head ( $H_{nas} - H_B$ ) is used to overcome resistances to motion of the fuel in the pipes to the tanks and the height  $h_B - h_A$ .

This method can also be used when the branches from the main line to the tanks are not all at the same point B, but at different points; in this case, it is necessary to plot three curves instead of the single  $H_{A-B} = f(d)$  curve.

### Footnotes

Manu-  
script  
page

222

<sup>1</sup>In this case, regime can be determined by comparing  $H_{\text{rasp}}$  with its approximate critical value  $H_{\text{kr}}$ , which can be expressed from (11.1) and (11.2) as follows:

$$H_{\text{kp}} = \Delta z + \frac{128\nu l Q_{\text{kp}}}{\pi g d^4} = \Delta z + \frac{32\nu l Q_{\text{kp}} \nu d}{g d^2 \cdot \nu d} = \Delta z + \frac{32\nu^2 l}{g d^3} \text{Re}_{\text{kp}}.$$

223

<sup>2</sup>The flow regime can be determined by comparing  $H_{\text{rasp}}$  with  $H_{\text{kr}}$ , which equals (for a given Q)

$$H_{\text{kp}} = \Delta z + \frac{128\nu l Q}{\pi g d^4} = \frac{2.48\nu l Q^3}{2.48\nu l Q^3} \Delta z + \frac{\pi^3 \nu^2 \text{Re}_{\text{kp}}^4}{2.48 Q^3}.$$

228

<sup>3</sup>In aircraft systems the flow direction is often kept from reversing by insertion of check valves.

## Symbol List

Manu- script page	Symbol	English equivalent
220	потр	potr required
220	расп	rasp available
220	экв	ekv equivalent
220	т	t turbulent
232	нас	nas pump
234	к	k kerosene
235	т	t friction
235	ф	f filter
235	кр	kr valve
235	р	r flowmeter
235	уг	ug bends
235	б	b tank
235	р.б	r.b service tank
236	вх	vkh entry
236	о.к	o.k checkvalve
236	кол	kol elbows
236	тр	tr tee
236	вых	vykh exit
237	ш	sh hose
237	м	m main line
238	н	n pump
241	кр	kr critical

## C H A P T E R XII

### CENTRIFUGAL PUMPS

#### §52. PUMPS IN GENERAL

As we know, a pump is a machine that transfers fluid by pressure or, sometimes, by suction.

From the physical standpoint, the operating principle of a pump consists in its conversion of the mechanical energy of a motor (drive) into energy of the fluid, i.e., it imparts power to the stream of fluid flowing through it. The reserve of energy acquired by the fluid in the pump enables the flow to overcome hydraulic resistances and rise to a geometrical height.

The energy that each unit weight of the fluid acquires in the pump, i.e., the specific-energy increase, has the dimensions of length, and, as we noted above, represents the head created by the pump. It was shown in §51 that the head developed by a pump equals

$$H_{\text{net}} = \left( \frac{p_2}{\gamma} + a_2 \frac{v_2^2}{2g} \right) - \left( \frac{p_1}{\gamma} + a_1 \frac{v_1^2}{2g} \right)$$

or

$$H_{\text{net}} = \frac{p_2 - p_1}{\gamma} + \frac{a_2 v_2^2 - a_1 v_1^2}{2g}$$

In the general case, therefore, the head developed by a pump is composed of a piezometric-height (static-head) increment and an increment of specific kinetic energy (dynamic head).

However, the second term is usually much smaller than the first, and equals zero when the intake and delivery pipes have the same diameter ( $d_1 = d_2$ , and, consequently,  $v_1 = v_2$ ) and  $\alpha_1 = \alpha_2$ ; then

$$H_{\text{use}} = \frac{P_2 - P_1}{\gamma} = \frac{P_{\text{use}}}{\gamma}. \quad (12.1)$$

We shall call the flow rate of fluid delivered by the pump into the line the pump's useful delivery and denote it by  $Q$ .

The useful power of a pump, or its developed power, is the energy that the pump imparts to the entire fluid flow each second. By definition, this power equals

$$N = Q\gamma H_{\text{use}} [\text{W}] = 10^{-3} Q\gamma H_{\text{use}} [\text{kW}] \quad (12.2)$$

where  $Q$  is in  $\text{m}^3/\text{s}$ ,  $\gamma$  in  $\text{N}/\text{m}^3$  and  $H_{\text{use}}$  in meters, or

$$N = \frac{Q\gamma H_{\text{use}}}{75} [\text{hp}]. \quad (12.2')$$

where  $Q$  is in  $\text{m}^3/\text{s}$ ,  $\gamma$  in  $\text{kgf}/\text{m}^3$ , and  $H_{\text{use}}$  in meters.

Like any other machine, a pump requires more power than it puts out. The ratio of the power developed to the power used is the efficiency of the pump:

$$\eta = \frac{N}{N_0}. \quad (12.3)$$

Hence the power drawn by the pump equals

$$N_0 = \frac{Q\gamma H_{\text{use}}}{\eta}. \quad (12.4)$$

or, applying (12.1),

$$N_0 = \frac{Q p_{\text{use}}}{\eta} [\text{W}] \quad (12.4)$$

where  $Q$  is in  $\text{m}^3/\text{s}$  and  $p_{\text{use}}$  in  $\text{N}/\text{m}^2$ .

This formula is used in selection of pump drives.

The over-all efficiency of a pump takes account of three kinds of energy loss in the pump: hydraulic losses, i.e., head losses to friction and eddying, volume losses due to circulation of fluid through clearances in the pump, and mechanical losses, i.e., losses to mechanical friction in bearings and packings and certain other losses.

The pumps used in aviation and other fields of engineering would appear to come in a wide variety of designs and operating principles. However, almost all of them can be classified among three main types:

1) vane pumps, which include centrifugal, diagonal, and axial-flow pumps;

2) displacement pumps, which include piston and rotor types;

3) turbulence-type pumps.

In this chapter, we shall examine centrifugal pumps, which are being used on an expanding scale in aviation and rocket engineering, and touch briefly on turbulence pumps.

The next chapter is devoted to displacement pumps.

### §53. DERIVATION OF THE FUNDAMENTAL EQUATION OF THE CENTRIFUGAL PUMP

The operating principle of the centrifugal pump is as follows. The basic working element of the pump is a vane wheel or impeller (Fig. 153), which rotates at high speed to impart increased pressure to the fluid filling it and expel it at increased velocity into a scroll chamber (delivery pipe). As a result of the interaction between the wheel vanes and the fluid flow, drive energy is converted into stream energy.

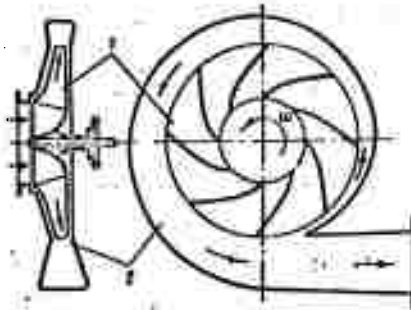


Fig. 153. Diagram of centrifugal pump. 1) impeller; 2) scroll chamber.

The scroll discharge pipe is snail-shaped and designed to catch the fluid issuing from the wheel and convert some of its kinetic energy into pressure energy.

The impeller of a centrifugal pump (Fig. 154) consists of two disks, one of which is bushed to the shaft, while the other, which has a central hole for passage of fluid, is secured to the first by the vanes. The latter are curved, with cylindrical or more complex space-curve shapes. The fluid comes into the wheel along its axis of rotation and is then directed into the spaces between the vanes; passing through these spaces, it exits through the slot between the impeller disks.

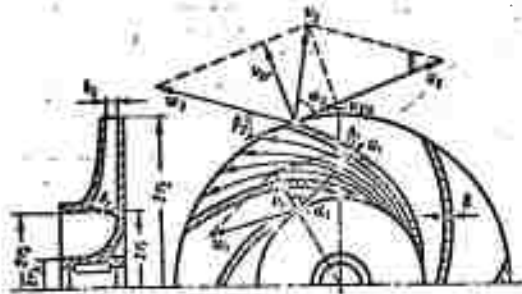


Fig. 154. Diagram of fluid flow through impeller.

The motion of the fluid in the passages between the vanes of the rotating impeller can be regarded as the sum of two motions: translational (rotation of the impeller) and relative (motion relative to the impeller). Thus, the absolute velocity vector  $\underline{v}$  of the fluid in the wheel can be found as the sum of the vectors of the circumferential velocity  $\underline{u}$  and the relative velocity  $\underline{w}$ . Examining a fluid particle as it slides over the surface of a vane, we can construct velocity parallelograms for the entrance of this particle onto the vane and its exit from the vane. Here it should be assumed that the relative velocity  $\underline{w}$  is directed along the tangent to the vane, while the circumferential component  $\underline{u}$  is tangential to the corresponding circle. The same velocity parallelogram can also be constructed for any intermediate point on the vane. Our convention here will be to denote all quantities pertaining to entrance onto the vane by the subscript 1, and quantities pertaining to the exit by subscript 2.

We shall denote the angle between the vectors of the circumferential and absolute velocities by  $\alpha$  and the angle between the tangent to the vane and the tangent drawn to the circumference of the impeller in the direction opposed to the rotation by  $\beta$  with the appropriate subscripts. In the general case, angle  $\alpha$  changes with a change in pump operating mode, i.e., on a change in impeller rpm  $n$  (velocity  $\underline{u}$ ) and flow rate  $Q$  (velocity  $\underline{w}$ ). The angle  $\beta$  determines the slope of the vane at each of its points and, consequently, does not depend on pump operating mode.

We shall adopt the following two assumptions to derive the basic equation of centrifugal-pump theory:

1. Let the pump have an infinite number of identical vanes ( $z = \infty$ ), and let the thickness of these vanes be zero ( $\delta = 0$ ). This implies a filamentary flow in the between-vanes passages of the wheel such that all filaments in the relative motion have exactly identical shapes conforming exactly to the shapes of the vanes, and that the velocities depend only on radius and do not vary on a circle of given radius. This situation can occur only when each filament is directed by its own vane. Figure 154 gives

a schematic representation of this filamentary flow in one of the between-vanes passages.

2. The efficiency of the pump is unity ( $\eta = 1$ ), i.e., there are no energy losses of any form in the pump and, consequently, all of the power used to turn the impeller is transmitted to the fluid. Such operation of the pump is possible only when an ideal fluid is being transferred, when there are no clearances in the pump, and in the absence of mechanical friction in the packings and bearings.

Thus, we have substantially idealized the working process of the centrifugal pump to facilitate theoretical investigation of its operation. We shall call this pump, for which  $z = \infty$  and  $\eta = 1$ , the ideal centrifugal pump. After examining the theory of the ideal pump, we shall, of course, pass to real pumps.

Let us write two equations: the equation of powers and the equation of moments. The first equation signifies that the power applied to the impeller shaft is equal to the energy acquired by the per-second flow of fluid in the pump, i.e.,

$$M\omega = Q\gamma H_{t\infty} \quad (12.5)$$

where  $M$  is the torque at the pump shaft,  $\omega$  is the angular velocity of the impeller, and  $H_{t\infty}$  is the head developed by the ideal pump, or the specific fluid-energy increment in the pump (the two subscripts  $\underline{t}$  and  $\infty$  correspond to the above two assumptions).

The sense of the second equation consists in the following: the torque at the pump shaft is equal to the per-second angular-momentum increment of the fluid in the impeller. Denoting by  $r_1$  the radius of the cylindrical surface on which the entry edges of the blades lie and by  $r_2$  the radius of the impeller outer circle, we have

$$M = \frac{Q\gamma}{g} (v_2 r_2 \cos \alpha_2 - v_1 r_1 \cos \alpha_1) \quad (12.6)$$

From the resulting equations (12.5) and (12.6), we find the head developed by the ideal pump:

$$H_{t\infty} = \frac{\omega}{g} (v_2 r_2 \cos \alpha_2 - v_1 r_1 \cos \alpha_1) \quad (12.7)$$

This equation is fundamental not only for centrifugal pumps, but also for all other bladed machines - fans, superchargers, and hydraulic turbines. In the latter case, we have a decrease rather than an increase in the angular momentum of the fluid as it passes through the impeller, i.e., energy is being taken from the fluid, so that the terms in parentheses must be written with the opposite signs. Equation (12.7) was derived by L. Euler and bears his name.

Attention should be drawn to the fact that the head developed by the ideal centrifugal pump and measured as the column of fluid being transferred does not depend on the kind of fluid, i.e., on its specific weight.

Usually, the fluid is not pretwisted before arriving at the impeller,<sup>1</sup> but is moving radially when it enters the between-vanes passages. This means that the vector  $v_1$  is radial and that the angle  $\alpha_1 = 90^\circ$ . Consequently, the second term in (12.7) vanishes and the equation assumes the form

$$H_{t\infty} = \frac{u}{g} v_2 r_2 \cos \alpha_2 = \frac{u_2 v_{2u}}{g}, \quad (12.8)$$

where  $u_2 = \omega r_2$  is the circumferential velocity at the exit from the impeller and  $v_{2u}$  is the projection of the absolute velocity at exit from the impeller onto the direction of the circumferential velocity, i.e., the tangential velocity component  $v_2$ .

Formula (12.8) indicates that to obtain large heads with a centrifugal pump, it is necessary to have, firstly, a high circumferential impeller speed and, secondly, a large enough value of vector  $v_{2u}$ , i.e., the impeller must impart sufficient twist to the fluid flow. The first requirement is met by adjustment of impeller rpm and diameter, and the second by providing an adequate number of vanes of the proper size and shape.

#### §54. CHARACTERISTIC OF THE IDEAL PUMP. PUMP REACTION RATIO

Equation (12.8) is inconvenient for use in calculations, since it does not contain the flow rate  $Q$ . We shall therefore transform this equation in such a way that the head  $H_{t\infty}$  is expressed as a function of flow rate  $Q$  and impeller dimensions.

We have from the velocity triangle at the exit from the impeller (Fig. 155)

$$v_{2u} = u_2 - v_{2r} \operatorname{ctg} \beta_2, \quad (12.9)$$

where  $v_{2r}$  is the projection of the absolute exit velocity onto the radius, i.e., the radial component of vector  $v_2$ .

The flow of fluid through the impeller can be expressed by the radial component  $v_{2r}$  and the dimensions of the wheel in the following manner:

$$Q = 2\pi r_2 b_2 v_{2r}, \quad (12.10)$$

where  $b_2$  is the width of the slot at the exit from the wheel (see Fig. 154).

<sup>1</sup>See page 290 for footnote.

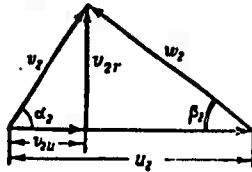


Fig. 155. Velocity triangle at exit from impeller.

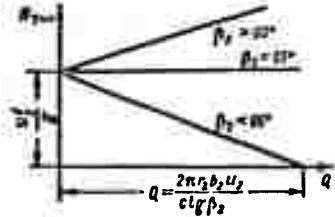


Fig. 156. Characteristics of ideal centrifugal pumps.

From this,

$$v_{2u} = \frac{Q}{2\pi r_2 b_2}$$

Substituting this expression into (12.9),

$$v_{2u} = u_2 - \frac{Q}{2\pi r_2 b_2} \cot \beta_2 \quad (12.11)$$

We now substitute our expression (12.11) for the tangential component  $v_{2u}$  in (12.8); the result is another form of the fundamental ideal-pump equation:

$$H_{t\infty} = \frac{u_2}{g} \left( u_2 - \frac{Q \cot \beta_2}{2\pi r_2 b_2} \right) \quad (12.12)$$

This equation enables us to construct the characteristic of the ideal centrifugal pump, i.e., a curve of the head developed by the pump as a function of flow rate at constant wheel rpm. As we see from (12.12), the characteristic of this pump is a straight line. However, its slope depends on the vane angle  $\beta_2$ . Here we must distinguish three cases:

- 1) angle  $\beta_2 < 90^\circ$ . In this case,  $\cot \beta_2$  is positive and the head  $H_{t\infty}$  diminishes with increasing flow rate;
- 2) the angle  $\beta_2 = 90^\circ$ ,  $\cot \beta_2 = 0$ , the head  $H_{t\infty}$  does not depend on flow rate, and equals  $H_{t\infty} = u_2^2/g$ ;
- 3) the angle  $\beta_2 > 90^\circ$ ,  $\cot \beta_2$  is negative, and head  $H_{t\infty}$  increases with increasing flow rate.

These three cases of the ideal centrifugal pump characteristic are shown in Fig. 156. Diagrams of the corresponding vanes and the velocity parallelograms are given in Fig. 157, a, b, and c, for the same  $u_2$  and  $v_{2r}$ .

Consequently, the bent-forward vane, i.e., one with  $\beta_2 > 90^\circ$ , gives the best results as far as head development is concerned. However, practice has shown that this produces low efficiencies.

The bent-backward vane, i.e., one with  $\beta_2 < 90^\circ$ , is more advantageous and therefore used most often; in most cases, this angle is made approximately equal to  $30^\circ$ . Radial vanes ( $\beta_2 = 90^\circ$ ) are also used, but this involves a certain loss of efficiency and is dictated by other considerations (bulk, strength).

To understand why the efficiency of the pump falls off with increasing angle  $\beta_2$ , it is necessary to examine the components of head  $H_{t\infty}$  and how their proportions change with changing  $\beta_2$ .

The head  $H_{t\infty}$ , or, in other words, the increment in the total specific energy of the fluid in the impeller, is composed of the specific pressure-energy increment and the specific kinetic energy increment, i.e.,

$$H_{t\infty} = \frac{p_2 - p_1}{\gamma} + \frac{v_2^2 - v_1^2}{2g} \quad (12.13)$$

or, in other terms,

$$H_{t\infty} = H_p + H_v. \quad (12.13')$$

Expressing the velocities  $v_1$  and  $v_2$  in terms of their radial and tangential components, we have

$$v_2^2 - v_1^2 = v_{2u}^2 + v_{2r}^2 - v_{1u}^2 - v_{1r}^2.$$

Assuming approximately equal impeller entrance and exit areas, we can consider that  $v_{1r} = v_{2r}$ . Moreover, as we indicated above, the flow is normally not twisted before entrance into the impeller, so that  $v_{1u} = 0$ . Consequently, we have instead of the above

$$v_2^2 - v_1^2 \approx v_{2u}^2.$$

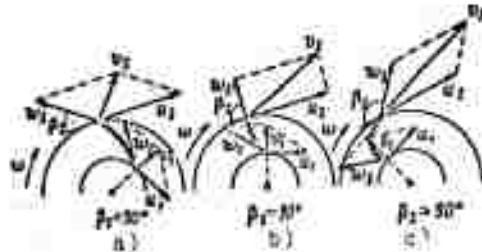


Fig. 157. Vane shapes and velocity parallelograms.

Applying this expression, we use (12.13) to find the pump reaction ratio, i.e., to determine the ratio of the head acquired by the fluid owing to the pressure increment to the total head:

$$\frac{H_p}{H_{t\infty}} = 1 - \frac{v_{2u}^2}{2gH_{t\infty}}.$$

With (12.8), we rewrite this last expression in the form

$$\frac{H_p}{H_{t\infty}} = 1 - \frac{v_{2u}}{2u_2}, \quad (12.14)$$

from which, after substituting  $v_{2u}$  by Formula (12.9), we obtain finally

$$\frac{H_p}{H_{t\infty}} = \frac{1}{2} \left( 1 + \frac{v_{2r}}{u_2 \tan \beta_2} \right). \quad (12.15)$$

We see from this expression that the larger  $v_{2r}/u_2$  and the smaller the angle  $\beta_2$ , the greater will be the part of head  $H_{t\infty}$  that is created by the pressure increment, i.e., the greater the pump reaction. With increasing  $\beta_2$ , on the other hand, the fraction of head  $H_{t\infty}$  developed in the form of the kinetic-energy increment becomes larger. But this means higher fluid exit velocities from the impeller, and this, in turn, results in larger energy losses and lower pump efficiencies. This is why there is no advantage in using vanes with large values of the angle  $\beta_2$ , i.e., forward-bent vanes.

For a radial vane ( $\beta_2 = 90^\circ$ ), as we see from (12.15), the reaction ratio is  $\frac{1}{2}$ , and with  $\beta_2 < 90^\circ$ , it is larger than  $\frac{1}{2}$ , but smaller than unity.

The change in the shape of the velocity parallelograms and the increase in absolute exit velocity  $v_2$  with increasing angle  $\beta_2$  are clearly seen in Fig. 157.

#### §55. TRANSITION TO FINITE NUMBER OF VANES

Up to this point, we have been discussing the operation of the ideal centrifugal pump, i.e., a pump with an infinite number of vanes and unit efficiency. The physical significance of these assumptions was analyzed above (see §54).

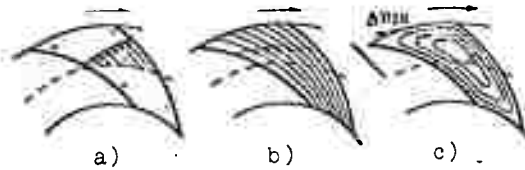


Fig. 158. Flow in passage between vanes.

To make a closer approach to the working process of the real pump, let us now begin by dropping the first of our assumptions, leaving the second in force, i.e., let us pass to a pump with a finite number of vanes.

In practice, there are normally from six to twelve vanes. In this case, the relative flow in the between-vanes passages of the impeller is no longer filamentary, as we assumed earlier, and the velocity distribution is nonuniform. On the leading surfaces of the vanes, which are marked by plus signs (Fig. 158a), the pressure is elevated and the velocity lowered; as a result, the distribution of velocities in the between-vanes passage is approximately as indicated on the same figure.

Here the velocity distribution can be regarded as the sum of two flows: a flow with uniform velocity distribution, as for  $z = \infty$  (Fig. 158b), and a rotational motion in the passage in the direction opposite to the rotation of the impeller (Fig. 158c). The latter occurs in its pure form at zero flow rate through the impeller ( $Q = 0$ ).

Because of the nonuniform distribution of both the relative and absolute velocities in the between-vanes passages when the number of vanes is finite, it is necessary to introduce the notion of average velocity on a circle of given radius. Of greatest interest to us is the average tangential component  $v'_{2u}$  of the absolute exit velocity from the impeller, which determines the head developed by the pump. With a finite number of vanes, this component is found to be smaller than for an infinite number, since an impeller with fewer vanes does not twist the flow as strongly. In the absence of vanes ( $z = 0$ ), there will be no twist either, i.e.,  $v'_{2u} = 0$ , and the (ideal) fluid will issue radially from the impeller.

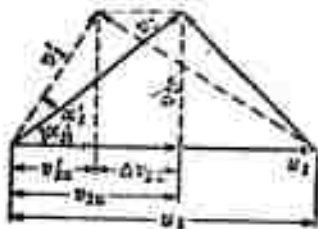


Fig. 159. Change in shape of velocity triangle on transition to finite number of blades.

As a result, the shape of the velocity triangle at the exit from the impeller changes. In Fig. 159, the solid lines indicate the velocity vectors for an infinite number of blades, and the dashed lines the same vectors for a finite number. The construction was made for identical  $u_2$  and  $v_{2r}$ , i.e., for identical rpm and equal flow rates. The velocity symbols for the finite number of vanes are primed.

The decrease in the tangential component  $v_{2u}$  on transition to the finite number of vanes results in a decrease in the head

The decrease in the velocity  $v_{2u}$  on transition to a finite number of vanes can also be explained by the secondary rotational motion referred to above. At the outer circumference of the impeller (see Fig. 158c), this relative motion gives rise to an additional absolute velocity  $\Delta v_{2u}$ , which is opposed to  $v_{2u}$  and, consequently, subtracts from the latter.

developed by the pump. Let us denote by  $H_{tz}$  the theoretical head with a finite number of vanes. This is the head that the pump would develop in the absence of head losses inside it; it is also known as the indicator head. On the basis of Formula (12.8), we have

$$H_{tz} = \frac{u_2^2 v_{2u}}{g}. \quad (12.16)$$

We shall call the ratio of  $H_{tz}$  to  $H_{t\infty}$  the influence coefficient of the number of vanes and denote it by  $\mu$ ; then

$$\mu = \frac{H_{tz}}{H_{t\infty}} = \frac{v_{2u}^2}{v_{2u}^2}, \quad (12.17)$$

whence the head of interest to us equals

$$H_{tz} = \mu H_{t\infty} = \mu \frac{v_2^2 v_{2u}}{g}. \quad (12.18)$$

The problem is now to find a way to determine the coefficient  $\mu$  numerically. Obviously, the coefficient  $\mu$  must be determined primarily by the number of vanes, although it is also influenced by the length of the vane, which depends on the ratio  $r_1/r_2$  and the pitch of the vane, i.e., the angle  $\beta_2$ .

Certain theoretical investigations [24] have shown that the coefficient  $\mu$  does not depend on pump operating mode, i.e., on  $Q$ ,  $H_{nas}$ , or  $n$ , but is determined entirely by the geometry of the impeller and is quite constant for a given impeller.

Without going into the theory of how the number of impeller vanes influences head, we cite only the ultimate results of this theory in the form of the Pfleiderer working formula for  $\mu$ :

$$\mu = \frac{1}{1 + \frac{2\psi}{z \left[ 1 - \left( \frac{r_1}{r_2} \right)^2 \right]}}, \quad (12.19)$$

where

$$\psi = (0.55 - 0.5z) + 0.6 \sin \beta_2.$$

According to the investigations of Prof. P.K. Kazandzhan,  $\psi = \pi/3$  for  $\beta_2 = 90^\circ$ .

By way of example, we present values of the coefficient  $\mu$  for  $\beta_2 = 30^\circ$  and  $r_1/r_2 = 0.5$  (Table 6).

TABLE 6

$z$	4	6	8	10	12	16	24
$\mu$	0.624	0.714	0.768	0.806	0.834	0.870	0.903

Thus,  $\mu \rightarrow 1$  as  $z \rightarrow \infty$ .

Since the relation between  $H_{tz}$  and  $H_{t\infty}$  remains constant in a given pump, the theoretical characteristic of a pump with a finite number of vanes, like the characteristic of the ideal pump at constant rpm ( $n = \text{const}$ ), is a straight line. For  $\beta_2 = 90^\circ$ , it runs parallel to the ideal-pump characteristic, and with  $\beta_2 < 90^\circ$  it intersects the latter at the axis of abscissas, since  $H_{tz} = 0$  and  $H_{t\infty} = 0$  at a given flow rate

$$Q = \frac{2\pi r_2 b_2 a_2}{c \lg \beta_2}.$$

This follows from Formulas (12.12) and (12.18).

#### §56. CONSIDERATION OF HYDRAULIC LOSSES IN THE PUMP. CONSTRUCTION OF DESIGN CHARACTERISTIC

We stated above that  $H_{tz}$  is the head that would be developed in the absence of head losses inside the pump. The actual head  $H_{nas}$  (see §53) is smaller than theoretical by the total head loss in the pump, i.e.,

$$H_{nas} = H_{tz} - \sum h_{nsc}, \quad (12.20)$$

where  $\sum h_{nas}$  is the total head loss in the pump (entry section of pump, impeller, and scroll chamber).

The ratio of the true to the theoretical head for a finite number of vanes (to the indicator head) is known as the hydraulic efficiency and denoted by  $\eta_g$ . Thus, we have

$$\eta_g = \frac{H_{nsc}}{H_{tz}} = \frac{H_{tz} - \sum h_{nsc}}{H_{tz}}. \quad (12.21)$$

The hydraulic efficiency of a pump is always greater than its total efficiency, since it takes account of only one form of energy loss in the pump - the hydraulic losses.

It follows from (12.18) and (12.21) that

$$H_{nsc} = \eta_g H_{tz} = \eta_g H_{t\infty}, \quad (12.21')$$

where  $H_{t\infty}$  is given by Formulas (12.7) and (12.12).

It is convenient to regard the hydraulic losses  $\sum h_{nas}$  in the pump as the sum of the following two components:

1. Ordinary hydraulic losses, i.e., head losses to friction and to some extent to eddying inside the pump. Since the fluid-flow regime in a centrifugal pump is normally turbulent, this form of head loss increases approximately in proportion to the square of flow rate and can be expressed by the formula



of two inclined straight lines for  $n = \text{const}$  (Fig. 161). Then, below the axis of abscissas, we construct the curves of the two components  $h_1$  and  $h_2$  of the total head loss in the pump. Adding the ordinates of these two curves, we obtain the curve of  $\sum h_{\text{nas}}$  as a function of flow rate. Then, in accordance with Formula (12.20), we subtract  $\sum h_{\text{nas}}$  from  $H_{tz}$  and obtain a curve of  $H_{\text{nas}} = f(Q)$ , i.e., the actual characteristic of the pump at constant speed.

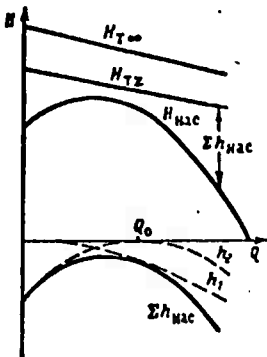


Fig. 161. Construction of design characteristics.

The  $H_{\text{nas}} = f(Q)$  curve shown in Fig. 161 is typical for a centrifugal pump. The maximum value of the head  $H_{\text{nas}}$  is usually obtained not at zero flow and not at  $Q = Q_0$ , but at a certain intermediate value of  $Q$ .

Pump characteristics obtained by this working method are not highly accurate because of the difficulty of evaluating the coefficients  $k_1$  and  $k_2$  in (12.22) and (12.23). Experimental pump characteristics are therefore preferred, i.e., the curves are obtained by testing the pump.

For this purpose, some sort of shut-off-and-regulating device - a cock, valve, or spool - is inserted at the exit from the pump, which is operated at constant rpm. During the test, the aperture of this device is progressively varied, for example, reduced from wide open, i.e., the line is throttled. During this process, the flow rate and the head developed by the pump are measured while holding rpm constant. With the valve wide open, the results are the maximum flow rate and minimum head, which is equal to the head lost in the line (point C in Fig. 162). As the valve is closed, flow rate decreases, but the head rises to its maximum (point B). As the flow rate is cut further, the head rises slightly and at  $Q = 0$  (point A), i.e., with the valve fully closed, the head usually has a value somewhat higher than the mean but smaller than the maximum.

Thus, reducing the pump delivery to zero by closing the line at constant rpm does not cause a head increase that is dangerous from the standpoint of pump and line strength. For this reason, centrifugal pumps, unlike displacement pumps, do not require safety valves.

## §57. PUMP EFFICIENCY

The energy losses in the pump, as indicated by the total efficiency  $\eta$ , are broken down into three types:

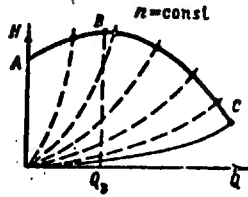


Fig. 162. Displacement of operating point on throttling.



Fig. 163. Leakage in centrifugal pump.

1. Hydraulic losses, which were considered in the previous section and are evaluated by the pump's hydraulic efficiency (12.21):

$$\eta_h = \frac{H_{tz} - \sum h_{nac}}{H_{tz}} = \frac{H_{nac}}{H_{tz}}$$

2. Volume losses. These energy losses result from the presence of backflow of fluid in the pump through the gap (seal) between the rotating impeller and the stationary casing of the pump. The impeller delivers fluid from the intake line into the delivery line, but owing to the pressure gradient that it creates, some part of this fluid returns through the clearance (Fig. 163).

In §53, we conventionally denoted by  $Q$  the flow rate into the line, i.e., the pump's useful delivery. Then the flow rate through the impeller will be

$$Q' = Q + q, \quad (12.25)$$

where  $q$  is the flow rate through the clearance, which is referred to as leakage.

The volume energy losses are evaluated by the so-called volume efficiency of the pump, which equals

$$\eta_v = \frac{Q}{Q + q} = \frac{Q}{Q'} \quad (12.26)$$

More detailed information on the numerical values of the volume losses and the coefficient  $\eta_v$  will be given later, in §60.

3. Mechanical losses. These include losses of energy to mechanical friction in the packings and bearings of the pump and to friction between the outer surface of the impeller (impeller disk) against the fluid. If the power lost to this friction is

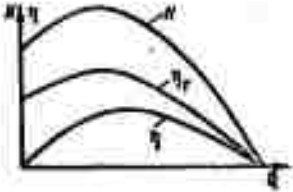


Fig. 164. Curves of  $H$ ,  $\eta$ , and  $\eta_g$  as functions of flow rate.

denoted by  $N_m$  and the total power drawn by the pump is  $N_0$ , the mechanical efficiency of the pump will be

$$\eta_m = \frac{N_0 - N_m}{N_0}. \quad (12.27)$$

(See §56 for the method used to find  $N_m$ ).

The numerator of this ratio is the so-called hydraulic or indicator power and can be expressed by the formula

$$N_r = N_0 - N_m = \frac{1}{75} (Q + q) \gamma H_{r,z}. \quad (12.28)$$

This is the power that the pump would develop in the absence of hydraulic and volume energy losses inside it.

We can now express the over-all pump efficiency as the ratio of developed power to the power drawn by the pump:

$$\eta = \frac{Q \gamma H_{r,z}}{75 N_0}$$

and multiply the numerator of this ratio by  $N_g$  and its denominator by the same quantity expressed by Formula (12.28):

$$\eta = \frac{Q \gamma H_{r,z}}{75 N_0} \frac{75 N_r}{(Q + q) \gamma H_{r,z}}$$

Cancelling and transposing multipliers,

$$\eta = \frac{H_{r,z}}{H_{r,z}} \frac{Q}{Q + q} \frac{N_r}{N_0} = \eta_r \eta_v \eta_m, \quad (12.29)$$

i.e., the over-all efficiency of the pump equals the product of its hydraulic, volumetric, and mechanical efficiencies.

The over-all efficiencies of centrifugal pumps vary from 0.7 to 0.85; small auxiliary pumps may have lower efficiencies.

Figure 164 presents curves that indicate the manner in which the over-all and hydraulic efficiencies of the pump vary, and also shows a constant-rpm characteristic.

## §58. SIMILARITY FORMULAS

Let us consider similar operating modes of centrifugal pumps that are geometrically similar to one another. As we noted earlier (§22), geometrical, kinematic, and dynamic similarity are required to ensure hydrodynamic similarity. For centrifugal pumps, kinematic similarity means similarity of the velocity triangles constructed for arbitrary corresponding points of the impellers.

To ensure dynamic similarity, the Reynolds numbers for the flows in the particular pumps must be equal.

In similar operating regimes of centrifugal pumps, proportionality is observed between the useful heads and the head losses in the pumps, as well as between the useful deliveries and leakage rates; we may therefore assume that if hydrodynamic similarity is observed in the pumps, their hydraulic and volumetric efficiencies will be equal.<sup>2</sup> Mechanical efficiency changes slightly on transition from one pump to another in spite of similarity, but we can assume without incurring any major error that the overall efficiency remains constant, as do  $\eta_g$  and  $\eta_0$ .

Let us consider similar operating modes of two geometrically similar centrifugal pumps. Quantities pertaining to the first pump will be denoted by the additional subscript I, and those pertaining to the second by II (Fig. 165).

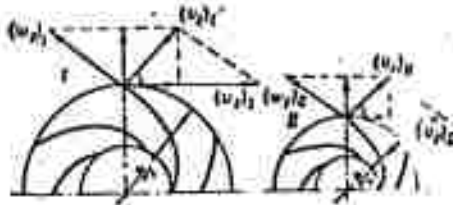


Fig. 165. Illustrating derivation of similarity formulas for centrifugal pumps.

Remembering that the circumferential velocities of the impellers are proportional to the products of the speed  $n$  by the diameters  $D$  of these impellers, the condition of kinematic similarity at the impeller exits can be written in the form of the following proportions:

$$\frac{(u_2)_I}{(u_2)_{II}} = \frac{(v_2)_I}{(v_2)_{II}} = \frac{(v_{2u})_I}{(v_{2u})_{II}} = \frac{(v_{2r})_I}{(v_{2r})_{II}} = \frac{(w_2)_I}{(w_2)_{II}} = \frac{(nD)_I}{(nD)_{II}}. \quad (12.30)$$

Since, in accordance with (12.10),

$$Q = \pi D v_2 b_2,$$

and we have from geometrical similarity

$$\frac{(D)_I}{(D)_{II}} = \frac{(b_2)_I}{(b_2)_{II}},$$

we can write on the basis of (12.30)

<sup>2</sup>See page 290 for footnote.

$$\frac{Q_I}{Q_{II}} = \frac{(nD^3)_I}{(nD^3)_{II}}. \quad (12.31)$$

This means that the flow rates in similar pumps operating in similar modes are related as the speeds and the cubes of the diameters.

The theoretical heads for infinite numbers of vanes are proportional, according to (12.8), to the product of two velocities: circumferential and tangential; the vane-number influence coefficient  $\mu$  is the same for the geometrically similar impellers, so that

$$\frac{(H, s)_I}{(H, s)_{II}} = \frac{(u, v_{2u})_I}{(u, v_{2u})_{II}}.$$

From this, applying the proportions (12.30), we obtain

$$\frac{(H, s)_I}{(H, s)_{II}} = \frac{(n^2 D^2)_I}{(n^2 D^2)_{II}}. \quad (12.32')$$

The actual head developed by the pump equals

$$H_{act} = \eta_r H_{t, act}$$

(this head  $H$  will henceforth be written without the subscript nas). But since  $(\eta_g)_I = (\eta_g)_{II}$ , we can write instead of (12.32')

$$\frac{H_I}{H_{II}} = \frac{(n^2 D^2)_I}{(n^2 D^2)_{II}}, \quad (12.32)$$

i.e., the actual heads developed by the similar pumps in similar operating modes are related as the squares of the products of speed by impeller diameter.

Proceeding from the expression for the power developed by the pump [Formula (12.2)] and using our new formulas (12.31) and (12.32), we can write the relation between the powers developed by similar pumps in similar operating modes:

$$\frac{N_I}{N_{II}} = \frac{Q_I H_I \gamma_I}{Q_{II} H_{II} \gamma_{II}} = \frac{n_1^3 D_1^5 \gamma_I}{n_2^3 D_1^5 \gamma_{II}}. \quad (12.33)$$

If we consider similar operating modes of a single pump at different speeds  $n_1$  and  $n_2$ , the above formulas (12.31), (12.32), and (12.33) are simplified, since they have the same  $D$  and  $\gamma$ , and assume the form (the subscripts 1 and 2 denote the different speeds):

$$\frac{Q_1}{Q_2} = \frac{n_1}{n_2}; \quad (12.34)$$

$$\frac{H_1}{H_2} = \left(\frac{n_1}{n_2}\right)^2; \quad (12.35)$$

$$\frac{N_1}{N_2} = \left(\frac{n_1}{n_2}\right)^3. \quad (12.36)$$

Formulas (12.34) and (12.35) are used to convert the pump characteristics from one speed to another. If a curve of  $H$  as a function of  $Q$  for  $n_1 = \text{const}$  is given, the analogous curve for  $n_2 = \text{const}$  can be obtained by converting the abscissas of points of the first curve (flow rates) in proportion to the ratio between the speeds and the ordinates (heads) in proportion to the square of this ratio (Fig. 166).

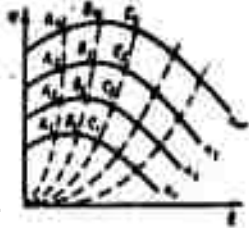


Fig. 166. Conversion of pump characteristics to a different speed.

Thus, we can convert and replot the pump characteristic for any other speed:  $n_2, n_3, n_4$ , and so forth, and obtain a whole series of characteristics of the same pump for different  $n$ .

On these curves, points connected with one another by the coordinate relationships (12.34) and (12.35), such as points  $A_1, A_2, A_3, A_4$ , etc., represent operating regimes that are similar to one another. Another series of points  $B_1, B_2, B_3$ , etc., represents a second series of similar regimes; points  $C_1, C_2, C_3$ , etc. represent a third series, etc.

It is easy to find the equation of the curves on which similar (in the sense of operating regime) points lie. According to (12.34) and (12.35), we can write for a series of points

$$\frac{H_1}{Q_1^2} = \frac{H_2}{Q_2^2} = \frac{H_3}{Q_3^2} = \text{const}_1.$$

From the above, we have for the series of mutually similar regimes

$$H = \text{const}_1 Q^2.$$

For another series

$$H = \text{const}_2 Q^2.$$

Consequently, the points representing similar regimes lie on second-degree parabolas emanating from the coordinate origin in  $H, Q$ -coordinates. They are known as similar-regime parabolas. In Fig. 166, they are indicated by dashed lines.<sup>3</sup>

On the basis of what we said above concerning the hydraulic and volumetric efficiencies in similar operating modes, it can be stated that the similar-regime parabolas are at the same time curves of constant  $\eta_g$  and  $\eta_0$ . It can be assumed in approximation that the over-all efficiency also remains constant along a similar-regime parabola.

<sup>3</sup>See page 290 for footnote.

The following question arises with regard to regime similarity in centrifugal-pump operation: when is similarity preserved and when is it violated on a change in the rpm of the centrifugal pump?

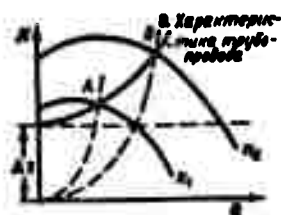


Fig. 167. Operating points on violation of similarity.

KEY: (a) pipeline characteristic.

abola. It may therefore be assumed that a change in pump speed will not disturb similarity of pump operating regimes in this case.

If, however, fluid is being transferred through the pipeline from a lower tank to a higher tank, i.e., if the level difference  $\Delta z \neq 0$ , the pipeline characteristic will take the form shown in Fig. 167. A change in pump speed from  $n_1$  to  $n_2$  will cause the operating point to shift from A to B. But points A and B are on different similar-regime parabolas, so that regime similarity is violated.

It follows from the above analysis that there are two possible ways of regulating a centrifugal pump: throttling as indicated in §57 and changing pump speed. In the case of throttling, the pipeline characteristic is changed and the operating point is shifted along a given pump characteristic (see Fig. 152), and when speed is changed, the pump characteristic changes and the operating point moves along the pipeline characteristic (see Fig. 166).

The second control method - varying speed - is more economical, since it permits us to maintain an approximately constant pump efficiency (if the pipeline characteristic starts from the origin). However, speed changing usually involves certain difficulties, since it requires additional equipment, and it is therefore simpler to control the pump by throttling. With throttling, the pump efficiency varies along the curve shown in Fig. 164 and, consequently, a substantial decrease in delivery is accompanied by a substantial decline in pump efficiency.

## §59. THE SPEED COEFFICIENT AND ITS RELATION TO IMPELLER SHAPE

Let us use the similarity formulas obtained above to derive a criterion that is of great importance in the calculation and design of centrifugal pumps and is known as the speed coefficient.

We can write on the basis of Formula (12.31)

$$\frac{D_1^3}{D_2^3} = \left(\frac{Q_1}{Q_2}\right)^{3/3} \left(\frac{n_1}{n_2}\right)^{-2/3}$$

Substituting this expression into (12.32), we obtain

$$\frac{H_1}{H_2} = \left(\frac{Q_1}{Q_2}\right)^{3/3} \left(\frac{n_1}{n_2}\right)^{4/3}$$

Grouping factors and raising to the 3/4 power,

$$\frac{n_1 \sqrt[3]{Q_1}}{H_1^{3/4}} = \frac{n_2 \sqrt[3]{Q_2}}{H_2^{3/4}} = \text{const.} \quad (12.37)$$

This expression is the same not only for two similar pumps I and II, but also for a whole series of mutually similar pumps operating in similar regimes.

Suppose that in this series of similar pumps we have one standard pump that develops a head  $H_e = 1$  m and a power  $N_e = 1$  hp at  $\gamma = 1000$  kg/m<sup>3</sup>.

The delivery of the standard pump is easily found from the power formula (12.2):

$$Q_e = \frac{75N_e}{H_e \gamma} = \frac{75 \cdot 1}{1 \cdot 1000} = 0,075 \text{ m}^3/\text{s} = 75 \text{ l/s.}$$

Let us now connect the parameters of the standard pump ( $Q_e$ ,  $H_e$ ,  $n_e$ ) with those of any other pump in the series ( $Q$ ,  $H$ ,  $n$ ) for similar operating regimes, i.e., let us apply (12.37):

$$\frac{n_e \sqrt[3]{Q_e}}{H_e^{3/4}} = \frac{n \sqrt[3]{Q}}{H^{3/4}}$$

Substituting the values of  $Q_e$  and  $H_e$ , we determine the rpm of the standard pump from the above equation:

$$n_e = \frac{1}{\sqrt[3]{0,075}} \frac{n \sqrt[3]{Q}}{H^{3/4}} = 3,65 \frac{n \sqrt[3]{Q}}{H^{3/4}}$$

This number is conventionally denoted by  $n_g$  and known as the speed coefficient or the specific rpm of the centrifugal pump. Thus, we have finally

$$n_s = 3.65 \frac{n \sqrt{Q}}{H^{3/4}} \quad (12.38)$$

As follows from its derivation, the sense of  $n_s$  is as follows: it is the speed of a standard pump that is similar to the given pump and develops a head  $H_s = 1$  m and a flow rate  $Q_s = 0.075$  m<sup>3</sup>/s in similar operation. It must be remembered that the hydraulic and volumetric efficiencies of these pumps are assumed to be the same.

The power developed by the standard pump will be 1 hp, but with the condition that  $\gamma = 1000$  kgf/m<sup>3</sup>. The power will be smaller for lighter fluids and greater for heavier ones. Thus it is better not to introduce the power value from the standpoint of generality in defining  $n_s$ .

The impeller diameter of the standard pump is easy to determine. According to (12.32), we can write

$$\frac{H_s}{H} = \frac{n_s^2 D_s^2}{n^2 D^2},$$

whence

$$D_s = \frac{nD}{n_s \sqrt{H}} \quad (12.39)$$

In using Formulas (12.38) and (12.39), it must be remembered that  $H$  is measured in meters,  $Q$  in m<sup>3</sup>/s, and  $n$  in rev/min.

Under certain conditions, the speed coefficient or specific rpm  $n_s$  characterises the ability of the pump to develop head ("head capacity") and feed fluid ("delivery capacity"). The larger the coefficient  $n_s$ , the smaller is the "head capacity" (for given  $Q$  and  $n$ ) and the greater the "delivery capacity" of the pump (for given  $H$  and  $n$ ).

The coefficient  $n_s$  is closely related to the shape of the pump's impeller.

Pumps with small  $n_s$  values have small impeller width ratios ( $b_2/D_2$ ), but large  $D_1/D_2$ , i.e., a longer vane than is required to produce a large head. Fluid flows through such an impeller in the plane perpendicular to its axis of rotation.

With increasing  $n_s$ , the ratio  $D_2/D_1$  (and  $D_2/D_0$ ) diminishes, i.e., the vanes become shorter and the relative width  $b_2/D_2$  of the impeller increases. In addition, the flow through the impeller leaves the plane of rotation and becomes increasingly three-dimensional. At the limit, for the maximum values of  $n_s$ , we obtain flow along the axis of rotation and the axial-flow impellers that correspond to this case.

As  $n_s$  increases from 40 to 200, the vane angle  $\beta$ , decreases from about 35 to about 15°.

Centrifugal pumps and other similar vane pumps are classified in the following varieties on the basis of the speed coefficient  $n_s$ :

- 1) slow-running:  $n_s < 80$ ,  $\frac{D_2}{D_1} = 2.2 + 3.5$ ;
- 2) normal:  $n_s = 80 + 150$ ,  $\frac{D_2}{D_1} = 2.2 + 1.8$ ;
- 3) fast-running:  $n_s = 150 + 300$ ,  $\frac{D_2}{D_1} = 1.8 + 1.3$ ;
- 4) diagonal or screw:  $n_s = 300 + 600$ ,  $\frac{D_2}{D_1} = 1.3 + 1.1$ ;
- 5) axial or screw-impeller:  $n_s = 600 + 1200$ ,  $\frac{D_2}{D_1} = 1$ .

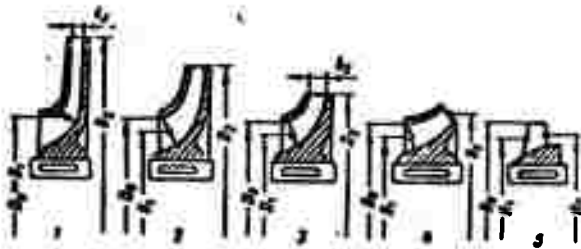


Fig. 168. Variations on the impeller.

Typical wheel designs corresponding to these pump varieties are represented in Fig. 168.

The first three pump varieties - slow, normal, and fast - are classed as centrifugal, but the last two - diagonal and screw-impeller - do not belong to this class. However, there are no sharp boundaries between these pump varieties; with increasing  $n_s$ , we have a gradual transition from the purely centrifugal wheel type to the diagonal and purely axial types.

#### §60. RELATION BETWEEN SPEED COEFFICIENT AND PUMP EFFICIENCY

Transition from one vane-pump variety to another, i.e., a change in the speed coefficient  $n_s$ , cannot but affect the efficiency of the pump. However, this influence of the coefficient  $n_s$  will be different for the hydraulic, volumetric, and mechanical efficiencies.

Research has shown [17] that hydraulic efficiency changes very slightly with a change in  $n_s$  and depends to a much greater

degree on the shape perfection of the flow section of the pump, its roughness, and the dimensions of the pump. As for the volumetric and mechanical efficiencies, they change very substantially as  $n_s$  approaches its lower limit.

With decreasing speed coefficient, the relative amount of power lost to friction between the lateral surfaces of the impeller (impeller disk) and the fluid increases substantially, i.e., the mechanical efficiency of the pump declines, and the amount of the flow that circulates through clearances in the pump also increases, i.e., the relative amount of leakage rises and volumetric efficiency falls off.

Thus, operation of a centrifugal pump with a small  $n_s$  entails a loss of over-all pump efficiency; this loss will be greater the smaller  $n_s$ . This fact determines the lower limit for  $n_s$ , which is dictated by economy considerations. The latter depend in turn on the specifics of the particular aircraft on which the pump is to be installed.

To permit judgments as to the minimum acceptable speed coefficient  $n_s$  and to facilitate numerical evaluation of pump efficiency for various  $n_s$ , we present working formulas for the relative energy losses in the pump and the corresponding efficiencies as functions of  $n_s$ .

Let us first examine the relative amount of flow that circulates through the packing clearance and find an expression for pump volumetric efficiency.

Flow through the packing clearance (leakage) can be expressed by the usual outflow formula:

$$q = \mu S \sqrt{2gH_{up}}$$

where  $S$  is the area of the gap, which equals (for the case of a one-sided packing)

$$S = \pi D_{up} \delta;$$

$D_{up}$  is the packing diameter;  $\delta$  is the clearance, which we shall assume proportional to the diameter  $D_{up}$ , i.e.,

$$\delta = \frac{D_{up}}{m};$$

$\mu$  is the flow rate coefficient for outflow through the gap, which equals  $\mu = 0.4-0.5$  for ordinary packings and 0.3 for special labyrinth packings;  $H_{up}$  is the head under which fluid flows out through the gap.

The quantity  $H_{up}$  can be found as the difference between the piezometric heights developed by the impeller (i.e., the head  $H_p$  for a finite number of vanes with consideration of hydraulic losses) minus the pressure drop in the space between the impeller and the casing due to rotation of the fluid. Since one of the walls of this space is stationary and the other moving, it is usually assumed that the fluid is in rotation at a speed equal to half the impeller speed.

Using Formula (3.3) for the pressure in the fluid at relative rest, we have with consideration of the above

$$H_{yn} = \mu \eta_p H_p - \frac{\omega^2}{32g} (D_s^2 - D_{yn}^2).$$

The head  $H_{up}$  can be assumed approximately proportional to the head developed by the pump and expressed as follows:

$$H_{yn} = k_{up} H_p.$$

where  $k_{up} = 0.6-0.85$ .

The packing diameter  $D_{up}$  is approximately equal to the entry diameter  $D_0$ , which, as will be shown in the next section, should be set equal for design purposes to

$$D_1 = k_0 \sqrt[3]{\frac{Q}{n}}.$$

where the coefficient  $k_0 = 4.2-4.5$ .

Substituting the above values into the equation for leakage, we find the ratio of this leakage to the useful flow rate as a function of the speed coefficient  $n_s$ :

$$\frac{q}{Q} = \frac{\mu \pi D_{yn}^2 \sqrt{2gk_{yn}H}}{mQ} = \frac{\mu \pi k_0^2 \sqrt{2gk_{yn}}}{m} \frac{H^{1.2}}{Q^{1.2} n^{0.2}}.$$

Using Expression (12.38) for the speed coefficient, we obtain

$$\frac{q}{Q} = A_1 \frac{1}{\left(\frac{n \sqrt{Q}}{H^{3/4}}\right)^{2/3}} = A_1 \frac{3.65^{2/3}}{n_s^{2/3}} = \frac{A}{n_s^{2/3}},$$

where

$$A = \frac{\mu \pi k_0^2 \sqrt{2gk_{yn}} \cdot 3.65^{2/3}}{m}.$$

For  $m = 300$ ,  $\mu = 0.5$ ,  $K_{up} = 0.8$ , and  $k_0 = 4.5$ , the constant  $A$  is found to equal  $A \approx 1.0$ . A curve of the leakage ratio  $q/Q$  through a one-way packing as a function of the speed coefficient  $n_s$  has

been plotted in Fig. 169 for this value of A. The diagram clearly shows the increase in the importance of leakage with decreasing pump speed. For two-way packing, A would be twice as large.

Pump volumetric efficiency can be expressed in terms of the speed coefficient by the following formula:

$$\eta_v = \frac{Q}{Q + q} = \frac{1}{1 + \frac{q}{Q}} = \frac{1}{1 + \frac{A}{n^2}} \quad (12.40)$$

Figure 169 also shows a curve of the volumetric efficiency  $\eta_v$ .

Friction between the impeller disk and the fluid usually occurs in turbulent flow, so that the tangential stress  $\tau$ , as in the case of turbulent flow in pipes, can be regarded as proportional to the product of fluid specific weight by the velocity head. In this case, the latter must be expressed in terms of the impeller's circumferential velocity, which varies in proportion to radius; thus, we have

$$\tau = c_f \gamma \frac{u^2}{2g}$$

where  $c_f$  is a dimensionless proportionality coefficient known as the coefficient of friction.

The power lost to friction between the impeller disk and the fluid can be computed by integrating the expression for the elementary frictional moment multiplied by the impeller angular velocity, i.e.,

$$N'_{fp} = k\omega \int_0^{D/2} \tau r dS,$$

where  $dS$  is an elementary area equal to

$$dS = 2\pi r dr;$$

$r$  is the radius in question and  $k$  is a coefficient that takes account of the fraction of total impeller disk area that is subject to friction; usually,  $1 < k < 2$ .

Substituting the earlier expression for  $\tau$ , remembering that  $u = \omega r$ , and assuming, in first approximation, that the turbulent-flow coefficient of friction  $c_f$  is constant over the entire disk area, we can perform integration in the form

$$N'_{fp} = C_1 \gamma \omega^3 \int_0^{D/2} r^4 dr = C_2 \gamma \omega^3 D^5$$

or

$$N'_{fp} = C \gamma u_2^3 D^2,$$

where  $C$  is a constant that incorporates the numerical coefficients,  $k$ ,  $c_f$ , and the other constants.

Research has shown that the constant  $C$  can be assumed equal to  $C = 1.2 \cdot 10^{-8}$  in the engineering system of units for approximate calculations in the case of highly finished surfaces; the power  $N_{tr}$  will then be obtained in horsepower.

Let us find the ratio of the friction power to the hydraulic power of the pump (see §57):

$$\frac{N'_{fp}}{N_r} = \frac{C_1 n_2^3 D^3}{Q \sqrt{H}} 75 \eta_0 \eta_r.$$

We express the impeller diameter  $D$  in terms of the circumferential velocity  $u_2$  and the speed  $n$  and the circumferential velocity in terms of head with the aid of the following relationships:

$$u_2 = \frac{\pi D n}{60} \quad \text{and} \quad H = k_1 \frac{u_2^2}{2g}.$$

from which

$$D = \frac{60 u_2}{\pi n} = \frac{60}{\pi n} \sqrt{\frac{1}{k_1} 2gH}.$$

Substituting the previous expression into the basic equation

$$\frac{N'_{fp}}{N_r} = 75 \left(\frac{60}{\pi}\right)^3 C \left(\frac{2g}{k_1}\right)^{3/2} \frac{H^{3/2}}{Q n^2}$$

or, introducing the speed coefficient  $n_s$  and using the expression found above for  $\eta_0$  in terms of  $n_s$ :

$$\frac{N'_{fp}}{N_r} = \frac{B}{n_s^3} \frac{1}{1 + \frac{A}{n_s^2}} \quad (12.41)$$

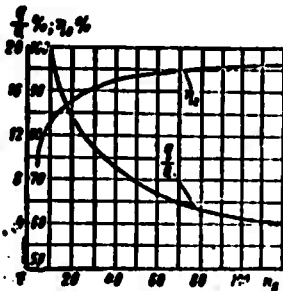


Fig. 169. Diagram of  $\eta_0$  and  $q/Q$  as functions of  $n_s$ .

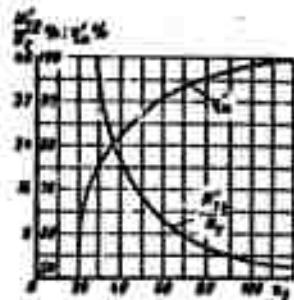


Fig. 170. Diagram of  $\eta_m$  and  $N'_{fp}/N_r$  as functions of  $n_s$ .

where  $n = 3,652.75 \cdot C \left(\frac{60}{\pi}\right)^2 \cdot \left(\frac{2g}{k_1}\right)^{3/2} \eta_r$ ; for  $k_1 = 1.2$ , we have  $\eta_g = 0.80$ ,  $C = 1.2 \cdot 10^{-6}$ , and  $B = 377$ .

The curve of  $N'_{tr}/N_g$  as a function of  $n_s$  for the value found for B and for  $A \approx 1.0$  appears in Fig. 170, from which we see how significantly the relative power losses due to friction between the impeller disk and the fluid increase with decreasing  $n_s$ .

To convert from  $N'_{tr}/N_g$  to pump mechanical efficiency, we regard the latter conventionally as the product

$$\eta_m = \eta'_m \eta''_m,$$

where  $\eta'_m$  is the efficiency with consideration of power losses to friction between the impeller disk and the fluid and therefore equals

$$\eta'_m = \frac{N_r}{N_r + N'_{tr}} = \frac{1}{1 + \frac{N'_{tr}}{N_r}}; \quad (12.42)$$

$\eta''_m$  is the efficiency with consideration of the power lost to friction in the packings and bearings and equals

$$\eta''_m = \frac{N_0 - N'_{tr}}{N_0} = \frac{N_r + N'_{tr}}{N_0}.$$

In the last expression,  $N'_{tr}$  is the power lost to friction in the packings and bearings and  $N_0$  is the total power drawn by the pump, which equals the sum

$$N_0 = N_r + N'_{tr} + N''_{tr}.$$

Using the relation obtained above for  $N'_{tr}/N_0$  as a function of the coefficient  $n_s$ , we can plot a curve of  $\eta'_m$  as a function of  $n_s$  for the above values of the constants A and B. The coefficient  $\eta'_m$  can be regarded as independent of  $n_s$  and equal, for example, to 0.95.

A curve showing the decrease in the coefficient  $\eta''_m$  with decreasing  $n_s$  also appears in Fig. 170.

It should be remembered that when the slots leading from the space between the impeller and the stationary walls to the scroll chamber is reasonably dimensioned (of the order of 3% of the wheel diameter on either side), some of the energy lost to friction between the impeller disk and the fluid can be recovered by utilizing the kinetic energy of the fluid picked up by the disk. Thus, the actual mechanical efficiency may be somewhat higher than the calculated figure.

In using the above curves of  $q/Q$ ,  $N'_{tr}/N_g$ ,  $\eta_o$ , and  $\eta'_m$  vs.  $n_s$ , it is necessary to remember that they are approximate. To obtain more accurate values for these quantities, it is necessary to recompute the constants A and B each time for the specific data.

No analytical expression can be given for the sum of the hydraulic losses in the pump or, consequently, for  $\eta_g$ , since this quantity depends on a whole series of factors whose influence has not yet been adequately studied. For high-head (slow-running) impellers, the hydraulic efficiencies vary from 0.70 to 0.90, with the lower limit pertaining to small  $n_s$  and small impeller dimensions, of the order of  $D = 100-200$  mm, while the upper limit corresponds to  $n_s = 90-120$  and  $D = 500-600$  mm.

#### §61. CALCULATIONS FOR PUMP SCROLL CHAMBER

The scroll chamber of a centrifugal pump is a unit that receives the fluid thrown off by the impeller and directs it into the pressure line.

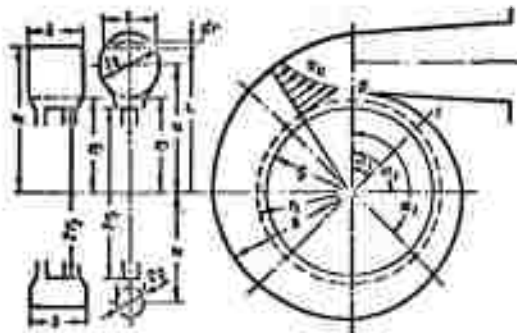


Fig. 171. Diagram of scroll chamber.

Calculation and design of the chamber are based on the assumption that the circumferential velocity component in the spiral varies in inverse proportion to radius (law of velocity distribution over cross section of vortex, or law of conservation of angular momentum), so that with a finite number of vanes we have

$$v'_c = \frac{\Gamma}{2\pi r},$$

where  $\Gamma$ , the so-called circulation through the closed contour including the wheel, is a constant for a given chamber and a given pump operating mode.

With increasing radius, the velocity  $v_u$  diminishes, and the pressure rises accordingly. Consequently, a process of conversion of fluid kinetic energy into pressure energy begins with flow in the scroll and continues in the diffuser that is usually connected to the scroll (Fig. 171).

The circulation  $\Gamma$  can easily be found from the head  $H$  developed by the pump and from  $\eta_g$ . In fact, since according to Formula (12.16)

$$H_{1,2} = \frac{u_2^2 v_{2u}^2}{g} = \frac{\omega}{g} r_2 v_{2u}^2,$$

we have on the basis of the above

$$\Gamma = 2\pi r_2 v_{2u}^2 = 2\pi \frac{g H_{1,2}}{\omega} = 2\pi \frac{g H}{\omega \eta_g}.$$

In an arbitrary section of the scroll, the flow rate can be considered to increase in proportion to the inclination angle  $\alpha$  of the section, reckoned from the initial section of the scroll (which is also its final section), i.e.,

$$Q_\alpha = \frac{\alpha^\circ}{360} Q,$$

where  $Q$  is the pump's delivery into the line.

We have for the elementary flow rate through an elementary area of dimensions  $b \times dr$  and taken at radius  $r$  in an arbitrary cross section of the scroll

$$dQ_\alpha = b v_u^2 dr = \frac{\Gamma}{2\pi r} b dr,$$

from which

$$Q_\alpha = \frac{\alpha^\circ}{360} Q = \frac{\Gamma}{2\pi} \int_{r_1}^{r-R} \frac{b}{r} dr,$$

where  $r_1 = (1.03-1.05)r_2$  is the radius of the cylindrical surface enclosing the wheel and tangent to the cross sections through the scroll chamber.

For the simplest case, in which the scroll has a rectangular cross section of constant width ( $b = \text{const}$ ), we obtain from the above

$$\frac{\alpha^\circ}{360} = \frac{\Gamma}{2\pi Q} b \ln \frac{R}{r_1} = \frac{g H}{\omega \eta_g Q} \ln \frac{R}{r_1}.$$

Assigning a series of values from 0 to  $360^\circ$  to the angle  $\alpha$ , at, for example,  $45^\circ$  intervals, we obtain a series of  $R$ -values ranging from  $r_1$  to  $R_{\text{max}}$ , i.e., we obtain a trace of the scroll.

For a scroll with a circular cross section of variable radius  $\rho$ ,

$$b = 2\sqrt{a^2 - (r-a)^2}$$

( $a$  is the distance from the center of the cross section to the wheel axis) and, consequently,

$$Q_a = \frac{\Gamma}{\pi} \int_{a-\rho}^{a+\rho} \frac{\sqrt{a^2 - (r-a)^2}}{r} dr = \Gamma (a - \sqrt{a^2 - \rho^2})$$

Substituting  $\frac{a^*}{360} Q$  for  $Q_a$  and  $r_3 + \rho$  for  $a$  in this expression, we obtain after solving for  $\rho$

$$\rho = \frac{a^*}{360k} + \sqrt{\frac{2}{k} \frac{a^*}{360} r_3} \quad (12.43)$$

where

$$k = \frac{\Gamma}{Q} = \frac{2\pi g H}{\omega \eta_r Q}$$

This formula enables us to make a complete calculation of the dimensions and outlines of a round-section scroll chamber. Numerical integration is necessary for arbitrary cross-sectional shapes.

## §62. CAVITATION CALCULATIONS FOR CENTRIFUGAL PUMPS (METHOD OF S.S. RUDNEV)

Any centrifugal pump or any other type of pump will perform normally only if the absolute pressure at its intake is not too low. Otherwise, cavitation will arise in the intake section of the pump or, more precisely, where the fluid enters the between-vanes spaces of the impeller, where the absolute pressure is lowest (see §23).

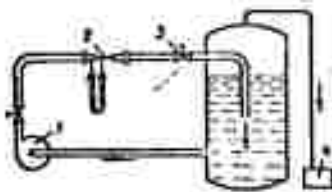


Fig. 172. Diagram of pump-testing apparatus. 1) test pump; 2) flowmeter; 3) choke; 4) vacuum pump.

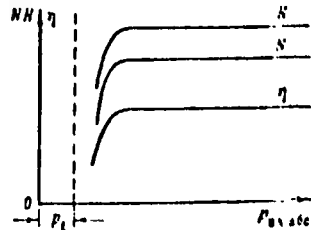


Fig. 173. Cavitation characteristic of pump.

When a pump is operated with cavitation, continuity of the flow is disrupted by the release of vapor and dissolved gases;

water hammer on condensation of vapor bubbles produces a characteristic noise, and the delivery, head, and efficiency of the pump decline. The severity of these phenomena increases with decreasing absolute pressure before the impeller intake, as is evident from the so-called cavitation characteristic of the centrifugal pump. The latter is a diagram of the head, power, and efficiency of the pump as functions of the absolute fluid pressure before the impeller intake. Characteristics of this kind are usually obtained as a result of special tests in which the pump speed and flow rate are held constant (by throttling with a valve or spool); during the test, the absolute pressure before the impeller intake is gradually lowered, for example, by evacuating air from the tank.<sup>4</sup> Figure 172 shows a diagram of an apparatus for this test. The pump head, power, and efficiency remain constant at first (Fig. 173), and then, when the pressure has been lowered substantially, the characteristic noise is heard and these quantities drop off sharply owing to the onset and steady increase of cavitation in the entry section of the pump.

An increase in the speed of the pump and the fluid flow rate (delivery) increases velocities and lowers absolute pressure at the entrance onto the vanes of the pump and, consequently, contributes to cavitation in the pump. It is therefore sometimes necessary to limit pump flow rate and speed to prevent cavitation.

Below we examine the flow of fluid at the entry into the impeller, determine the entrance diameter of the impeller from cavitation conditions, and derive a cavitation criterion by the method of Prof. S.S. Rudnev.

Let the fluid's velocity be  $v_{vkh}$  and the absolute pressure  $p_{vkh}$  directly before the entrance into the pump; then the fluid's specific energy at the pump intake will equal

$$H_{bx} = \frac{p_{bx}}{\gamma} + \frac{v_{bx}^2}{2g}.$$

As the fluid advances onto the impeller vanes, there is a further pressure drop proportional to the velocity head calculated from the relative entrance velocity, but cavitation will not occur until the absolute pressure of the fluid exceeds its saturation vapor pressure at the given temperature.

Thus, the condition for prevention of cavitation in the pump can be expressed by the following inequality:

$$H_{bx} = \frac{p_{bx}}{\gamma} + \frac{v_{bx}^2}{2g} > h_1 + \frac{v_1^2}{2g} + \lambda \frac{w_1^2}{2g},$$

where  $v_1$  is the absolute velocity at which the fluid enters onto the vane, and is approximately equal to the velocity  $v_0$  of entry into the impeller;  $w_1$  is the relative velocity at which the fluid

<sup>4</sup>See page 290 for footnote.

enters onto a vane;  $h_t$  is the saturation vapor pressured divided by  $\gamma$ , i.e.,

$$h_t = \frac{p_t}{\gamma};$$

$\lambda$  is a coefficient that depends on vane shape and on the fluid-flow conditions;  $\lambda \frac{w_1^2}{2g}$  is the pressure decrease as the fluid moves onto the vane.

The same inequality can be written

$$H_{\text{ex}} - h_t > \frac{v_1^2}{2g} + \lambda \frac{w_1^2}{2g}.$$

The left side of the inequality represents the available fluid specific energy at entry into the pump, which may, at the limit, equal the right side. This equality will correspond to the onset of cavitation, so that we shall call the difference  $H_{\text{vkh}} - h_t$  the critical difference if it is equal to the right member, i.e.,

$$(H_{\text{ex}} - h_t)_{\text{kp}} = \frac{v_1^2}{2g} + \lambda \frac{w_1^2}{2g}.$$

Since normally  $w_1^2 = v_1^2 + u_1^2$ , we have

$$(H_{\text{ex}} - h_t)_{\text{kp}} = (1 + \lambda) \frac{v_1^2}{2g} + \lambda \frac{u_1^2}{2g}.$$

It is helpful to have  $(H_{\text{vkh}} - h_t)_{\text{kr}}$  as small as possible, since the smaller  $(H_{\text{vkh}} - h_t)_{\text{kr}}$ , the greater will be the pump's stability as regards cavitation. As we see from the above, the value of  $(H_{\text{vkh}} - h_t)_{\text{kr}}$  depends on the velocities  $v_1$  and  $u_1$ , which depend, in turn, for given  $Q$  and  $n$ , on the diameter  $D_1$ , which is approximately equal to  $D_0$  (see Fig. 154). This prompts the question as to how to select the entrance diameter of the impeller in order to guarantee the smallest value of  $(H_{\text{vkh}} - h_t)_{\text{kr}}$ . To find the dimension  $D_1$  that is optimal from the standpoint of cavitation, we express the velocities  $v_1$  and  $u_1$  in terms of  $D_1$  and investigate for the minimum. We have

$$(H_{\text{ex}} - h_t)_{\text{kp}} = \frac{1}{2g} \left[ (1 + \lambda) \frac{16Q^2}{\pi^2 D_1^4} + \lambda \frac{\pi^2 D_1^2 n^2}{60^2} \right].$$

Differentiating with respect to  $D_1$  and equating the derivative to zero, we obtain

$$\frac{d}{dD_1} (H_{\text{ex}} - h_t)_{\text{kp}} = -4(1 + \lambda) \frac{16Q^2}{\pi^2 D_1^5} + 2\lambda \frac{\pi^2}{60^2} D_1 n^2 = 0,$$

whence

$$D_{opt} = \sqrt[3]{\frac{4.60}{\pi^2} \sqrt{2} \sqrt[6]{\frac{1+\lambda}{\lambda}} \sqrt[3]{\frac{Q}{n}}} = 3.25 \sqrt[3]{\frac{1+\lambda}{\lambda}} \sqrt[3]{\frac{Q}{n}}.$$

Finally, we obtain the following expression for the optimum diameter:

$$D_{opt} = k_0 \sqrt[3]{\frac{Q}{n}}, \quad (12.44)$$

where the coefficient  $k_0$  varies in the range  $k_0 = 4.3-4.5$  as a function of  $\lambda$ .

For practical calculations, it is recommended that the upper limit be taken to avoid overloading the pump.

Using this expression for the optimum diameter, we find the minimum value of  $(H_{vkh} - h_t)_{kr}$ :

$$((H_{vkh} - h_t)_{kr})_{min} = \frac{D_{opt}^3}{2g} \left[ (1+\lambda) \frac{16Q^2}{\pi^2 D_{opt}^6} + \lambda \frac{\pi^2}{60^2 n^2} \right].$$

or, after substitution, rearranging, and solving

$$((H_{vkh} - h_t)_{kr})_{min} = \frac{1}{20} \sqrt[3]{\frac{\pi^2 s}{15} \sqrt{\lambda^2(1+\lambda)}} \frac{Q^{2/3} n^{4/3}}{2g} - s \frac{(Qn^2)^{2/3}}{2g}.$$

where  $s$  is a coefficient that is fully determined by  $\lambda$ ; for  $\lambda = 0.25$ ,  $s \approx 0.02$ .

Tests run on pumps indicate that this value of the coefficient  $s$  can be used in practical calculations for impellers of the conventional form. For special wheels, such as those with increased width  $b_1$ , the values of  $s$  decrease to 0.012-0.013 [18].

Thus, if the optimum inlet diameter  $D_1$  is taken, the anti-cavitation condition for the pump will be the inequality

$$H_{vkh} - h_t > s \frac{(Qn^2)^{2/3}}{2g}. \quad (12.45)$$

Thus, our coefficient  $s$  is a criterion of cavitation in the pump that enables us to carry out check calculations and calculations to determine the maximum allowable pump speed for given  $Q$  and  $H_{vkh}$  or the lowest admissible absolute pressure at the pump entrance.

The latter, as follows from the nomenclature adopted above and the above inequality, is determined from the condition

$$(h_{min})_{in} = \gamma \left( H_{vkh} - \frac{v_{2x}^2}{2g} \right) \geq \left[ s \frac{(Qn^2)^{2/3}}{2g} + h_t - \frac{v_{2x}^2}{2g} \right] \gamma.$$

The velocity head in the brackets is often neglected, since this increases the cavitation reliability of the pump, and the difference  $p_{vkh} - p_t$  is referred to as the pressure cavitation margin.

To find the maximum permissible pump speed, we solve (12.45) for  $n$ :

$$n_{max} = \left(\frac{2g}{s}\right)^{3/4} \frac{(H_{vx} - h_t)^{3/4}}{\sqrt{Q}}$$

After multiplying and dividing the right member of the equation by  $10^{3/4}$ , we obtain Prof. S.S. Rudnev's formula as it is most frequently encountered in the literature:

$$n_{max} = c_{kp} \frac{1}{\sqrt{Q}} \left(\frac{H_{vx} - h_t}{10}\right)^{3/4}, \quad (12.46)$$

where  $c_{kr}$  is a constant with the dimensions  $m^{3/4} s^{-3/2}$  and equals

$$c_{kp} = \left(\frac{2g}{s} \cdot 10\right)^{3/4};$$

$Q$  is the delivery in  $m^3/s$ , and  $H_{vkh} - h_t$  is given in meters.

Introduction of the multiplier  $10^{3/4}$  results from the fact that the formula was originally intended for pumps working on water with  $\gamma = 1000 \text{ kgf/m}^3$ , so that the pressure could be obtained in  $\text{kgf/cm}^2$  by dividing the head  $H_{vkh} - h_t$  expressed in meters by 10.

If we substitute the corresponding pressures  $p_{vkh}$  and  $p_t$  divided by the fluid specific weight  $\gamma$  for the heads  $H_{vkh}$  and  $h_t$ , Formula (12.46) can also be reduced to the form

$$n_{max} = c_{kp} \frac{1}{\sqrt{Q}} \left(\frac{p_{vx} - p_t}{\gamma}\right)^{3/4},$$

where  $Q$  is expressed in  $m^3/s$ ,  $p$  in  $\text{kgf/cm}^2$ ,  $\gamma$  in  $\text{kgf/l}$ , and  $c_{kr}$  has the same dimensions as in Formula (12.46).

This inhomogeneity in the dimensions of the quantities appearing in this last formula must be remembered and taken into consideration when it is used.

The constant  $c_{kr}$  for a given pump is known as its critical cavitation coefficient. This quantity and the dimensionless coefficient  $s$  in Formula (12.45) characterize the cavitation properties of the pump, i.e., the predisposition of the pump to cavitation when the absolute pressure at its intake decreases. The larger  $c_{kr}$  and the smaller  $s$ , the less susceptible will the pump be to cavitation; this is an advantage that becomes especially

valuable for pumps in liquid rocket engines. Conversely, the lower the value of  $c_{kr}$  and the higher  $\underline{s}$ , the greater will be the tendency of the pump to cavitation, a highly undesirable phenomenon in any pump.

The coefficients  $c_{kr}$  and  $\underline{s}$  are uniquely related by the formula given above.

The accuracy of the cavitation calculation for a centrifugal pump, i.e., that of the calculation to determine  $n_{max}$  or  $(p_{vkh})_{min}$ , is determined by correct selection of the numerical value of  $c_{kr}$  or  $\underline{s}$ .

For conventional centrifugal pumps, the coefficient  $c_{kr}$  ranges from 800 to 1200, depending on the shape of the vane entry section and the intake plumbing ( $s = 0.025-0.015$ ).

Very recent studies indicate that for special impellers with high anticavitation properties and expanded entry sections, the coefficient  $c_{kr}$  reaches values of 2000-2200 or  $s = 0.008-0.007$ .

The following measures are taken to prevent cavitation in the pumps of aircraft hydraulic systems and in liquid rocket engines:

a) the gas pressure in the tank from which fluid is drawn is increased. However, this may result in a weight penalty on the tanks, and the tank pressures are therefore held comparatively low (1-3 atm);

b) an auxiliary booster pump is inserted at the beginning of the intake pipeline. But this can be done only if power, e.g., electric power, can be supplied to the point of installation of the booster to drive it;

c) an axial or screw wheel (worm) is mounted directly in front of the main impeller and on the same shaft to raise the pressure and twist the flow. The twist results in a certain decrease in the relative velocity  $\omega_1$ , and this also improves the operating conditions of the main impeller.

This auxiliary wheel can provide full insurance against cavitation in the main impeller of the pump, but, since it has the same speed  $\underline{n}$  and passes the same flow rate  $Q$ , it may itself become a locus of cavitation. Hence the best solution will be a device in which the speed of the auxiliary wheel is lower than that of the main wheel.

#### §63. DETERMINATION OF THE ALTITUDE CAPABILITY OF AIRCRAFT FUEL SYSTEMS WITH CENTRIFUGAL BOOSTER PUMPS

In §51, in our discussion of intake pipelines, we set forth the principle on which the altitude capability of aircraft

hydraulic systems with tanks communicating with the atmosphere is determined. We also indicated an effective method of increasing the altitude capability of these systems, which consisted in installation of a booster pump at the beginning of the intake line (or directly in the tank). This method is widely used in the fuel systems of modern aircraft, with centrifugal pumps serving as the boosters. Hence determination of the altitude ability of aircraft fuel systems is closely related to the cavitation characteristics of centrifugal pumps.

Let us take a typical layout of the main part of an aircraft fuel system running from the service tank, to which fuel is supplied from other tanks, to the main high-pressure pump (see Fig. 147) and consider the method of determining the altitude capability of this system.

The excess air (gas) pressure  $\Delta p_{1zb}$  in the fuel tanks, i.e., the amount by which the absolute pressure in the tanks exceeds atmospheric pressure at the particular flight altitude  $H$ , and its dependence on  $H$  are determined by the tank-venting system. The latter may be open, semiopen, or closed.

In the open system, the excess pressure in the tanks is developed by using a velocity head, and, consequently,

$$\Delta p_{1zb} = k \rho_H \frac{V^2}{2}.$$

where  $\rho_H$  and  $V$  are the density and flight speed, respectively, at altitude  $H$ ;  $k$  is the coefficient of utilization of the velocity head, which is usually somewhat smaller than unity.

In semiopen systems, the gradient  $\Delta p_{1zb}$  is created by using velocity head and turbocompressor pressure simultaneously. This ensures a practically constant  $\Delta p_{1zb}$  irrespective of altitude.

In closed systems, the fuel tanks do not communicate with the atmosphere, and the required tank pressure is provided by turbocompressor or bottled compressed air (gas) carried by the airplane.

The booster pump is usually placed inside or at the bottom of the service tank, so that there are practically no hydraulic losses at the pump intake and the pressure  $p_{vkh}$  differs from the tank pressure only by the velocity head.

We shall assume that we know all dimensions of the system, the resistance coefficients of the components ( $\zeta$ ), the physical properties of the fuel ( $\gamma$ ,  $\nu$ ,  $p_t$ ), the excess pressure  $\Delta p_{1zb}$  in the tank, the engine's fuel consumption as a function of altitude at top speed of the airplane (Fig. 174a), and, finally, the characteristics of the booster pump.

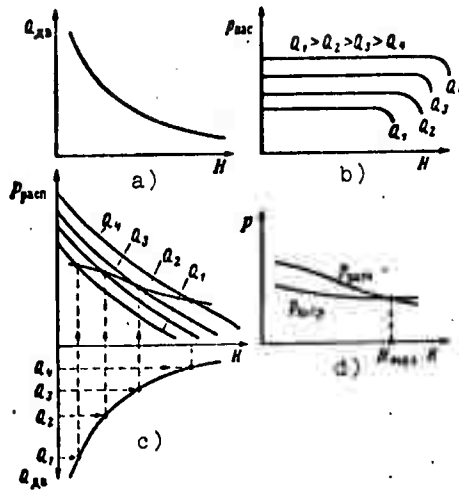


Fig. 174. Illustrating determination of altitude capability of aircraft fuel system.

It is desirable to have the cavitation characteristics of the booster pump constructed in the form of curves of the pressure (or head) developed by the pump ( $p_{nas}$ ) as a function of altitude  $H$  for various pump deliveries  $Q$  (Fig. 174b). However, special cavitation tests cannot normally be relied upon to produce such characteristics. It is easier to obtain the normal characteristic of the pump, i.e., a curve of  $p_{nas} = f(Q)$  for  $n = \text{const}$ .

This characteristic can be used to determine the pressure  $p_{nas}$  for selected deliveries  $Q$ , thereby obtaining the horizontal segments of the curves in Fig. 174b. The values of  $H$  at which these lines begin to curve, i.e., those at which cavitation begins, can be determined with S.S. Rudnev's formula (12.46), in which it is necessary to set

$$H_{max} = (p_A + \Delta p_{hst})^{-1/3}$$

Using (12.46), we determine the atmospheric pressure  $p_A$  at altitude  $H$  for each of the  $Q$ , and the altitude  $H$  from the  $p_A$ .

The pressure at the delivery end of the booster pump must be sufficient to overcome all hydraulic resistances in the main line from the booster pump to the main high-pressure pump ( $\Sigma p$ ) and the inertial pressure ( $\Delta p_{in} = \Delta H_{in} \gamma$ ) and provide a pressure  $p'_{vkh}$  at the entry into the main pump at which it can function normally

and without cavitation. The pressure  $p'_{vkh}$  is, in turn, composed of the fuel vapor pressure and the cavitation margin, the latter determined by the type of the main pump, its speed, and certain other factors.

Thus, the required absolute pressure at the booster-pump exit is

$$p_{potr} = \sum p + \Delta p_{rs} + p'_{vkh}. \quad (12.47)$$

Owing to the decrease in fuel consumption and, consequently, of  $\Sigma p$  with altitude, the pressure  $p_{potr}$  also diminishes somewhat with increasing  $H$ .

To obtain the available absolute pressure  $p_{rasp}$  at the booster output as a function of altitude  $H$ , we replot the pump characteristics given in Fig. 174b. Instead of  $p_{nas}$ , we compute

$$p_{rasp} = p_A + \Delta p_{rs} + p'_{vkh}$$

and construct curves of  $p_{rasp}$  as a function of  $H$  for the same  $Q$  (Fig. 174c). It is convenient to mark out a curve of engine fuel consumption versus altitude below these curves and, assigning a series of consumption values for which  $p_{rasp}$  curves have been constructed, to determine the corresponding altitudes  $H$ . By erecting verticals to the intersections with the corresponding  $p_{rasp}$  curves, we obtain a series of system operating points.

The curve connecting these points determines the available pressures  $p_{rasp}$  for each of the altitudes  $H$ .

If we now make a joint plot of two curves - available pressure  $p_{rasp}$  and required pressure  $p_{potr}$ , the latter calculated by Formula (12.47), as functions of flight altitude  $H$ , their point of intersection (Fig. 174d) will determine the maximum altitude at which the booster pump is capable of developing the required pressure. At lower altitudes,  $p_{rasp} > p_{potr}$  and, consequently, the necessary amount of fuel will be delivered automatically. At  $H > H_{max}$ , transfer of fuel is not guaranteed, and if the altitude  $H_{max}$  determined from the calculation is smaller than that required, measures must be taken to improve system altitude capability. This property of the fuel system should not limit the altitude capability of the vehicle as a whole. On the other hand, the altitude capability of the fuel system should be several thousand meters greater than that of the vehicle as determined by its powerplant and aerodynamic properties.

The basic ways to increase the altitude capability of fuel systems are as follows:

- 1) to increase the excess air (gas) pressure in the fuel tanks;
- 2) to install a more powerful booster pump in the service tank and booster pumps in the other tanks;
- 3) to lower the hydraulic resistance of the pipelines;
- 4) to use a fuel with a lower saturation vapor pressure;
- 5) to reduce the necessary cavitation pressure margin of the main fuel pump by lowering its speed.

However, use of any of these methods will result in greater weight of the fuel-system elements. The designer's problem is to secure the required system altitude capability with a minimal weight penalty.

#### §64. SELECTION OF PUMP TYPE. FEATURES OF CENTRIFUGAL PUMPS USED IN AVIATION AND ROCKET ENGINEERING

Pump type selection and design are usually based on  $Q$ ,  $H$ , and  $n$  as initial data. These quantities are a basis for computing the coefficient  $n_s$ , which immediately gives an idea as to which variety of vane-wheel pump is required for the specific conditions. The design procedure for the centrifugal pump is indicated in an example in this chapter.

If the  $n_s$  given by the calculation is too large (for example, greater than 1200), this means that not one, but several pumps connected in parallel must be used.

If, on the other hand,  $n_s$  is too small (see §60) and it is impossible to increase the speed  $n$ , it is necessary to use a multistage pump, i.e., one with  $z$  impellers in sequence on the same shaft. The head developed by each impeller will be one- $z$ th that of a single-stage pump, and the  $n_s$  of each impeller will be larger by a factor of  $z^{3/4}$ .

If this construction is undesirable, recourse is taken to turbulence or rotary-displacement pumps. Then, however, such properties of the fluid as viscosity, chemical activity, etc., must be taken into account.

On aircraft with gas-turbine engines, centrifugal pumps have thus far been used chiefly in fuel systems as booster pumps. Most of them are made with closed-type impellers (Fig. 175a) or semi-open impellers, i.e., impellers consisting only of a single disk with vanes on one side (see Fig. 175b);<sup>5</sup> open impellers (Fig. 175c) are used less often.

<sup>5</sup>See page 290 for footnote.



Fig. 175. Centrifugal-pump impellers.

When a booster pump is placed inside a tank, an axial wheel (vane wheel) is usually mounted on the same shaft at the entrance into the main impeller. Its function is to improve the operating conditions of the centrifugal booster pump, and to separate the fluid, i.e., to free it of vapor and gases. The axial wheel is designed for a delivery substantially larger than that of the centrifugal pump, since some of the fluid that it feeds is slung off.

Booster pumps normally operate at speeds of the order of  $(6-10) \cdot 10^3$  rev/min and develop pressures from 0.6 to 1.2 atm. The speed coefficients of these pumps vary from 100 to 200, i.e., they are classed as normal or even fast-running centrifugal pumps.

A current trend is to use centrifugal pumps as main fuel pumps on gas turbine engines. This is because the required fuel deliveries (flow rates) are increasing and less viscous fuel grades with higher volatilities are being used. At the same time, it is possible to operate the pumps at very high angular velocities (several tens of thousands of revolutions per minute).

Under these conditions, centrifugal pumps are capable of delivering the required amount of fuel under a high enough pressure at smaller bulk and weight than other pump types. These pumps have the same characteristic peculiarities as those used in liquid-rocket engines.

In LRE's, centrifugal pumps are widely used to supply fuel and oxidizer from the tanks to the engine's combustion chamber. These pumps must develop enough head to overcome all resistances in the pipelines and the combustion-chamber back pressure, as well as to ensure the necessary pressure drop across the injectors. As a result, the required head becomes quite large and is reckoned in hundreds of meters, while the pressures range into the tens of atmospheres.

Usually, displacement pumps are used to produce such high pressures, but if a substantial flow rate is required at the same time (as is the case in LRE's) and a high-rpm drive, such as a gas turbine, can be used, use of the centrifugal pump is more rational.

High pressures are obtained from a centrifugal pump by use of high impeller speeds and special impeller designs. As follows from §59, this is the construction typical of the so-called slow-running centrifugal pumps, i.e., those with the smallest speed coefficients (specific rpm  $n_s$ ).

It must be remembered that the term "slow-running" refers to a small specific rpm figure and has no relation at all to the actual (operating) pump speed, which may be very high.

Thus, the basic peculiarity of the centrifugal pumps used in LRE's is a very small value of the speed coefficient  $n_s$  with all of its consequences (see §60).

As a result, the impellers of LRE pumps are usually purely radial, i.e., of the type in which the flow moves in a plane normal to the axis of rotation. These impellers are characterized by large relative diameters  $D_2/D_1$  and small relative impeller width  $b_2/D_2$ . As we said in §60, a decrease in  $n_s$  increases the relative energy losses to fluid leakage inside the pump (volume losses) and to friction between the impeller disk and the fluid, i.e., it lowers the coefficients  $\eta_0$  and  $\eta_m'$  and, consequently, the over-all efficiency of the pump. For this reason, LRE centrifugal pumps usually have modest efficiencies.

The physical designs of LRE centrifugal-pump impellers may be of the ordinary closed type used in booster pumps, i.e., with two disks, then of the semiopen type with one disk, and, finally, of the open type without disks and with cantilevered vanes (Fig. 175). In the first two cases, the optimum backward-bent ( $\beta_2 < 90^\circ$ ) vane is used, but in the third the vanes are made radial for strength reasons. We have substantially smaller disk-friction power losses in impellers of the semiopen type and even smaller losses in the open type as compared to closed-type impellers, but the volume losses increase.

The method set forth in §60 for calculation of the friction-power ratio  $N_{tr}/N_g$  is also applicable to semiopen impellers, but with appropriate selection of the coefficient  $k$  in the formula for  $N_{tr}$ . As for determination of the volume losses in this case, this is a special problem.

Yet another peculiarity of centrifugal pumps used in LRE is the fact that they usually operate close to the cavitation point because of their high speeds. As a result, the cavitation calculation examined above acquires particular importance.

**Example.** Calculate (in first approximation) the centrifugal-pump impeller dimensions of the LRE of the V-2 rocket [28] and determine the pressure required at the entry into the pump to suppress cavitation, using the following data:

fluid pumped: ethyl alcohol (75%),  $\gamma = 864 \text{ kgf/cm}^3$ ,  $h_c = 44 \text{ mmHg}$ ;

gravimetric flow rate (pump delivery)  $G = 56 \text{ kgf/s}$ ;

pressure developed by pump  $p_{nas} = 20.7 \text{ atm}$ ;

impeller speed  $n = 3800 \text{ rev/min}$ .

**Solution.** 1. We determine the volumetric flow rate  $Q$ , the head  $H$  of the pump, and its speed coefficient  $n_s$ .

$$Q = \frac{G}{\gamma} = \frac{56}{864} = 0,065 \text{ m}^3/\text{s}; H = \frac{P_{\text{pac}}}{\gamma} = \frac{20,7 \cdot 10^4}{864} = 240 \text{ m};$$

$$n_s = 3,65 \frac{n \sqrt{Q}}{H^{3,4}} = 3,65 \frac{3800 \sqrt{0,065}}{240^{3,4}} \approx 60.$$

2. From the value of  $n_s$  and statistical data (see §60), we approximate the following quantities:

$$\frac{D_2}{D_1} = 2,5; \beta_2 = 30^\circ; \eta_0 = 0,88; \eta_{\text{st}} = 0,92; \eta_{\text{m}} = 0,97; \eta_r = 0,85;$$

from which

$$\eta = 0,88 \cdot 0,92 \cdot 0,97 \cdot 0,85 = 0,67.$$

3. The power required by the pump

$$N_0 = \frac{Q\gamma H}{75\eta} = \frac{0,065 \cdot 240 \cdot 864}{75 \cdot 0,67} = 238 \text{ hp.}$$

4. Fluid flow rate through impeller

$$Q' = \frac{Q}{\eta_0} = \frac{0,065}{0,88} = 0,074 \text{ m}^3/\text{s}.$$

5. The optimum diameter of the impeller intake orifice  $D_{\text{opt}}$  according to Formula (12.44)

$$D_{\text{opt}} = k_0 \sqrt[3]{\frac{Q'}{n}} = 4,5 \sqrt[3]{\frac{0,074}{3800}} = 0,120 \text{ m}.$$

The result is the so-called reduced diameter without consideration of flow displacement by the impeller hub. When the latter is taken into account, the area equality gives a somewhat larger diameter  $D_0$ , i.e.,

$$D_0 = \sqrt{D_{\text{opt}}^2 + d_{\text{vt}}^2},$$

where  $d_{\text{vt}}$  is the hub diameter, which equals  $d_{\text{vt}} = (1.15-1.25)d_v$  and  $d_v$  is the diameter of the shaft, which is determined by strength considerations. Without carrying out the strength calculation for the shaft here, let us assume that  $D_0 \approx 140 \text{ mm}$ . The diameter  $D_1$  will be equal to or slightly smaller than  $D_0$  owing to the inclination of the vane entry edge.

6. Setting the radial velocity ratio  $v_{2r}/v_{1r}$  equal to 1.0 and  $v_0 \approx v_{1r}$ , we obtain

$$v_{2r} = v_0 = \frac{4Q}{\pi D_{\text{opt}}^2} = \frac{4 \cdot 0,074}{\pi \cdot 0,12^2} = 6,5 \text{ m/s}.$$

7. The influence coefficient of the number of vanes is found by Formula (12.19) by setting (tentatively)  $z = 7$ :

$$\frac{1}{\mu} = 1 + \frac{2(0,6 + 0,6 \cdot 0,5)}{7(1 - 0,16)} = 1,30,$$

from which  $\mu = 0,77$ .

8. According to Formula (12.21'), the theoretical head for  $z = \infty$  is

$$H_{z=\infty} = \frac{H}{\mu \eta_r} = \frac{240}{0,77 \cdot 0,85} = 367 \text{ m.}$$

9. Substituting  $v_{2r}$  for the ratio  $Q/2\pi r_2 b_2$  in (12.12) and solving it as a quadratic equation, we get

$$v_{2r} = \frac{v_{2r}}{2 \lg \beta_2} + \sqrt{\frac{v_{2r}^2}{4 \lg^2 \beta_2} + g H_{z=\infty}} = \frac{6,5}{2 \cdot 0,578} + \sqrt{\frac{6,5^2}{4 \cdot 0,578^2} + 9,81 \cdot 367} = 65,5 \text{ m/s,}$$

from which

$$D_2 = \frac{60 u_2}{\pi n} = \frac{60 \cdot 65,5}{\pi \cdot 2800} = 0,33 \text{ m.}$$

10. The width of the impeller passage at the exit, with consideration of the coefficient of flow displacement by the vanes, which we assume equal to  $\psi_2 = 0,95$ , is

$$b_2 = \frac{Q'}{\pi D_2 v_{2r} \psi_2} = \frac{0,074}{\pi \cdot 0,33 \cdot 65,5 \cdot 0,95} = 0,012 \text{ m} = 12 \text{ mm.}$$

11. The width of the impeller channel at the entry (with  $\psi_1 = 0,85$ )

$$b_1 = \frac{Q'}{\pi D_1 v_{1r} \psi_1} = \frac{0,074}{\pi \cdot 0,14 \cdot 65,5 \cdot 0,85} = 0,03 \text{ m} = 30 \text{ mm.}$$

12. The inclination angle of the vane at the entry, on the basis of nonseparating flow of fluid over the entry edge of the vane, is

$$\beta_1 = \arctg \frac{v_{1r}}{u_1} = \arctg \frac{6,5 \cdot 370}{65,5 \cdot 140} = \arctg 0,23 = 13^\circ.$$

Usually, the calculated angle  $\beta_1$  is increased by  $3-5^\circ$  for cavitation reasons in the event of a flow rate overload.

13. This is followed by improvement of the impeller dimensions, i.e., the calculation is repeated in the same procedure, but on the basis of the values finally selected for  $\beta_2$  and  $\underline{z}$  and the more accurate values of the coefficients  $\eta$ ,  $\mu$ ,  $\psi_1$  and  $\psi_2$ . The latter are figured by the formulas

$$\psi_1 = 1 - \frac{z \delta}{\pi D_1 \sin \beta_1}$$

and

$$\zeta_2 = 1 - \frac{\delta^3}{\pi D_2 \sin \beta_2}$$

where  $\delta$  is the thickness of the vane.

14. The dimension of the final scroll-chamber section (radius  $\rho$ ) is, according to Formula (12.43) for  $\alpha = 360^\circ$  (taking  $r_3 = 1.05$ ,  $r_2 = 173$  mm)

$$\begin{aligned} Q_{360} = \frac{1}{k} + \sqrt{\frac{2}{k} r_3} = \frac{\omega \eta_r Q}{2\pi g H} + \sqrt{\frac{2\omega \eta_r Q}{2\pi g H} r_3} = \frac{398 \cdot 0,85 \cdot 0,065}{2\pi \cdot 9,81 \cdot 240} + \\ + \sqrt{\frac{398 \cdot 0,85 \cdot 0,065}{\pi \cdot 9,81 \cdot 240} 0,173} = 0,023 \text{ m.} \end{aligned}$$

15. The required head at the entrance into the impeller according to Formula (12.45):

$$H_{ax} = h_t + s \frac{(Qn^2)^2}{2g} = 0,011 \frac{13600}{861} + 0,02 \frac{(0,065 \cdot 3,82 \cdot 10^5)^2}{19,6} = 10,5 \text{ m}$$

or, neglecting the velocity head,

$$P_{ax} = 10,5 \cdot 891 \cdot 10^{-4} = 0,91 \frac{\text{kgf}}{\text{cm}^2}$$

## §65. BASIC INFORMATION ON TURBULENCE PUMPS

The turbulence pump is superficially similar to the centrifugal pump - it consists of an impeller 1 with short radial vanes and a stationary casing 2, which is fitted with intake 3 and delivery 4 pipes (Fig. 176). In the turbulence pump, the intake and delivery pipes are not hermetically separated, i.e., like all vane pumps, it is a continuous-flow type.

In operating principle, however, turbulence pumps differ substantially from both impeller and displacement pumps, and are therefore regarded as an independent type.

In turbulence pumps, motor energy is converted into fluid-flow energy in a process of vigorous eddying and entrainment of slow fluid particles in the passage surrounding the impeller 5 by fast fluid particles in the slots of the impeller. A vapor vortex (see arrows in Fig. 176) forms in the rotating impeller, which has cells on both sides, and in the passage running around the impeller. This results in a continuous exchange of fluid particles between the cells and the passage.

Like centrifugal pumps, turbulence pumps are usually used to transfer light fluids - water, kerosene, acids, etc. Characteristically, these pumps have comparatively small deliveries and relatively high heads, 4-10 times those of centrifugal pumps at the same impeller circumferential speeds. This corresponds to speed coefficients  $n_s = 10-40$ , i.e., to the range of  $n_s$  in which the use of single-stage centrifugal pumps is difficult because of their low efficiencies and the need to use a high-speed drive.

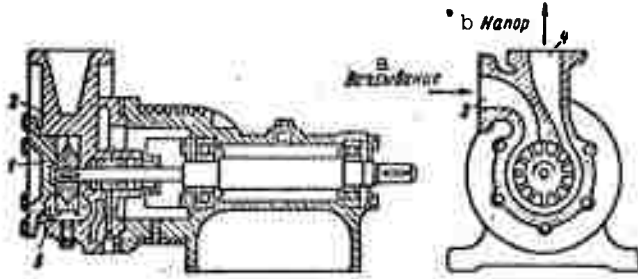


Fig. 176. Diagram of turbulence pump.  
KEY: (a) intake; (b) delivery.

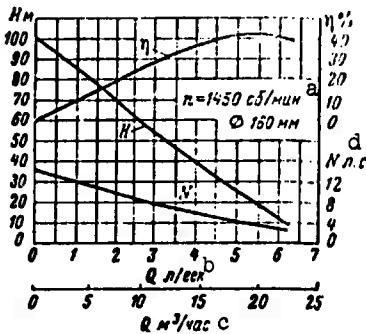


Fig. 177. Characteristics of turbulence pump.  
KEY: (a) rev/min; (b) l/s; (c) m<sup>3</sup>/h; (d) hp.

Other advantages of turbulence pumps, in addition to their high head capacities, are simplicity of design, small size, and light weight. Their basic disadvantage lies in their comparatively low efficiencies (25-50%).

Minor improvement makes the turbulence pump self-priming, i.e., enables it to produce enough vacuum in the airspace to raise fluid through the intake line, which was previously filled with air.

Multistage turbulence pumps are used to obtain pressures of the order of several tens of kgf/cm<sup>2</sup>. As in multistage centrifugal pumps, the fluid passes through several impellers connected in series.

Figure 177 shows an experimental characteristic for a turbulence pump with an impeller diameter of 160 mm in the form of curves of the head  $H$  in mm of water, power in hp, and pump efficiency  $\eta$  as functions of delivery  $Q$  in l/s at a constant speed  $n = 1450$  rev/min. As we see from the diagram, the characteristic of the turbulence pump differs substantially from that of the centrifugal pump. With increasing delivery, the head developed by the pump diminishes along a nearly straight line. At the same time, the required power does not increase, as it does for the centrifugal pump, but decreases. For this reason, it is recommended that the pump be started with the valve (spool) in the delivery line open.

In view of the very sharp rise in head as  $Q \rightarrow 0$ , turbulence pumps are often fitted with safety valves.

Turbulence pumps are subject to the same similarity formulas as centrifugal pumps, and pump characteristics are converted from one speed to another in the same way as was described in §58 for centrifugal pumps.

Turbulence pumps are used on aircraft fueling trucks and in a number of other fields.

### Footnotes

Manu-  
script  
page

- 248      <sup>1</sup>An exception is the case in which an auxiliary impeller or screw wheel (worm) is mounted in front of the main impeller (see below).
- 259      <sup>2</sup>In practice, equality of the coefficients  $\eta_g$  and  $\eta_0$  is sometimes violated to some degree on passage from one pump to another because of a change in the relative roughness of the flow passages, which influences  $\eta_g$  (the so-called scale effect), and also because of relatively unequal leakage-determining clearances in the pumps.
- 261      <sup>3</sup>It should be noted that  $Re$  varies to some extent along a similar-regime parabola, but research has shown that the flow regimes in centrifugal pumps are very close to self-similar, i.e., to those that are practically uninfluenced by  $Re$ . Kinematic similarity is of decisive importance in this case.
- 274      <sup>4</sup>It is also possible to obtain the cavitation characteristic with the valve or choke in a fixed position, i.e., as the pump's delivery decreases owing to cavitation.
- 282      <sup>5</sup>The peculiarities of these impellers will be discussed below.

### Symbol List

Manu- script page	Symbol		English equivalent
244	нас	nas	pump
247	т	t	theoretical
254	г	g	hydraulic
258	м	m	mechanical
263	э	e	standard
266	уп	up	packing
268	тр	tr	friction
274	вх	vkh	entry
274	абс	abs	absolute
275	кр	kr	critical
276	опт	opt	optimum
279	изб	izb	excess
280	дв	dv	engine
280	расп	rasp	available
280	ин	in	inertial
281	потр	potr	required
285	вт	vt	hub
285	в	v	shaft

## C H A P T E R   X I I I

### DISPLACEMENT PUMPS

#### §66. BASIC CONCEPTS. PISTON PUMPS

The operating principle of the displacement pump differs fundamentally from that of the vane-wheel pump.

A displacement pump is a pump in which fluid is moved by expellers that press it out of the pump's chambers.

The chamber of a displacement pump is a space that communicates by turns with the pump's receiving (intake) space during the filling stroke and with its delivery (pressure) space during the pressure stroke. A displacement pump may have one or more working chambers.

The expeller is the component of a displacement pump that directly accomplishes the work of expulsion (and sometimes also of induction). The number of expellers in a pump may be equal to or smaller than the number of chambers.

Thus, the action of a displacement pump consists in periodic delivery of definite, characteristic volumes (portions) of fluid from an intake line into a delivery line with a simultaneous rise in fluid pressure. Consequently, the delivery of a displacement pump, unlike that of a vane-wheel pump, is always more or less nonuniform, and for this reason the time-averaged delivery is usually considered.

Another peculiarity of displacement pumps is the fact that the receiving spaces are always hermetically separated from the delivery spaces. The sealing may be absolute or relative (practical). In the latter case, there is a possibility of minor fluid leakage (seepage) through the clearances in quantities that are small by comparison with the pump's delivery rate.

Finally, a third peculiarity of the displacement is their self-priming property. In principle, all displacement pumps are self-priming, i.e., they are capable in operation on air (without fluid) of developing rather good partial vacuums and drawing fluid through the intake line from a tank below the pump, provided that the geometrical intake height does not exceed a certain limit, which depends on a number of factors. In addition, the self-priming property of displacement pumps is often defeated in practice by inadequately tight sealing or inadequate speed.

The above operating principle of the displacement pump makes it possible to write a general expression for the time-averaged theoretical (geometrical) delivery per unit of time. By the theoretical or geometrical delivery of the pump, we mean the delivery of an incompressible fluid by a perfectly sealed pump, i.e., in the total absence of internal and external fluid seepage through clearances and in normal, cavitation-free operation of the pump, in which the chambers are filled with single-phase fluid.

Thus, we have for the theoretical per-second delivery of the pump

$$Q_t = \frac{Wn}{60} = \frac{wzn}{60} \text{ [m}^3\text{/s]} \quad (13.1)$$

where  $W$  is the so-called swept displacement of the pump, i.e., the volume of incompressible fluid that a perfectly sealed pump delivers in one revolution of the drive shaft in cavitation-free operation;  $w$  is the volume delivered (expelled) under the above conditions from each pump chamber during one pump-shaft revolution, or the useful chamber displacement;  $z$  is the number of chambers of the pump;  $n$  is the number of revolutions of the pump shaft per minute.

Since the theoretical delivery of a displacement pump is independent of the pressure (head) developed by the pump, the theoretical characteristic of a displacement pump in  $p, Q$ -coordinates at  $n = \text{const}$  is a straight line parallel to the axis of ordinates.

Displacement pumps fall into two basic classes - piston and rotor - depending on the nature of the expulsion process.

A piston pump is a displacement pump in which fluid is displaced from stationary chambers as a result of pure straight-line reciprocating motion of the expelling components relative to these chambers.

Thus, the piston pump is characterized by stationary chambers and straight-line reciprocating absolute motion of the expellers.

The class of piston pumps includes, in addition to piston pumps proper, plunger pumps, diaphragm pumps, and certain other types with the same kind of expulsion process and differing only in design or in the form of the expellers.

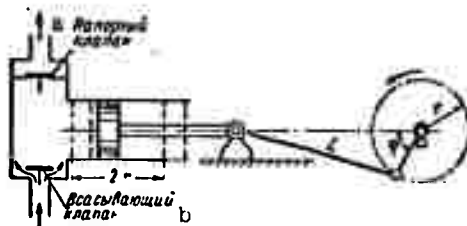


Fig. 178. Diagram of single-action piston pump.  
KEY: (a) delivery valve; (b) intake valve.

The expellers (piston, plunger, etc.) are most frequently set in reciprocating motion by means of a crank mechanism, but other mechanisms are also used (cam and eccentric mechanisms, etc.).

Conventional piston pumps are characterized by the presence of intake and delivery valves that regulate the motion of fluid through their chambers. As the chamber fills with fluid, the intake valve is open, and the delivery valve is closed. When fluid is being expressed (delivered), and the expeller is moving in the opposite direction, the intake valve is closed and the delivery valve is open. These valves are usually self-operating, i.e., they open only under a pressure gradient and close by gravity or under spring tension.

Piston pumps are classified as single-action ( $z = 1$ ), double-action ( $z = 2$ ), triple-action ( $z = 3$ ), etc., on the basis of the number of chambers.

Figure 178 shows a schematic diagram of a single-action piston pump, and Fig. 179 that of a double-action pump.

If we assume that the length of connecting rod  $L$  is infinite by comparison with the crank arm  $r$ , it follows that the speed of piston motion varies sinusoidally as a function of crank turn angle  $\phi$  or of time. The deliveries of the pumps shown in the diagrams will vary according to the same law and, consequently, so will the fluid flow rates in the intake and delivery pipelines.

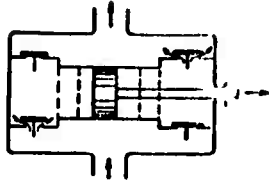


Fig. 179. Diagram of double-action piston pump.

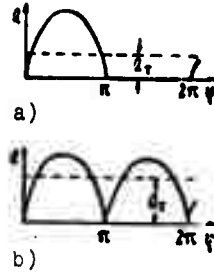


Fig. 180. Diagrams showing variation of piston-pump delivery.

Figure 180 shows curves of delivery  $Q$  vs. turn angle  $\phi$ : curve a for a single-action pump and curve b for a double-action pump. In the single-action pump, delivery occurs only during a half-turn of the crank; induction takes place during the other half-turn, while delivery is zero, i.e., delivery is extremely nonuniform.

For the double-action pump, the delivery during one revolution is represented by two sinusoids with different amplitudes (the second is smaller than the first because of the rod area), and delivery drops twice to zero and twice reaches a maximum. The delivery is not as nonuniform as in the preceding case, but it is still quite uneven.

The detrimental effect of delivery nonuniformity on pump operation consists primarily in the fact that, owing to the nonsteady flow in the pipelines, the fluid pressure at the piston varies greatly over its stroke. During the accelerating motion of the piston and the fluid in the intake line, the pressure at the piston drops further, giving rise to an inertial head (see §45), and cavitation and even complete detachment of the fluid from the piston are possible.

Moreover, the strong delivery nonuniformity makes it necessary to use additional power for the periodic increase in head loss to fluid friction in the intake and delivery lines.

To mitigate these undesirable effects, single- and double-action piston pumps are equipped with air bells. These air-filled tanks are mounted in the immediate vicinity of the pump - one at the end of the intake pipeline and the other at the beginning of the delivery line. The air bells function as quick-action accumulators which, given adequate volumes, can substantially improve the uniformity of delivery from the pump.

Properly manufactured piston pumps are capable of producing very high pressures, ranging into the tens, hundreds, and in some cases even thousands of atmospheres. Of all known pump types, the piston pumps are capable of producing the highest heads.

However, piston pumps can be operated only at comparatively low speeds, not above 300-500 rev/min. At higher speeds, the self-operating intake and delivery valves cannot function normally. Because of this slow-running property, piston pumps are substantially larger than centrifugal pumps designed for the same parameters (delivery and pressure). For this reason, piston pumps have been supplanted by centrifugal and rotor pumps in water-supply and other engineering branches.

Piston pumps are now used chiefly in the petroleum and chemical industries in the form of powerful mechanically driven units for the transfer of heavier fluids, and at thermal power plants to supply high-pressure steam boilers.

Piston pumps are also used in all specialized fields in which very high pressures are required.

The class of piston pumps can be broken down into two subclasses that differ in the type of motion of the driving element - direct-action and shaft types. In the former, the driving element - the piston rod - executes only reciprocating motion, while in the latter the driver is a rotating shaft.

A direct-action piston pump usually has a rod rigidly coupled to the rod of the piston-type drive engine (steam, compressed-air, or internal-combustion) and has no shaft or other rotating parts.

In the shaft-type piston pump, the rotary motion of the drive shaft is converted into reciprocating motion of the expeller by a crank or cam mechanism. As a result, shaft-type piston pumps are classified as crank and cam types.

Cam-type piston pumps with valveless fluid control bear a strong resemblance to the rotary-piston pumps that will be discussed in the next section. The classification of displacement pumps (and the terminology) given here and continued in the next section has been recommended by the USSR Academy of Sciences Committee on Scientific and Technical Terminology [36]. However, this classification is not the only one possible. We might, for example, make the primary classification of displacement pumps on the basis of another criterion - the type of motion of the driving element - into direct-action and shaft types, and then further classify the shaft types as piston and rotor.

## §67. ROTOR PUMPS; FEATURES AND VARIETIES

Rotor pumps represent the class of pumps that is now most extensively used in aviation engineering. They include rotary, gear, screw, rotary-plate, rotary-piston, rotary-plunger, and other types. All of these pumps, which differ considerably in design, have much in common in their working processes and characteristics.

Like piston pumps, rotor pumps are displacement pumps, i.e., pumps that work on the displacement principle. However, the

fluid-displacement process in rotor pumps differs essentially from the process in piston pumps.

The working process of rotor pumps is characterized, firstly, by transfer of the chambers from the receiving space of the pump to the delivery space and, secondly, by rotational or more complex (rotational and translational) absolute motion of the expellers.

Thus, we can offer the following definition of the rotor pump: it is a displacement pump in which fluid is displaced from moving chambers as a result of a rotational or compound motion of the expellers with respect to a stator.

The stator is the stationary part of the pump, its casing, and incorporates the receiving (intake) and delivery (pressure) spaces. The part of a rotor pump that is turned directly by the drive shaft is called the rotor. A rotor pump also usually has one or more expellers (see §66), which perform some type of cyclic motion relative to the rotor.

The chamber transfer in a rotor pump makes the intake and delivery valves superfluous. A characteristic feature of all rotor pumps that originates from their expulsion process is the absence of valve control of the fluid. In addition, rotor pumps lack the usual crank mechanism.

By virtue of the absence of intake and delivery valves, rotor pumps are reversible, i.e., they can work as hydraulic motors when fluid is supplied to them under pressure. This useful property of rotor pumps has been responsible for their extensive use in the so-called hydraulic transmissions (see below).

Rotor pumps are usually considerably faster-running than piston pumps, something that is also associated with the absence of valve distribution. Rotor pumps are currently being used at speeds up to 3000-5000 rev/min, and in some cases run even faster.

Rotor pumps deliver fluid much more smoothly than piston types, and this is another advantage.

The theoretical delivery of rotor pumps, like that of other displacement pumps, is determined by Formula (13.1). However, rotor pumps are further distinguished in this respect by the fact that the number of characteristic volumes  $z$  delivered in one shaft revolution is usually substantially higher than in the case of piston pumps. While  $z = 1-3$  for the latter,  $z = 4-12$  and more for rotor pumps. In addition, these characteristic volumes are delivered by a rotor pump not strictly in sequence, but with a certain amount of overlap: one volume has not yet been fully delivered before delivery of a second begins, then a third, and so forth (for greater detail, see below). This explains why rotor pumps deliver fluid more uniformly than piston pumps.

Other advantages of rotor pumps are compactness of construction, small dimensions, and light weight per unit of developed power. For modern aviation-type rotor pump and hydraulic motors used in hydraulic power systems, this specific weight is 0.2-0.3 kgf/kW, or only 10-20% of the analogous specific weight of similarly rated electrical machines.

The pressures that modern aviation rotor pumps are capable of delivering range up to 250-300 kgf/cm<sup>2</sup>, and further increases are possible and are the trend. However, such high pressures are not inherent to all rotor pumps, but to only one variety - the rotary-piston (or rotary-plunger) type, and then only when they are manufactured to very high precision. On the whole, the heads developed by rotor pumps are somewhat smaller than those of piston pumps because of the absence of valve control.

The working process of each element of a rotor pump is composed of the following three phases:

- 1) filling of the chambers by fluid;
- 2) closing of the chambers, i.e., their isolation from the receiving and delivery spaces of the pump and their transfer from the receiving space to the delivery space;
- 3) displacement of fluid from the chambers.

Below, as we discuss the basic varieties of rotor pumps, these phases of the working process and other features of the pumps will be indicated on specific diagrams.

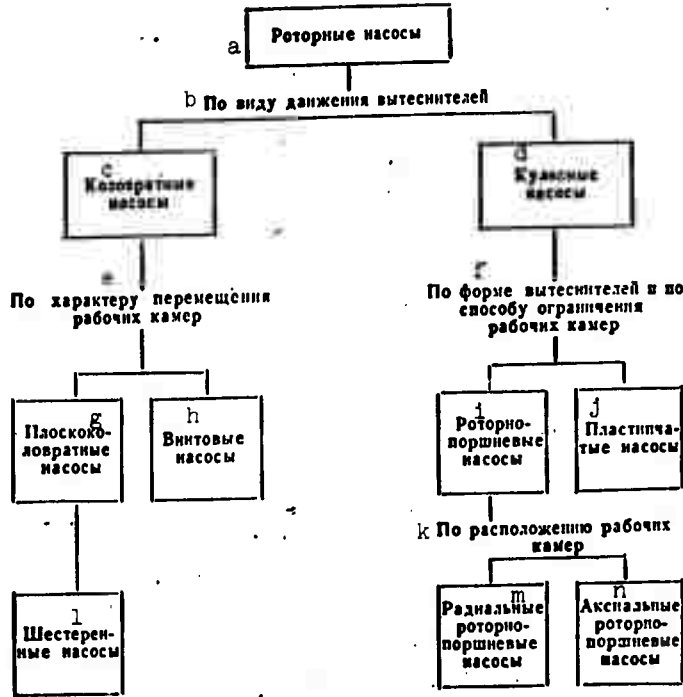
Let us examine a classification of rotor pumps (see Diagram 1).

All rotor pumps can be classified as rotary and slideblock types. In rotary pumps, the expellers execute only rotational motion with respect to their axes, and are supported in stationary bearings. In slideblock pumps, the expellers, while rotating around the stator axis, simultaneously perform straight-line reciprocating motion relative to the rotor.

According to the type of chamber transfer (type of motion of fluid displaced in the pump), rotary pumps are classified as flat-rotary and screw types. Chamber and fluid transfer occurs in a plane normal to the rotor axis in a flat rotary pump and along the rotor axis in a screw pump. The basic form of the flat-rotary pump is the well-known gear pump (Figs. 181, 182). The other varieties are seldom used and will not be examined here. The basic variety of the screw pump is the triple-screw pump (Fig. 183).

A feature of all rotary pumps is that fluid is displaced in them by the expeller and the rotor simultaneously, or only by the rotor, which is also acting as an expeller. In the latter

Diagram 1



KEY: (a) rotor pumps; (b) by type of expeller motion; (c) rotary pumps; (d) slideblock pumps; (e) by type of chamber motion; (f) by shape of expellers and by method of limiting chambers; (g) flat rotary pumps; (h) screw pumps; (i) rotary-piston pumps; (j) rotary-plate pumps; (k) by position of chambers; (l) gear pumps; (m) radial rotary-piston pumps; (n) axial rotary-piston pumps.

case, the pump must have one or more "locks," moving elements that disconnect the pump's receiving and delivery spaces without expressing fluid.

Slideblock pumps are subclassified as rotary-plate and rotary-piston types in accordance with the method used to limit (lock) the chambers and the shape of the expellers.

In the rotary-plate pump, the chambers are limited by two adjacent expellers and the rotor and stator surfaces, and the expellers take the form of plates (Figs. 184 and 185).

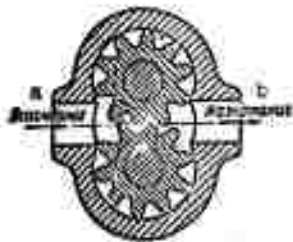


Fig. 181. Diagram of gear pumps.  
KEY: (a) intake; (b) delivery.

In the rotary-piston pump, the chambers are locked off by expellers in cylindrical hollows in the rotor, and the expellers are cylindrical (sometimes spherical) in shape (Figs. 186-189).

Rotary-piston pumps are classified as radial (Fig. 186) and axial (Figs. 187 and 189) in accordance with the positions of the chambers (cylinders) with respect to the rotor axis.

Let us examine the scheme on which each of these rotor-pump varieties operates and derive formulas for calculation of the averaged theoretical delivery. The next section will deal with the true deliveries of these pumps.

The gear pump (see Fig. 181) is usually made in the form of a pair of identical involute gears enclosed in a tight-fitting housing, the stator. The driving gear is considered to be the rotor and the driven gear the expeller. In the pump's receiving space, fluid fills the slot between the teeth of both gears, and these volumes are then locked (isolated) and transferred along circular arcs to the delivery (pressure) section of the pump.

As it meshes, each tooth on each gear fits into the slot corresponding to it and displaces the fluid from that slot. Since the volume of a slot is greater than the volume of a tooth, a certain amount of fluid returns into the intake space at the point of meshing.

Thus, both gears, i.e., the rotor and the expeller, perform the function of displacing fluid simultaneously in this pump, and its working chambers are the slots between gear teeth. However, as we see from the above, it would be more correct to consider the tooth volume rather than the slot volume as the useful chamber displacement  $w$  to be substituted into the general formula (13.1), i.e.,  $w = w_{\text{zub}}$ . The number of these volumes delivered during one pump-shaft revolution equals the total number of teeth on the two gears ( $2z$ ). Hence the averaged theoretical delivery of a gear pump per second is

$$Q_{\text{т}} = \frac{2z w_{\text{zub}} n}{60} [\text{m}^3/\text{s}]. \quad (13.2)$$

Since calculation of the volume  $w_{\text{zub}}$  requires measurement of the tooth area, recourse is usually taken to the following approximate formula, which has been derived on the assumption that the pump delivers a continuous layer of fluid with a thickness  $2h = 2m$  and width  $b$  at a speed equal to the circumferential velocity  $u$  of the gears on their pitch circles, i.e.,

$$Q_1 = uS = \frac{2\pi Rn}{60} 2hb = \frac{1}{15} \pi Rnbm \text{ [m}^3/\text{s]}, \quad (13.3)$$

where  $S$  is the cross-sectional area of the fluid layer, which equals  $2hb$ ;  $h$  is the height of the gear tooth, which is equal to its modulus  $\bar{m}$ ;  $R$  is the pitch-circle radius of the gears [meters].



Fig. 182. Diagram of internal-mesh gear pump.

Gear pumps are capable of pressures up to 100-150 kgf/cm<sup>2</sup>, and sometimes even higher. However, for pressures above 100 kgf/cm<sup>2</sup>, it is necessary to provide the pump with a device for automatic control of the face clearances on the gears. This unit consists of two floating sleeves that are pressed against the faces of the gears by fluid pressure and thereby reduce the face clearance, improving the internal seal of the pump.

Multistaged gear pumps are sometimes used to obtain very high pressures. Such a pump is built up from several gear pumps which are connected in series, and develops a pressure equal to the sum of the pressures developed by all of the stages. To ensure reliable filling, the delivery from each preceding stage of the multistage pump must be greater than the flow rate through the next stage. The excess delivery is diverted through special drainage passages provided in each stage and designed for the appropriate pressure.

Gear pumps are used extensively in aviation engineering, and especially in aircraft hydraulic power systems. However, their basic disadvantage is the impossibility of simple control of swept volume.

The internal-mesh gear pump is also used (see Fig. 182). In this pump, the driving gear (rotor) is usually the larger of the internally-toothed gears. A stationary crescent-shaped part of the pump's stator projects between it and the smaller gear (the expeller), to provide for locking of the chambers, i.e., the slots between the teeth of the gears. The motion of fluid in the pump is indicated by the arrows. Obviously, a volume of fluid equal to the volume of twice the number of driving-gear teeth is delivered during one revolution of the driving gear. This volume does not depend on the number of driven-gear teeth.

An internal-mesh gear pump delivers at a somewhat higher rate than an external-mesh pump of the same size. In addition, the internal-mesh pumps have an advantage in the symmetrical position of the drive shaft relative to the casing. However, these pumps are more complex in manufacture, and their head capacities are somewhat lower than those of the external-mesh types. This is explained by the fact that the chamber-transfer distances in these pumps are much shorter than in external-mesh pumps and, consequently, sealing is not as good.

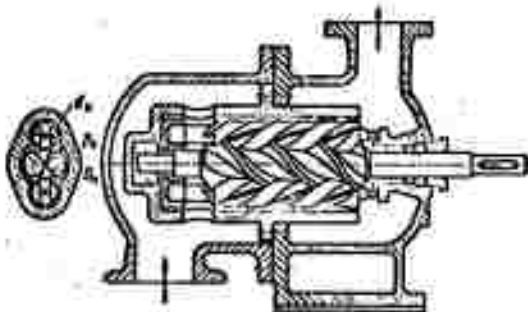


Fig. 183. Diagram of triple-screw pump.

Pumps of this type are used on some aircraft fuel trucks where high pressures are unnecessary.

A screw pump with three screws enclosed in a case with receiving and delivery spaces appears in Fig. 183. The middle screw is the driving unit, and the two lateral screws are driven. A special cycloidal screw profile is required to ensure tight locking of the chambers and, consequently, separation of the receiving and delivery spaces of the pump. This profile is convex on the driving screw and concave on the driven screws (see left diagram of Fig. 183, which shows a cross section through the screws). The screw thread is usually cut two-start. The transmission ratio from the driving to the driven screws is unity.

The working chambers in this pump are bounded by the threads of all three screws and the stator surfaces. As the screws turn, the closed chambers are transferred with the fluid along the axis of rotation.

The screws are profiled in such a way that the two driven screws are fully relieved of torque, with the driving screw taking all of it and performing the work of expulsion. It is therefore rotor and expeller at the same time. The driven screws, on the other hand, function as so-called locks - moving elements of the pump mechanism that merely separate the receiving and delivery spaces of the pump without moving fluid.

The theoretical delivery of a screw pump is determined by the expression

$$Q_t = \frac{S \pi n}{60},$$

where  $S$  is the cross-sectional area of the pump chambers normal to the axes of rotation and equals  $S = 2.4 D_v$ ;  $D_v$  is the inside diameter of the driving-screw thread, and is equal to the outside diameter of the driven screw (see Fig. 183):

$$D_s = d_s;$$

$t$  is the pitch of the screws, which usually equals  $t = (10/3)D_v$ .

Triple-screw pumps can develop pressures up to 100-200 kgf/cm<sup>2</sup>. The higher the pressure for which the pump is designed, the longer must be the chamber transfer path and, consequently, the screws.

The minimum screw length needed to provide sealing in the pump is considered to be 1.25t. In practice, this length is taken in the range (1.5-8)t, depending on the required pressure.

This pump delivers very smoothly, is capable of operating at very high speeds (up to 3000-5000 rev/min), and is quiet and dependable. However, it has the same shortcoming as the gear pump: the impossibility of adjusting swept volume during operation. In addition, the screw pump is quite complex to manufacture.

Nevertheless, the cycloidal triple-screw pump is quite promising. It is being used in a number of engineering fields, including aviation, where it is the main hydraulic power system pump on certain foreign aircraft.

Double-screw and single-screw (gyrotor) pumps are sometimes used. However, their data are usually inferior to those of triple-screw pumps with cycloidal profiles, primarily because they are not capable of maintaining good internal seals.

Rotary-plate pumps are often used in aviation in the form of four-plate units with single-plane kinematics (see Fig. 184). The rotor is a hollow cylinder with radial slots in which the expeller plates slide. The rotor is positioned eccentrically with respect to the inner cylindrical surface of the stator, which is bored round, so that as the rotor turns the plates reciprocate in and out of it. Under the action of centrifugal force, the outer faces of the plates are pressed against the stator inner surface and slide along it, while the inner faces roll around the so-called floating shaft, which has no bearings.

Fluid fills the space between two adjacent plates and the rotor and stator surfaces. This is the working chamber, whose volume increases as the rotor turns and then, after reaching a maximum, is sealed off and transferred to the delivery side of the pump. Expulsion of an amount of fluid equal to the chamber useful volume  $w$  begins simultaneously.

Let  $R$  denote the radius of the inside surface of the stator,  $e$  the eccentricity, i.e., the distance between the rotor and stator axes,  $z$  the number of plates (expellers), which equals the number of chambers in the pump,  $b$  the axial dimension of the plates, and  $\delta$  the thickness of the plates.

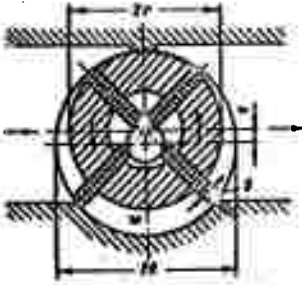


Fig. 184. Diagram of rotary-plate pump.

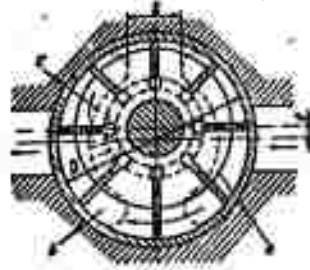


Fig. 185. Diagram of rotary-plate pump with plates operated by fluid pressure.

Then the useful chamber volume can be approximated by the formula

$$w = \left[ \frac{2\pi(R-e)}{z} - z \right] 2eb, \quad (13.4)$$

and the averaged theoretical per-second delivery according to (13.1) will be

$$Q_1 = \frac{wzn}{60} = [2\pi(R-e) - z] 2eb \frac{n}{60} \text{ [m}^3\text{/s]}.$$

Since the chamber transfer distance is reduced to a minimum in the rotary-plate pump, and the receiving and delivery spaces are separated only by the contact between the face of the plate and the stator, the pump is not particularly tightly sealed. As a result, the pressure developed by a rotary-plate pump is usually somewhat lower than the pressures put out by other rotor pumps.

Pumps built according to the diagram of Fig. 184 are used as gasoline pumps for piston aircraft engines and as fuel booster and oil pumps on some gas-turbine-engined aircraft. In these cases, pressures of only a few atmospheres are required of the pumps.

Rotary-plate pumps are used in metal-cutting machine tools and certain other machines in the form of more powerful units with up to 10-12 and more plates and with devices that improve internal sealing. This makes it possible to obtain pressures up to 70 kgf/cm<sup>2</sup> from them, and in some cases even higher pressures.

Thus, in the pump shown in Fig. 185, the pressure of the plates against the stator is increased by supplying fluid under pressure from the delivery space to the annular passage C and, consequently, to the inner ends of the plates. Fluid is supplied to the working chambers and taken from these chambers through the sausage-shaped intake and delivery ports a and b,

which are connected to the intake and delivery pipes of the pump, respectively.

In contrast to rotary (gear, screw) pumps, the principle of rotary-plate pumps permits regulation of swept volume; this is easily accomplished by changing the eccentricity, i.e., shifting the rotor relative to the stator.

By reducing the eccentricity, we can reduce the delivery of the pump at a given speed and vice versa, but this naturally requires provision of the appropriate device in the design of the pump.

Double-action rotary-plate pumps, in which each expeller (plate) performs two reciprocating motions relative to the rotor during a single rotor revolution, are also in use. In these pumps, the inside of the stator must have a special cylindrical shape instead of being round.

Rotary-piston pumps, a class that also includes rotary-plunger types, are used with both single-plane and three-dimensional kinematics.

In the former version, which is known as the radial rotary-piston (or rotary-plunger) pump, rotor 1 is positioned eccentrically in stator 3 and fitted with radial cylindrical sockets (Fig. 186). The pistons (plungers) 2, which fit into these sockets and act as expellers, reciprocate relative to the rotor as the latter turns, with their ends sliding on the inner surface of the stator. Special rollers are sometimes used instead of allowing the pistons to slip.

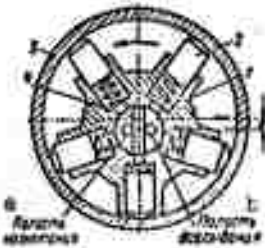


Fig. 186. Diagram of radial rotary-piston pump.

KEY: (a) delivery space; (b) intake space.

As we have noted, the chambers are bounded by expellers in cylindrical cavities (sockets) of the rotor. The chambers communicate by turns, through radial drilled passages, with the left and right halves of the central cavity, which is divided by vertical partition 4 into two chambers. The right-hand chamber in Fig. 186 is the receiving (intake) chamber, and the one on the left is the delivery (pressure) chamber; fluid proceeds from the former into the working chambers and then, after they are locked off and transferred, is displaced into the second, delivery chamber.

The chambers are locked when the radial hole reaches the partition. Consequently, each chamber is closed twice during each rotor revolution: once when its volume is greatest and again when its volume is smallest (the so-called dead space).

The useful chamber volume of this pump equals the volume displaced by each piston, i.e.,

$$w = \frac{\pi d^2}{4} 2e,$$

where  $d$  is the plunger diameter and  $e$  is the eccentricity.

The average theoretical per-second delivery for  $z$  plungers equals

$$Q_t = \frac{\pi d^2 e z n}{120} \text{ [m}^3/\text{s]}. \quad (13.5)$$

Radial rotary-piston pumps are built for pressures up to 200-300 kgf/cm<sup>2</sup>. Pumps with both constant and variable (adjustable) swept volumes are in use. In a radial rotary-piston pump, displacement is regulated in the same way as in a rotary-plate pump, by changing the eccentricity.

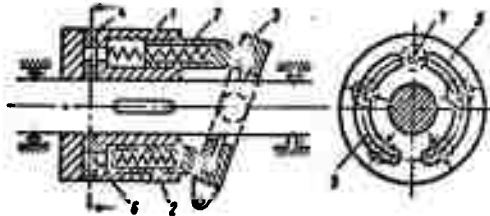


Fig. 187. Diagram of axial rotary-piston pump with inclined disk.

In axial rotary-piston pumps, the mechanism that transmits motion to the expellers (pistons, plungers) has a three-dimensional kinematics. The cylindrical chambers in the rotor are positioned parallel to its axis of rotation or at a small angle to this axis.

Axial rotary-piston pumps are made with an inclined disk or an inclined block (rotor). One of the possible arrangements for the former type is shown in Fig. 187.

The rotor 1 has sockets parallel to its axis of rotation, and the chambers are formed in these sockets. The ends of plungers 2, which are advanced out of the sockets by springs, slide (or roll) along the inclined thrust plate (disk) 3, which forces the plungers on the other semicircle back into their sockets.

This causes the plungers to reciprocate in the sockets and, consequently, to take fluid in and deliver it. The stationary part 4 of the pump, against which the end of the rotor runs, has two sausage-shaped ports 5, one of which communicates with the intake line and the other with the delivery line. As the rotor

turns, holes 6 move across ports 5 and, consequently, connect the sockets first with the intake line and then with the delivery line. When these holes reach partition 7, the chamber is locked, at maximum volume in the top position and minimum volume in the bottom position.

The inclined disk is hinged in such a way that it can be turned on an axis that intersects the rotor axis at a right angle, and this permits adjusting the disk angle  $\gamma$  to regulate the delivery.

The averaged per-second delivery of this pump is

$$Q_v = \frac{\pi d^2}{4} l z \frac{n}{60} = \frac{\pi D d^2 (z \gamma)^2}{4} \frac{n}{60} \quad (13.6)$$

where  $D$  is the diameter of the circle on which the cylinder axes lie in the rotor;  $d$  is the plunger (piston) diameter;  $z$  is the number of plungers;  $l$  is the plunger stroke.

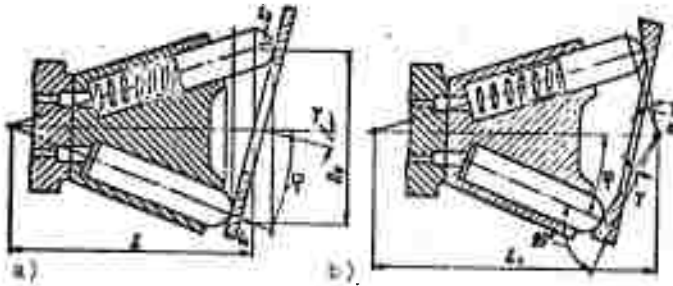


Fig. 188. Diagrams of inclined-piston rotary-piston pumps.

Quite often, the plungers of an inclined-disk pump are arranged at a certain angle  $\phi$  instead of parallel to the rotor axis (see Fig. 188). In this case, the plungers are expelled from their sockets not only by the spring forces, but also by components of the centrifugal forces that act on these plungers with rotation of the rotor; this makes it possible to use smaller springs.

With a flat inclined disk, the plunger stroke  $l$  can be determined from geometrical considerations on the assumption that each plunger contacts the disk at a point on the plunger axis (see Fig. 188a). On this basis, using the law of sines, we obtain

$$\frac{l_1}{\sin \gamma} = \frac{D_0}{2 \sin (90^\circ - \gamma + \phi)}$$

and

$$\frac{l_2}{\sin \gamma} = \frac{D_0}{2 \sin (90^\circ - \gamma - \varphi)}$$

where  $D_0$  is the diameter of the circle on which the points of contact between the plunger and the disk are situated at  $\gamma = 0$ .

Hence the plunger stroke equals

$$l = l_1 + l_2 = \frac{D_2}{2} \sin \gamma \left[ \frac{1}{\cos (\varphi - \gamma)} + \frac{1}{\cos (\varphi + \gamma)} \right],$$

and the average theoretical per-second delivery is determined by the expression

$$Q_v = \frac{\pi d^2}{4} \frac{l z n}{60} = \frac{1}{480} \pi d^2 D_0 z n \sin \gamma \left[ \frac{1}{\cos (\varphi - \gamma)} + \frac{1}{\cos (\varphi + \gamma)} \right] \quad (13.7)$$

With  $\phi = 0$ , this expression becomes Formula (13.6).

The inclined disk is often made conical in shape so that the plungers will be perpendicular to its thrust surface at  $\gamma = 0$ . For this condition, the angle at the vertex of this cone will be  $2\beta = (90^\circ - \phi)2$  (see Fig. 188b).

As above, we obtain the following expression for plunger stroke in this case:

$$l = D_0 \frac{\tan \gamma}{\cos \varphi},$$

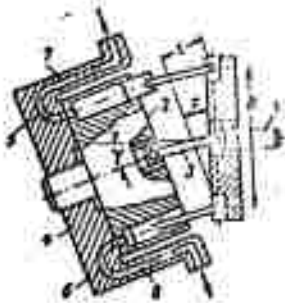


Fig. 189. Diagram of inclined-block axial rotary-piston pump.

and as the disk inclination angle  $\gamma$  is varied, the delivery of the pump will vary in proportion to  $\tan \gamma$  as in the case of the axial plunger arrangement.

Figure 189 shows a diagram of a rotary-piston pump with an inclined block (rotor). Rotation is transmitted from drive shaft 1 to rotor 2 through the universal joint 3, which makes it possible to change the angle between the shaft and rotor axes. The rotor is enclosed in a so-called cradle 4, whose base has two circular-arc grooves (intake 5 and delivery 6) similar to those in the inclined-disk pump. In the figure, the section through the cradle is conventional: in actuality, the intake and delivery passages of the pump (7 and 8) are at the sides. In an adjustable pump, this cradle can be turned to change the inclination angle  $\gamma$ . The pistons are connected to the drive-shaft disk by hinged rods.

If we disregard the angles that the axes of the piston rods form with the cylinder axes, the piston stroke is expressed, in contrast to the previous case, as follows:

$$l = D \sin \gamma,$$

where the dimension D is indicated in Fig. 189.

Inverted rotor pumps, which are sometimes used in aviation and other fields, can be regarded as rotor pumps in which the rotor has been stopped and the stator set in rotation. With this inversion, the rotary-piston pump is converted formally into a piston pump, since its chambers remain stationary and the absolute motion of the expellers becomes reciprocating. However, the design and properties of these pumps (unless valve control is used) resemble those of rotor pumps very closely. At the same time, it must be remembered that the hydraulic, dynamic, and cavitation properties of inverted rotor pumps differ to some extent from the properties of ordinary rotor pumps.

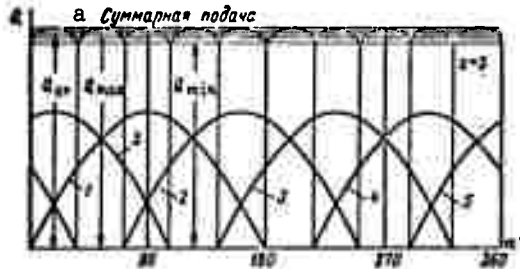


Fig. 190. Delivery diagram for five-plunger pump.  
KEY: (a) total delivery.

**Delivery nonuniformity of rotor pumps.** We stated above that rotor displacement pumps always deliver fluid with some unevenness. Investigation of the kinematics of the mechanisms used in rotary-piston pumps indicates that the relative velocity of the plungers, as in the case of the crank mechanism, can be regarded as approximately proportional to the sine of the rotor turn angle  $\phi$ . The delivery of fluid by each plunger varies as a function of angle  $\phi$  and time  $t$  in accordance with the same sinusoidal law. The total delivery of fluid by all plungers of the pump can be found by adding the ordinates of these sinusoids, as indicated in Fig. 190 for  $z = 5$  plungers.

The unevenness of delivery decreases with increasing number of expellers (plungers, pistons, or plates) in the pump. It is important to note, however, that it is much more advantageous from the standpoint of improving pump-delivery uniformity to use an odd number of expellers  $z$ .

The degree of delivery nonuniformity for odd  $z$  can be evaluated by the following approximate formula, which is due to Prof. N.S. Acherkan:

$$\sigma = \frac{Q_{\max} - Q_{\min}}{Q_{cp}} = \frac{125}{z^2} \rho_0,$$

while for even  $z$

$$\sigma = \frac{500}{z^2} \%.$$

A calculation by these formulas gives the following values for the coefficient  $\sigma$  for various  $z$ .

$z$	5	6	7	8	9	10	11	12
$\sigma$ , %	5,0	13,9	2,6	7,8	1,5	5,0	1,0	3,5

As a result, an odd number of pistons (plungers) - 5, 7, or 9 - is usually used in rotary-piston pumps.

The comparatively strong nonuniformity of delivery with an even number of expellers is explained by the fact that two chambers are locked simultaneously and the delivery of fluid from these chambers drops to zero, while only one chamber is closed at a time if  $z$  is odd.

### §68. CHARACTERISTICS OF ROTOR DISPLACEMENT PUMPS

Let us now examine the general hydraulic properties of all of the rotor displacement pumps, i.e., their characteristics. Earlier (§§51 and 55), we defined the characteristic of a pump as the curve of the head (or pressure) that it develops versus its delivery (flow rate) at constant rpm.

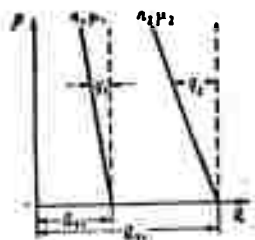


Fig. 191. Characteristics of rotor pump for  $n_1$ ,  $\mu_1$  and  $n_2$ ,  $\mu_2$ .

From Formula (13.1), which is common for all rotor displacement pumps,

$$Q_t = \frac{V n}{60}$$

it follows that the theoretical delivery of a rotor displacement pump is independent of pressure. Hence the theoretical characteristic of such a pump in the coordinates  $p$  (or  $H$ ) and  $Q$  with  $n = \text{const}$  is a straight line running parallel to the axis of ordinates all the way to infinity. The theoretical characteristics of a rotor displacement pump for two different speeds are indicated by broken lines in Fig. 191.

This means that theoretically, any displacement pump is capable of producing any desired pressure, irrespective of speed and flow rate. In practice, the situation is somewhat different, and the actual characteristic of the displacement pump differs from the theoretical due to leakage. This is because any pump has larger or smaller clearances between its moving and stationary parts, i.e., between the rotor, expellers, and stator. Under the pressure developed by the pump, a certain amount of fluid flows back through these clearances, i.e., from

the delivery zone to the intake zone. As in the case of the centrifugal pump, the amount of fluid flowing back through the clearances per unit of time is referred to as leakage and denoted by  $q$ .

Because of the small clearances in the rotor pump, fluid flow in these pumps is laminar. The quantity  $q$  is therefore directly proportional to the pressure developed by the pump and inversely proportional to the absolute viscosity of the fluid, but not to its first power; experiments have indicated that the exponent  $m$  is smaller than unity. For gear pumps,<sup>1</sup> we can set  $m = 1/2$ , but there are no reliable data for other pumps, although  $m$  must obviously be of the same order.

Thus, we have

$$q = A \frac{P_{psc}}{\mu^m}, \quad (13.8)$$

where  $A$  is a constant that depends on the design of the pump and its clearances and is indicated by experiment to be practically independent of pump speed.

That the exponent  $m$  is not equal to unity is explained by the fact that when fluid flows through gaps there are always quite substantial energy losses per unit weight of fluid; as a result, the fluid is heated in the gaps and its viscosity decreases below that of the main stream.

The actual delivery  $Q$  from the pump, i.e., the fluid flow that it delivers into the line, is smaller than the theoretical delivery  $Q_t$  by the amount of leakage; consequently,

$$Q = Q_t - q = \frac{Wn}{60} - A \frac{P_{psc}}{\mu^m} \quad (13.9)$$

or

$$Q = \eta_0 Q_t,$$

where  $\eta_0$  is the pump's volumetric efficiency.

It follows from the above that the true characteristics of the rotor displacement pump, which are indicated by the solid lines in Fig. 191, will be inclined and will intersect the theoretical characteristics at  $P_{nas} = 0$ , i.e., on the axis of abscissas, where  $q = 0$  and  $Q = Q_t$ .

The higher the viscosity of the fluid, the less seepage will there be through the clearances and the steeper will the pump characteristic become. Slight inflections of the real characteristic that are sometimes observed are explained by abnormalities of pump operation - poor filling of the chambers or cavitation.

<sup>1</sup>See page 321 for footnote.

A method of converting and replotting these characteristics from one set of pump operating conditions ( $n_1, \mu_1$ ) to another ( $n_2, \mu_2$ ) proceeds from the construction of the true characteristic of the rotor displacement pump by Formula (13.9).

First, we recompute the initial abscissas of the characteristics, i.e.,

$$\frac{Q_{t1}}{Q_{t2}} = \frac{n_1}{n_2},$$

from which

$$Q_{t2} = Q_{t1} \frac{n_2}{n_1}. \quad (13.10)$$

Then we express the leakage ratio for the different pressures, i.e., for  $p_{1nas} = p_{2nas}$ ,

$$\frac{q_1}{q_2} = \left( \frac{\mu_2}{\mu_1} \right)^m,$$

from which

$$q_2 = q_1 \left( \frac{\mu_1}{\mu_2} \right)^m. \quad (13.11)$$

Using the values found for  $Q_{t2}$  and  $q_2$ , we construct a new characteristic as shown in Fig. 191 for the case in which

$$n_2 > n_1 \text{ and } \mu_2 < \mu_1.$$

The results of tests of rotor pumps at a given  $\mu = \text{const}$  are usually represented by curves of the flow rate  $Q$  as a function of speed  $n$  for a series of constant pressures  $p_{nas}$  developed by the pump (Fig. 192). The result is a series of straight lines that are approximately parallel to one another (owing to the independence of  $q$  of  $n$ ), each corresponding to a constant  $p_{nas}$ . Here, the larger  $p_{nas}$ , the lower is the line, since the seepage  $q$  is larger.

Since the characteristic of the rotor displacement pump in  $p, Q$ -coordinates is usually very steep, a decrease in pump delivery, e.g., resulting from an increase in line resistance, causes a quite substantial pressure rise. Special devices must be provided to protect the pump and the system connected to it from excessive overpressures when delivery drops off.

One such device is the so-called overflow (bleeder) valve (Fig. 193), which opens under elevated pressure and passes part of the flow rate in the reverse direction. The pump characteristic then changes as indicated in Fig. 194a. The valve is closed on segment AB, since the pressure is moderate. Point B marks the beginning of opening; the pressure being developed by the pump is equal here to the spring force  $P_{pr}$  divided by the area  $S_{k1}$  of the valve. On segment BC, the fluid delivery into the line equals

$$Q = Q_T - Q_{un} - q,$$

where  $Q_{kl}$  is the flow rate through the valve.

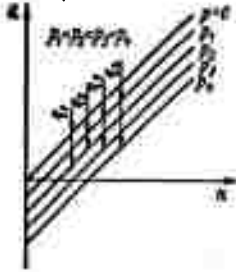


Fig. 192. Delivery of rotor pump as a function of speed.

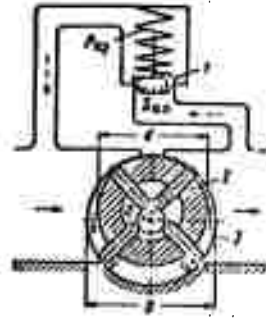


Fig. 193. Diagram of pump with adjustable valve. 1) overflow valve; 2) rotor; 3) stator.

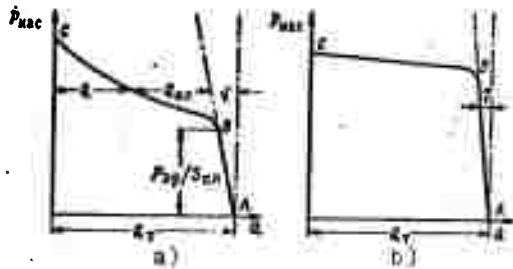


Fig. 194. Characteristic of pump with overflow valve (a) and with automatic delivery control system (b).

Point C corresponds to total closing of the line; all fluid delivered by the pump is fed back through the valve.

A device taking the form of a servomotor consisting of a cylinder, piston, and rod and operating on an adjustable pump is an improvement (Fig. 195).

When the pressure  $p_{nas}$  reaches a definite value, it acts on piston 1, compresses spring 2, and causes disk 3 to turn through a smaller angle  $\gamma$ . This reduces delivery, so that there is practically no increase in pressure. The corresponding pump characteristic appears in Fig. 194b. On segment AB, the disk is at its maximum angle. At point B, the angle  $\gamma$  begins to decrease, and at point C is it only a fraction of a degree, which is necessary to compensate seepage.

If the pressure in the pump servocylinder chamber with the spring (on the right of the piston in Fig. 195) were constant at, for example, atmospheric pressure, the slope of the pump characteristic on segment BC would be determined only by the stiffness of the spring. To obtain a flat pump characteristic, it would be necessary to use a softer spring, but one that was at the same time very strong, i.e., large.

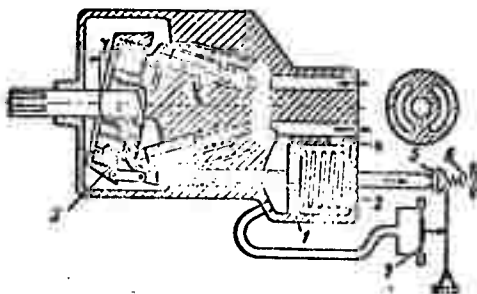


Fig. 195. Diagram of rotary-piston pump with automatic delivery control.

To reduce the dimensions of the spring and obtain the flattest possible pump characteristic on segment BC, the spring chamber of the servomechanism is opened. Fluid enters it through nozzle 4 from the pressure line and then passes under valve 5, which is loaded by spring 6 and by the force from membrane 7, which is under the delivery pressure. When the pump disk has its greatest inclination ( $\gamma_{\max}$ ), the valve is closed and the pressures on the two sides of the piston are the same and equal to the delivery pressure. The disk is held in its tilted position by the spring force and by the fluid pressure on the piston, which is directed from right to left.

When the delivery pressure rises, the valve is lifted, fluid begins to flow back, and the pressure in the servocylinder flow chamber drops. The fluid-pressure force on the piston, which now acts from left to right, compresses the spring and resets the disk at a smaller angle.

This device is used both on gas-turbine-engine fuel pumps and in aircraft hydraulic-transmission pumps.

#### §69. FUNDAMENTALS OF THE GENERAL THEORY OF ROTOR PUMPS AND HYDRAULIC MOTORS

The specifics of the previously described (see §67) fluid-displacement process in rotor pumps and the associated absence of intake and delivery valves result in clearances in the pump between the stationary and moving walls; it is in these gaps that the basic energy losses occur.

These energy losses are: (Newtonian) fluid-friction losses, dry (Coulomb) friction losses, and losses to seepage from the high-pressure space to the low-pressure space (Poiseuille losses). The remaining types of energy losses in rotor pumps (hydraulic losses in the pump channels, fluid-twisting losses in the rotor, etc.) are usually small by comparison with the basic losses and are included in the latter.

Because of the reversibility property of rotor pumps, all of the above applies equally to pumps that are converted to hydraulic motors. In the exposition to follow, therefore, we shall speak of rotor-type hydraulic machines in general, indicating, where necessary, the differences between the pump and the hydraulic motor.

The operating regime of a hydraulic machine is determined by the following three parameters: pressure gradient  $\Delta p$ , rotor angular velocity  $\omega$ , and the dynamic coefficient of viscosity  $\mu$  of the fluid.

In theoretical bookkeeping, the size of a hydraulic machine is usually evaluated by a linear quantity - a characteristic dimension equal to

$$D = \sqrt[3]{W'}$$

where  $W'$  is the so-called characteristic volume, i.e., the volume of incompressible fluid passing through the machine in the absence of leakage during a one-radian turn of the rotor.

The characteristic volume  $W'$  is connected with the swept displacement  $W$  of the machine (see §66) by the obvious relation

$$W' = \frac{1}{2\pi} W.$$

A second linear dimension that is usually introduced into consideration is the equivalent clearance  $\delta$ , i.e., the clearance in which the energy losses are equal to the corresponding losses in all clearances of a specific hydraulic machine. For complete geometric similarity of two hydraulic machines, it is necessary that the ratios  $\delta/D$  also be identical. Otherwise, the geometrical similarity between the machines will be only partial.

Assuming laminar fluid flow in the clearances, let us express the leakage in the hydraulic machine in accordance with Poiseuille's law

$$q = k_u \frac{\Delta p}{\mu} \delta^3,$$

where  $k_u$  is a proportionality factor that is the same for an entire series of geometrically similar hydraulic machines.

Multiplying the flow rate  $q$  by the pressure gradient  $\Delta p$ , we obtain an expression for the seepage power loss:

$$N_y = k_y \frac{\Delta p^2}{\mu} \delta^3 = k_y \frac{\Delta p^2}{\mu} D^3 = k_y \frac{\Delta p^2}{\mu} W, \quad (13.12)$$

where  $k_y = k'_y \left(\frac{\delta}{D}\right)^3$  is the leakage (or tightness) coefficient of the hydraulic machines.

The liquid-friction force in a hydraulic machine is proportional, according to Newton's law, to the viscosity  $\mu$  of the fluid, the area of the rubbing surfaces ( $\sim D^2$ ), and the velocity gradient ( $\sim D\omega/\delta$ ). Since the relative velocity of displacement is proportional to  $\omega D$ , the power lost to liquid friction in the machine will equal

$$N'_z = k'_z \mu D^2 \left(\frac{D\omega}{\delta}\right) (D\omega) = k_z \mu \omega^2 D^3 = k_z \mu \omega^2 W', \quad (13.13)$$

where  $w'_{zh}$  is a proportionality coefficient that is the same for an entire series of geometrically similar hydraulic machines and  $k_{zh} = k'_z D/\delta$  is the coefficient of the fluid-friction losses.

The expression for the power lost to "dry" friction can be written on the basis of Coulomb's law if it is remembered that the normal force is approximately proportional to  $\Delta p D^2$ , while the relative velocity of displacement is proportional to  $\omega D$ :

$$N_{,p} = k_{,p} \Delta p \omega D^3 = k_{,p} \Delta p \omega W'. \quad (13.14)$$

The coefficient of friction is incorporated into the proportionality factor  $k_{tr}$ , which can be assumed constant for a series of geometrically similar machines.

The power of a hydraulic machine in the absence of the above losses is known as its indicator power and expressed as follows:

$$N_i = \Delta p Q_i = M\omega = \Delta p D^3 \omega,$$

since

$$\frac{Q_i}{\omega} = \frac{M}{\Delta p} = W' = D^3.$$

Here  $M$  is the torque on the shaft of the machine at  $N_{zh} = N_{tr} = 0$  and  $Q_t$  is the flow rate at  $q = 0$ .

In actuality, the pump will delivery less than  $Q_t$  because of leakage, and the power required will be greater than  $N_i$  because of fluid and dry friction. Hence the efficiency of the pump (subscript 1) can be expressed thus:

$$\eta_1 = \frac{N_1 - N_f}{N_1 + N_m + N_{fp}} = \frac{\Delta p D^3 \omega - k_f \frac{\Delta p^2}{\rho} D^3}{\Delta p D^3 \omega + k_{mp} D^3 \omega^2 + k_{fp} \Delta p D^3 \omega}$$

After dividing the numerator and denominator by  $N_1$ , we obtain finally

$$\eta_1 = \frac{1 - \frac{k_f}{\sigma}}{1 + k_{fp} + k_{m\sigma}} = \eta_{v1} \eta_{m1} \quad (13.15)$$

where  $\sigma = \mu\omega/\Delta p$  is a dimensionless number known as the isogonality coefficient;<sup>2</sup>  $\eta_{v1}$  and  $\eta_{m1}$  are the volumetric and mechanical efficiencies of the pump, respectively, and equal

$$\eta_{v1} = 1 - \frac{k_f}{\sigma} \quad \text{and} \quad \eta_{m1} = \frac{1}{1 + k_{fp} + k_{m\sigma}}$$

The power developed by a hydraulic motor is smaller than the indicator power  $N_1$  because of dry- and fluid-friction losses, and the power that it requires exceeds  $N_1$  because of seepage, which moves in the same direction as the main flow in a hydraulic motor, in contrast to the case of the pump. Hence the motor efficiency (subscript 2) is expressed by the formula

$$\eta_2 = \frac{N_1 - N_{fp} - N_m}{N_1 + N_f} = \frac{N_1 - k_{mp} \sigma}{1 + \frac{k_f}{\sigma}} = \eta_{v2} \eta_{m2} \quad (13.16)$$

where the volumetric and mechanical efficiencies of the motor equal respectively

$$\eta_{v2} = \frac{1}{1 + \frac{k_f}{\sigma}} \quad \text{and} \quad \eta_{m2} = 1 - k_{mp} - k_{m\sigma}$$

As we see from these formulas, the efficiencies of rotor-type hydraulic machines (pumps and hydraulic motors) are uniquely expressed in terms of the isogonality factor  $\sigma$ . It can be shown that this coefficient is proportional to the ratio of the frictional flow rate, which is governed by the motion of one wall of the gap relative to the other (see §26), and the flow rate of the delivery flow created by the pressure gradient. Dividing Formula (6.15) by (6.13) and setting  $p_{tr} = \Delta p$ ,  $a = \delta$ ,  $U \sim \omega D$  and  $l \sim D$ , we have

$$\frac{Q_{fp}}{Q_{min}} \sim \frac{L^2 \mu \omega}{\delta^2 \Delta p} = \frac{\Omega^2}{\delta^2} \sigma$$

where  $\sim$  is the proportionality symbol.

<sup>2</sup>See page 321 for footnote.

Thus, the coefficient  $\sigma$  is a kinematic-similarity criterion for geometrically similar rotor-type hydraulic machines, as well as a quantity that characterizes the operating regime of a given hydraulic machine.

Figure 196 presents curves of pump (a) and motor (b) efficiencies as functions of the coefficient  $\sigma$ . As the diagrams show, the over-all efficiency curves of the pump and hydraulic motor (solid lines) have maxima at certain values of  $\sigma = \sigma^*$ .

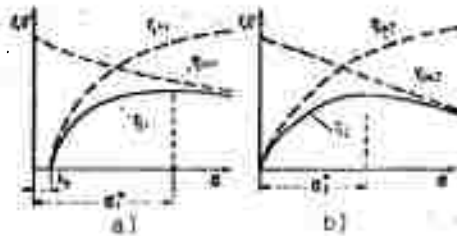


Fig. 196. Pump (a) and hydraulic-motor (b) efficiencies as functions of isogonality coefficient.

For the pump,  $\sigma^*$  is obviously found from the condition  $d\eta_1/d\sigma=0$ , which leads us to the quadratic equation

$$(\sigma_1^*)^2 - 2k_y(\sigma_1^*) - \frac{k_y}{k_x k_m}(1 + k_{tp}) = 0,$$

from which

$$\sigma_1^* = k_y \left( \sqrt{\frac{1 + k_{tp}}{k_x k_m} + 1} + 1 \right), \tag{13.17}$$

while for the motor it is found from the condition  $d\eta_2/d\sigma=0$ :

$$(\sigma_2^*)^2 + 2k_y(\sigma_2^*) - \frac{k_y}{k_x}(1 - k_{tp}) = 0,$$

from which

$$\sigma_2^* = k_y \left( \sqrt{\frac{1 - k_{tp}}{k_x k_m} + 1} - 1 \right). \tag{13.18}$$

For pumps and hydraulic motors, the quantities

$$\frac{1 + k_{tp}}{k_y k_m} \quad \text{and} \quad \frac{1 - k_{tp}}{k_y k_m}$$

are large by comparison with unity and larger the higher the efficiency of the machine. Hence Expressions (13.17) and (13.18) can be replaced by the approximate relationships

$$\sigma_1^* = \sqrt{\frac{k_y}{k_x} (1 + k_{1p})} \quad \text{and} \quad \sigma_2^* = \sqrt{\frac{k_y}{k_x} (1 - k_{1p})}. \quad (13.19)$$

Because of the flatness of the  $\eta_1$  and  $\eta_2$ -curves near the maxima, determination of  $(\eta_1)_{\max}$  and  $(\eta_2)_{\max}$  from approximate values of  $\sigma_1^*$  and  $\sigma_2^*$  gives quite high accuracy. Substituting Expressions (13.19) into (13.15) and (13.16), we obtain the maximum efficiencies of the pump and hydraulic motor:

$$(\eta_1)_{\max} = \frac{1 - \sqrt{\frac{k_y k_x}{1 + k_{1p}}}}{1 + k_{1p} + \sqrt{k_x k_y (1 + k_{1p})}} \quad (13.20)$$

and

$$(\eta_2)_{\max} = \frac{1 - k_{1p} - \sqrt{k_y k_x (1 - k_{1p})}}{1 + \sqrt{\frac{k_x k_y}{1 - k_{1p}}}} \quad (13.21)$$

The general theory of rotor-type hydraulic machines set forth above was worked out during the prewar years by Prof. V.V. Mishke (Bauman Higher Technical Institute at Moscow), and has been developed further since the war in the studies of Prof. V.N. Prokov'yev and abroad.

а) Тип гидромашинны	$k_y$	$k_x$	$k_{1p}$	$\eta$ %
б) Пластинчатый насос	9·10 <sup>-8</sup>	2·10 <sup>5</sup>	0	76
с) Шестеренный насос	2·10 <sup>-9</sup> —1·10 <sup>-7</sup>	3·10 <sup>6</sup> —1·10 <sup>5</sup>	0—0,2	79—85
д) Роторно-поршневой насос	9·10 <sup>-10</sup> —15·10 <sup>-9</sup>	(0,2—2)·10 <sup>6</sup>	0—0,15	87—92
е) Пластинчатый гидромотор	1,5·10 <sup>-7</sup>	1,5·10 <sup>5</sup>	0,1	65
ф) Шестеренный гидромотор	(3—5)·10 <sup>-7</sup>	3·10 <sup>4</sup> —1·10 <sup>5</sup>	0—0,19	55—80
г) Роторно-поршневой гидромотор	1,1·10 <sup>-8</sup>	4·10 <sup>5</sup>	0,07	80

KEY: (a) type of hydraulic machine; (b) rotary-plate pump; (c) gear pump; (d) rotary-piston pump; (e) rotary-plate hydraulic motor; (f) gear hydraulic motor; (g) rotary-piston hydraulic motor.

The expressions derived can be used to evaluate the change in the efficiency of a hydraulic machine in the event of relatively small changes in the regime indicators  $\omega$ ,  $\Delta p$ , and  $\mu$ , changes such that  $\sigma$  would change by no more than  $\pm 50\%$ . They can also be used to determine the optimum operating mode for a hydraulic machine and its maximum efficiency value.

However, the approximate nature of this theory must be borne in mind. Inaccuracies stem mainly from the fact that the fluid viscosity in the clearances is assumed constant and equal to the viscosity of the main stream. In actuality, as we noted earlier (§68), the fluid is heated to some degree in the clearances as a result of friction and its viscosity drops. Fluid pressure also influences the viscosity.

Attempts have been made to take account of fluid heating in the clearances by introducing the Prandtl number into the basic relationships of the theory of rotor hydraulic machines.

The table on the previous page gives experimental values of the coefficients  $k_u$ ,  $k_{zh}$ , and  $k_{tr}$  and the over-all efficiency calculated by Formulas (13.20) and (13.21) for the principal varieties of the rotor-type hydraulic machine according to Soviet [5] and foreign sources.

### Footnotes

Manu-  
script  
page

311       <sup>1</sup>See [9].

317       <sup>2</sup>Sometimes the reciprocal of the above quantity is also  
called the isogonality coefficient.

### Symbol List

Manu- script page	Symbol	English equivalent	
293	т	t	theoretical
300	зуб	zub	tooth
302	в	v	inside
303	н	n	outside
309	ср	sr	average
311	нас	nas	pump
312	пр	pr	spring
312	кл	kl	valve
315	у	u	leakage
316	ж	zh	fluid
316	тр	tr	friction
317	м	m	mechanical
317	фр	fr	friction
317	нап	nap	head, pressure

## C H A P T E R   X I V

### HYDRAULIC DRIVES AND HYDRAULIC TRANSMISSIONS

A hydraulic transmission is a device for the transfer of mechanical energy and the conversion of motion by the use of fluid.

A hydraulic transmission consists of the following two basic elements: a pump, which converts mechanical to hydraulic (fluid-flow) energy, and a hydraulic motor, which reverses this energy transformation.

The hydraulic motor sets a driven element in reciprocating or rotary motion. Hydraulic transmissions are classified into two basic types on the basis of this kinematic criterion: reciprocating hydraulic transmissions and rotary hydraulic transmissions. Both types are used in aviation and rocketry. A further classification of hydraulic transmissions will be given below.

A hydraulic drive is a device that consists of a hydraulic transmission, a control system, and accessories. Thus, the hydraulic transmission is the actuating element of the hydraulic drive.

#### §70. RECIPROCATING HYDRAULIC TRANSMISSIONS

General information. The hydraulic motors used in reciprocating hydraulic transmissions are hydraulic power cylinders with pistons and rods that execute reciprocating motions under the action of working-fluid pressure. Double-action hydraulic

cylinders, in which the driven element can move in two opposite directions under the action of fluid pressure, are used most frequently.

The so-called hydraulic torque cylinders, in which the driven element (a shaft) executes reversible rotary motions through an angle smaller than  $360^\circ$ , are sometimes used along with hydraulic power cylinders.

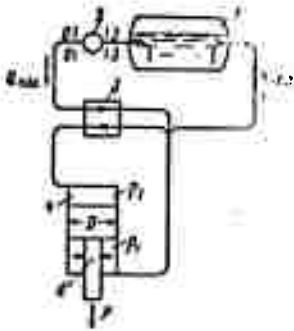


Fig. 197. Diagram of elementary hydraulic transmission.

Reciprocating hydraulic transmissions are used very extensively on aircraft, usually not in the form of simple transmissions, but as transmission systems composed of one or more displacement pumps and several hydraulic motors. The latter are connected to one another by main lines (pipelines) and perform various functions simultaneously or at different times (the functions performed by these hydraulic motors were enumerated in §1).

A special hydraulic system (a system of boosters or hydraulic amplifiers) built with backup and emergency systems is usually provided for control of the aircraft in view of the importance of this function and the high power required. Another, general-purpose, hydraulic transmission system serves the other functions on the airplane.

Such a hydraulic transmission system usually consists of a main (pump) line and several parallel-connected actuator mains with the appropriate hydraulic cylinders, each of which is designed to perform a definite function: control of landing gear, flaps, etc.

Figure 197 shows a schematic diagram of an elementary reciprocating-action hydraulic transmission with one actuator main and one hydraulic power cylinder. The transmission includes: tank 1, an intake main, pump 2, a pressure main with certain general-purpose units on it running to the control unit (distributor) 3, and actuator and return lines.

The actuator main begins at the distributor; it is followed by a length of main that supplies fluid to hydraulic cylinder 4 and a return length of main running from the hydraulic cylinder to the distributor. When the hydraulic motor is reversed by switching the distributor, the supply and return lines exchange functions.

Figure 198 shows a diagram of an aircraft hydraulic transmission system with only one of the actuator mains indicated by

way of example - the main for operation of the flaps (legend items 1-4 are the same as in Fig. 197).<sup>1</sup>

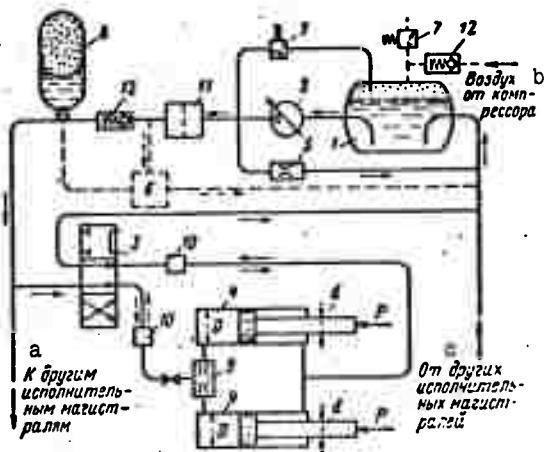


Fig. 198. Diagram of aircraft hydraulic transmission system.  
KEY: (a) to other actuator mains; (b) air from compressor; (c) from other actuator mains.

The arrangement of the main hydraulic line depends on the kind of pump used in the hydraulic system - adjustable or non-adjustable. Gear (nonadjustable) and rotary-piston (adjustable) pumps are used in aircraft hydraulic systems. The adjustable pumps are usually fitted with appropriate devices (see §68) for maintenance of practically constant pressure and reduction of delivery to a certain minimum in the absence of a demand for fluid. This minimum should compensate only internal leakage in the system and provide for pump cooling, which is accomplished by constant circulation of fluid through a high-resistance choke 5.

If, on the other hand, a nonadjustable pump is used in the system, its delivery is practically constant (at constant speed). In the absence of a demand for working fluid, therefore, this delivery must be returned to the tank with minimum resistance. The automatic pump-relief device 6, which switches the pump to "idle" (see broken lines on the figure) serves this purpose.

Safety valve 7 is usually inserted in all hydraulic systems to protect them from excessive pressure in the event of failure of the pump automatic control, the automatic relief device, or the air-pressure regulator in the tank pressurizing system.

<sup>1</sup>See page 367 for footnote.

Hydraulic accumulator 8 accumulates working fluid under pressure when the hydraulic motors are idle for subsequent use, together with pump delivery, when the demand for fluid reaches its maximum. The accumulator also smooths out pump-delivery unevenness, softens water hammer, and replenishes fluid leakage from the high-pressure line into the return line in automatically relieved systems.

As we stated in §42, the distributor is a control device by means of which one or another chamber of a hydraulic cylinder (actuating mechanism) is connected to the system pressure line or disconnected from this line. The squares on the diagram represent the various possible line connections, i.e., distributor positions.

The flow divider or batcher 9 is used when it is necessary to synchronize the motions of various mechanisms (such as flaps). Also shown here is a batchmeter 10 — a device that prevents working fluid from escaping the system when a pipeline ruptures.

Filter 11 has the function of trapping solid particles in the fluid. The purpose of the check valve 12 is to pass a stream of fluid (or air) in one direction and block it in the opposite direction.

For more detailed information on the units of aircraft hydraulic systems listed above and on certain others, the reader is referred to §72.

The basic working fluid used in aircraft hydraulic systems is AMG-10, a heavy kerosene to which a special thickener (Vinipol) has been added to increase its viscosity. The physical properties of AMG-10 fluid were given in Table 1 (see Chapter I). AMG-10 moves in laminar flow in pipelines at low temperatures. However, because of the comparatively low viscosity of AMG-10 fluid, the laminar flow regime yields to turbulent flow in some parts of the aircraft hydraulic system. In winter, for example, during retraction of landing gear, laminar flow is established in the return line, but the flow may be turbulent in the pressure line, where the fluid is heated.

**Principle of calculation.** In the mathematical design of such a hydraulic transmission, it should be regarded as a closed pipeline with pump delivery of fluid, and the power cylinder as a special local resistance that causes a pressure drop  $\Delta p_{ts}$  equal to the difference between the pressures on the two sides of the piston, i.e.,

$$\Delta p_{ts} = p_1 - p_2.$$

It can be assumed in first approximation that the delivery of fluid from the accumulator is zero, i.e., that the piston is moved solely by pump operation.<sup>2</sup>

<sup>2</sup>See page 367 for footnote.

The gradient  $\Delta p_{ts}$  can be expressed as follows on the basis of the equilibrium equation of the piston (see Fig. 197):

$$\frac{\pi}{4}(D^2 - d^2)p_1 = P + \frac{\pi D^2}{4}p_2,$$

from which

$$\Delta p_a = p_1 - p_2 = \frac{4P}{\pi(D^2 - d^2)} + \frac{d^2}{D^2 - d^2}p_2. \quad (14.1)$$

The quantity  $p_2$  is approximately equal to the total pressure loss in the return line; consequently, the second term in (14.1) is a function of flow rate or piston speed. This term is usually far smaller than the first and is often dropped.

Thus, the pressure required for a given system when the pump delivers  $Q_{nas}$  must be found by adding the gradient  $\Delta p_{ts}$  to the total pressure loss in the entire system, i.e.,

$$P_{nop} = \Delta p_a + \sum p_{rp}. \quad (14.2')$$

In determining the return-line hydraulic losses, it must be remembered that during motion of a piston with a rod on one end, the fluid flow rate  $Q_{s1}$  in the return line is not equal to the flow  $Q_{nas}$  in the delivery line, since the piston area is larger on one side than on the other. For this purpose, we introduce a coefficient  $\underline{a}$ , which equals

$$a = \frac{Q_{c2}}{Q_{nac}} = \frac{D^2}{D^2 - d^2}$$

when the piston rises (see Fig. 197).

Let us assume that we have the particular case in which flow is laminar in the return line and turbulent in the delivery line.

Then, applying Formula (14.1) and the expression for the coefficient  $\underline{a}$ , and grouping terms in accordance with the type of dependence on  $Q_{nas}$ , we obtain from (14.2')

$$P_{nop} = \frac{4P}{\pi(D^2 - d^2)} + a^2 k_1 \gamma Q_{nac} + k_2 \gamma Q_{nac}^2. \quad (14.2)$$

Here the first term in the right-hand member is the basic term in the expression for  $\Delta p_{ts}$ , the second term is the pressure loss in the return line plus the second term in (14.1), and the third term is the pressure loss in the delivery line (from the tank to the cylinder).

The sense of the coefficients  $k_1$  and  $k_2$  is the same as in §47.

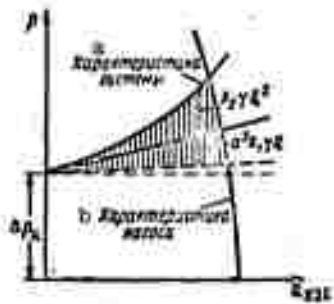


Fig. 199. Graphical determination of hydraulic transmission operating regime.  
 KEY: (a) system characteristic; (b) pump characteristic.

From this equation, we construct the system characteristic (Fig. 199) and enter the pump characteristic on the same diagram. The intersection point of these two lines determines the system operating regime, i.e.,  $Q_{nas}$  and  $P_{nas}$ . If the load  $P$  along the rod does not vary over the stroke of the piston, dividing the cylinder volume by the flow rate gives the time to execute the operation or the time required to traverse the piston from one extreme position to the other.

An aircraft landing-gear hydraulic system usually has three power cylinders connected in parallel. In this case, the system should be regarded for design purposes as a complex closed pipeline and, in addition to the instructions given above, recourse should be taken to the characteristic-plotting method (see §50).

**Calculation for nonsteady regime.** The dynamics of the motion is not taken into account in the method set forth above for synthesis of the hydraulic transmission (hydraulic system), since it was assumed that the fluid flow is fully stabilized over the entire span of the working cycle from the time at which the piston(s) begin to move to the time at which they stop.

In actuality, the motions of the fluid and piston are non-uniform, and for this reason dynamic pressures usually arise in the system and must be taken into account when large masses are being moved with large accelerations and abrupt load changes.

Suppose we have a given law of variation of the external load on the rod as a function of piston movement  $P = f(x)$ . It is required to determine the time of displacement of the piston from one extreme position to the other with consideration of inertial pressures.

Let us write the fundamental equation of nonsteady motion (10.6) for the flow of fluid (see Fig. 197) from the pump outlet (section 0-0) to the pump inlet (section 3-3) with consideration of the pressure losses in the hydraulic power cylinder to handle the load and the inertia of the moving parts.

Disregarding the velocity-head difference, we have

$$P_0 = P_3 + \Delta P_u + \sum P_{1,1} + P_{1,2} + P_{1,3} + P_{r,3} \quad (14.3')$$

\*See page 367 for footnote.

where  $\sum p_{tr} = kQ_{nas}^2$  is the sum of the pressure losses in the pipelines;  $\Delta p_{ts} = P/S_p$  is the pressure loss to start the load moving;  $p_{in1}$  and  $p_{in2}$  are the inertial pressures used to accelerate the fluid in the delivery and return lines, respectively, and are equal to (see §45)

$$p_{in1} = \rho \frac{l_1}{S_1} \frac{dQ_{nac}}{dt} \quad \text{and} \quad p_{in2} = \rho \frac{l_2}{S_2} \frac{dQ_{ra}}{dt}$$

( $l$  and  $S$  are the lengths and sectional areas of the pipes, respectively);  $p_{in3}$  is the inertial pressure used to accelerate the piston and the masses of the moving mechanisms reduced to the piston, and equals

$$p_{in3} = M_p \frac{j_p}{S_p} = M_p \frac{dQ_{nac}}{dt} \frac{1}{S_p^2}$$

Here,  $S_p$ ,  $j_p$  and  $M_p$  are the area, acceleration, and mass of the piston, respectively (and of the other moving parts reduced to the piston).

Since  $Q_{s1} = aQ_{nas}$ , we have

$$p_{in2} = aQ \frac{l_2}{S_2} \frac{dQ_{nac}}{dt}$$

and the fundamental equation (14.3') can be rewritten

$$p_{nac} = p_0 - p_s = kQ_{nac}^m + \frac{P}{S_n} + \frac{M}{S_1^2} \frac{dQ_{nac}}{dt}, \quad (14.3)$$

where  $p_{nas}$  is the pressure developed by the pump, which we shall assume constant, and  $M$  is the reduced mass of all of the fluid and moving parts, which equals

$$M = \rho \left( S_1 l_1 + a \frac{S_1^2}{S_2} l_2 \right) + \frac{S_1^2}{S_n^2} M_p$$

In the case of a constant load along the piston rod ( $P = \text{const}$ ), Eq. (14.3) is easily solved for linear ( $m = 1$ ) or square-law ( $m = 2$ ) resistances.

If the load is variable, it is recommended that the problem be solved by numerical integration.

The initial value of the derivative  $(dQ_{nac}/dt)_0$  is found from (14.3) with the initial values  $P = P_0$  and  $Q = 0$ . Then we take a short time segment  $\Delta t$ , and find the flow rate increment

$$\Delta Q_1 = \left( \frac{dQ_{nac}}{dt} \right)_0 \Delta t_1$$

The fluid volume entering the hydraulic cylinder during time  $\Delta t_1$  is

$$\Delta W_1 = \frac{1}{2} \Delta t_1 \Delta Q_1,$$

while the piston travels a distance

$$\Delta x_1 = \frac{\Delta W_1}{S_0}$$

A new value of the load  $P_1$  is found from  $\Delta x_1$ , and the time derivative of flow rate at the end of segment  $\Delta t_1$  is found from (14.3) with the substitution  $Q_1 = \Delta Q_1$  and  $P = P_1$ .

We then take a new time segment  $\Delta t_2$  and, assuming that the derivative value  $(\frac{dQ_{nas}}{dt})_1$  calculated in the first cycle is constant for this segment, we determine the flow rate increment

$$\Delta Q_2 = \left( \frac{dQ_{nas}}{dt} \right)_1 \Delta t_2,$$

and then the flow rate and volume increment

$$Q_2 = \Delta Q_1 + \Delta Q_2; \quad \Delta W_2 = \frac{\Delta t_2}{2} (\Delta Q_1 + \Delta Q_2)$$

and so forth.

The third and subsequent cycles are analogous to the above. The limits of integration are the beginning and end of the working stroke. The unknown time is found as the sum of the segments  $\Delta t$ .

### §71. HYDRAULIC SERVO DRIVE (HYDRAULIC BOOSTER)

In the hydraulic transmission examined in the preceding section, we had a simple displacement of the piston from one extreme position to the other, during which it overcomes a load  $P$  along the piston rod.

In other cases, it is necessary to secure a more complex piston (rod) motion. Thus, in aircraft control systems, the rod of the hydraulic power cylinder must automatically follow the motion of the control lever, and a definite rod position must correspond to each position of that lever.

These are systems of the hydraulic servo type, and the hydraulic cylinder is called a hydraulic booster or amplifier in this case, since its actuating rod does not simply repeat the motion of the control lever, but also develops a force considerably greater than that applied to the control.

As a rule, modern high-speed aircraft and helicopters are controlled with the aid of hydraulic boosters, since the effort

required at the control surfaces is often many times the muscular strength of the pilot.

Figure 200 shows a schematic diagram of a hydraulic amplifier (booster). By moving the control 1, for example to the right, the pilot traverses command slidevalve 2, which directs fluid under pressure through passage 3 into the left chamber of cylinder 4 and connects its right chamber with the return line. Under the pressure developed by the pump, piston 5 moves to the right together with the spool of slidevalve 6 until the slidevalve passages through which fluid enters the cylinder and leaves it are covered.

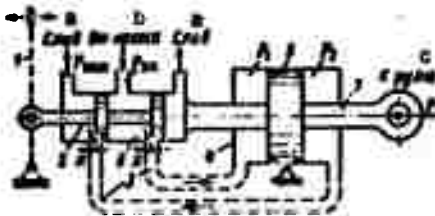


Fig. 200. Schematic diagram of hydraulic amplifier (booster).  
KEY: (a) return; (b) from pump;  
(c) to control surface.

When the stick and slidevalve are moved to the left, pressure will be supplied to the right chamber of the cylinder and the piston will move to the left.

Thus, the actuating rod 7, which is connected in the example to a control surface of the airplane, follows all motions of slidevalve 2, but the force that it develops is many times that which the pilot applies to the slidevalve.

Let us now examine the basic characteristics of the hydraulic booster as a power drive. We shall derive formulas for the effort at the actuating rod of the booster, its efficiency, and the power that it develops.

The pressure supplied to the hydraulic booster is used to overcome the force  $P$  acting along the actuator rod and hydraulic resistances, i.e.,

$$p_0 = \Delta p_u + \sum p. \quad (14.4)$$

where  $p_0 = p_{vkh} - p_{vykh}$  is the fluid pressure at the inlet of the booster minus the pressure at the outlet;  $\Delta p_{ts} = p_1 - p_2$  is the pressure drop in the cylinder, which equals  $\Delta p_{ts} = P/S$ ;  $S$  is the

piston area less the rod area;  $\sum p$  is the total pressure loss on the path of the fluid from the inlet into the booster to its outlet.

Assuming that the hydraulic losses take place basically in two partially covered slide-valve ports and that these losses are square-law functions of velocity (flow rate), we can write

$$\sum p = \zeta \frac{\rho}{2g} v^2$$

where  $\zeta$  is the resistance coefficient of the slidevalve port and  $v$  is the velocity of fluid outflow through it.

Since the slidevalve ports are usually rectangular, with one side of the rectangle constant and equal to  $b$ , which the other is variable and equal to  $x$  (see Fig. 200), we can write the flow rate equation in the form

$$Q = VS = vbx,$$

where  $V$  is the speed of the piston.

Expressing  $v$  in terms of  $Q$  in accordance with the above, and then substituting it into the formula for  $\sum p$  and (14.4), we obtain

$$p_0 = \Delta p_a + \zeta \gamma \frac{Q^2}{2g(bx)^2}$$

or

$$p_0 = \Delta p_a + k \frac{Q^2}{x^2}, \quad (14.4')$$

where

$$k = \frac{\zeta \gamma}{2g b^2}$$

The quantity  $k$  can be assumed approximately constant and independent of flow rate. If the booster is supplied by an adjustable constant-pressure pump (see Fig. 195), and if the hydraulic losses in the supply pipes can be disregarded, the pressure  $p_0$  will also be constant at the pressure developed by the pump.

In the absence of a load on the actuator rod ( $P = 0$  and  $\Delta p_{ts} = 0$ ) and with the slidevalve ports wide open ( $x = x_{\max} = t$ ), the delivery (flow rate) of fluid to the booster will be  $Q = Q_{\max}$ . We then obtain from (14.4')

$$k = p_0 \frac{x_{\max}^2}{Q_{\max}^2}$$

After substituting this expression into (14.4') and solving it for  $\Delta p_{ts}$ ,

$$\Delta p_{ts} = p_0 \left( 1 - \frac{Q^2}{Q_{\max}^2} \right)$$

where  $\bar{Q} = \frac{Q}{Q_{max}} = \frac{V}{V_{max}} = \bar{V}$  is the relative flow rate or the relative speed of the actuator rod;  $\bar{x} = \frac{x}{x_{max}}$  is the percentage opening of the slidevalve ports. From the above, the force acting along the actuator rod (the load) will be

$$P = \Delta p_e S = p_0 S \left(1 - \frac{\bar{Q}^2}{\bar{x}^2}\right), \quad (14.5')$$

and the relative load  $\bar{P}$  is found by dividing  $P$  by  $P_{max} = p_0 S$ , i.e.,

$$\bar{P} = \frac{P}{p_0 S} = 1 - \frac{\bar{Q}^2}{\bar{x}^2} = 1 - \frac{V^2}{x^2}. \quad (14.5)$$

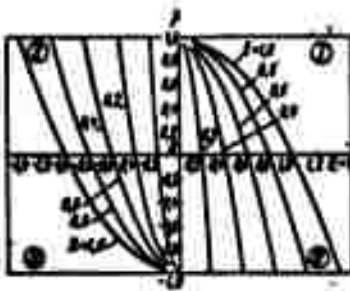


Fig. 201. Static characteristics of hydraulic booster.

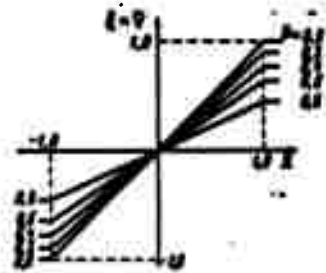


Fig. 202. Alternate method of plotting static characteristics of hydraulic booster.

This equation can be used to construct a net of so-called static characteristics of the hydraulic booster, i.e., curves of  $\bar{P}$  as a function of  $\bar{Q}$  for various  $\bar{x}$  (Fig. 201). This diagram is constructed for positive and negative  $\bar{Q}$  and  $\bar{x}$ , i.e., for motion of the slidevalve and rod and, consequently, of the fluid in either direction.

We see from the diagram that the force on the actuator rod approaches the largest possible value  $P_{max} = p_0 S$  only at low speeds  $V$  of the rod. The faster the motion of the rod, the smaller the load that it will handle.

The load on the rod changes sign where the curves cross the axis of abscissas, i.e., the load is transformed into a force that pulls the rod in the direction of motion. This results in a further increase in its speed, and the hydraulic cylinder works in the pump mode. Thus, in quadrants I and III on the diagram, the hydraulic cylinder is operating as a motor performing work to overcome the load, and in quadrants II and IV it is a pump supplying fluid in the same direction as the main pump.

The static characteristics of a hydraulic booster can also be constructed in another coordinate system. Let us solve Eq. (14.5) for  $\bar{Q} = \bar{V}$ :

$$\bar{Q} = \bar{V} = \bar{x} \sqrt{1 - \beta} \quad (14.6)$$

and plot  $\bar{Q} = \bar{V}$  as a function of  $\bar{x}$  for various values of  $\beta$  (Fig. 202). We obtain a series of straight lines whose inclination to the  $\bar{x}$ -axis is smaller the greater the load on the booster actuating rod. At  $\beta = 1$ , the booster characteristic coincides with the axis of abscissas, and this means that the rod speed is zero.

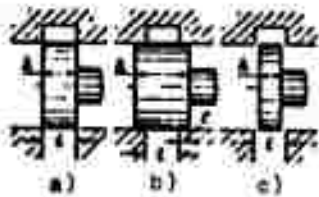


Fig. 203. Diagrams of slidevalves. a) ideal; b) with positive overlap; c) open.

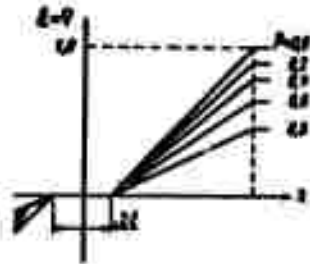


Fig. 204. Characteristic of hydraulic booster with positive overlap.

The characteristics of the booster are also influenced by the so-called overlap of the slidevalve, i.e., the relation between the width  $h$  of the slidevalve spool and the width  $t$  of its ports. We therefore distinguish the ideal slidevalve, in which  $h = t$  (Fig. 203a), the positive-overlap slidevalve, in which  $h > t$  (Fig. 203b), and the negative-overlap or open slidevalve, in which  $h < t$  (Fig. 203c). The overlap is taken as

$$c = \frac{h-t}{2} \quad \text{or} \quad \bar{c} = \frac{h-t}{2t}$$

The characteristic shown in Fig. 202 is that of an ideal slidevalve ( $c = 0$ ). A dead zone of width  $2c$  appears on the characteristic of the positive-overlap slidevalve — a disadvantage, but one that improves sealing (Fig. 204).

In the open slidevalve, fluid seeps from the delivery line to the return line and, consequently, power is lost. However, there is practically no dead zone, since when the spool is shifted even very slightly from its neutral position, a pressure gradient appears in the hydraulic power cylinder.

The efficiency  $\eta$  of a hydraulic booster will be represented here as the ratio of the work done by the actuator rod per second to the power that the fluid flow applies to the hydraulic booster, i.e.,

$$\eta = \frac{PV}{P_0Q} = \frac{\Delta P_0 SV}{P_0 VS} = \frac{\Delta P_0}{P_0} = \bar{P}. \quad (14.7)$$

Consequently, the efficiency of the booster is numerically equal to the relative load on the rod and varies in accordance with the same law as  $\bar{P}$ .

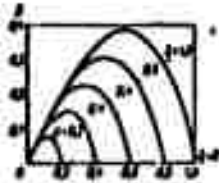


Fig. 205. Relative power curves of hydraulic booster.

The useful power of the booster is

$$N = PV,$$

and the relative power is determined by the ratio

$$\bar{N} = \frac{PV}{P_0 SV_{\max}} = \bar{P} \bar{V}.$$

Applying (14.5) and remembering that  $\bar{V} = \bar{Q}$ , we obtain

$$\bar{N} = \left[1 - \frac{\bar{Q}^2}{\bar{x}}\right] \bar{Q}. \quad (14.8)$$

Figure 205 gives curves of the relative power  $\bar{N}$  as a function of  $\bar{Q} = \bar{V}$  for various  $\bar{x}$ , as plotted by Formula (14.8).

Let us find the value of the relative flow  $\bar{Q}$  at which the power reaches its maximum.

For  $\bar{x} = 1$ , we obtain instead of (14.8)

$$\bar{N}_{\bar{x}=1} = (1 - \bar{Q}^2) \bar{Q}.$$

After differentiating with respect to  $\bar{Q}$ , we equate the derivative to zero:

$$\frac{d\bar{N}}{d\bar{Q}} = 1 - 3\bar{Q}^2 = 0.$$

Hence the optimum relative flow rate

$$\bar{Q}_{\text{opt}} = \bar{V}_{\text{opt}} = \frac{1}{\sqrt{3}} = 0.58,$$

and the maximum relative power

$$\bar{N}_{\max} = \left(1 - \frac{1}{3}\right) \frac{1}{\sqrt{3}} = 0.385.$$

Then, according to Formulas (14.5) and (14.7), the relative rod load and the booster efficiency are equal to

$$\bar{P} = \eta = \frac{2}{3}.$$

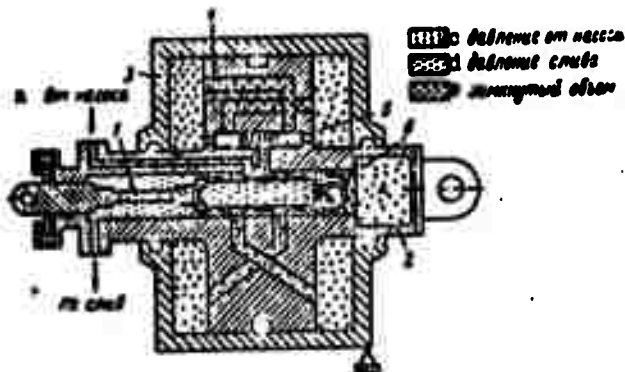


Fig. 206. Diagram of hydraulic booster with internal slidevalve.

KEY: (a) from pump; (b) return; (c) pressure from pump; (d) return pressure; (e) closed volume.

The absolute value of the maximum power will be

$$N_{max} = \frac{2}{3\sqrt{3}} p_0 S V_{max} = \frac{2}{3\sqrt{3}} Q_{max} p_0$$

where  $Q_{max}$  can be found from the expression derived above for  $k$ , i.e.,

$$Q_{max} = x_{max} \sqrt{\frac{p_0}{k}}$$

After substitution in the above expression, we finally obtain

$$N_{max} = \frac{2}{3\sqrt{3}} \frac{x_{max}}{\sqrt{k}} p_0^{3/2} \quad (14.9)$$

Figure 206 shows the design layout of a booster whose slide valve is accommodated inside the actuating rod 2. When command spool 1 shifts, fluid from the pump is directed through passages 7 into one of the chambers of cylinder 3 and is drained from the other.

In addition to the cylinder-piston group 4 and the slide valve, aircraft hydraulic boosters also have the following auxiliary devices.

1. A cylinder-bypass system, which provides for automatic interconnection of both cylinder chambers in the event of a pressure drop in the hydraulic system. This is necessary to permit free movement of the booster actuator rod by means of the control

stick on switching to manual control, when the booster does no work at all and is reduced to a simple kinematic element.

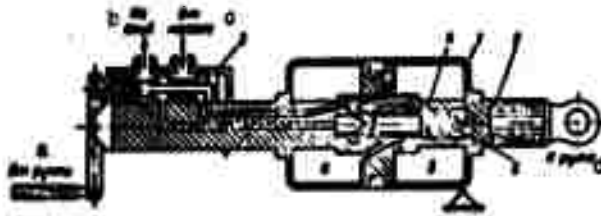


Fig. 207. Diagram of hydraulic booster with external slidevalve.  
KEY: (a) from stick; (b) return; (c) from pump; (d) to control surface.

In Fig. 206, the cylinder chambers are connected by the bypass plungers 5. Obviously, when there is no pressure in the system, movement of the piston by an external force will move the bypass plungers to open the passages, through which fluid can flow without hindrance from one chamber of the cylinder into the other.

2. The slidevalve damper in Fig. 206 is made in the form of a one-way ball valve 6. Together with this valve, the slidevalve acts as a pump that continuously exhausts fluid from damper chamber A, where a vacuum is created as a result. Thus, a constant unidirectional load acts on the end of the slidevalve; tests indicate that this protects the booster from self-oscillation.

Figure 207 shows another design version of the hydraulic booster. It differs from the previous one primarily in the external position of slidevalve 3, whose shell is also rigidly coupled to actuator rod 2. The bypass system is also different in design. In the absence of pressure in the booster, the bypass valve 4 is transferred by spring 6 to its extreme left position (as shown on the diagram) and joins the left chamber of cylinder 1 with its right chamber. If fluid is supplied to the booster under pressure, this pressure moves the bypass valve to the right, where it covers hole 5 and blocks communication between the booster chambers.

A booster is connected either reversibly or irreversibly into the aircraft's control system.

In the former case, a small part of the effort from the controls is transmitted to the pilot. In the latter case, the entire load is offset by hydraulic force, and nothing but the force of friction in the command slidevalve is transmitted back to the control stick.

Figure 208 represents the operation of a hydraulic booster in a reversible control system. If we imagine a reversing rod

to be rigidly attached as shown and the center of rotation of the rocker to be transferred from point A to point B, the reversible control system becomes an irreversible system.

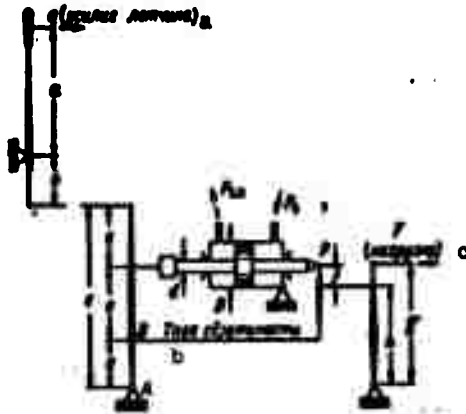


Fig. 208. Diagram of transmission from control stick through hydraulic booster to control surface.  
KEY: (a) pilot effort; (b) reversing rod; (c) load.

A numerical example will clarify the function of the hydraulic booster in the reversible system.

Example. Given (see Fig. 208):

Diameter of booster cylinder  $D = 50$  mm.

Diameter of actuating rod  $d = 30$  mm.

Booster efficiency  $\eta = 0.90$  (with consideration of friction in the cylinder).

Load from control surfaces  $F = 960$  kgf.

Arm ratios:  $\frac{a}{b} = 4$ ;  $\frac{c}{e} = 3$ ;  $\frac{e}{f} = 4$ ;  $\frac{g}{h} = \frac{3}{2}$ .

Determine:

1) the pressure  $p_0$  at the entry into the booster if the pressure in the return line  $p_{s1} = 3$  kgf/cm<sup>2</sup>.

2) the stick effort  $q$  in the presence and absence of pressure in the hydraulic booster.

Solution. 1. We determine the force  $P$  on the booster actuating rod:

$$P = F \cdot \frac{f}{b} \cdot \frac{e-f}{e} = 900 \cdot \frac{3}{2} \left(1 - \frac{1}{4}\right) = 1050 \text{ kgf.}$$

2. We determine the pressure  $p_0$  at the entrance into the booster. Since

$$P = \frac{\pi}{4} (D^2 - d^2) (P_0 - P_1) \eta,$$

we have

$$P_0 = \frac{4D}{\pi \eta (D^2 - d^2)} + P_1 = \frac{4 \cdot 1050}{3,14 \cdot 0,9 (5^2 - 3^2)} + 3 = 99,6 \text{ kgf/cm}^2.$$

3. We find the effort at the control stick in the presence of pressure in the booster.

The transmission ratio  $i_1$  (the so-called "reversibility factor") equals

$$i_1 = \frac{b}{a} \cdot \frac{e}{e'} \cdot \frac{f}{e} \cdot \frac{f'}{b} = \frac{1}{4} \cdot \frac{1}{3} \cdot \frac{1}{4} \cdot \frac{3}{22} = \frac{1}{32}.$$

The stick effort is  $F_1 = i_1 F = \frac{1}{32} 900 = 28 \text{ kgf.}$

4. We find the stick effort in the absence of booster pressure.

In this case, the transmission ratio is

$$i_2 = \frac{b}{a} \cdot \frac{a}{e'} \cdot \frac{f}{b} = \frac{b}{a} \cdot \frac{e-f}{e} \cdot \frac{f}{b} = \frac{7}{32}.$$

The stick effort  $F_2 = i_2 F = \frac{7}{32} 900 = 210 \text{ kgf}$ , i.e., manual control of the airplane in this flight mode is impossible; for this reason, a reserve power source must be provided against the eventuality of hydraulic system failure.

## §72. BASIC SUBUNITS OF AIRCRAFT HYDRAULIC SYSTEMS

The components of aircraft hydraulic power systems (hydraulic transmission systems) include, first of all, those that perform the functions of control devices (see §43) - distributors, pressure regulators, and flow regulators - and certain units with other functions - filters, accumulators, etc.

Let us begin our examination of these units with the control devices, whose function is to direct the flow of working fluid in the hydraulic system.

Distributors, like other control devices, are classified as choke and valve types on the basis of working principle (see §43). Most commonly used are the choke distributors, whose geometrical characteristics or percentage openings do not depend on the parameters of the flow through them. However, valve-type distributors are nevertheless used in the form of adjustable valves.

A classification on the basis of control method distinguishes manually, electrically, hydraulically, and pneumatically controlled distributors.

Depending on the number of external lines (pipelines) through which working fluid is supplied to the distributor and removed from it, we distinguish three-line, four-line, etc., types. They are also said to be three-way, four-way, etc.

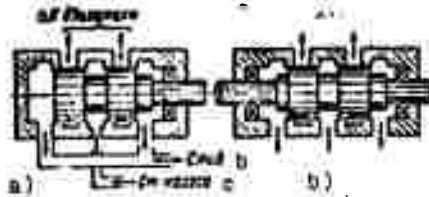


Fig. 209. Diagram of four-line slidevalve distributor.  
KEY: (a) to motor; (b) return; (c) from pump.

The four-line distributor, to which fluid is supplied from a pump, removed to one of the chambers of a hydraulic motor, supplied from the other motor chamber, and returned to the tank, is used most frequently.

Choke distributors are classified as spool and valve types. The difference is that the working element reciprocates in the former type and rotates in the latter.

The slide valve distributor, also known simply as the slidevalve, is the most common type of distributor in aircraft hydraulic systems.

The working element of a slidevalve distributor is a rod fitted with two, three, or four spools and capable of axial movement inside the slidevalve's cylinder (sleeve). The latter is provided with ports for intake and outflow of fluid. Figure 209 is a diagram of a four-line (four-way) slidevalve distributor without (a) and with (b) compensation of the axial force.

The hydraulic properties of a slidevalve distributor are determined by its flow rate coefficient  $\mu$  (or resistance coefficient) and by the axial and radial forces acting on the spool rod.

The flow rate coefficient of a slidevalve is determined by the formula

$$\mu = \frac{Q}{\delta x \sqrt{2\epsilon \frac{\Delta p}{\gamma}}}$$

where  $b$  is the width of the slidevalve port;  $x$  is the percentage opening of the port;  $\Delta p$  is the pressure loss in one branch of the slidevalve.

Experiments have shown that the coefficient  $\mu$  varies very slightly with varying percentage opening of the ports and with Reynolds number. This coefficient depends much more strongly on the ratio of port width  $b$  to spool diameter  $b/d$ . Figure 210 shows the flow rate coefficient  $\mu$  as a function of  $Re$  for a series of  $b/d$  values for various percentage openings of the slidevalve ports.<sup>4</sup>

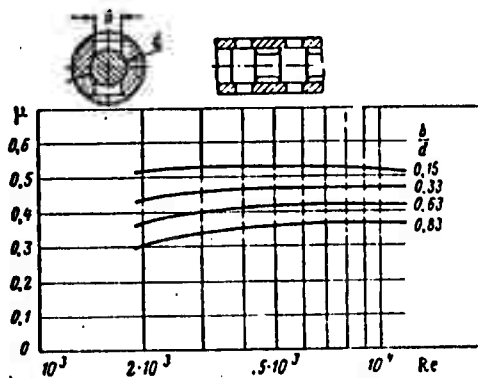


Fig. 210. Flow rate coefficient of slidevalve as a function of Reynolds number and ratio  $b/d$ .

As we see from the diagram, the flow rate coefficient decreases from 0.53 to 0.35 as the ratio  $b/d$  is increased from 0.15 to 0.83. This is because the fraction of the resistance contributed by the supply passages increases with increasing relative port size.

The resistance coefficient of a slidevalve, which is equal to the ratio of the head loss to the velocity head in the port, is found with consideration of the above from the formula

$$\zeta' = \frac{\Delta p 2g}{\gamma v^2} = \frac{2g \Delta p (\delta x)^2}{Q^2 \gamma}$$

Consequently, a resistance coefficient  $\zeta'$  equal to 3.55 to 8.15 will correspond to the flow rate-coefficient values given above. These large coefficients  $\zeta'$  are explained by the fact that the jet is compressed during outflow through the slidevalve ports, but we have attributed the flow decrease due to jet compression to resistance, i.e., we set  $\epsilon = 1$  for the same  $\mu$ . Moreover, the coefficient  $\zeta'$  also takes account of the energy loss to sudden

<sup>4</sup>See page 367 for footnote.

expansion on issuance from the port. This is the difference between the coefficient  $\zeta'$  and the  $\zeta$  that we used in §38.

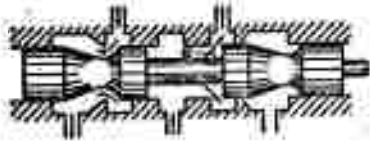


Fig. 211. Diagram of four-line slidevalve with axial-force compensation.

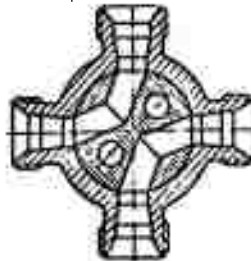


Fig. 212. Valve distributor.

The axial force acting on the slidevalve rod may consist of static and dynamic components. The former arises when the return-line pressure acts on the end of the rod. To offset this force, the rod is made longer and extended to the outside of the sleeve (as shown in Fig. 209b), or other measures are taken.

The axial dynamic component appears as a result of the momentum  $Qqv \cos \alpha$  that the jet carries with it through the partially opened port (Fig. 211).

This force is compensated by using the reaction of the jet issuing from the opposite chamber of the hydraulic motor. For this purpose, the slidevalve rod is profiled approximately as shown in Fig. 211.

The possible appearance of a radial force in the slidevalve poses a very important problem, since this force may throw the rod out of alignment and jam the spools in the sleeve, causing failure of the slidevalve.

To eliminate the possibility of radial reaction forces, the slidevalve ports are usually made in the form of a pair of diametrically opposed holes that communicate with one another through grooves, or else the port is made annular, i.e., with a width equal to the perimeter of the spool cross section,  $b = \pi d$ .

The influence of the clearance between the spools and sleeve, eccentricity, and spool taper is analyzed in detail in [5].

Valve distributors (Fig. 212) are usually simplest in construction. However, the torques required to operate them are quite substantial. Devices that reduce these torques complicate the design.

Mushroom-valve distributors are also used in aviation hydraulic systems; like the valve-controlled piston pumps, they have an advantage in their very tight internal sealing. Figure 213 presents a schematic diagram of a four-line mushroom-valve

distributor. It is controlled by turning shaft 1, which carries four cams 2. The latter operate valves 3, opening either the first and third or the second and fourth, i.e., one intake and one return valve at a time. The directions of the fluid flows are marked on the diagram.

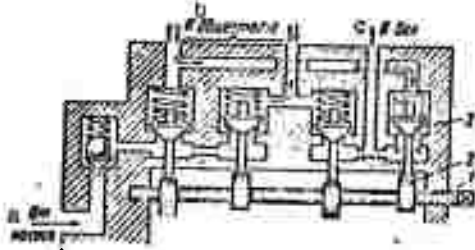


Fig. 213. Four-line mushroom-valve distributor.  
KEY: (a) from pump; (b) to motor;  
(c) to tank.

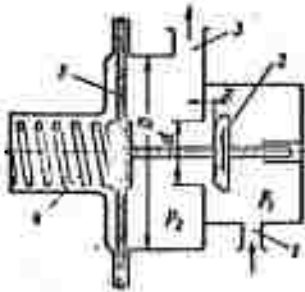


Fig. 214. Diagram of reduction valve (pressure reducer).

This distributor has a disadvantage in the large efforts required to open the valves. A variety of methods may therefore be used to relieve the valves, or so-called servo-action valves may be employed. In the latter case, the main valves are equipped with small auxiliary valves. Opening of an auxiliary valve, which requires little effort, causes the main valve to open under fluid pressure.

Pressure regulators are used in aviation hydraulic systems in the form of various types of valves - reduction, safety, bypass, pressure, etc.

A reduction valve or pressure reducer has the function of lowering the pressure of fluid coming from the pump to the appliance and maintaining the reduced pressure within specified limits.

This becomes necessary when an appliance in a system with a common pump requires a lower pressure than that delivered by the pump.

A schematic diagram of a reduction valve appears in Fig. 214. Fluid under pressure  $p_1$  enters through passage 1, passes under valve 2, where it is throttled, and exits through passage 3 at a lower pressure  $p_2$ . Spring 4 tends to open the valve, while the fluid pressures on membrane 5 and on valve 2 act in the direction

<sup>5</sup>See page 367 for footnote.

to close it. As a result, when pressure  $p_2$  rises to a certain limit, the valve shuts, and when the pressure drops, the valve opens. Thus, pressure  $p_2$  is held within the required range as fluid flow rate varies.

To obtain the fundamental equation reflecting the operation of the reduction valve, we write the following initial equations: the equation of the flow rate through the valve

$$Q = \mu \pi d x \sin \alpha \sqrt{2g \frac{p_1 - p_2}{\gamma}}$$

and the equilibrium equation of the valve

$$P_{sp0} - Cx - \frac{\pi d^2}{4} (p_1 - p_2) - \frac{\pi D^2}{4} p_2 = 0,$$

where  $\mu$  is the flow rate coefficient of the valve (see §42),  $x$  is the lift of the valve (percentage opening),  $d$  and  $D$  are the diameters of the valve seat and membrane,  $P_{sp0}$  is the spring force with the valve shut (at  $x = 0$ ),  $C$  is the spring constant, and  $\alpha$  is the taper angle of the valve.

The equilibrium equation for the valve has been written on the assumption that the pressures  $p_1$  and  $p_2$  are distributed uniformly over the area  $\pi d^2/4$  of the valve. This can occur only at small (by comparison with  $d$ ) valve openings  $x$ . At large  $x$ , the equilibrium equation requires corrections.

Determining  $x$  from the equilibrium equation and substituting into the flow rate equation, we have

$$Q = \mu \pi d \sin \alpha \frac{1}{c} \left[ P_{sp0} - p_1 - p_2 \left( \frac{D^2}{d^2} - 1 \right) \right] \sqrt{2g \frac{p_1 - p_2}{\gamma}}, \quad (14.10)$$

where

$$c = \frac{4C}{\pi d^2} \quad \text{and} \quad P_{sp0} = \frac{4P_{sp0}}{\pi d^2}.$$

This equation connects the two basic variables  $Q$  and  $p_2$ . The pressure  $p_1$  can be considered constant in systems with an adjustable pump.

The equilibrium equation can be used to determine the maximum (for a given  $p_1$ ) pressure  $p_2$  at the reducer outlet, which corresponds to a closed valve; setting  $x = 0$ , we obtain

$$(p_2)_{\max} = \frac{P_{sp0} - p_1}{\frac{D^2}{d^2} - 1}.$$

It is evident from this that for a given reducer, the pressure  $(p_2)_{\max}$  increases with decreasing pressure  $p_1$ .

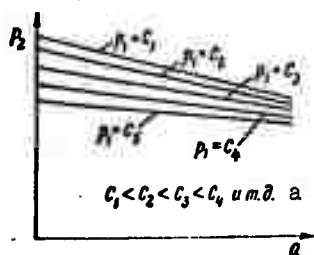


Fig. 215. Characteristic of reduction valve.  
KEY: (a) and so forth.

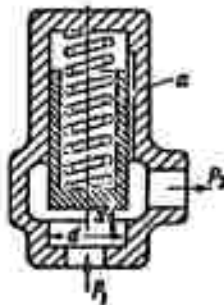


Fig. 216. Diagram of bypass valve.

Equation (14.10) can be used to construct the characteristic of the reduction valve, which is most conveniently presented as a curve of  $p_2$  vs.  $Q$  for a series of constant  $p_1$  equal to  $C_1, C_2, C_3$ , etc. The typical form of these curves is shown in Fig. 215, from which we see that the extent of the  $p_2$  drop with increasing flow rate  $Q$  is greater the lower the pressure  $p_1$  at the inlet into the reducer.

A pressure valve, in contrast to the reduction valve, is designed to limit the pressure in the flow of working fluid supplied to it. If, in this process, the valve maintains a specified fluid pressure by bleeding fluid continuously, it is called a bypass valve.

The design of the bypass valve is most frequently that of a spring-loaded plunger valve (Fig. 216). Such a valve must be fitted with a damper for oscillatory motions, e.g., in the form of the narrow passage  $a$ , through which fluid flows from the chamber above the valve to the chamber below it and back.

The relation between the pressures  $p_1$  at the entry to the valve and  $p_2$  at its outlet, and their relation to the fluid flow rate  $Q$  through the valve can be obtained by simultaneous solution of two equations - the flow rate and equilibrium equations of the valve. Assuming that pressure  $p_1$  is distributed uniformly over the valve area  $\pi d^2/4$ ,

$$Q = \mu \pi dx \sqrt{2g \frac{p_1 - p_2}{\gamma}}$$

and

$$P_{sp0} + Cx = (p_1 - p_2) \frac{\pi d^2}{4},$$

whence

$$Q = \mu \pi d \left[ \frac{\pi d^2}{4C} (p_1 - p_2) - \frac{P_{sp0}}{C} \right] \sqrt{2g \frac{p_1 - p_2}{\gamma}}, \quad (14.11)$$

where  $\mu$ ,  $x$ ,  $P_{sp0}$ , and  $C$  have the same meanings as for the reduction valve (see above).

As the flow rate rises from zero to  $Q_{max}$ , the pressure  $p_1$  does not remain constant, but rises to some degree. This equation can be used to estimate the extent of the  $p_1$  increase with increasing flow rate and at  $p_2 = \text{const}$ , and to ascertain the influence of  $p_2$ .

To obtain the flattest possible valve characteristic, i.e., to reduce the influence of fluid flow rate on the pressure  $p_1$ , it is necessary to increase the diameter  $d$  of the valve and lower the spring stiffness  $C$ .

A safety valve is another variety of the pressure valve; its function is to bleed fluid in the event of an overpressure. Thus, the safety valve functions only episodically, when the pump-regulating mechanism or automatic relief valve malfunctions.

Both ball and conical valves, usually spring-loaded, are used as safety valves.

A safety valve must be designed to open at a given pressure and pass a definite flow of fluid, preventing the pressure from exceeding a certain maximum.

Flow rate regulators, which hold fluid flow rate constant in a given hydraulic line, are used in aviation hydraulic systems when it is necessary to stabilize the speed at which a hydraulic motor moves - for example, that of an antenna motor.

Figure 217 shows a diagram of such a flow regulator. Diaphragm 1, which is its sensitive element, is installed at the inlet into the regulator. When fluid passes through it, a pressure difference  $\Delta p_d$  appears and acts on piston 2. The size of the throttling slot 3 is basically determined by the ratio of the pressure force on piston 2 and the force of spring 4. When the flow rate increases, the pressure on the piston rises, and the piston, together with slidevalve 5, moves to the left, increasing the size of the throttling slot. On a decrease in flow rate, the slidevalve and piston move in the opposite direction.

Construction of the regulator's static characteristic in the form of a curve of  $Q$  as a function of the pressure drop  $\Delta p_{reg}$  across the regulator requires simultaneous solution of the following five equations.

1. The equation of the flow rate through the diaphragm:

$$Q = \mu_d S_d \sqrt{2g \frac{\Delta p_A}{\gamma}}$$

where  $\mu_d$  and  $S_d$  are the flow rate coefficient and hole area of the diaphragm.

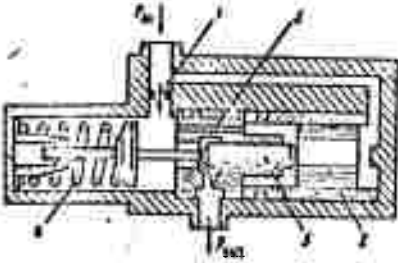


Fig. 217. Diagram of flow regulator.

2. The equation of the flow rate through the throttling slot:

$$Q = \mu_{shch} S_{shch} \sqrt{2g \frac{\Delta p_{shch}}{\gamma}}$$

where  $\mu_{shch}$  and  $S_{shch}$  are the flow rate coefficient and area of the throttling slot;  $\Delta p_{shch}$  is the pressure drop across the throttling slot.

3. The equilibrium equation of the piston and slidevalve:

$$P_{sp0} - Cx - \Delta p_A S_p - P_z = 0,$$

where  $P_{sp0}$  is the spring force at  $x = 0$ , when  $S_{shch} = (S_{shch})_{min}$ ;  $C$  is the spring stiffness;  $S_p$  is the piston area;  $P_z$  is the unbalanced pressure force on the slidevalve.

4. The pressure drop across the regulator as the sum of the pressure drops across the diaphragm and in the slot:

$$\Delta p_{reg} = \Delta p_A + \Delta p_{shch}$$

5. Law of variation of slot area with slidevalve stroke (for tapered shape of slidevalve in slot):

$$S_{shch} = (S_{shch})_{min} + \pi d s \sin \alpha x.$$

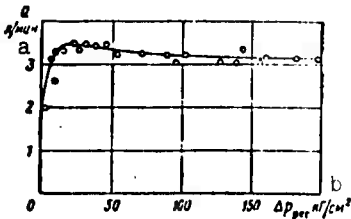


Fig. 218. Characteristic of flow rate regulator. KEY: (a) 1/min; (b) kgf/cm<sup>2</sup>.

The slidevalve must have a special profile in order to obtain more precise regulation of flow rate constancy.

Figure 218 shows the typical form of a static regulator characteristic as plotted by the method of A.V. Polozov, together with the experimental points. With  $\Delta p_{reg} < 15$  kgf/cm<sup>2</sup>, flow rate is not regulated; the regulator functions as a simple choke because  $S_{shch} = (S_{shch})_{min} = \text{const}$ . With the

subsequent increase of the gradient  $\Delta p_{reg}$  to 200 kgf/cm<sup>2</sup>, flow rate diminishes by about 10%.

The divider valve, flow divider, or metering valve is another flow rate regulator that operates on the valve principle and is used to maintain a given relationship among working-fluid flow rates in several parallel flows when they are divided. A requirement for such flow division arises in aircraft hydraulic systems when it is necessary to synchronize the operation of two or more hydraulic motors, e.g., hydraulic cylinders for operation of flaps, slats, or airbrakes.

A diagram of a divider valve designed to split the flow into halves appears in Fig. 219. The flow is divided immediately upon entry into the unit (see arrows); then each flow passes through a fixed multistage choke 1 and enters sleeve 2, which holds floating piston 3. The latter acts as a valve, moving in one direction or the other in accordance with the pressure difference acting upon it. This pressure difference arises when, as a result of load differences, the fluid flow in one branch differs from that in the other and, consequently, the pressure loss in one throttle is greater than in the other. Moving in the direction of the lower pressure, e.g., to the right, piston 3 reduces the area of holes 5 and increases the area of holes 4. The piston stops when the pressures in the right and left chambers of the sleeve and, consequently, the flow rates through these chambers have become equal.

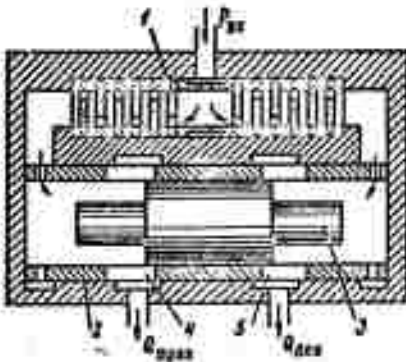


Fig. 219. Diagram of divider valve (metering valve).

To evaluate the flow rate error of such a divider, let us write the equation of the flow rate through a fixed choke.

$$Q = \mu S \sqrt{2g \frac{\Delta p_{sp}}{\gamma}} = C \sqrt{\Delta p_{sp}}$$

Since the variable exit orifice is fully opened in the more heavily loaded branch and does not offer an additional resistance the pressure drop  $\Delta p_{dr}$  across the choke can be assumed equal to that across the divider:  $\Delta p_{dr} = \Delta p_d = p_{vkh} - p_{vykh}$ .

We differentiate the above equation with respect to  $\Delta p_d$  and solve the result simultaneously with the initial equation. After converting to finite differences, which we shall denote by the letter  $\delta$ , we obtain

$$\frac{\delta Q}{Q} = \frac{C^2}{2} \frac{\delta(\Delta p_d)}{Q^2} = \frac{\delta(\Delta p_d)}{2\Delta p_d}$$

Thus, the relative flow rate error of the divider is inversely proportional to the pressure drop  $\Delta p_d = \Delta p_{dr}$  or to the square of flow rate. Consequently, it is necessary to increase the resistance coefficient  $\zeta_{dr}$  of the choke in order to improve the precision of division.

Since the floating piston 3 is acted upon only by pressure and friction forces, we can write

$$\delta(\Delta p_x) = \Delta p_{tr},$$

where  $\Delta p_{tr}$  is the pressure difference across the piston necessary to overcome friction and start it moving.

Thus the error equation can be written

$$\frac{\delta Q}{Q} = \frac{\Delta p_{tr}}{2\Delta p_x}. \quad (14.12)$$

This means that friction is the only cause of the flow-division error.

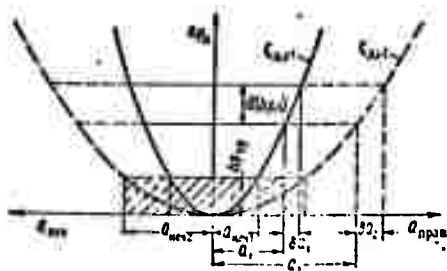


Fig. 220. Characteristic of metering-valve sensitive element.

As flow rate diminishes, the flow-division error rises substantially. It follows from the above that  $\delta Q/Q = 1$  at  $\Delta p_{tr} = 2\Delta p_d$ . This last equality defines the flow rate sensitivity limit of a flowmeter, i.e., the flow rate at which (and below which) the divider is insensitive to flow rate change:

$$Q_{min} \leq \mu S \sqrt{2g \frac{\Delta p_{tr}}{\gamma}}.$$

Figure 220 shows curves of  $\Delta p_d$  as a function of  $Q_{prav}$  and  $Q_{lev}$  for two choke resistance coefficients  $\zeta_{dr1}$  and  $\zeta_{dr2}$ , with  $\zeta_{dr1} > \zeta_{dr2}$ . The corresponding insensitivity ranges of the divider are indicated by the cross hatching (solid and broken lines).

It must be remembered that this flow divider is not reversible, i.e., it cannot combine flows in a given (1:1) ratio. It is easily seen that when the directions of the fluid flows are reversed, the difference between the flow rates will increase and the branch with the lower flow rate may even close completely. For this reason, two independent units - a flow divider and a flow adder - are installed in actuator mains of hydraulic systems when it is necessary to synchronize hydraulic-motor operation; one of these units is automatically shut off when the other is operating. Sometimes a reversible divider is used in the form of a single unit with a system of check valves and a special floating-piston design that provides for regulation of the flow rates in either direction.

Division can be accomplished with higher precision if the fixed choke in the divider is replaced by a variable choke that operates on the valve principle. However, this divider will not be considered here.

The batchmeter, a diagram of which appears in Fig. 221, can perform either of two functions. The first, protective function is to shut off the flow of fluid to a damaged section of pipeline and thereby prevent expulsion of fluid from the system. At the normal flow rate through the batchmeter, the pressure drop in chambers a and b due to the resistance of holes 1 is not enough to compress spring 2. However, when the flow rate increases excessively owing to rupture of a pipeline, this gradient increases and acts on the piston, which compresses spring 2 and closes hole 4 with valve 3. When the fluid stops moving, the pressure on the right of the valve has become equal to the pressure developed by the pump, while that on the left is equal to atmospheric, and the valve is held in the closed position.

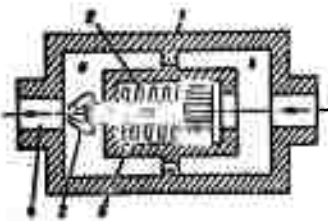


Fig. 221. Diagram of batchmeter.

Thus, the batchmeter performs the function of a flow regulator or limiter. The maximum flow rate at which the valve closes can be found from the equations

$$Q_{\max} = \mu S_0 \sqrt{2g \frac{\Delta p}{\gamma}},$$

$$\Delta p S_p = P_{\text{pr}0} + C x_{\max},$$

where  $\mu$  is the flow rate coefficient of holes 1;  $S_0$  is the total area of these holes;  $S_p$  is the piston area;  $\Delta p$  is the pressure drop across the piston;  $P_{\text{pr}0}$  is the spring force pressing the piston against its stop;  $x_{\max}$  is the maximum piston travel.

The second possible function of this unit, and the one from which it gets its name, consists in batching of fluid, i.e.,

passing a definite fluid volume when a flow rate  $Q > Q_{max}$  is delivered to the valve. The volume batched through will be equal to the volume displaced by the piston through jet tube 5 plus a certain amount of fluid that manages to get through hole 1 and the valve before the latter closes.

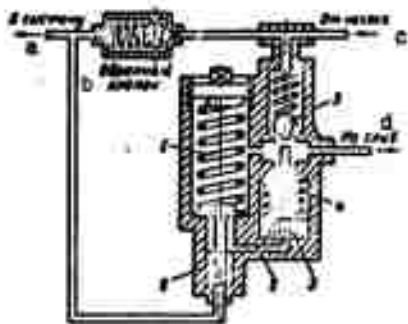


Fig. 222. Diagram of automatic pump-relief valve.  
KEY: (a) to system; (b) check valve; (c) from pump; (d) return.

open ball valve 5. Working fluid from the pump passes under this valve and is returned. The pump goes into no-load operation. When the system pressure drops to the minimum  $p_{min}$  as a result of seepage, spring 1 extends and piston 6 moves down to open valve 2 to the return line. Piston 4 descends and valve 5 closes; the pump delivery is again directed into the system.

The pressures  $p_{max}$  and  $p_{min}$  determine the basic dimensions of the automatic relief system and the characteristics of springs 1 and 4.

The maximum and minimum spring forces 1 can be found from  $P_{max}$ ,  $P_{min}$ , and the area  $S_6$  of piston 6:

$$P_{max} = (p_{s1} - p'_{s1})S_6 \quad \text{and} \quad P_{min} = (p_{s1} - p'_{s1})S_6$$

where  $p_{s1}$  and  $p'_{s1}$  are the return line pressures and the spring stiffness is determined as the quotient of the difference  $P_{max} - P_{min}$  divided by piston stroke, which is equal to the length of piston 6 plus the width of passage 2.

The maximum force ( $F_{max}$ ) of spring 4 depends on the pressures  $p_{max}$  and  $p_{s1}$ , the area of piston 3 ( $S_3$ ), the force of spring

7 (Q), which operates valve 5, and the area  $S_5$  of the seat of this valve, and can be found from the equation (without considering friction)

$$F_{\max} = (p_{\max} - p_{c2})S_3 - Q - (p_{\max} - p_{c2})S_5$$

The force  $F_{\min}$  must be large enough to overcome only the friction of the unloaded piston 3. The stroke of piston 3 must be such as to ensure wide enough opening of valve 5 and, consequently, minimum resistance of this valve. The stroke of piston 3 and the forces  $F_{\max}$  and  $F_{\min}$  determine the stiffness of spring 4.

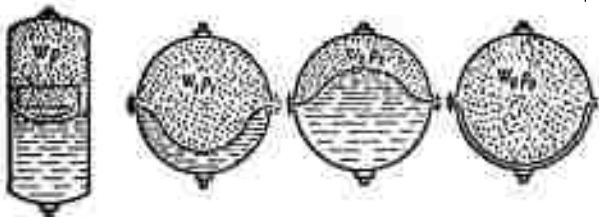


Fig. 223. Diagrams of pneumatic accumulators.

The hydraulic accumulator, whose function was indicated above, may be of the pneumatic or spring type. Spherical or cylindrical pneumatic accumulators are used most frequently in aviation hydraulic systems. In pneumatic accumulators, the gas must not come into contact with the fluid, since it would dissolve in it. As a rule, therefore, the accumulators have partitions in the form of pistons or membranes.

Cylindrical accumulators are most frequently of the piston type, while the spherical ones are always diaphragmed (Fig. 223).

When the accumulator is charged, the gas is compressed, its temperature rises, and the heat transfer through the wall to the environment increases. The reverse takes place during discharging: expansion of the gas, lowering of the temperature, and an inflow of heat from the outside. The charging and discharging times are usually reckoned in seconds. As a result, the compression and expansion processes of the gas cannot be adiabatic any more than they are isothermal. Experiments have shown that these processes are actually intermediate, i.e., polytropic with a variable polytropic exponent of the order of  $n = 1.1-1.2$ . The expansion and compression process is often assumed to be isothermal to simplify calculations.

The basic operating parameters of an accumulator are the pressures at the beginning ( $p_{\min} = p_1$ ) and end of charging ( $p_{\max} = p_2$ ), the total (design) volume  $W_0$  of the accumulator, the

initial pressure  $p_0$  in it when it is filled only with gas, and its useful volume, which equals the difference  $W_p = W_1 - W_2$ , where  $W_1$  and  $W_2$  are the volumes of the gas at pressures  $p_1$  and  $p_2$ .

A relation between these parameters is easily obtained by writing the following approximate polytrope equations (see Fig. 223):

$$\frac{W_1}{W_0} = \left(\frac{p_0}{p_1}\right)^{\frac{1}{n}} \quad \text{and} \quad \frac{W_2}{W_0} = \left(\frac{p_0}{p_2}\right)^{\frac{1}{n}}.$$

From this

$$\frac{W_p}{W_0} = \frac{W_1 - W_2}{W_0} = \left(\frac{p_0}{p_1}\right)^{\frac{1}{n}} - \left(\frac{p_0}{p_2}\right)^{\frac{1}{n}}$$

or

$$\frac{W_p}{W_0} = \left(\frac{p_0}{p_2}\right)^{\frac{1}{n}} \left[ \left(\frac{p_2}{p_1}\right)^{\frac{1}{n}} - 1 \right]. \quad (14.13)$$

In the isothermal process,  $n = 1$ , and the above expression is simplified.

The pressure  $p_2 = p_{\max}$  is determined by the head capacity of the pump and the pressure limit established for the particular hydraulic system. In a system with an unregulated pump and an automatic relief unit, the pressure  $p_1 = p_{\min}$  is determined by the time interval between switching of the pump off and on and by the demand for fluid. In these systems, we usually have  $p_2 = (1.25-1.65)p_1$  (for further details, see [9]).

In hydraulic systems with regulated pumps,  $p_1$  is less determinate, since it depends on the maximum working-fluid flow rate, the time for which it is in demand, and other factors.

As we see from (14.13), it is advisable to make the initial pressure  $p_0$  as high as possible, i.e., approximate it to  $p_1$ , in order to increase the useful volume  $W_p$  of the accumulator for given  $p_1$  and  $p_2$ . In practice, therefore, it is usually assumed that

$$p_0 = (0.9-1.0)p_1.$$

Energy capacity is an important characteristic of any accumulator. Let us find the reserve of energy of a pneumatic accumulator of volume  $W_0$  when it is charged to pressure  $p_2$  and can be discharged to a pressure  $p_1$ . We shall assume the expansion of the gas in the accumulator to be isothermal.

The elementary energy (or work) equals

$$dE = p dW = W_0 p_0 \frac{dW}{W}.$$

After integrating from  $W = W_2$  to  $W = W_1$ , we have

$$E = W_0 p_0 \ln \frac{W_1}{W_2} = W_0 p_0 \ln \frac{p_2}{p_1}.$$

Thus, like the useful volume of the accumulator, the energy capacity increases in proportion to the initial pressure  $p_0$ ; it is therefore advantageous to set  $p_0 = p_1$ . We then have

$$E = W_0 p_1 \ln \frac{p_2}{p_1}.$$

If we assume that the maximum pressure  $p_2$  and the accumulator volume  $W_0$  are given, we can find  $p_1$  (or  $p_2/p_1$ ) from the above formula; the maximum energy store will correspond to this pressure. Assuming  $W_0$  and  $p_2$  constant, we find the derivative  $dE/dp_1$  and equate it to zero:

$$\frac{dE}{dp_1} = W_0 (\ln p_2 - \ln p_1 - 1) = 0$$

or

$$\ln \frac{p_2}{p_1} = 1.$$

Hence the optimum pressure ratio

$$\left(\frac{p_2}{p_1}\right)_{opt} = e = 2.72.$$

In practice, as we noted above, it is usually necessary to use pressure ratios  $p_2/p_1$  that are substantially smaller than the optimum, since operational conditions prohibit excessive lowering of the pressure. In certain cases, however, as in airbrake hydraulic systems, it is necessary to have a comparatively moderate pressure in the actuating mechanisms; for this reason, the accumulators have a substantially wider pressure range and the ratio  $p_2/p_1$  often even exceeds the optimum.

The filters used in aircraft hydraulic systems are classified as coarse and final filters. The former have comparatively low hydraulic resistance and are therefore usually installed at the beginning of the intake main, in the tank. They are made in the form of screen or plate units and are capable of trapping particles down to 50-100  $\mu\text{m}$  in size.

Final filters offer substantial hydraulic resistance (see Fig. 89); they can therefore be installed only in delivery lines or directly behind the pump, or else before the most critical actuator mechanisms, those requiring highly purified fluid, such as hydraulic boosters.

The element of a fine filter is made of felt, serge-woven metal mesh, paper, or some other porous material. Such filtering elements trap particles in the size range from 5 to 15  $\mu\text{m}$  and up.

Because of the small size of the pores in the filtering elements and, consequently, the small Reynolds numbers of flows in these pores, the pressure gradient across a fine filter is usually linear, and the resistance coefficient of such a filter is inversely proportional to  $Re$ .

For more detailed information on filtration of the working fluid in aircraft hydraulic systems and on filters, we refer the reader to [5].

### §73. ROTARY DISPLACEMENT-TYPE HYDRAULIC TRANSMISSIONS

Hydraulic transmissions for rotary motion (like pumps) are classified as hydrodynamic (impeller) or displacement (hydrostatic) types. We shall examine the latter type first and in greater detail.

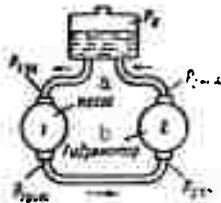


Fig. 224. Diagram of rotary displacement hydraulic transmission.  
KEY: (a) pump; (b) hydraulic motor.

The rotary-displacement hydraulic transmission is a combination of a pump and a rotor-displacement hydraulic motor. In design, the motor is simply another converted pump. All displacement rotor pumps have the property of reversibility, i.e., they can be used either as pumps or as hydraulic motors. This means that if fluid is supplied to a rotor pump under enough pressure, its rotor will turn and perform work.

The basic advantage of the rotary-action hydraulic transmission over the conventional mechanical transmission is the possibility of smooth (stepless) variation of transmission ratio and torque conversion, as will be shown below.

Figure 224 is a schematic diagram of a so-called simple displacement-rotor hydraulic transmission (hydraulic drive), i.e., a pump, hydraulic motor, and fluid tank connected together by pipelines. The tank included in the system is necessary to compensate external fluid leakage and temperature changes in the volume of the fluid, and also to hold down heating of the fluid during operation. In addition, the elevated air pressure in the tank provides the necessary intake-line conditions to prevent cavitation in the pump.

It is possible to build a closed-type hydraulic transmission, i.e., one with no tank in the main fluid-circulation system.

However, this is detrimental to fluid-cooling conditions. A pressurized tank or a tank with a booster pump must then be connected to the intake line, in much the same way as was indicated for the closed pipeline (see Fig. 143).

Let us examine the fundamental relationships for a hydraulic transmission operating on the scheme indicated, using the subscript 1 for quantities pertaining to the pump and 2 for the hydraulic motor.

The useful pump delivery equals the actual flow rate through the hydraulic motor, i.e.,

$$Q_1 = Q_2, \quad (14.14)$$

Let us convert from actual to theoretical flow rates and take into account that the actual flow rate through the motor is greater than the theoretical rate, since the leakage in the motor has the same direction as the main flow. We have instead of Formula (14.14)

$$Q_{t1} \eta_{o1} = \frac{Q_{t2}}{\eta_{o2}},$$

where  $\eta_{o1}$  is the volumetric efficiency of the pump;  $\eta_{o2}$  is the volumetric efficiency of the motor, which, unlike  $\eta_{o1}$ , is usually defined as the ratio of the theoretical flow rate to the actual flow rate.

Hence the volumetric efficiency of the entire hydraulic transmission ( $\eta_{o.per}$ ) will equal

$$\eta_{o.per} = \eta_{o1} \eta_{o2} = \frac{Q_{t2}}{Q_{t1}}. \quad (14.15)$$

Assuming that the pump and motor can be regulated, let us introduce the coefficient of regulation  $\psi$ , which equals  $e/e_{max}$  for pumps and rotors with eccentric motors (see §67) and  $-(\tan \gamma / \tan \gamma_{max})$  for rotary-plunger hydraulic machines with inclined plates (blocks).<sup>6</sup> Obviously, the coefficients  $\psi$  can vary from 0 to 1 during regulation of the machines.

Then, expressing the theoretical flow rates in terms of the maximum working volumes  $W$ , the coefficients  $\psi$ , and the speeds  $n$ , we obtain

$$\eta_{o.per} = \frac{\psi_2 W_2 n_2}{\psi_1 W_1 n_1} = \frac{\psi_2 W_2}{\psi_1 W_1} \frac{1}{i}, \quad (14.16')$$

where  $i$  is the transmission ratio and equals

$$i = \frac{n_1}{n_2} = \frac{\psi_2 W_2}{\psi_1 W_1} \frac{1}{\eta_{o.per}}. \quad (14.16)$$

<sup>6</sup>See page 367 for footnote.

Owing to the hydraulic losses in the pipelines connecting the pump, motor, and tank, the pressure developed by the pump ( $p_1$ ) will be greater than the pressure used by the motor ( $p_2$ ). The ratio of the latter to the former is known as the hydraulic efficiency of the drive, i.e.,

$$\eta_{\text{recp}} = \frac{p_2}{p_1}. \quad (14.17)$$

It must be remembered that here (see Fig. 224)

$$p_2 = p_{212} + p_{2012};$$

$$p_1 = p_{1121} + p_{1021}.$$

Subtracting the first equation from the second, we obtain

$$p_1 - p_2 = (p_{1021} - p_{2012}) + (p_{212} - p_{121}) = \sum p_{1p},$$

i.e., the difference between the pressure developed by the pump and the pressure used by the motor equals the total pressure loss in the pipelines (in the delivery, intake, and return lines).

Let us now write the energy equations for the pump and motor, i.e., expressions for the power used to turn the pump ( $N_1$ ) and the power developed by the motor ( $N_2$ ). Applying (12.4), we have for the pump

$$N_1 = M_1 \omega_1 = \frac{p_1 Q_1}{\eta_{01} \eta_{m1}}, \quad (14.18)$$

and for the motor

$$N_2 = M_2 \omega_2 = p_2 Q_2 \eta_{02} \eta_{m2}, \quad (14.19)$$

where the  $M$  are the torques, the  $\omega$  are the angular velocities, and the  $\eta_m$  are the mechanical efficiencies, which take account of friction in the machines.

The hydraulic efficiencies of rotor-type hydraulic machines, both pumps and motors, are usually considered equal to unity, since the basic losses in these machines are volumetric and mechanical; the hydraulic losses are included in the mechanical losses.

Dividing the second equation by the first, we find the overall efficiency of the drive, which, on the one hand, will equal

$$\eta_{\text{recp}} = \frac{N_2}{N_1} = \frac{M_2 \omega_2}{M_1 \omega_1} = \frac{k}{i}, \quad (14.20)$$

where  $k$  is the torque conversion ratio.

On the other hand, applying (14.14) and (14.17), we obtain by the same division

$$\eta_{\text{неп}} = \frac{P_2}{P_1} \eta_{01} \eta_{02} \eta_{\text{м1}} \eta_{\text{м2}} = \eta_{\text{г}} \eta_{\text{неп}} \eta_{\text{о}} \eta_{\text{неп}} \eta_{\text{м}} \eta_{\text{неп}} = \eta_{\text{г}} \eta_1 \eta_2 \quad (14.21)$$

i.e., the over-all efficiency of the hydraulic transmission is equal to the product of its hydraulic, volumetric, and mechanical efficiencies or to the product of the hydraulic efficiency (with consideration of losses in the connecting lines) by the over-all efficiency of the pump and the over-all efficiency of the motor.

The over-all efficiencies of rotor-type hydraulic transmissions vary from 0.7 to 0.85.

One of the following methods can be used to regulate hydraulic transmissions in order to change the transmission ratio  $\underline{i}$  and the torque conversion ratio  $\underline{k}$ :

- 1) regulation of the pump, i.e., changing its eccentricity or block inclination;
- 2) regulation of the hydraulic motor, i.e., changing its eccentricity or block inclination;
- 3) bleeding out of the pump's delivery through a valve.

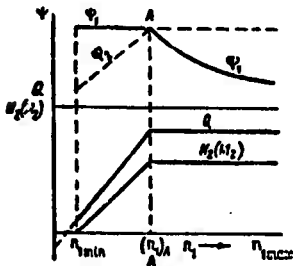


Fig. 225. Regulation diagram of hydraulic transmission.

The first regulation method is most frequently used, and the hydraulic transmission consists of a regulated pump and an unregulated hydraulic motor. Use of the second control method may be expedient as a supplement to the first. Both of the hydraulic machines forming the transmission in this case must be adjustable. The third regulation method is uneconomical, and its use can be defended only when the hydraulic transmission operates for short times.

The most important example of use of rotary-displacement hydraulic transmissions on aircraft is found in the hydraulic transmission from the engines to the stable-frequency alternators. The latter must turn at constant speed despite variations in engine speed and in the load on the electrical system. Under these conditions, the speed of the hydraulic motor connected to the generator  $n_2 = \text{const}$ , while that of the pump,  $n_1$ , varies in a certain range, depending on the type of engine. Consequently, the transmission ratio of the hydraulic drive must vary smoothly and, in addition, automatically.

Figure 225 shows a diagram of hydraulic-drive regulation for this example, i.e., the dependence of the coefficients  $\psi_1$  and  $\psi_2$ ,

the flow rate  $Q$ , and the power  $N_2$  (and the torque  $M_2$ ) at constant pressure and speed  $n_2$ , on the speed  $n_1$  of the drive (pump) shaft.

The vertical line A-A corresponds to the case in which both hydraulic machines have their largest working volumes, i.e.,  $\psi_1 = \psi_2 = 1$ . To the right of vertical A-A, we have the range of pump regulation, where the coefficient  $\psi_1$  decreases hyperbolically [see Formula (14.16)], and to the left of vertical A-A the range of hydraulic-motor regulation, where the coefficient  $\psi_2$  increases linearly.

The flow rate is determined by the relationship

$$Q = \psi_1 W_1 n_1 - \psi_2 W_2 n_2 + q,$$

and, consequently, is represented on the diagram for constant  $p_1 = p_2 = p$  as a straight line with an inflection at line A-A. This means that flow rate remains constant when the pump is regulated and diminishes linearly when the hydraulic motor is regulated.

The useful power  $N_2$  of the hydraulic motor, which is determined by Formula (14.19), is represented in about the same way as the flow rate with the assumptions that we have adopted, and its torque in exactly the same way as the power.

The minimum drive-shaft speed  $n_{1\min}$  and  $\psi_{2\min}$  are determined by the self-braking of the hydraulic motor, i.e., by the equality  $M_2 = 0$ .

The maximum speed  $n_{1\max}$  and  $\psi_{1\min}$  are determined by the upper-limit service speed of the pump. For modern rotary-plunger pumps, it can be assumed that  $n_{1\max} \approx 4500$  rev/min.

Applying Eq. (14.16) to the transmission operating mode in which  $\psi_1 = \psi_2 = 1$  and  $n_1 = (n_1)_A$ , and then to the regime of maximum pump speed  $n_{1\max}$ , we obtain after dividing one equation by the other

$$\frac{n_{1\max}}{(n_1)_A} = \frac{1}{(\psi_1)_{\min}}.$$

This speed ratio is known as the range of speed regulation with preservation of constant power.

If we assume that, as is frequently the case,  $n_2 = (n_1)_{\max}$ , we obtain from the same equation (14.16)

$$(\psi_1)_{\min} = \frac{W_2 n_2}{W_1 (n_1)_{\max}} \frac{1}{\eta_o} = \frac{W_2}{W_1} \frac{1}{\eta_o}$$

or

$$\frac{n_{1max}}{(n_1)_A} = \frac{W_1}{W_2} \eta_o.$$

Thus, if we wish to provide a range of constant-power regulation of, say, two, the working volume of the pump must be approximately two times that of the hydraulic motor.

The above makes it clear that the range of speed variations can be broadened by regulating the hydraulic motor, but then power no longer remains constant.

#### §74. HYDRAULIC-MECHANICAL TRANSMISSIONS

A hydraulic-mechanical transmission is a geared differential mechanism the two elements of which are connected by a hydraulic transmission. In such devices, most of the power is usually transmitted mechanically, and only a certain part of the total power in one direction or the other through the hydraulic transmission.

Let us consider the operating principle of hydraulic-mechanical transmissions in which the hydraulic section consists of two displacement-rotor-type hydraulic machines.

Use of such a device makes it possible to increase the overall efficiency of a transmission and lower its weight and bulk by comparison with the simple displacement-type hydraulic transmission.

In the design operating mode of a hydraulic-mechanical transmission (at the design drive-shaft rpm), all of the power is transmitted through the mechanical part with maximum efficiency, and the hydraulic transmission merely produces the necessary torque on the idle element of the differential mechanism. The greater the deviation of drive-shaft rpm from the design figure, the greater is the amount of power transmitted hydraulically.

The hydraulic-mechanical transmission, together with an appropriate automatic control system that varies the working volume of one of the hydraulic transmission's machines, makes up the so-called hydraulic-mechanical drive. This drive is capable of holding driven-shaft speed constant when the drive-shaft speed and the load on the driven shaft are variables. Precisely this requirement arises on aircraft carrying stable-frequency alternators. As we indicated in §73, the latter must run at strictly constant speed as the rpm of the engine and the load vary. For this reason, the hydraulic-mechanical drive is coming into steadily increasing use on aircraft with stable-frequency alternating-current electrical systems whose generators have powers above 15-20 kW.

The differential mechanism has three external shafts and three elements: the driving element, which is connected to the drive-motor shaft, the driven element, which is connected in our case to the generator shaft, and an auxiliary element connected

to one of the hydraulic machines forming the hydraulic transmission. At design drive-shaft (drive-element) rpm, the auxiliary element of the differential mechanism remains stationary, but when the rpm increase or decrease from the design value, this element and the hydraulic machine connected to it rotate in one direction or the other to supply or take off the necessary power.

The maximum power transmitted through a hydraulic transmission is determined by the range of drive-shaft speed variation and the selection of the design operating mode.

Variation of the load in the generator line causes a change in the torque on the drive's output shaft, and this, in turn, results in a proportional change in the working-fluid pressure of the hydraulic transmission.

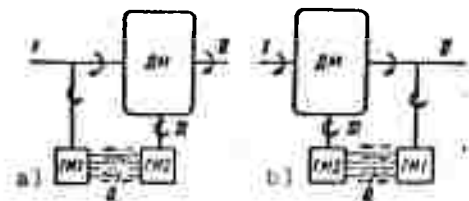


Fig. 226. Structural diagrams of hydraulic-mechanical transmissions.

There are very many possible different combinations of the differential mechanism with the hydraulic transmission, i.e., the shafts of the differential mechanisms can be connected in a variety of ways with the external shafts and the shafts of the hydraulic transmission. However, any of these variants can be classified into one of the following two basic hydraulic-mechanical-transmission design layouts, which we shall call schemes a and b.

Scheme a (Fig. 226) is characterized by insertion of the hydraulic transmission between the driving I and auxiliary III shafts of the differential mechanism, i.e., by branching of the power at the drive shaft. Characteristic of scheme b is insertion of the hydraulic transmission between the auxiliary III and driven II shafts, i.e., branching of the power on the driven shaft.

On the conventional diagrams shown here, DM is a differential mechanism, GM1 is a hydraulic machine connected to the driving or driven shafts, and GM2 is a hydraulic machine connected to the auxiliary shaft of the differential mechanism. Machine GM1 is nonreversible and must be regulated, i.e., its working volume must be varied automatically; machine GM2 is generally reversible and may be unregulated. Each of these hydraulic machines can operate either as a pump or as a hydromotor, e.g., when the first

operates as a pump, the second works as a motor, and vice versa.

An energy analysis of these schemes indicate that preference should be given to scheme a as a drive for aircraft alternators, since it requires regulation of only the one hydraulic machine GM1 and has better data from the standpoint of uniformity of hydraulic-transmission loading at the operating extremes. In practice, however, hydraulic-mechanical transmissions (drives) patterned after both scheme a and scheme b are used.

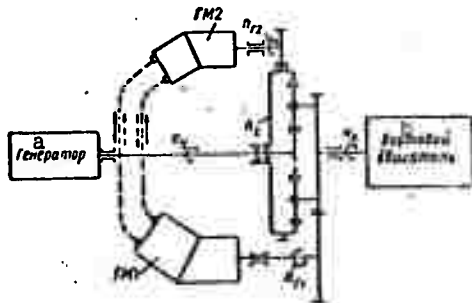


Fig. 227. One of the layout variations of the scheme-a hydraulic-mechanical transmission.  
KEY: (a) generator; (b) auxiliary motor.

Figure 227 shows one of the six possible variations of external-shaft connection to the elements of the differential mechanism in scheme a, in which the driving shaft (from the auxiliary motor) is connected to the planet carrier and the driven shaft (generator shaft) to the sun gear, while the auxiliary shaft is that of the crown gear connected to hydraulic machine GM2.

The regulated hydraulic machine GM1 is connected by a gear transmission to the auxiliary-motor shaft, and by pipelines (dashed lines on the diagram) to hydraulic machine GM2.

The unit operates as follows in response to a change in drive-shaft rpm  $n_x$ .

At a certain intermediate design rpm  $n_x = n'_x$ , hydraulic machine GM1 has a coefficient of regulation (see §73)  $\psi = \psi'$ , at which it provides only for compensation of seepage in the system and maintains the necessary pressure, but does not deliver fluid to machine GM2 ( $Q = 0$ ). As a result, the rotor of machine GM2 is stationary and, consequently, so is the crown gear. All power is transmitted to the generator mechanically. The speed of the sun gear and generator is  $n_y$ .

When  $n_x < n'_x$ ,  $\psi > \psi'$  and machine GM1 functions as a pump, delivering fluid to machine GM2. The latter, operating in the motor mode, turns the crown gear in such a way that the speeds of the sun gear and generator remain the same at  $n_y = \text{const}$ . The missing power is supplied to the generator shaft hydraulically.

When  $n_x > n'_x$ ,  $\psi < \psi'$ , the inclined disk of machine GM1 (or the cylinder block) is inclined in the other direction and machine GM1 now functions as a hydraulic motor, receiving fluid under pressure from machine GM2, which operates as a pump.

Machine GM2 and the crown gear turn in the opposite direction, holding generator speed constant. The excess power from the generator shaft is now diverted hydraulically.

The automatic control system of this drive has a device that responds to a change in generator speed or current frequency and sends appropriate signals to an amplifier. The latter controls hydraulic machine GM1 by varying its coefficient of regulation  $\psi$  and hence also its working volume. When  $n_x = n_x \text{ min}$ ,  $\psi = 1$ , i.e., the working volume  $W_1$  of machine GM1 has its maximum value. As  $n_x$  increases,  $W_1$  diminishes; near the design mode ( $n_x = n'_x$ ),  $W_1$  vanishes at  $\psi = 0$  and then assumes negative values with  $\psi < 0$ , indicating transition from the pump to the motor mode.

As we noted above, use of a hydraulic-mechanical drive, e.g., for aircraft alternators, makes it possible to obtain a substantial efficiency increase by comparison with the simple hydraulic drive. Heating of the working fluid is substantially reduced as a result.

In addition, the dimensions and weight of the hydraulic-mechanical drive are smaller than those of the simple hydraulic drive. The differential mechanism can usually be made quite compact, and the hydraulic section is relatively small in size because only part of the nominal drive power is transmitted through it.

For the theoretical fundamentals and design of hydraulic-mechanical transmissions, the reader is referred to [21] and the author's other works.

#### §75. VANE-WHEEL HYDRAULIC TRANSMISSIONS (HYDRODYNAMIC TRANSMISSIONS)

A hydrodynamic (vane-wheel or impeller) transmission is a combination of impeller-type hydraulic machines - a centrifugal pump and a hydraulic turbine - whose rotors are brought as close together as possible and housed coaxially in a common casing.

Hydrodynamic transmissions are subclassified as hydraulic clutches (hydraulic couplings) and hydraulic converters. The

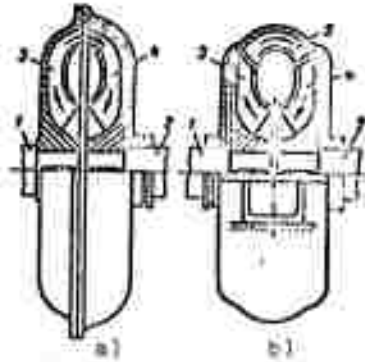


Fig. 228. Diagrams of vane-wheel (hydrodynamic) transmissions.

fundamental difference between them is that the former do not change torque when they transmit power, while the latter increase or decrease it, i.e., they convert torque.

A diagram of a hydraulic coupling appears in Fig. 228, where 1 is the driving shaft, 2 is the driven shaft, 3 is the pump rotor, and 4 is the turbine rotor. On rotation of the pump rotor, which is rigidly attached to the driving shaft, fluid shifts toward the periphery and is slung off into the turbine rotor.

The flow acts powerfully on the vanes of the turbine rotor and yields the energy that it acquired in the pump rotor to the driven shaft. Thus, fluid circulates continuously in the closed working space of the hydraulic coupling, and power is transmitted from one shaft to the other without a solid coupling between them.

If we disregard friction between the outer surfaces of the rotors and the fluid, we can assume that the torques on the driving and driven shafts are equal, i.e.,

$$M_1 = M_2, \quad (14.22)$$

and that the efficiency  $\eta_{gm}$  of the hydraulic coupling is determined by the speed ratio:

$$\eta_{gm} = \frac{n_2}{n_1} = \frac{1}{i}. \quad (14.23)$$

The difference between unity and the coupling's efficiency is known as the slip ratio, i.e.,

$$s = 1 - \eta_{gm}.$$

Usually, hydraulic couplings are designed in such a way that the slip  $s$  is only a few percent (for example, 2-4%) in the steady-state design operating mode, while the transmission ratio and the efficiency  $\eta_{gm}$  are close to unity. Usually, when the torque to be transmitted increases above the design torque, i.e., when the coupling is overloaded, slip increases, the speed of the turbine rotor decreases, and the efficiency  $\eta_{gm}$  declines.

Hydraulic converters are used when it is necessary to transmit power with a change in torque and at transmission ratios substantially different from unity, but without an unacceptable sacrifice of efficiency. Characteristically, an impeller-type hydraulic converter has a fixed guide-vane assembly or stator 5 (see Fig.

228b), i.e., an additional impeller wheel that is rigidly attached to the casing, between the pump and turbine rotors.

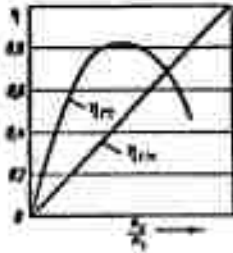


Fig. 229. Efficiencies of hydraulic coupling and hydraulic converter as functions of  $n_2/n_1$ .

Instead of (14.22), we have for the hydraulic converter

$$M_1 + M_{n.a} = M_2,$$

where  $M_{n.a}$  is the reaction torque that arises on the stator vanes.

In the above notation, the torque  $M_{n.a}$  is positive when the converter is used to reduce speed and increase torque as it transmits power, and negative in the opposite case. In the former case, therefore, the stator increases the twist imparted to the flow by the impeller, increasing  $M$ , while in the latter case it reduces this twist.

The following expression for efficiency applies for the hydraulic converter,<sup>7</sup> just as it does for a rotary-displacement hydraulic transmission:

$$\eta_{gt} = \frac{M_2 n_2}{M_1 n_1}.$$

or, introducing the torque conversion ratio  $k$ ,

$$\eta_{gt} = \frac{k}{i}.$$

Figure 229 shows the efficiencies of a hydraulic clutch ( $\eta_{gm}$ ) and a hydraulic converter ( $\eta_{gt}$ ) for  $k > 1$  as functions of the speed ratio  $n_2/n_1$ .

The former is represented by a straight line in accordance with (14.23), while the latter takes the form of a curve with a maximum at an  $n_2/n_1$  of about 0.5.

Comparison of these relationships indicates that the hydraulic converter is more economical than the hydraulic coupling at large transmission ratios  $i$  (small  $n_2/n_1$ ). On the other hand, the coupling becomes more economical as  $i$  approaches unity. However, the basic advantage of the hydraulic converter over the hydraulic clutch at large  $i$  consists in its ability to multiply torque, a requirement that arises in a number of practical cases.

Hydrodynamic transmissions are coming into increasing use on ground vehicles (automobiles, tractors, etc.) and aboard ships. In all of these cases, it is very important, as the vehicle moves

<sup>7</sup>See page 367 for footnote.

away from a standing start, to obtain an increase in the torque at the driven shaft over that on the drive shaft, and this is the function of the hydraulic converter. As the machine accelerates further, the transmission ratio of this drive decreases smoothly, and this is followed either by direct coupling of the engine shaft to the driven shaft or automatic conversion of the converter to a coupling (compound hydraulic transmission). This conversion is brought about by locking the stator to the pump (or turbine) rotor, so that it begins to turn as a single unit with the latter.

Hydrodynamic couplings are used in aviation engineering to transmit rotation from starter motors to the rotors of the main gas-turbine engines.

## Footnotes

Manu-  
script  
page

- 325       <sup>1</sup>Symbol usage on the diagram conforms to the GOST 1967 project. The arrow on the pump symbol indicates that it is regulated.
- 326       <sup>2</sup>No particular difficulty is encountered in taking fluid delivery from the accumulator into account, the more so since research [9] has shown that the expansion process of the air in the accumulator can be considered isothermal.
- 328       <sup>3</sup>Hydraulic-system calculations for nonsteady modes have been developed by Prof. P.I. Blandov (see collection "Voprosy proyektirovaniya gidrosistem letatel'nykh apparatov" [Problems in the design of aircraft hydraulic systems], Mashinostroyeniye, 1967).
- 341       <sup>4</sup>The experimental data were reduced by V.V. Shul'gin.
- 343       <sup>5</sup>A piston of the same diameter may be used instead of the membrane.
- 356       <sup>6</sup>If the plungers are set at an angle  $\phi$  to the axis of revolution, the coefficient  $\psi$  can be expressed in the same way without incurring major error.
- 365       <sup>7</sup>The rotary hydraulic transmissions described in §65 are also hydraulic converters, but of a different class - that of the rotary-displacement type.

## Symbol List

Manu- script page	Symbol		English equivalent
324	нас	nas	pump
324	сл	sl	return
326	ц	ts	cylinder
327	потр	potr	required
328	тр	tr	pipeline
328	ин	in	inertia
329	п	p	piston
331	вх	vkh	inlet
331	вых	vykh	outlet
335	опт	opt	optimum
344	пр	pr	spring
346	д	d	diaphragm
346	рег	reg	regulator
347	щ	shch	slot
347	з	z	slidevalve
348	прав	prav	right
348	лев	lev	left
348	др	dr	choke
349	тр	tr	friction
349	неч	nech	insensitive
353	п	p	useful
356	пер	per	transmission
356	т	t	theoretical
357	г	g	hydraulic
357	м	m	mechanical
361	ДМ	DM	differential mechanism
361	ГМ	GM	hydraulic machine

Symbol List (Cont'd.)

Manu- script page	Symbol		English equivalent
362	г	g	hydraulic machine
364	гм	gm	hydraulic coupling
365	н.а	n.a	guide-vane assembly, stator
365	гт	gt	hydraulic converter

## C H A P T E R   X V

### FUNDAMENTALS OF THE DESIGN OF GAS LINES

As we know, the basic difference between a gas and a dropping fluid is that the density and temperature of a gas change with pressure, while density usually remains constant in the case of a dropping fluid.

Thus, the laws of motion of a gas are more general than those of an incompressible fluid, and the latter can be derived from the former as a particular case by setting  $\rho = \text{const.}$

Naturally, the motion of a gas is described by substantially more complex equations than the motion of a liquid. This is clearly seen from the elementary continuity equation for a one-dimensional-steady state flow (the equation of gravimetric flow rate), which is written as follows for a gas:

$$G = S_1 v_1 \gamma_1 = S_2 v_2 \gamma_2 = \text{const.}$$

With a change in flow cross section, both velocity and pressure will change and, consequently, so will density; here, pressure and density usually increase with increasing velocity and vice versa. Consequently, velocity and density vary in opposite directions, with the result that a definite conclusion as to the relation between cross section and velocity can no longer be drawn from the flow rate equation.

It can be shown that for subsonic flows, the dependence of velocity on change in cross section remains qualitatively the same as for a fluid, while for supersonic flows the relationship

will be reversed, i.e., velocity will increase with an increase in cross section.

In the present chapter, we shall consider the simplest cases of outflow and pipe motion of a gas, assuming this motion to be uniform. This analysis will enable us to solve the problems of gas-line design with sufficient accuracy.

#### §76. EQUATION OF MOTION FOR AN INVISCID GAS

To obtain the fundamental equation of motion of an inviscid gas, which is analogous to the Bernoulli equation for an incompressible fluid, we shall use the differential equation in the form of (4.15')

$$g dz + \frac{1}{\rho} dp + \frac{1}{2} d(v^2) = 0. \quad (15.1)$$

We shall assume the gas to be ideal, i.e., subject to the equation of state

$$\frac{p}{\rho} = RT, \quad (15.1')$$

where R is the gas constant in the SI system of units and equals 287.14 m<sup>2</sup>·deg for air.

We shall disregard heat transfer between the flow of gas and the external environment, so that the variable density  $\rho$  of the gas can be related to pressure by the adiabatic (isentropic) equation

$$\rho = \rho_1 \left( \frac{p}{p_1} \right)^{\frac{1}{k}}, \quad (15.2)$$

where  $\rho_1$  and  $p_1$  are the density and pressure of the gas, respectively, in the initial section through the flow.

Integrating (15.1),

$$gz + \int \frac{dp}{\rho} + \frac{v^2}{2} = \text{const} \quad (\text{along a filament}), \quad (15.3')$$

where, with (15.2),

$$\int \frac{dp}{\rho} = \frac{p_1^{\frac{1}{k}}}{\rho_1} \int \frac{dp}{p^{\frac{1}{k}}} = \frac{k}{k-1} \frac{p_1^{\frac{1}{k}}}{\rho_1} p^{\frac{k-1}{k}}.$$

Since Formula (15.2) can be written

$$\frac{p_1^{\frac{1}{k}}}{\rho_1} = \frac{p^{\frac{1}{k}}}{\rho},$$

the above integral can be written

$$\int \frac{dP}{\rho} = \frac{k}{k-1} \frac{P}{\rho}.$$

On substituting into (15.3') and dividing by  $\rho$ , we have

$$z + \frac{k}{k-1} \frac{P}{\rho} + \frac{v^2}{2g} = \text{const.} \quad (15.3)$$

The second term in the left member of this equation can be broken up into two terms, as follows:

$$\frac{k}{k-1} \frac{P}{\rho} = \frac{P}{\rho} + \frac{1}{k-1} \frac{P}{\rho}$$

and the second summand expressed in terms of temperature by the equation of state:

$$\frac{1}{k-1} \frac{P}{\rho} = \frac{r}{\rho} + \frac{RT}{(k-1)g}.$$

Now Eq. (15.3) can be rewritten

$$z + \frac{P}{\rho} + \frac{v^2}{2g} + \frac{RT}{(k-1)g} = \text{const (along a filament)}. \quad (15.4)$$

Equation (15.4) differs from the Bernoulli equation for an incompressible ideal (inviscid) fluid in the presence of the term

$$\frac{RT}{(k-1)g}.$$

Applying the thermodynamic relationships for an ideal gas

$$R = c_p - c_v \quad \text{and} \quad k = \frac{c_p}{c_v}, \quad (15.5)$$

where  $c_p$  and  $c_v$  are the heat capacities of the gas at constant pressure and constant volume in the SI system, i.e., in J/kg·deg, we transform this term as follows:

$$\frac{RT}{(k-1)g} = \frac{c_p - c_v}{(k-1)g} T = \frac{c_v}{g} T = U \quad [J \cdot s^2 / \text{kg} \cdot \text{m} = J / N = \text{m}].$$

It is clear from the above that the term  $U$  represents the internal energy of a unit weight of gas (one Newton), and that the physical significance of (15.4) is analogous to that of the Bernoulli equation for the ideal incompressible fluid and consists in constancy of the total energy of the gas along a filament.

A fourth form of energy is added to the three forms considered earlier (see §16): internal energy, which must be taken into account in analysis of gas motion.

If we multiply (15.3) by  $g$ , it will express the total energy of the gas per unit of mass. The levelling heights  $z$  usually have very little influence on the variables of the gas, and are therefore usually omitted from (15.3). Equation (15.3), written for any two sections 1-1 and 2-2 of a filament, assumes the form

$$\frac{k}{k-1} \frac{p_1}{\rho_1} + \frac{v_1^2}{2} = \frac{k}{k-1} \frac{p_2}{\rho_2} + \frac{v_2^2}{2} = \frac{k}{k-1} \frac{p_0}{\rho_0}, \quad (15.6)$$

where  $p_0$  and  $\rho_0$  are the pressure and density of the gas at the stagnation point, i.e., at  $v = 0$ .

If it is necessary to know the temperature change of the gas that results from a change in its velocity, the above equation can be brought to the following form with the aid of the equation of state:

$$\frac{k}{k-1} RT_1 + \frac{v_1^2}{2} = \frac{k}{k-1} RT_2 + \frac{v_2^2}{2} = \frac{k}{k-1} RT_0. \quad (15.7)$$

where  $T_0$  is the stagnation temperature.

Applying (15.5), we can rewrite (15.7) in still another form:

$$i_1 + \frac{v_1^2}{2} = i_2 + \frac{v_2^2}{2} = i_0. \quad (15.8)$$

where  $i$  is the enthalpy of the gas and equals  $i = c_p T$ .

The above equations have been derived from the Euler differential equations on the assumption of adiabatic flow for a filament of inviscid ideal gas. However, it can be shown that Eq. (15.8) and its preceding forms are also valid for any adiabatic motion of a gas, even in the presence of friction. Disregarding the velocity-distribution nonuniformity, these equations are applied not only for filaments, but also for real gas flows. The only necessary conditions are the absence of heat exchange with the environment and validity of the equation of state.

#### §77. OUTFLOW OF GAS THROUGH HOLES AND MOUTHPIECES

Let us apply the equation obtained for the energy of a moving gas to solution of the following practically important problem. Determine the velocity and gravimetric flow rate of a gas in its outflow from a tank through a hole or short pipe (mouthpiece) into a medium with pressure  $p$ . We shall use the subscript 0 for the gas variables in the tank. The velocity  $v_0$  in the tank may be set equal to zero.

We apply Eq. (15.8) to two cross sections, placing one in the tank and the other at the exit from the hole or mouthpiece. Then

$$i + \frac{v^2}{2} = i_0.$$

whence the gas outflow velocity equals

$$v = \sqrt{2(i_0 - i)}.$$

For an ideal gas, we obtain for the selected cross sections from (15.6)

$$v = \sqrt{2g \frac{k}{k-1} \left( \frac{p_0}{\gamma_0} - \frac{p}{\gamma} \right)}. \quad (15.9)$$

Disregarding friction, we apply the equation of the ideal adiabatic curve; then

$$v = \sqrt{2g \frac{k}{k-1} \frac{p_0}{\gamma_0} \left[ 1 - \left( \frac{p}{p_0} \right)^{\frac{k-1}{k}} \right]}. \quad (15.9)$$

and the gravimetric flow rate equals

$$G = Sv\gamma = S \sqrt{2g \frac{k}{k-1} p_0 \gamma_0 \left[ \left( \frac{p}{p_0} \right)^{\frac{2}{k}} - \left( \frac{p}{p_0} \right)^{\frac{k+1}{k}} \right]}. \quad (15.10)$$

where S is the area of the hole.

The influence of resistance and constriction of the jet during outflow of a gas can be taken into account by introducing coefficients of velocity  $\phi$  and compression  $\epsilon$ , whose product, as in the case of outflow of an incompressible fluid, is equal to the flow rate coefficient  $\mu$ . The numerical values of these coefficients for low velocities can be assumed in first approximation to be the same as for the incompressible fluid, i.e., they can be determined from the shape of the hole (or mouthpiece) and the Reynolds number. The error incurred here will be greater the closer the outflow velocity to the speed of sound, which, as we know from physics, equals

$$a = \sqrt{k \frac{p}{\rho}} = \sqrt{kRT}.$$

As we see from Formula (15.10), the gravimetric flow rate of the gas at finite S is zero in two cases: when  $p/p_0 = 1$  and when  $p/p_0 = 0$ . Consequently, the flow rate will be at a maximum at a definite  $p/p_0$ . Let us find the critical pressure ratio  $(p/p_0)_{cr}$  at which the gravimetric flow reaches its maximum value  $G_{max}$ .

For this purpose, we differentiate the expression in brackets under the radical in Formula (15.10) with respect to  $p/p_0$  and equate the derivative to zero. We have

$$\frac{2}{k} \left( \frac{p}{p_0} \right)^{\frac{2-k}{k}} - \frac{k+1}{k} \left( \frac{p}{p_0} \right)^{\frac{1}{k}} = 0,$$

whence

$$\left(\frac{p}{p_0}\right)_{sp} = \left(\frac{2}{k+1}\right)^{\frac{k}{k-1}}. \quad (15.11)$$

For  $k = 1.4$  (for air and diatomic gases), the critical pressure ratio equals

$$\left(\frac{p}{p_0}\right)_{sp} = \left(\frac{2}{2.4}\right)^{\frac{1.4}{1.4}} = 0.528. \quad (15.11)$$

Substituting (15.11) into (15.10), we get

$$G_{\max} = S \sqrt{2g \frac{k}{k-1} \left[ \left(\frac{2}{k+1}\right)^{\frac{2}{k-1}} - \left(\frac{2}{k+1}\right)^{\frac{k+1}{k-1}} \right] \rho_0 v_0}$$

or

$$G_{\max} = S \sqrt{gk \left(\frac{2}{k+1}\right)^{\frac{k+1}{k-1}} \rho_0 v_0} = \psi S \sqrt{\rho_0 v_0}. \quad (15.12)$$

where  $\psi = 2.15$  for  $k = 1.4$ .

Let us now find the outflow velocity that corresponds to  $G_{\max}$  and  $(p/p_0)_{kr}$ . This velocity, which is called the critical velocity, is determined by Eq. (15.9) on substitution of (15.11) in it:

$$v_{sp} = a_{sp} = \sqrt{2g \frac{k}{k+1} \frac{p_0}{\gamma_0}} = \sqrt{\frac{2k}{k+1} RT_0}. \quad (15.13)$$

If we now use (15.9), setting  $v = v_{kr}$ , we obtain after simple transformations with (15.11)

$$v_{sp} = \sqrt{k \frac{p}{\rho}} = a, \quad (15.13')$$

i.e., the outflow velocity is equal to the speed of sound calculated from the gas variables at the exit from the hole or mouthpiece.

Thus, the maximum gravimetric gas flow rate is obtained when the outflow velocity in a given exit section is equal to the speed of sound. We note that in outflow through a hole or through a cylindrical or tapering mouthpiece, the pressure in the exit section remains equal to the ambient pressure only until the velocity in this section reaches the speed of sound. On a further increase in the initial pressure  $p_0$  or on a decrease in the ambient pressure  $p$ , the pressure in the exit section is found to be greater than the ambient pressure and is determined by (15.11);

accordingly, the velocity in the exit section is in this case equal to that of sound.

We draw attention to the fact that a decrease in the ambient pressure does not influence gas flow rate when the speed of sound is reached in the exit section. To obtain a supersonic outflow velocity, it is necessary to use a special mouthpiece known as the Laval nozzle, whose shape resembles that of the diffuser mouthpiece examined earlier (see Fig. 98). In the throat section of the Laval nozzle, the gas flow velocity equals the local speed of sound, and a further increase in velocity occurs in the expanding section.

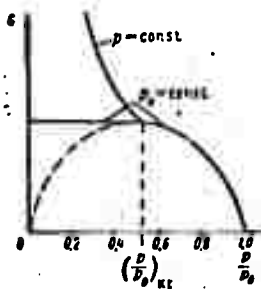


Fig. 230. Gravimetric gas flow rate as a function of the ratio  $p/p_0$ .

The following conclusion may be drawn from the above. In determining the gravimetric gas flow rate issuing from a tank through a mouthpiece, the pressure ratio  $p/p_0$  should be determined first and compared with the critical ratio, as defined by (15.11). If  $p/p_0 > (p/p_0)_{kr}$ , the gas flow rate must be found by Formula (15.10), and the outflow velocity from Formula (15.9). If  $p/p_0 < (p/p_0)_{kr}$ , the air flow rate is determined by Formula (15.12) and the outflow velocity by (15.13), in terms of  $p_0$  and  $\gamma_0$ . Figure 230 gives curves corresponding to Formulas (15.10) and (15.12).

#### §78. MOTION OF VISCOUS GAS IN CYLINDRICAL PIPE

For steady motion of a viscous gas along a constant-section pipe, we can write, by virtue of the constancy of gravimetric flow rate along the stream,

$$\frac{G}{S} = v_1 \gamma_1 = v_2 \gamma_2 = v \gamma = \text{const (along the stream)}, \quad (15.14)$$

where  $v$  is the average flow velocity in the given pipe section,  $\gamma$  is the specific weight of the gas in the same section, and  $S$  is the cross-sectional area of the pipe.

The greatest practical interest attaches to two cases of flow: adiabatic and isothermal.

In the absence of heat exchange with the external environment, the expansion of the gas will be adiabatic, even though its density is not related to pressure by the adiabatic equation (15.2), which applies only in the absence of friction. Here, the temperature of the gas along the pipe will be related to the flow velocity by (15.7). The other case will be that of heat exchange with the environment such that the temperature of the gas remains constant along the pipe, i.e., the process is isothermal. In actuality, we usually observe some sort of intermediate process.

Here, the shorter the gas line and, consequently, the shorter the time required by a gas particle to move through it, the closer will be the approach of the process to adiabatic. Conversely, the greater the length ratio of the gas line, the more nearly isothermal will the process become.

Let us express the Reynolds number for a gas flow in a pipe in terms of the gravimetric gas flow rate and the dynamic viscosity coefficient of the gas:

$$Re = \frac{vd}{\nu} = \frac{4G}{\pi g d \mu}$$



Fig. 231. Illustrating problem of gas flow in a cylindrical pipe.

It is clear from this that the Reynolds number may vary along the stream in a pipe of constant diameter only as a result of a change in the viscosity  $\mu$ . But the viscosity  $\mu$  of ideal gases does not depend on pressure, being determined solely by temperature. In the isothermal process of pipe flow of the gas, therefore, the Reynolds number will remain constant. In the adiabatic process, it will change slightly as a result of a temperature change, but this variation is usually insignificant.

result of a temperature change, but this variation is usually insignificant.

Let us isolate an element of length  $dx$  from a horizontal cylindrical pipe by passing two sections through it at an infinitesimal distance from one another (Fig. 231). Disregarding the nonuniformity of the velocity distribution over the cross sections, we denote the velocity in the left-hand section of the pipe by  $v$  and that in the right section by  $v + dv$ , and the respective pressures by  $p$  and  $p + dp$ .

We apply the momentum-change theorem of mechanics to our elementary volume. The per-second momentum increment in the direction of the flow equals

$$M dv = \rho S v dv$$

This increment results from the action of two external forces: a pressure force and a friction force.

The per-second impulse of the resultant force equals

$$dR = [p - (p + dp)]S - \tau_0 \Pi dx = -S dp - \tau_0 \Pi dx,$$

where  $\tau_0$  is the tangential stress at the pipe wall and  $\Pi$  is the perimeter of the pipe cross section.

Equating the per-second impulse of the forces to the momentum increment, we obtain

$$-S dp - \tau_0 \Pi dx = -\rho S v dv$$

or

$$dp + \rho d\left(\frac{v^2}{2}\right) + \lambda \frac{\tau_0}{R_g} dx = 0,$$

where  $R_g = S/\Pi$  is the hydraulic radius, which equals  $R_g = d/4$  for a round pipe.

We express  $\tau_0$  in terms of  $\lambda$  and  $v^2$  in accordance with (4.22) and divide the entire equation by  $\gamma = \rho g$ :

$$\frac{dp}{\gamma} + d\left(\frac{v^2}{2g}\right) + \lambda \frac{dx}{d} \frac{v^2}{2g} = 0, \quad (15.15)$$

where the last term is the head loss to friction on length  $dx$  and  $\lambda$  is a loss coefficient that depends on flow regime and Reynolds number (see §§24 and 28).

We now integrate (15.15) for the two cases: adiabatic and isothermal gas flows.

For adiabatic flow, we use (15.6), from which we find the pressure:

$$p = \frac{\gamma}{\gamma_1} p_1 = \frac{(k-1)\gamma}{2gk} (v_1^2 - v^2). \quad (15.16)$$

Here and below, the gas variables with the subscript 1 pertain to the initial section through the gas line, and those without a subscript to an arbitrarily chosen section.

We then find from Condition (15.14)

$$\gamma = \frac{\gamma_1 v_1}{v}; \quad \frac{\gamma}{\gamma_1} = \frac{v_1}{v}.$$

Now, using the expressions derived, we can rewrite the earlier equation in the form

$$p = \frac{v_1}{v} p_1 + \frac{k-1}{2gk} \gamma_1 \left( \frac{v_1^2}{v} - v v_1 \right).$$

We find the derivative

$$\frac{dp}{dv} = -\frac{k-1}{2gk} \gamma_1 \left( \frac{v_1^2}{v^2} + v_1 \right) - \frac{v_1}{v^2} p_1.$$

We substitute the resulting expression into (15.15); substituting  $\gamma$  in this equation according to (15.14), we obtain after simple manipulation

$$\lambda \frac{dx}{d} = 2g \frac{p_1}{\gamma_1} \frac{dv}{v^3} + \frac{k-1}{k} \left( \frac{v_1^2}{v^3} + \frac{1}{v} \right) dv - \frac{d(v^2)}{v^2}.$$

Extending integration from the initial cross section of the gas line to a certain arbitrary section (for example, the final section), which is at a distance  $l$  from the initial section, and regarding  $\lambda$  as constant along the stream, we have

$$\lambda \frac{l}{d} = \left( g \frac{p_1}{\gamma_1} + \frac{k-1}{2k} v_1^2 \right) \left( \frac{1}{v_1^2} - \frac{1}{v^2} \right) - \frac{k+1}{k} \ln \frac{v}{v_1}. \quad (15.16')$$

We can write on the basis of (15.6) and (15.7)

$$g \frac{p_1}{\gamma_1} + \frac{k-1}{2k} v_1^2 = g \frac{p_{01}}{\gamma_{01}} = RT_0.$$

Here and from now on, the subscript 01 will be applied to the stagnation parameters in the initial cross section of the gas line, those that the gas acquires if it is stagnated adiabatically and without friction, i.e., so as to observe the isentropic equation (15.2). We may therefore assume that the variables of the gas in the tank (bottle) from which the gas line runs and in which the velocity  $v = v_0 = 0$  will also be the same.

We note in passing that in adiabatic gas flow, the stagnation temperature remains constant along the flow, i.e.,  $T_{0,1} = T_0 = \text{const}$ , while the stagnation pressure  $p_0$  decreases because of friction.

With consideration of the above, the result of integration (15.16) can be written

$$\lambda \frac{l}{d} = RT_0 \left( \frac{1}{v_1^2} - \frac{1}{v^2} \right) - \frac{k+1}{k} \ln \frac{v}{v_1}, \quad (15.16'')$$

and, using (15.13), we can write Eq. (15.16'') in dimensionless quantities:

$$\bar{l} = \frac{k+1}{2k} \left( \frac{1}{\bar{M}_1^2} - \frac{1}{\bar{M}^2} - 2 \ln \frac{\bar{M}}{\bar{M}_1} \right), \quad (15.16)$$

where  $\bar{M}_1 = v_1/a_{kr}$  and  $\bar{M} = v/a_{kr}$  are the so-called relative velocities in the initial and final cross sections of the gas line and  $\bar{l} = \lambda l/d$  is the reduced relative length of the line.

If we again differentiate this expression with respect to  $\bar{M}$ , assuming  $\bar{M}_1 = \text{const}$  and express  $d\bar{M}$  in terms of  $d\bar{l}$ , we can easily show that the velocity increases in a cylindrical pipe in subsonic gas flow, and decreases in supersonic flow, but that passage through the speed of sound is impossible in a cylindrical pipe in adiabatic flow.

Equation (15.16'') or (15.16) is not sufficient for full solution of the problem of gas flow along a pipe from a receiver to a final (or arbitrary) cross section. It is necessary to derive a second working equation linking  $\bar{M}_1$ ,  $\bar{M}$ , and the ratio of the pressure in the receiver (the stagnation pressure in the

initial pipe section)  $p_{01}$  to the pressure  $p$  in the final section.

For this purpose, we obtain from Eq. (15.7), written for the receiver and the initial pipe section,

$$v_1^2 = \frac{k}{k-1} 2RT_0 \left(1 - \frac{T_1}{T_0}\right). \quad (15.17)$$

Thereafter, we use the following equation system:

1) the equations of state for the initial and final pipe sections:

$$p_1 = \rho_1 RT_1 \text{ and } p = \rho RT;$$

2) the ideal adiabatic equation for the tank and the initial pipe cross section

$$\frac{p_{01}}{p_1} = \left(\frac{T_{01}}{T_1}\right)^{\frac{k}{k-1}};$$

3) Eq. (15.14) for the initial and final pipe cross sections

$$\frac{v_1}{v} = \frac{\rho}{\rho_1};$$

4) Eq. (15.7) for the receiver and the final pipe cross section

$$\frac{k}{k-1} RT_0 = \frac{k}{k-1} \frac{p}{\rho} + \frac{v^2}{2}, \text{ where } T_0 = T_{01}.$$

With the above equations, we can reduce Formula (15.17) by successive exclusions to the form

$$v_1^2 = \frac{2k}{k-1} RT_0 \left[1 - \left(\frac{pv}{\rho_0 v_1}\right)^{k-1} \cdot \left(1 - \frac{k-1}{k} \frac{v^2}{2RT}\right)^{1-k}\right]. \quad (15.17')$$

Introducing the relative velocities  $\bar{M}$  into (15.17') and solving it for  $p/p_{01}$ , we obtain

$$\frac{p}{p_{01}} = \left(1 - \frac{k-1}{k+1} \bar{M}_1^2\right)^{\frac{1}{k-1}} \cdot \left(1 - \frac{k-1}{k+1} \bar{M}^2\right) \frac{\bar{M}_1}{\bar{M}}. \quad (15.18)$$

The system of equations (15.16) and (15.18) enables us to construct a family of  $p/p_{01} = f(\bar{M})$  curves of adiabatic gas flow for a series of constant relative velocities  $\bar{M}_1$  in the initial cross section of the pipe and to plot on the same diagram curves of constant  $\bar{M}$ . This family of curves is very convenient for calculation of gas lines for adiabatic flow. In Fig. 232, the curves were plotted for  $k = 1.4$ ; the solid lines represent  $\bar{M}_1 = \text{const}$ , and the dashed lines  $\bar{M} = \text{const}$ .

Curve AB corresponds to the limiting value  $\bar{M} = 1$ , i.e., to the speed of sound in the final (or subject) cross section. Consequently, curve AB is the boundary between the region of subsonic flows (above curve AB) and the region of supersonic flows in the gas line.

For  $\bar{M}_1 = \bar{M} = 1$ , Formula (15.16) gives  $\bar{x} = 0$ , and it follows from (15.18) that

$$\frac{p}{p_{01}} = \left( \frac{2}{k+1} \right)^{\frac{k}{k-1}} = 0,528,$$

i.e., we obtain the case of gas outflow through a hole at the critical velocity.

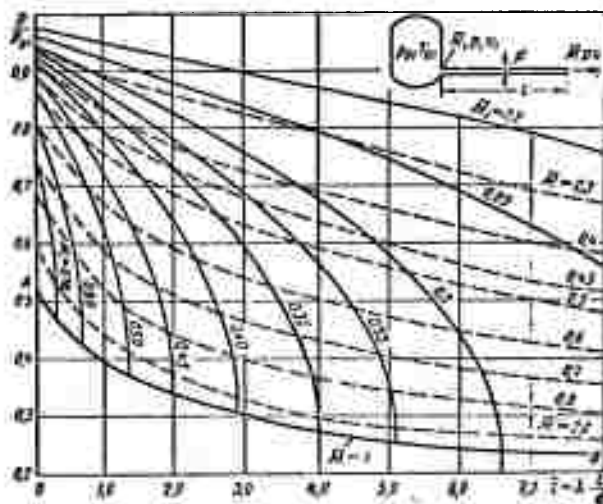


Fig. 232. Illustrating design of gas lines for adiabatic flow.

The method by which these curves are used will be demonstrated below.

For isothermal flow we have the following relation between pressure and density:

$$\frac{p_1}{\rho_1} = \frac{p}{\rho}.$$

Applying (15.14) and differentiating, we obtain

$$dp = -\rho_1 \frac{v_1}{v^2} dv.$$



Differentiating (15.20) with respect to  $M$ , assuming  $M_1 = \text{const}$ , and determining  $dM$ , we obtain

$$dM = \frac{M d\bar{l}}{2\left(\frac{1}{kM^2} - 1\right)}.$$

Analyzing this equation, we conclude that in the case of isothermal flow with  $M^2 < 1/k$  in a cylindrical pipe, velocity increases downstream (for  $d\bar{l} > 0$  and  $dM > 0$ ), while for  $M^2 > k$ , it decreases downstream. Consequently, the value of  $M = 1/\sqrt{k}$  for isothermal pipe flow is just as critical as  $M = 1$  for adiabatic flow. Passage through this value of  $M$ , which equals  $M_{kr} = 0.845$  for  $k = 1.4$ , with preservation of isothermal flow is impossible, since the slightest upward deviation of  $M$  from the critical value changes the sign of the increment  $dM$  and returns the flow to the critical state.

To obtain our second working equation, we proceed, as in the case of adiabatic flow, from Eq. (15.17) and the four-equation system that follows it, except for the last, instead of which we use the isotherm equation

$$\frac{p}{\gamma} = \frac{p_1}{\gamma_1}.$$

This equation system enables us to bring (15.17) to the form

$$v_1^2 = \frac{2k}{k-1} R' l_{01} \left[ 1 - \left( \frac{p v}{p_{01} v_1} \right)^{\frac{k-1}{k}} \right].$$

Then on introducing  $M$  and solving for  $p/p_{01}$ , we obtain instead of the above

$$\frac{p}{p_{01}} = \frac{M_1}{M \left( 1 + \frac{k-1}{2} M_1^2 \right)^{\frac{k}{k-1}}}. \quad (15.21)$$

With Eqs. (15.20) and (15.21), we can construct a family of  $p/p_{01} = f(\bar{l})$  curves of isothermal flow for a series of constant  $M_1$  (in the initial cross section of the pipe), and plot curves of constant  $M$  on the same diagram (Fig. 233). Curve AB corresponds to the limiting value  $M = M_{kr} = 1/\sqrt{k} = 0.845$ .

#### §79. POSSIBLE PROBLEMS IN THE SYNTHESIS OF GAS LINES

We shall examine problems of this type that are likely to come up in practice and their solution by means of the diagrams that we have constructed. These problems are formulated in much the same way as those pertaining to the simple pipeline, which were examined in §47. We shall consider all problems in two variants: for adiabatic and isothermal flows in the gas line. The difference in the

formulation of the problems for these two variants will be in the temperatures assumed to be given:  $T_{01}$  in the receiver for adiabatic flow and  $T = T_1 = \text{const}$  along the gas line, which is equal to the ambient temperature, in the case of isochermal flow.

Since the actual flow process is intermediate, it is recommended that the problem be solved in the general case in these two variants, so that the limits between which the real answer lies will be known. We shall assume that the properties of the gas, i.e.,  $k$ ,  $R$ , and  $\mu$ , are given in all cases. The frictional loss coefficient  $\lambda$  for the gas line is determined by the same formulas as for a liquid.

#### Problem 1.

Given: Gravimetric gas flow rate  $G$ , ambient pressure  $p$  at exit from pipeline, and the dimensions of the gas line,  $l$  and  $d$ .

Find the required receiver pressure  $p_{01}$ .

#### Solution:

1. For the adiabatic case, we assign an average gas temperature in the gas line<sup>1</sup> and determine the average viscosity  $\mu$  from it. We find  $Re$  from  $G$ ,  $d$ , and  $\mu$ , and then determine the coefficient  $\lambda$  and the reduced length  $\bar{l} = \lambda l/d$ .

Then, on the basis of (15.6) and (15.7), we write the equation for the flow from the receiver to the final section of the gas line:

$$\frac{k}{k-1} RT_{01} = \frac{k}{k-1} \frac{p}{\gamma} + \frac{v^2}{2g},$$

where

$$\gamma = \frac{4G}{\pi d^2 v}.$$

Eliminating  $\gamma$  from the first equation, we solve it as a quadratic equation in  $v$ . Then we determine  $a_{kr}$  and  $M = v/a_{kr}$  from (15.13).

We then turn to the diagram of Fig. 232 and determine  $p/p_{01}$  for the  $\bar{l}$  and  $M$ , and then find  $p_{01}$ .

If the result places the calculated point below curve AB in Fig. 232, this means that in actuality,  $M = 1$  and  $v = a_{kr}$  will apply in the final section. The pressure ratio  $p/p_{01}$  is determined by the intersection point of curve AB in Fig. 232 with the vertical corresponding to  $\bar{l}$ . In this case, the pressure in the final section of the gas line will exceed the pressure of the medium into which the gas is escaping and, consequently, is unknown.

<sup>1</sup>See page 389 for footnote.

In this case, we proceed as follows to determine  $p_{01}$ . From the indicated intersection on the diagram, we determine  $\bar{M}_1$  and then  $v_1 = a_{kr} \bar{M}_1$  and

$$\gamma_1 = \frac{4G}{\pi d^2 v_1}.$$

We then have from (15.7), written for the receiver and the initial cross section,

$$T_1 = T_{01} - \frac{k-1}{kR} \frac{v_1^2}{2},$$

and from the equation of state

$$p_1 = \frac{\gamma_1 R T_1}{g}.$$

Using the ideal adiabatic equation known from thermodynamics, we find the unknown receiver pressure

$$p_{01} = p \left( \frac{T_{01}}{T_1} \right)^{\frac{k}{k-1}}.$$

In the case of laminar flow, when the coefficient  $\lambda$  varies substantially with  $Re$ , we can determine the temperature and improve the calculation.

2. In the isothermal case, we find  $\mu$  from the temperature  $T = T_1$ , and then  $Re$ ,  $\lambda$ , and  $\bar{V}$ . We use the equation of state to determine  $\gamma$  from  $T$  and  $p$ , and then find the velocity in the final section of the gas line:

$$v = \frac{4G}{\pi d^2 \gamma}.$$

We determine  $a$  from (15.13') and then  $M = v/a$ . We then determine  $p/p_{01}$  for the  $\bar{L}$  and  $M$  on the diagram of Fig. 233, and this gives us  $p_{01}$ .

If the calculated point is below curve AB on Fig. 233, this means that  $M = 0.845$  and the calculation is carried out as in the preceding case for  $\bar{M} = 1$ . The only difference will be that the temperature  $T_1$  is known and  $T_{01}$  is not known.

### Problem 2.

Given: Pressure  $p_{01}$  in receiver, pressure  $p$  of medium at exit from gas line, and gas line dimensions  $\bar{L}$  and  $\bar{d}$ .

Find the gravimetric gas flow rate  $G$ .

Solution:

1. For the adiabatic case, we assign a value to the coefficient  $\lambda$  on the assumption of turbulent flow ( $\lambda = 0.02-0.03$ ). We determine the reduced gas line length  $\bar{\ell}$  and find  $\bar{M}_1$  from  $p/p_{01}$ , with the aid of Fig. 232. Next, we determine  $a_{kr}$  from (15.13), and then  $v_1 = a_{kr}\bar{M}_1$ . We determine  $T_1$  from Eq. (15.7), written for the receiver and the initial pipeline cross section:

$$T_1 = T_{01} - \frac{k-1}{kR} \frac{v_1^2}{2}.$$

We then apply the ideal adiabatic equation of thermodynamics:

$$\frac{y_1}{y_{01}} = \left( \frac{T_1}{T_{01}} \right)^{\frac{1}{k-1}}$$

and the equation of state

$$y_{01} = \frac{p_{01} \bar{\ell}}{RT_{01}},$$

from which we determine the specific weight of the gas in the initial cross section.

The unknown gas flow rate is determined in first approximation by the formula

$$G = v_1 y_1 \frac{\pi d^2}{4}.$$

We then determine the Reynolds number from  $G$  and  $T_{sr}$ , check the flow regime, and figure the coefficient  $\lambda$  from Re. The gas flow rate can then be determined in the same way in second approximation and, if necessary, third and subsequent approximations, but two or three are usually sufficient.

2. For the isothermal case, we again assign a coefficient  $\lambda$ , determine  $\bar{\ell}$ , and find  $\bar{M}$  from  $p/p_{01}$ , with the diagram of Fig. 233. Using (15.13'), we determine  $a$  and then  $v = a\bar{M}$ . Using  $T$  and  $p$  with the equation of state, we find  $\gamma$ , and then the unknown gas flow rate in first approximation:

$$G = v\gamma \frac{\pi d^2}{4}.$$

Then, as before, we improve the solution, i.e., compute Re and  $\lambda$  and repeat the same procedure until we obtain satisfactory convergence.

If the calculated point on Fig. 232 or 233 is below curve AB when this problem is solved, this means, as in Problem 1, that the flow rate  $G$  is determined from the intersection point of curve AB with the vertical corresponding to  $\bar{\ell}$ .

### Problem 3.

Given: Gravimetric gas flow rate  $G$ , receiver pressure  $p_{01}$ , pressure  $p$  in medium at exit from gas line, and length  $l$  of gas line.

Find the diameter  $d$  of the gas line.

The solution is carried out as follows in both cases (adiabatic and isothermal). We assign a series of values to the diameter  $d$  (3-4 values). Here it is helpful to make an approximate determination of the diameter corresponding to  $\bar{L}_{kr}$ , at which the assigned pressure ratio  $p/p_{01}$  will yield the limiting velocity value at the exit from the gas line (if  $p/p_{01} < 0.528$ ), and to include this diameter among the assigned values. Then we solve the first problem for each of these diameters, i.e., we find the  $p_{01}$  for adiabatic and isothermal flows or for only one of them. We then plot a curve of  $p_{01}$  as a function of  $d$  and use it to find the necessary diameter from the assigned  $p_{01}$ ; we then select the next larger standard diameter.

An approximate formula for synthesis of gas lines on the assumption of isothermal flow can be derived from (15.19) by applying (15.14) and the equations of state and the isotherm. We first solve (15.19) for  $v_1$  and then transform and write an expression for the gravimetric gas flow rate

$$G = \frac{\pi d^2}{4} \gamma_1 v_1 = \frac{\pi d^2}{4} \sqrt{\frac{(p_1^2 - p^2)}{\left(\lambda \frac{l}{d} + 2 \ln \frac{p_1}{p}\right) RT}} \quad (15.22)$$

where  $T$  is the constant temperature along the gas line.

This formula can be used when it is known that  $M = 0.845$  at the end of the gas line and when the pressure  $p_1$  in the initial cross section of the gas line is given. If, on the other hand, the latter is unknown, we can assume in approximation that  $p_1 = p_{01}$  at low gas velocities in the initial cross section, i.e., we can disregard the pressure drop from the receiver to the initial gas line cross section.

The problem of determining the initial pressure  $p_1$  for given  $G$  and  $p$  with Formula (15.22) can be solved only by trial and error. But if the reduced length  $\lambda l/d$  is large enough by comparison with  $2 \ln(p_1/p)$ , the latter can be disregarded; (15.22) then gives

$$p_1^2 = p^2 + \frac{16}{\pi^2 d^4} \lambda \frac{l}{d} RTG^2.$$

It must be remembered that here and everywhere else  $R$  has been the gas constant in SI units and  $p$  the pressure in  $N/m^2$ . If, however, the old engineering system of units is used and pressure

is expressed in  $\text{kgf/m}^2$ , the last formula will be written somewhat differently:

$$p_1^2 = p^2 + \frac{16}{\pi^2 g d^4} \lambda \frac{l}{d} R T G^2.$$

Footnote

Manu-  
script  
page

384

<sup>1</sup>This temperature can be assumed approximately equal to  
 $T_{sr} = 0.9T_{01}$ .

### Symbol List

Manu- script page	Symbol		English equivalent
374	kp	kr	critical
378	r	g	hydraulic
386	cp	sr	average

### References

1. Abramovich, G.N. Prikladnaya gazovaya dinamika (Applied Gasdynamics), GTTI, 1953.
2. Al'tshul', A.D. and Kiselev, P.G. Gidravlika i aerodinamika (Hydraulics and Aerodynamics), Stroyizdat, 1965.
3. Al'tshul', A.D. Ob istechenii zhidkostey znachitel'noy vyazkosti (Outflow of higher-viscosity fluids), Zhurnal tekhnicheskoy fiziki, Izd. AN SSSR, 1957.
4. Al'tshul', A.D. Mestnyye gidravlicheskiye soprotivleniya pri dvizhenii vyazkikh zhidkostyy (Local hydraulic resistances in motion of viscous fluids), Gostoptekhzdat, 1962.
5. Bashta, T.M. Raschet i konstruktsii samoletnykh gidravlicheskiykh ustroystv (Synthesis and design of aircraft hydraulic devices), Oborongiz, 1961.
6. Bashta, T.M. Mashinostroitel'naya gidravlika (Hydraulics for Mechanical Engineers), Mashgiz, 1963.
7. Burago, G.F. Kurs gidravliki (Textbook of hydraulics), Izd. VVIA im. N.Ye. Zhukovskogo, 1946.
8. Butayev, D.A., Kalmykova, Z.A., Podvidz, L.G., Popov, K. N., Rozhdestvenskiy, S.N., and Yan'shin, B.I. Zadachnik po gidravlike (Problem book in hydraulics), Edited by Prof. I.I. Kukolevskiy, Gosenergoizdat, 1960.
9. Voskoboynik, M.S. and Mokrushin, L.V. Osnovy proyektirovaniya samoletnykh gidravlicheskiykh sistem (Fundamentals of the

design of aircraft hydraulic systems), Izd. Rzhskogo vysshego inzhenerno-aviatsionnogo voyennogo uchilishcha (Riga Higher Aviation Engineering Military Academy Press), 1954.

10. Grigor'yev, A.I. Aviatsionnyye goryuchsmazochnyye materialy (Aviation lubricant fuels), Izd. VVIA im. N.Ye. Zhukovskogo, 1957.

11. Zhovinskiy, N.Ye. Penyaz'kov, Ye.I., Yundev, N.L. Oborudovaniye silovyykh aviatsionnykh ustanovok i ikh ekspluatatsiya (Equipment of aircraft power systems and their operation), Izd. VVIA im. N.Ye. Zhukovskogo, 1957.

12. Idel'chik, I.Ye. Gidravlicheskiye soprotivleniya (Hydraulic resistances), Gosenergoizdat, 1954.

13. Izbash, S.V. Osnovy gidravliki (Fundamentals of Hydraulics), Gosstroyizdat, 1952.

14. Kosourov, K.F. Osnovy obshchey i aviatsionnoy gidravliki (Fundamentals of general and aviation hydraulics), Izd. Leningradskoy voyenno-vozdushnoy inzhenernoy akademii (Leningrad Air Force Engineering Academy Press), 1952.

15. Kopyrin, M.A. Gidravlika i gidravlicheskiye mashiny (Hydraulics and hydraulic machines), Izd-vo "Vysshaya shkola", 1961.

16. Kulagin, A.V., Prokof'yev, V.N., Demidov, Yu.S. and Kondakov, L.A. Osnovy teorii i konstruirovaniya ob'emnykh gidroperedach (Fundamentals of the theory and design of displacement-type hydraulic transmissions), Izd-vo "Vysshaya shkola", 1967.

17. Lomakin, A.A. Tsentrobezhnyye i propellernyye nasosy (Centrifugal and screw-impeller pumps), Mashgiz, 1950.

18. Levkoyeva, N.V. O vliyani chisla Reynol'dsa na velichinu koefitsiyentov soprotivleniya diafragm (Influence of Reynolds number on resistance coefficients of diaphragms), Izvestiya vuzov, seriya "Aviatsionnaya tekhnika," No. 2, 1959.

19. Mikheyev, M.A. Osnovy teploperedachi (Fundamentals of heat transfer), Gosenergoizdat, 1956.

20. Nekrasov, B.B. Gidravlika (Hydraulics), Voenizdat, 1960.

21. Nekrasov, B.B. Badikov, G.I. and Kravchuk, M.V. O gidravlicheskom privode samoletnykh sinkhronnykh generatorov (Hydraulic drives for aircraft synchronous generators), Izd. VVIA im. N.Ye. Zhukovskogo, 1956.

22. Prokof'yev, V.N. Gidromekhanicheskiye peredachi (Hydro-mechanical transmissions), Mashgiz, 1957.

23. Prokof'yev, V.N. Gidravlicheskiye peredachi. Rotornyye nasosy (Hydraulic transmissions. Rotor pumps), Entsiklopedicheskiy spravochnik mashinostroyeniya (Encyclopedic Handbook of Mechanical Engineering), Mashgiz, Vol. 12, 1948.

24. Pfleyderer, K. Tsentrobezhnyye i propellernyye nasosy (Centrifugal and screw-impeller pumps), ONTI NKTP, 1937.

25. Podvidz, L.G. and Yan'shin, B.I. Gidravlika (Hydraulics), Spravochnik mashinostroitelya (Mechanical engineer's handbook), Mashgiz, Vol. 2, 1960.

26. Rabinovich, Ye.Z. Gidravlika (Hydraulics), Fizmatgiz, 1963.

27. Rozhdestvenskiy, B.S. Issledovaniye gidravlicheskogo udara primenitel'no k gidrosistemam letatel'nykh apparatov (Investigation of water hammer in aircraft hydraulic systems), Izvestiya vuzov, seriya "Aviatsionnaya tekhnika", No. 2, 1965.

28. Satton, D. Raketnyye dvigateli (Rocket engines), IL, 1952.

29. Sinyarev, G.B. and Dobrovol'skiy M.V. Zhidkostnyye raketnyye dvigateli (Liquid rocket engines), Oborongiz, 1957.

30. Uginchus, A.A. Gidravlika i gidravlicheskiye mashiny (Hydraulics and hydraulic machines), Gosenergoizdat, 1953.

31. Fabrikant, N.Ya. Aerodinamika. Obshchiy kurs (Aerodynamics: a general textbook), Izd-vo "Nauka", 1964.

32. Frenkel', N.Z., Gidravlika (Hydraulics), Gosenergoizdat, 1956.

33. Shiukov, A.G. Nasosy i forsunki gasoturbinnykh dvigatelay (Pumps and injectors of gas-turbine engines), Izd. VVIA im. N. Ye. Zhukovskogo, 1954.

34. Yur'yev, B.N. Eksperimental'naya aerodinamika (Experimental aerodynamics), ONTI NKTP, Part I, 1936.

35. Yablonskiy, V.S. Kratniy kurs tekhnicheskoy gidromekhaniki (Concise Textbook of Engineering Hydromechanics), Fizmatgiz, 1961.

36. Ob"yemnyy gidroprivod. Sbornik rekomenduyemykh terminov Komiteta nauchno-tekhnicheskoy terminologii AN SSSR (The displacement-type hydraulic drive. List of terms recommended by the USSR Academy of Sciences Committee on Scientific and Technical Terminology), No. 66, Izd-vo "Nauka", 1964.

**DATA HANDLING PAGE**

01-ACCESSION NO. TM0000109		98-DOCUMENT LOC		39-TOPIC TAGS hydraulic pump, hydraulic fluid, hydraulic pressure amplifiers, hydraulics, fluid flow, turbulent flow, centrifugal pump	
09-TITLE HYDRAULICS AND ITS APPLICATIONS ON AIRCRAFT. -U-					
47-SUBJECT AREA 13, 20					
42-AUTHOR CO-AUTHORS NEKRASOV, B. B.				10-DATE OF INFO ----67	
43-SOURCE GIDRAVLIKA I YEYE PRIMENIENIYE NA LETATEL'NYKH APPARATAKH, MOSCOW, IZD-VO "MASHINOSTROYENIYE" (RUSSIAN)				60-DOCUMENT NO. HT-23-242-69 69-PROJECT NO. 72301-78	
63-SECURITY AND DOWNGRADING INFORMATION UNCL. 0			64-CONTROL MARKINGS NONE		97-HEADER CLASS UNCL
76-REEL/FRAME NO. 1891 0477	77-SUPERSEDES	78-CHANGES	40-GEOGRAPHICAL AREA UR	NO. OF PAGES 393	
CONTRACT NO. F33657-68-D-0866P002	X REF ACC. NO. 65- AM8014380	PUBLISHING DATE 94-	TYPE PRODUCT TRANSLATION	REVISION FREQ NONE	
STEP NO. 02-UR/0000/67/000/000/0001/0368					
<p>ABSTRACT</p> <p>(U) The book is intended for use as a textbook by students of higher educational institutes for aviation, and in some machine building higher educational institutes. The author discusses problems of general hydraulic control, hydrostatic laws, fluid flow level in tubes, as well as laws for the flow of fluid through orifices and nozzles. Hydraulic calculations are presented as applied to fluid flow in tubes. Centrifugal and positive-displacement pumps as applied in aircraft, as well as fluid flow and the practical application of its theories, are discussed. The author thanks N. Ya. Fabrikant, K. F. Kosourov, S. S. Rudnev, A. S. Shifrin, V. N. Prokof'yev, V. V. Shul'gin, B. Ya. Shumatskiy, and B. P. Borisov for participation in the compilation of this book.</p>					